Pumping new life into preclinical pharmacokinetics: exploring the pharmacokinetic application of ex vivo organ perfusion
Stevens, L.J.

Pumping new life into preclinical pharmacokinetics:

exploring the pharmacokinetic
application of ex vivo organ perfusion

L.J. Stevens

Pumping new life into preclinical pharmacokinetics; exploring the pharmacokinetic application of ex vivo organ perfusion

Proefschrift

ter verkrijging van
de graad van doctor aan de Universiteit Leiden,
op gezag van rector magnificus prof.dr.ir. H. Bijl,
volgens besluit van het college voor promoties
te verdedigen op dinsdag 29 oktober 2024
klokke 14.30 uur

door

Lida Joanne Stevens

geboren te Twello
in 1992

PROMOTOREN

Prof. dr. I.P.J. Alwayn
Prof. dr. C.A.J. Knibbe

CO-PROMOTOR

Dr. E. van de Steeg   TNO

LEDEN PROMOTIECOMMISSIE
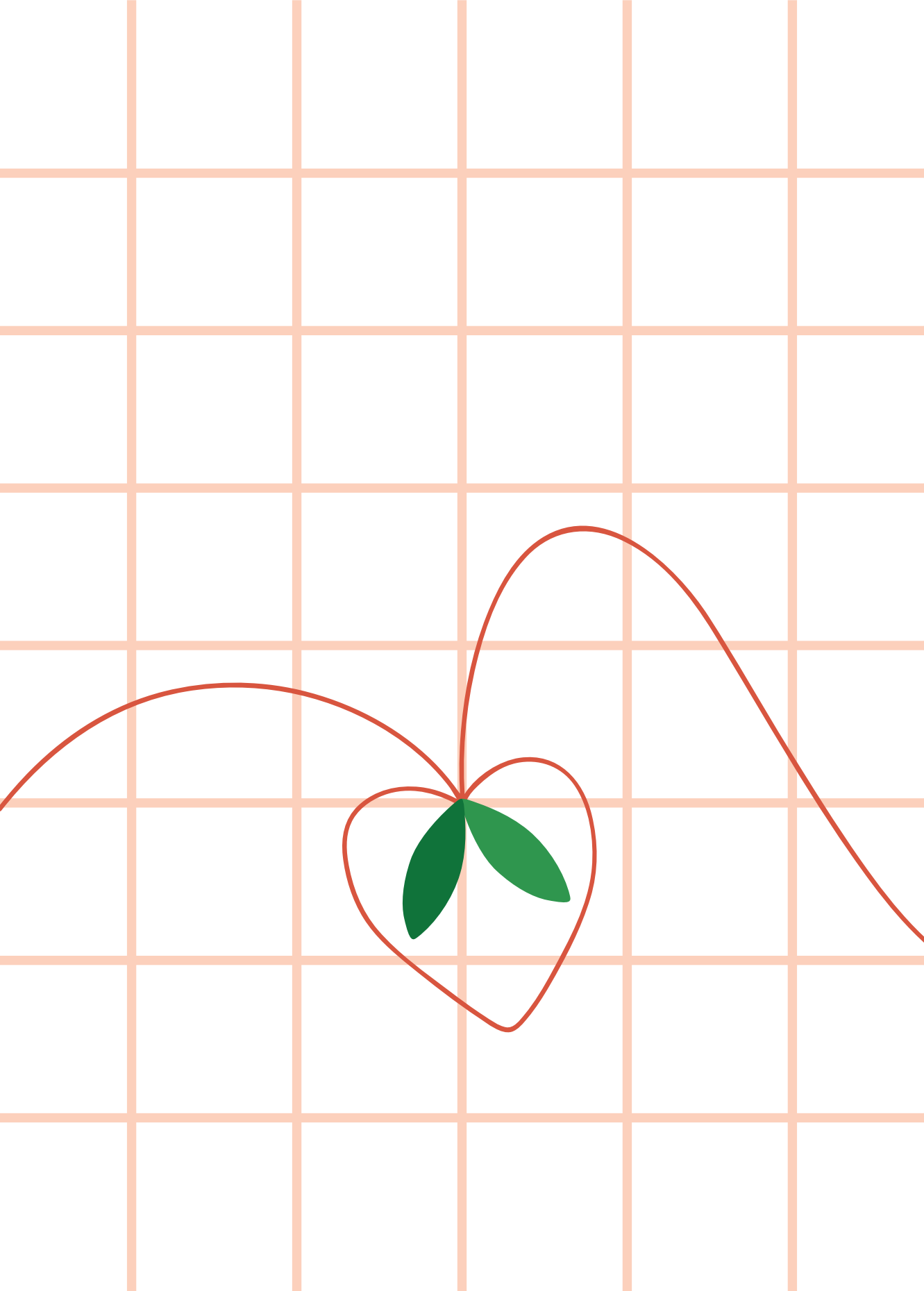
Dr. M.A. Engelse
Prof. dr. T. van Gelder
Prof. dr. S.F.J. van de Graaf   Amsterdam University Medical Center
Prof. dr. R. Masereeuw   Utrecht University
Prof. dr. F.G.M. Russel   Radboud University Medical Center
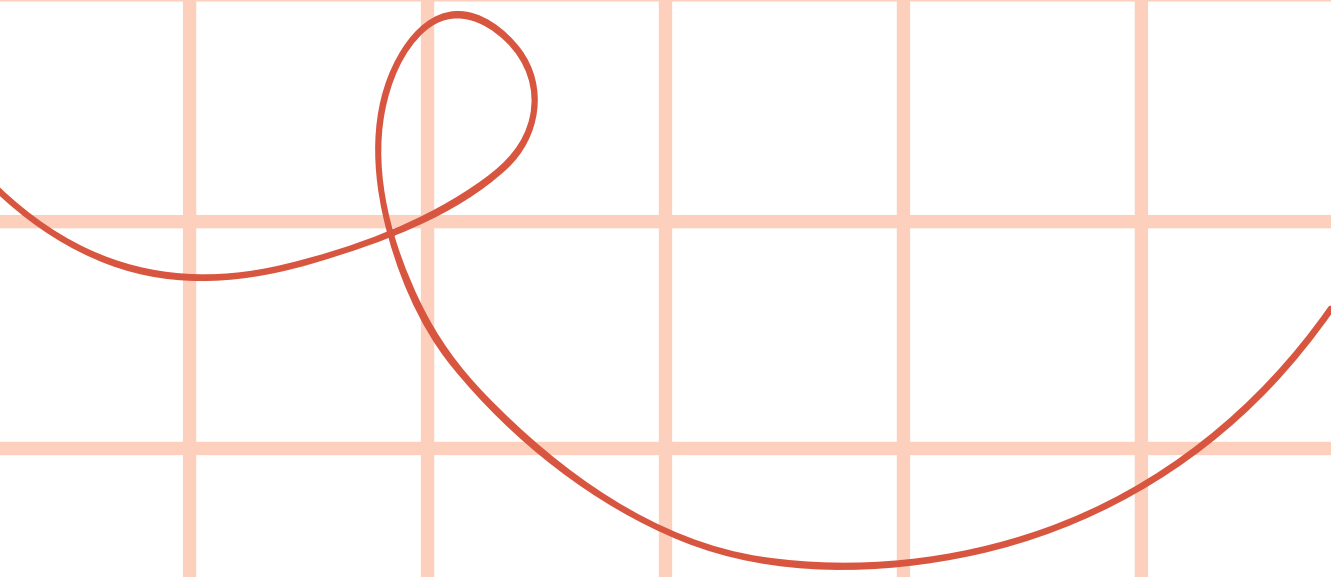
Table of contents

PART I

Exploring pharmacokinetics
through ex vivo models

CHAPTER 01

General introduction, scope
and outline of the investigation

General introduction

Drug development process

The drug development process is a comprehensive and multi-stage procedure that involves discovery, compound identification, preclinical testing and clinical trials. This is a costly and long process as it takes on average 10-15 years and $1-2 billion for each new drug to be approved for clinical use[1]. It is observed that 90% of drug candidates to not make it do the market[1-3]. A majority of drugs in development tend to fail in phase II of phase III due to the inability to predict toxicity and efficacy *in vivo*[4,5]. The disparate findings during the preclinical phase using animal models and human clinical trials typically manifest during late-stage clinical assessment or during post-market stages[3]. To illustrate, recently the drug fenebrutinib for the treatment of multiple sclerosis resulted in elevated levels of hepatic transaminases and elevated bilirubin levels in some patients in a phase III clinical trial, suggesting a potential risk for drug-induced liver injury[6]. Besides drug induced toxicity, drug-drug interactions (DDI) are also major concerns during the drug development process[7,8]. DDI can occur when patients use multiple drugs which can affect the systemic concentration of the drug. This can potentially result in reduced efficacy, severe adverse reactions or can even result in toxicity leading to withdrawal from the market[7]. It is observed that compounds which are inhibitors or substrates of hepatic transporters are more prone to cause DDI and/or drug induced liver injury, therefore assessment of the hepatic first pass effect and biliary excretion of drugs in development is of major importance. An example is a phase I study where Mita et al.[9] demonstrated that a compound showed non-linear kinetics at the highest dose levels. This could possibly be the effect of saturation in biliary excretion pathway of the compound, as a biphasic plasma profile was observed in the lower dose levels, demonstrating enterohepatic circulation of the compound, however this was not observed in preclinical models and animal studies. Current models that predict biliary excretion often fail due to species differences (rodent/dog) or due to differences in transporter expression in *in vitro* assays (e.g. sandwich cultured hepatocytes)[10-12]. Thus characterization of these complex pharmacokinetic (PK) processes request comprehensive, complete and dynamic preclinical models which can recapitulate the complexity of the human body[13,14], which is crucial to enhance the likelihood of successfully concluding a clinical trial and obtaining approval for a new drug[15]. Developing physiologically relevant models is not only limited to study the DDI potential of newly developed drugs but also to study the outcomes of polypharmacy.

Patients and elderly patients in particular, often receive more than one drug at the same time as they can suffer from multiple conditions. As a result, the uptake or excretion can be mediated by the same transporters and thereby interfering which each other's clearance[16-18].

Drug ADME processes and models involved

Intestine

Oral delivery of a drug is the most preferred route of administration in terms of costs and medication adherence[13]. After oral absorption, the gastrointestinal tract serves as the first barrier for the entry of drugs into the bloodstream. After passive or active (transporter-mediated) absorption, drugs can be metabolized by cytochrome P450 (CYP450) enzymes located within the gut-wall[19]. These drug transporters and CYP450 enzymes are broadly and heterogeneously expressed along the gastrointestinal tract and they can have a major impact on the drug absorption into the portal vein[20]. The intestinal tract expresses a broad range of efflux transporters which belong to the ATP-binding cassette (ABC) family, using ATP as energy source to efflux drugs and endogenous compounds out of cells[21,22]. Main transporters in the intestine are multidrug resistance protein 1 (MDR1), also known as P-glycoprotein (Pgp), breast cancer resistance protein (BCRP) and multidrug resistance protein 2 (MRP2) and they belong to the ABC transporter family and efflux compounds from the apical membrane back into the lumen, thereby limiting the absorption of substrates for these transporters such as rosuvastatin and digoxin[23]. Additionally, CYP450 drug metabolism by the gut wall, which is known as the intestinal extraction (E_G), contributes to the first-pass effect and thereby limits the oral bioavailability[24,25]. Midazolam for instance, a CYP3A4 substrate, undergoes partial metabolism in the gut wall before reaching the liver[24,26,27]. Multiple intestinal preclinical models have been established to measure the absorption from the lumen (apical side) to the portal venous blood (basolateral side). The Caco-2 transwell model is often used to study intestinal permeability[28]. However a major drawback of this cell-based model is the limited expression of CYP450 enzymes and altered transporter protein expression levels compared to human intestinal tissue[29]. The use of *ex vivo* intestinal tissue models is therefore preferred since the morphological structure is intact as well as the presence of uptake and efflux transporters and CYP450 enzymes thereby properly reflecting *in vivo* conditions[30]. In preclinical intestinal models, the intestinal transport is reflected as the apparent

permeability (P_{app}) which represents the apical to basolateral permeability per centimeter per second[30,31]. Subsequently, the P_{app} can be incorporated in physiologically based pharmacokinetic modelling (PBPK) modeling to predict the intestinal absorption and clearance[32]. Current intestinal models are predominantly static, while in vivo, the intestinal luminal flow as well as the superior mesenteric artery flow affect the absorption and metabolism of drugs[33,34]. This shows the importance of incorporation of flow in preclinical intestinal models to properly predict absorption and metabolism. The developments in the field or organ on-a-chip have therefore the capacity of better reflecting the *in vivo* intestinal transport[35-37].

Liver

After intestinal absorption, the drug reaches the liver via the portal vein. Similar to the intestine, transporter proteins and CYP450 enzymes play an important role in the uptake, efflux and metabolism of drugs and endogenous compounds. The organic anion transporting peptides (OATPs) belong to the superfamily of the solute carrier class of organic anion transporters and are key uptake transporters expressed on the basolateral membrane of hepatocytes[38]. This is exemplified by guidelines from the FDA for drugs in development, emphasizing the significance of testing whether a drug is a substrate for OATP1B1/1B3 when biliary secretion of hepatic metabolism constitutes ≥25% of the total drug clearance[39]. Moreover, OATP1B1/1B3 play also an important role in the uptake of endogenous compounds and toxins. (Un)conjugated bilirubin, coproporphyrin I (CPI) and III and (un)conjugated bile acids are for instance transported by OATP1B1/1B3 into the hepatocyte. Clinical studies[42,43] showed that direct bilirubin, CPI and also the bile acids like glycochenodeoxycholic acid-sulphate (gCDCA-S) are elevated upon dosing the OATP1B1/1B3 inhibitor rifampicin. Utilization of endogenous biomarkers is particularly valuable in *in vivo* studies to enhance drug safety, serving as an early indicator for potential transporter-mediated drug-drug interactions. Besides the expression of OATPs, other important proteins expressed on the basolateral membrane are the organic cation transporters (OCTs) and the natrium taurocholate transporting peptide (NTCP) which are uptake transporters and MRP3 and MRP4 which are efflux transporters[44,45]. Next to basolateral transporters, CYP450 enzymes are abundantly present in the liver, to a higher extent than in the intestine[26]. This higher abundance in the liver plays a crucial role in the hepatic extraction (E_H), which represents the fraction of a drug that is extracted by the liver (converted to metabolites of excreted

into the bile) during one passage through the liver[46]. The clearance of a drug by the liver is affected by transporter mediated uptake, CYP450 metabolism and hepatic blood flow[46]. The hepatic clearance refers to the amount of drug removed from the blood flow per unit of time and a greater (portal) blood flow will therefore lead to faster absorption into the hepatocytes. Liver diseases as non-alcoholic-fatty liver disease (NAFLD), currently known as metabolic associated fatty liver disease (MAFLD), alcoholic liver disease (ALD) and primary sclerosing cholangitis (PSC) can affect the hepatocellular function and lead to fibrosis which can progress to liver cirrhosis[47]. Subsequently, cirrhosis can affect the hepatic blood flow and lead to an increased resistance in the hepatic vascular bed resulting in a decreased portal hepatic flow[48,49]. Rane et al.[50] reported that the clearance of hepatically cleared drugs with a high extraction ratio are related to blood flow and thus a major decrease in portal flow as in cirrhosis can dramatically affect the first passage across the liver[50,51]. Therefore, it is of major importance and of interest to include (portal)flow into hepatic preclinical models to better predict clinical outcome.

After CYP450 metabolism (phase I metabolism), drugs and endogenous compounds can undergo phase II metabolism (conjugation) which involves glucuronidation or sulfation by uridine diphosphate-glucuronosy-ltransferases (UGTs) or sulfotransferase (SULT) enzymes respectively[52,53]. Thereafter, carrier mediated processes are required to transport phase II conjugated across the canalicular or basolateral membrane or transport the parent compound in unchanged form[53,54]. Drugs and endogenous compounds can also be excreted into the bile which is a carrier-mediated and energy-dependent process. BCRP, MRP2, P-gp, multidrug and toxin extrusion proteins 1 (MATE-1) and bile salt export pump (BSEP) are located on the canalicular membrane of the hepatocyte and are involved in the excretion of drugs, metabolites and endogenous compound as unconjugated and conjugated bile acids[55]. BSEP, and MRP2 to a lesser extent, are considered important transporters involved in the efflux of conjugated bilirubin and bile acids into the bile making them noteworthy endogenous biomarkers[56]. After a meal, the gallbladder contracts and the bile is excreted into the duodenum enhancing digestion of lipids and aid in the absorption of fat-soluble nutrients[57]. In the intestine the biliary excreted drug metabolite can undergo hydrolysis back to parent compound by the microbiome, whereafter the parent compound can be re-absorbed by the intestine ending up in the portal venous blood again. This is known as the enterohepatic circulation (EHC). These dynamic liver processes which include

portal and arterial flow, interplay between drug transporters and phase I, phase II metabolism and biliary excretion is challenging to mimic in preclinical models[12]. In *in vitro* studies, microsomal fractions and hepatocyte cultures are often applied to determine the hepatic clearance of drugs. By measuring the rate of unbound drug elimination followed by scaling the incubation cell content to average liver cell content, an estimate of the hepatic clearance is generated[58,59]. More advanced models which are used are precision cut liver slices, the isolated perfused liver, sandwich cultured hepatocytes or the liver-duct-on a chip which have the ability to study phase I and II metabolism and/or biliary excretion[12,60,61]. Although the isolated perfused liver model closely mimics the *in vivo* conditions by incorporating flow and allowing the measurement of biliary excretion, its primary application in studying drug pharmacokinetics is currently restricted to rodents[62].

Kidney

After gut-wall and hepatic metabolism, known as the first-pass effect, the drug reaches the systemic circulation. Systemic bioavailability after oral absorption is defined as (F) = fraction absorbed (F_a) * fraction escaping gut metabolism, (F_G) * fraction escaping hepatic metabolism (F_H)[63], showing the influence of the intestine (F_a and F_G) and the liver (F_H). After reaching the systemic circulation, the drug reaches various organs including the kidneys. The kidneys are responsible for the elimination of mainly hydrophilic drugs. The renal clearance is the result of glomerular filtration, tubular secretion and reabsorption[64]. The basolateral and apical membrane of the proximal tubule cell contain many different transporters which play a pivotal role in the elimination of drugs and metabolites which function in a secretive or a reabsorptive manner[64]. Organic anion transporter 1 (OAT1) and OAT3, and OCT2 and OCT 3 are important uptake transporters on the basolateral membrane. On the apical membrane, MATE1 and MATE2 and BCRP have a significant role in the elimination. The FDA and the international transporter consortium recommended evaluation of OAT1, OAT3, OCT2 and MATE transporter involvement when the active secretion of the drugs is ≥25% of the systemic clearance[39,65]. This is primarily since their significant role in drug clearance and inhibition of these transporters can result in potential DDI and renal toxicity[65]. Endogenous markers have also been established for several kidney transporters as early indicators in plasma and urine to investigate potential transporter mediated DDI. Taurine, the bile acid gCDCA-S and creatinine are known to be transporter into the renal proximal cells by OAT1, OAT3 and OCT2, respectively. Subsequently, creatinine

and thiamine are known to be excreted by MATE into the urine[66]. In general it is considered that the kidney has less metabolizing capacity compared to liver and intestine given the net weight of the organ and the microsomal content[67]. Preclinical renal clearance is often assessed using primary human cells or immortalized cells to study transporter affinity and transporter involvement in the renal uptake and efflux of compounds[68,69]. Nowadays, renal clearance is assessed in more complex preclinical models like the isolated kidney perfusion model, proximal tubule on a chip, or animal studies[70-74].

Currently, PBPK modeling is broadly applied in drug discovery to estimate the PK profile of a compound based on the preclinical absorption, distribution, metabolism and elimination (ADME) data[75]. Prediction could aid in the determination of the first dose for a clinical trial in the absence of *in vivo* data, assess dose regimen or to study potential population variability[76]. The more accurate the input data into these models, the more reliable the outcome which could facilitate early identification of drug with a high potential for DDI in the drug discovery process[77]. To exemplify, the use of isolated intestine, liver and kidney perfusion in the past have demonstrated to be value models gaining mechanistic insights into the physiology and the role of transporters and enzymes including their interplay in the organs[78]. Using *ex vivo* organ perfusion with rat organs, Pang et al., demonstrated important DMPK concepts as hepatic zonation, hepatic and renal metabolism and blood flow dependent hepatic elimination[79-83]. For the isolated organ perfusion experiments mainly rodent organs are used, however translation of these findings to clinical practice remains challenging due to, among others, species differences in transporter expression[11,84]. Currently, advancements in the development and application of *ex vivo* organ perfusion are occurring in the field of organ transplantation. The use of pressure driven machine perfusion facilitates organ preservation under hypothermic conditions and also provides the opportunity to assess organ viability and functionality under normothermic conditions[85-88]. The use of these novel pressure driven perfusion machines opens new opportunities for the field of pharmacology since it allows to study the function of human or porcine whole organ(s) under conditions that are as close as possible to the *in vivo* situation[89]. The inclusion flow, intact cellular morphology and preservation of excretion pathways make the model attractive to study pharmacological processes such as the hepatic first pass effect, renal clearance, biliary and urinary elimination or DDI. Compared to the isolated perfused-organ systems using rat organs, the human/porcine machine perfusion models have

relatively high circulating perfusion volume and urinary and biliary output which allows easy sample collection to assess drug PK[89]. Furthermore, and of utmost significance, the use of human organs enables direct translation of the findings to the human in vivo condition.

The objective of this thesis

The aim of this thesis was to explore the applicability of pressure driven normothermic organ perfusion to study pharmacological processes in the liver, intestine and kidney.

Outline of this thesis

Preclinical models are a crucial part of the drug development process, however to study complex ADME processes more advanced preclinical models are needed. The first part of this thesis, **chapter 2**, provides an overview of the currently used *ex vivo* models in drug development research. The review describes the novel developments using *ex vivo* tissues to improve the predictions of human ADME profiles and DDIs in health and disease.

In part II of this thesis, the focus is on *ex vivo* liver perfusion to study drug pharmacokinetic processes and endogenous substrate handling. Porcine organs are often used for method validation and device development and it has been shown that normothermic machine perfusion (NMP) of the porcine liver is an excellent platform to study hepatic processes[90,91]. Additionally, the pig liver model is considered a proper translational model because of anatomical, physiological and biochemical similarity to humans and nowadays this model is increasingly used in biomedical research[92,93]. In **chapter 3**, we evaluate the use of normothermic machine perfusion of porcine livers as a novel model to predict pharmacokinetic processes. Using three statins as OATP1B1/1B3 substrate model drugs (rosuvastatin, atorvastatin and pitavastatin) we studied the transporter mediated hepatic extraction and biliary excretion. Furthermore, we examined the effect of rifampicin on the disposition of these three statins. In clinical data, a rank-order relationship has been observed in the DDI with rifampicin and we aimed to study if the *ex vivo* liver perfusion model could mimick the rank-order relationship.

Established *in vitro* and animal models are often used to study the pathology and pharmacological characteristics of drugs of varying diseases. However,

translation of these findings to clinical practice remains challenging due to, among others, species differences in transporter expression and the difficulty to mimic dynamic liver processes[61,84]. In **chapter 4**, we developed a novel hepatic model using diseased explanted human livers. Four model drugs (rosuvastatin, digoxin, furosemide and metformin) with and without perpetrator drugs were used to study hepatic extraction, clearance, biliary excretion and DDI. These model drugs are known substrates for different important hepatic uptake and efflux transporters and enabled comparison of the model to *in vivo* reported data.

In the field of *ex vivo* liver perfusion, limited research is performed regarding characterization of bile acid composition, cholesterol homeostasis and transporter gene expression during *ex vivo* liver perfusion. Moreover, in the *ex vivo* perfused liver model the enterohepatic circulation is absent. Nevertheless, the bile acid recirculation plays a crucial role, particularly in supporting the function of specific drug transporters and homeostasis of cholesterol levels[94-96]. In **chapter 5**, we aimed to characterize the de novo bile acid production, cholesterol levels and transporter gene expression during *ex vivo* liver perfusion in pig and human livers. Additionally, we aimed to decreased the metabolic burden of the *de novo* bile acid synthesis by incorporating a pool of (un)conjugated bile acids during *ex vivo* liver perfusion and study subsequently its effects.

Part III is aimed to unravel drug pharmacokinetics through multi-organ perfusion. While the majority of organ perfusion studies focus on perfusion with a single organ, a few studies have investigated the possibility of a multi-organ perfusion model to study physiological processes[97-100]. The possibly to perfuse multiple organs allows in-depth analysis of ADME processes like gut wall metabolism, portal vein concentrations, hepatic uptake and biliary excretion and thus generating novel pharmacological insights. In **chapter 6**, we aimed to explore the applicability of a porcine *ex vivo* perfusion model to study gut-hepatobiliary metabolism by characterization of oral absorption, gut wall metabolism, pre-systemic hepatic metabolism and biliary excretion using midazolam as a CYP3A4 model compound.

In part IV – **chapter 7**, the results and conclusions of this thesis are summarized, discussed and future perspectives are presented. As the application of *ex vivo* organ perfusion for pharmacokinetic research is quite

novel, major potential lies ahead for future pharmacokinetic questions regarding DDI, studying the first-pass effect and the enterohepatic circulation in the multi-organ model and the use of explanted human diseased livers. Furthermore, the first steps towards translation of *ex vivo* data to *in vivo* PK profiles will be shown and discussed.

References

1. Sun D, Gao W, Hu H, Zhou S. Why 90% of clinical drug development fails and how to improve it? Acta Pharmaceutica Sinica B 2022;12:3049-3062.
2. Brodniewicz T, Grynkiewicz G. Preclinical drug development. Acta Pol Pharm 2010;67: 578-585.
3. Visk D. Will advances in preclinical in vitro models lower the costs of drug development? Applied In Vitro Toxicology 2015;1:79-82.
4. Klopman G, Stefan LR, Saiakhov RD. ADME evaluation: 2. A computer model for the prediction of intestinal absorption in humans. European journal of pharmaceutical sciences 2002;17: 253-263.
5. Selimović Š, Dokmeci MR, Khademhosseini A. Organs-on-a-chip for drug discovery. Current opinion in pharmacology 2013;13:829-833.
6. Genentech. Fenebrutinib multiple sclerosis clinical trial program update. In; 2023.
7. Kusuhara H. How far should we go? Perspective of drug-drug interaction studies in drug development. Drug metabolism and pharmacokinetics 2014;29:227-228.
8. Malone DC, Armstrong EP, Abarca J, Grizzle AJ, Hansten PD, Van Bergen RC, Duncan-Edgar BS, et al. Identification of serious drug–drug interactions: results of the partnership to prevent drug–drug interactions. Journal of the American Pharmacists Association 2004;44: 142-151.
9. Mita MM, LoRusso PM, Papadopoulos KP, Gordon MS, Mita AC, Ferraldeschi R, Keer H, et al. A phase I study of ASTX660, an antagonist of inhibitors of apoptosis proteins, in adults with advanced cancers or lymphoma. Clinical Cancer Research 2020;26:2819-2826.
10. Kimoto E, Bi Y-A, Kosa RE, Tremaine LM, Varma MV. Hepatobiliary clearance prediction: species scaling from monkey, dog, and rat, and in vitro–in vivo extrapolation of sandwich-cultured human hepatocytes using 17 drugs. Journal of pharmaceutical sciences 2017;106:2795-2804.
11. Wang L, Prasad B, Salphati L, Chu X, Gupta A, Hop CE, Evers R, et al. Interspecies variability in expression of hepatobiliary transporters across human, dog, monkey, and rat as determined by quantitative proteomics. Drug Metabolism and Disposition 2015;43: 367-374.
12. Ghibellini G, Leslie EM, Brouwer KL. Methods to evaluate biliary excretion of drugs in humans: an updated review. Molecular pharmaceutics 2006;3:198-211.
13. Keuper-Navis M, Walles M, Poller B, Myszczyszyn A, van der Made TK, Donkers J, Amirabadi HE, et al. The application of organ-on-chip models for the prediction of human pharmacokinetic profiles during drug development. Pharmacological research 2023;195: 106853.
14. Lee J, Park D, Seo Y, Chung JJ, Jung Y, Kim SH. Organ‐level functional 3D tissue constructs with complex compartments and their preclinical applications. Advanced Materials 2020;32: 2002096.
15. Honek J. Preclinical research in drug development. Medical Writing 2017;26:5-8.
16. Franz CC, Egger S, Born C, Rätz Bravo AE, Krähenbühl S. Potential drug-drug interactions and adverse drug reactions in patients with liver cirrhosis. European journal of clinical pharmacology 2012;68:179-188.
17. Ito K, Iwatsubo T, Kanamitsu S, Ueda K, Suzuki H, Sugiyama Y. Prediction of pharmacokinetic alterations caused by drug-drug interactions: metabolic interaction in the liver. Pharmacological reviews 1998;50:387-412.
18. Rodrigues AD. Drug-drug interactions: CRC Press, 2019.
19. Thelen K, Dressman JB. Cytochrome P450-mediated metabolism in the human gut wall. Journal of pharmacy and pharmacology 2009;61:541-558.
20. van de Kerkhof EG, de Graaf IA, Groothuis GM. In vitro methods to study intestinal drug metabolism. Current drug metabolism 2007;8:658-675.
21. Teodori E, Dei S, Martelli C, Scapecchi S, Gualtieri F. The functions and structure of ABC transporters: implications for the design of new inhibitors of Pgp and MRP1 to control multidrug resistance (MDR). Current drug targets 2006;7:893-909.
22. Liu X. ABC family transporters. Drug transporters in drug disposition, effects and toxicity 2019:13-100.

23. Berggren S, Gall C, Wollnitz N, Ekelund M, Karlbom U, Hoogstraate J, Schrenk D, et al. Gene and protein expression of P-glycoprotein, MRP1, MRP2, and CYP3A4 in the small and large human intestine. Molecular pharmaceutics 2007;4:252-257.
24. Paine MF, Shen DD, Kunze KL, Perkins JD, Marsh CL, McVicar JP, Barr DM, et al. First-pass metabolism of midazolam by the human intestine. Clinical Pharmacology & Therapeutics 1996;60:14-24.
25. Thummel KE, O'Shea D, Paine MF, Shen DD, Kunze KL, Perkins JD, Wilkinson GR. Oral first-pass elimination of midazolam involves both gastrointestinal and hepatic CYP3A-mediated metabolism. Clinical Pharmacology & Therapeutics 1996;59:491-502.
26. Galetin A, Houston JB. Intestinal and hepatic metabolic activity of five cytochrome P450 enzymes: impact on prediction of first-pass metabolism. Journal of Pharmacology and Experimental Therapeutics 2006;318:1220-1229.
27. Kato M. Intestinal first-pass metabolism of CYP3A4 substrates. Drug metabolism and pharmacokinetics 2008;23:87-94.
28. Angelis ID, Turco L. Caco-2 cells as a model for intestinal absorption. Current protocols in toxicology 2011;47:20.26. 21-20.26. 15.
29. Vaessen SF, van Lipzig MM, Pieters RH, Krul CA, Wortelboer HM, van de Steeg E. Regional expression levels of drug transporters and metabolizing enzymes along the pig and human intestinal tract and comparison with Caco-2 cells. Drug Metabolism and Disposition 2017;45:353-360.
30. Rozehnal V, Nakai D, Hoepner U, Fischer T, Kamiyama E, Takahashi M, Yasuda S, et al. Human small intestinal and colonic tissue mounted in the Ussing chamber as a tool for characterizing the intestinal absorption of drugs. European Journal of Pharmaceutical Sciences 2012;46: 367-373.
31. Lennernas H, Nylander S, Ungell A-L. Jejunal permeability: a comparison between the ussing chamber technique and the single-pass perfusion in humans. Pharmaceutical research 1997;14:667.
32. CY Chow E, Sandy Pang K. Why we need proper PBPK models to examine intestine and liver oral drug absorption. Current Drug Metabolism 2013;14:57-79.
33. Fine KD, Santa Ana CA, Porter JL, Fordtran JS. Effect of changing intestinal flow rate on a measurement of intestinal permeability. Gastroenterology 1995;108:983-989.
34. Pang KS, Peng HB, Noh K. The Segregated Intestinal Flow Model (SFM) for drug absorption and drug metabolism: Implications on intestinal and liver metabolism and drug–drug interactions. Pharmaceutics 2020;12:312.
35. Yang Y, Chen Y, Wang L, Xu S, Fang G, Guo X, Chen Z, et al. PBPK modeling on organs-on-chips: An overview of recent advancements. Frontiers in Bioengineering and Biotechnology 2022;10:900481.
36. Milani N, Parrott N, Franyuti DO, Godoy P, Galetin A, Gertz M, Fowler S. Application of a gut–liver-on-a-chip device and mechanistic modelling to the quantitative in vitro pharmacokinetic study of mycophenolate mofetil. Lab on a Chip 2022;22:2853-2868.
37. Amirabadi HE, Donkers JM, Wierenga E, Ingenhut B, Pieters L, Stevens L, Donkers T, et al. Intestinal Explant Barrier Chip: Long-term intestinal absorption screening in a novel microphysiological system using tissue explants. Lab on a Chip 2022;22:326-342.
38. van de Steeg E, Wagenaar E, van der Kruijssen CM, Burggraaff JE, de Waart DR, Elferink RPO, Kenworthy KE, et al. Organic anion transporting polypeptide 1a/1b–knockout mice provide insights into hepatic handling of bilirubin, bile acids, and drugs. The Journal of clinical investigation 2010;120.
39. U.S. Department of Health and Human Services FaDA, Center for Drug Evaluation and Research (CDER). In Vitro Drug Interaction Studies — Cytochrome P450 Enzyme- and Transporter-Mediated Drug Interactions Guidance for Industry. In; 2020.
40. Frank M, Doss MO. Relevance of urinary coproporphyrin isomers in hereditary hyperbilirubinemias. Clinical Biochemistry 1989;22:221-222.

41. van de Steeg E, Stránecký V, Hartmannová H, Nosková L, Hřebíček M, Wagenaar E, van Esch A, et al. Complete OATP1B1 and OATP1B3 deficiency causes human Rotor syndrome by interrupting conjugated bilirubin reuptake into the liver. The Journal of clinical investigation 2012;122:519-528.
42. Takehara I, Yoshikado T, Ishigame K, Mori D, Furihata K-i, Watanabe N, Ando O, et al. Comparative study of the dose-dependence of OATP1B inhibition by rifampicin using probe drugs and endogenous substrates in healthy volunteers. Pharmaceutical research 2018;35: 1-13.
43. Mori D, Kashihara Y, Yoshikado T, Kimura M, Hirota T, Matsuki S, Maeda K, et al. Effect of OATP1B1 genotypes on plasma concentrations of endogenous OATP1B1 substrates and drugs, and their association in healthy volunteers. Drug metabolism and pharmacokinetics 2019;34:78-86.
44. Jetter A, Kullak-Ublick GA. Drugs and hepatic transporters: A review. Pharmacological research 2020;154:104234.
45. Faber KN, Müller M, Jansen PL. Drug transport proteins in the liver. Advanced drug delivery reviews 2003;55:107-124.
46. Mehvar R. Application of organ clearance to estimation of the in vivo hepatic extraction ratio. Current Clinical Pharmacology 2016;11:47-52.
47. Zhou W-C, Zhang Q-B, Qiao L. Pathogenesis of liver cirrhosis. World journal of gastroenterology: WJG 2014;20:7312.
48. Grabner G. Einige methodische, pathophysiologische und klinische Probleme des enterohepatalen Kreislaufes. Wien. Z. Inn. Med 1963;44:221-305.
49. Moreno AH, Burchell AR, Rousselot LM, Panke WF, Slafsky SF, Burke JH. Portal blood flow in cirrhosis of the liver. The Journal of clinical investigation 1967;46:436-445.
50. Rane A, Wilkinson G, Shand D. Prediction of hepatic extraction ratio from in vitro measurement of intrinsic clearance. Journal of Pharmacology and Experimental Therapeutics 1977;200: 420-424.
51. Delco F, Tchambaz L, Schlienger R, Drewe J, Krähenbühl S. Dose adjustment in patients with liver disease. Drug safety 2005;28:529-545.
52. Zhou X, Cassidy KC, Hudson L, Mohutsky MA, Sawada GA, Hao J. Enterohepatic circulation of glucuronide metabolites of drugs in dog. Pharmacology Research & Perspectives 2019;7:e00502.
53. Zamek-Gliszczynski MJ, Hoffmaster KA, Nezasa K-i, Tallman MN, Brouwer KL. Integration of hepatic drug transporters and phase II metabolizing enzymes: mechanisms of hepatic excretion of sulfate, glucuronide, and glutathione metabolites. European journal of pharmaceutical sciences 2006;27:447-486.
54. Váradi A, Sarkadi B. Multidrug resistance-associated proteins: Export pumps for conjugates with glutathione, glucuronate or sulfate. Biofactors 2003;17:103-114.
55. Thompson DC, Mitchell MD. The Role of Liver Transporters in Drug-Drug Interactions. Biofiles 2013:1022-1023.
56. Chu X, Chan GH, Evers R. Identification of endogenous biomarkers to predict the propensity of drug candidates to cause hepatic or renal transporter-mediated drug-drug interactions. Journal of pharmaceutical sciences 2017;106:2357-2367.
57. Maldonado-Valderrama J, Wilde P, Macierzanka A, Mackie A. The role of bile salts in digestion. Advances in colloid and interface science 2011;165:36-46.
58. Sodhi JK, Benet LZ. Successful and unsuccessful prediction of human hepatic clearance for lead optimization. Journal of medicinal chemistry 2021;64:3546-3559.
59. Benet LZ, Sodhi JK. Investigating the theoretical basis for in vitro–in vivo extrapolation (ivive) in predicting drug metabolic clearance and proposing future experimental pathways. The AAPS journal 2020;22:120.
60. Du Y, Khandekar G, Llewellyn J, Polacheck W, Chen CS, Wells RG. A bile duct-on-a-chip with organ-level functions. Hepatology 2020;71:1350-1363.
61. Guillouzo A. Liver cell models in in vitro toxicology. Environmental health perspectives 1998;106:511-532.

62. Bessems M, 't Hart N, Tolba R, Doorschodt B, Leuvenink H, Ploeg R, Minor T, et al. The isolated perfused rat liver: standardization of a time-honoured model. Laboratory animals 2006;40:236-246.

63. Varma MV, Obach RS, Rotter C, Miller HR, Chang G, Steyn SJ, El-Kattan A, et al. Physicochemical space for optimum oral bioavailability: contribution of human intestinal absorption and first-pass elimination. Journal of medicinal chemistry 2010;53:1098-1108.

64. Miners JO, Yang X, Knights KM, Zhang L. The role of the kidney in drug elimination: transport, metabolism, and the impact of kidney disease on drug clearance. Clinical Pharmacology & Therapeutics 2017;102:436-449.

65. Giacomini KM, Huang S-M, Tweedie DJ, Benet LZ, Brouwer KLR, Chu X, Dahlin A, et al. Membrane transporters in drug development. Nature Reviews Drug Discovery 2010;9: 215-236.

66. Chu X, Liao M, Shen H, Yoshida K, Zur AA, Arya V, Galetin A, et al. Clinical probes and endogenous biomarkers as substrates for transporter drug-drug interaction evaluation: perspectives from the international transporter consortium. Clinical Pharmacology & Therapeutics 2018;104:836-864.

67. Knights KM, Rowland A, Miners JO. Renal drug metabolism in humans: the potential for drug–endobiotic interactions involving cytochrome P450 (CYP) and UDP-glucuronosyltransferase (UGT). British journal of clinical pharmacology 2013;76: 587-602.

68. Hsueh CH, Hsu V, Zhao P, Zhang L, Giacomini K, Huang SM. PBPK modeling of the effect of reduced kidney function on the pharmacokinetics of drugs excreted renally by organic anion transporters. Clinical Pharmacology & Therapeutics 2018;103:485-492.

69. Chu X, Bleasby K, Evers R. Species differences in drug transporters and implications for translating preclinical findings to humans. Expert opinion on drug metabolism & toxicology 2013;9:237-252.

70. Watanabe T, Maeda K, Kondo T, Nakayama H, Horita S, Kusuhara H, Sugiyama Y. Prediction of the hepatic and renal clearance of transporter substrates in rats using in vitro uptake experiments. Drug metabolism and disposition 2009;37:1471-1479.

71. Sirianni GL, Pang KS. Organ clearance concepts: new perspectives on old principles. Journal of pharmacokinetics and biopharmaceutics 1997;25:449-470.

72. Morrissey KM, Stocker SL, Wittwer MB, Xu L, Giacomini KM. Renal transporters in drug development. Annual review of pharmacology and toxicology 2013;53:503-529.

73. Vriend J, Nieskens TT, Vormann MK, van den Berge BT, van den Heuvel A, Russel FG, Suter-Dick L, et al. Screening of drug-transporter interactions in a 3D microfluidic renal proximal tubule on a chip. The AAPS journal 2018;20:1-13.

74. Jang K-J, Mehr AP, Hamilton GA, McPartlin LA, Chung S, Suh K-Y, Ingber DE. Human kidney proximal tubule-on-a-chip for drug transport and nephrotoxicity assessment. Integrative Biology 2013;5:1119-1129.

75. Zhuang X, Lu C. PBPK modeling and simulation in drug research and development. Acta Pharmaceutica Sinica B 2016;6:430-440.

76. Jones HM, Gardner IB, Watson KJ. Modelling and PBPK simulation in drug discovery. The AAPS journal 2009;11:155-166.

77. Jones HM, Mayawala K, Poulin P. Dose selection based on physiologically based pharmacokinetic (PBPK) approaches. The AAPS journal 2013;15:377-387.

78. Fan J, Chen S, CY Chow E, Sandy Pang K. PBPK modeling of intestinal and liver enzymes and transporters in drug absorption and sequential metabolism. Current drug metabolism 2010;11:743-761.

79. Abu-Zahra TN, Pang KS. Effect of zonal transport and metabolism on hepatic removal: enalapril hydrolysis in zonal, isolated rat hepatocytes in vitro and correlation with perfusion data. Drug metabolism and disposition 2000;28:807-813.

80. de Lannoy I, Nespeca R, Pang K. Renal handling of enalapril and enalaprilat: studies in the isolated red blood cell-perfused rat kidney. Journal of Pharmacology and Experimental Therapeutics 1989;251:1211-1222.

81. Xu X, Hirayama H, Pang KS. First-pass metabolism of salicylamide. Studies in the once-through vascularly perfused rat intestine-liver preparation. Drug metabolism and disposition 1989;17:556-563.

82. Pang KS, Lee W-F, Cherry WF, Yuen V, Accaputo J, Fayz S, Schwab AJ, et al. Effects of perfusate flow rate on measured blood volume, disse space, intracellular water space, and drug extraction in the perfused rat liver preparation: characterization by the multiple indicator dilution technique. Journal of pharmacokinetics and biopharmaceutics 1988;16:595-632.

83. Pang KS, Koster H, Halsema I, Scholtens E, Mulder GJ, Stillwell R. Normal and retrograde perfusion to probe the zonal distribution of sulfation and glucuronidation activities of harmol in the perfused rat liver preparation. Journal of Pharmacology and Experimental Therapeutics 1983;224:647-653.

84. Nevzorova YA, Boyer-Diaz Z, Cubero FJ, Gracia-Sancho J. Animal models for liver disease–A practical approach for translational research. Journal of hepatology 2020;73:423-440.

85. van Leeuwen OB, de Vries Y, Fujiyoshi M, Nijsten MW, Ubbink R, Pelgrim GJ, Werner MJ, et al. Transplantation of high-risk donor livers after ex situ resuscitation and assessment using combined hypo-and normothermic machine perfusion: a prospective clinical trial. Annals of surgery 2019;270:906-914.

86. van Rijn R, Schurink IJ, de Vries Y, van den Berg AP, Cortes Cerisuelo M, Darwish Murad S, Erdmann JI, et al. Hypothermic machine perfusion in liver transplantation—a randomized trial. New England Journal of Medicine 2021;384:1391-1401.

87. Watson CJ, Kosmoliaptsis V, Pley C, Randle L, Fear C, Crick K, Gimson AE, et al. Observations on the ex situ perfusion of livers for transplantation. American journal of transplantation 2018;18:2005-2020.

88. Hosgood S, Barlow A, Hunter J, Nicholson M. Ex vivo normothermic perfusion for quality assessment of marginal donor kidney transplants. Journal of British Surgery 2015;102: 1433-1440.

89. Stevens LJ, Donkers JM, Dubbeld J, Vaes WH, Knibbe CA, Alwayn IP, van de Steeg E. Towards human ex vivo organ perfusion models to elucidate drug pharmacokinetics in health and disease. Drug metabolism reviews 2020;52:438-454.

90. Borie DC, Eyraud D, Boleslawski E, Lemoine A, Sebagh M, Cramer DV, Roussi J, et al. Funtional metabolic charactristics of intact pignlivers during prolonged extracorporeal perfusion: potential for a unique biological liver-assist device1. Transplantation 2001;72:393-405.

91. Eshmuminov D, Becker D, Borrego LB, Hefti M, Schuler MJ, Hagedorn C, Muller X, et al. An integrated perfusion machine preserves injured human livers for 1 week. Nature biotechnology 2020;38:189-198.

92. Helke KL, Swindle MM. Animal models of toxicology testing: the role of pigs. Expert opinion on drug metabolism & toxicology 2013;9:127-139.

93. Elmorsi Y, Al Feteisi H, Al-Majdoub ZM, Barber J, Rostami-Hodjegan A, Achour B. Proteomic characterisation of drug metabolising enzymes and drug transporters in pig liver. Xenobiotica 2020;50:1208-1219.

94. Chiang JY. Bile acid regulation of gene expression: roles of nuclear hormone receptors. Endocrine reviews 2002;23:443-463.

95. Chiang JY. Bile acids: regulation of synthesis: thematic review series: bile acids. Journal of lipid research 2009;50:1955-1966.

96. Chiang JY. Bile acid metabolism and signaling. Comprehensive physiology 2013;3:1191.

97. Chen C, Chen M, Lin X, Guo Y, Ma Y, Chen Z, Ju W, et al. En bloc procurement of porcine abdominal multiple organ block for ex situ normothermic machine perfusion: a technique for avoiding initial cold preservation. Annals of Translational Medicine 2021;9.

98. Chung WY, Gravante G, Al-Leswas D, Arshad A, Sorge R, Watson CC, Pollard C, et al. The development of a multiorgan ex vivo perfused model: results with the porcine liver-kidney circuit over 24 hours. Artificial Organs 2013;37:457-466.

99. He X, Ji F, Zhang Z, Tang Y, Yang L, Huang S, Li W, et al. Combined liver-kidney perfusion enhances protective effects of normothermic perfusion on liver grafts from donation after cardiac death. Liver Transplantation 2018;24:67-79.

100. Li J, Jia J, He N, Jiang L, Yu H, Li H, Peng Y, et al. Combined kidney-liver perfusion enhances the proliferation effects of hypothermic perfusion on liver grafts via upregulation of IL-6/Stat3 signaling. Molecular medicine reports 2019;20:1663-1671.
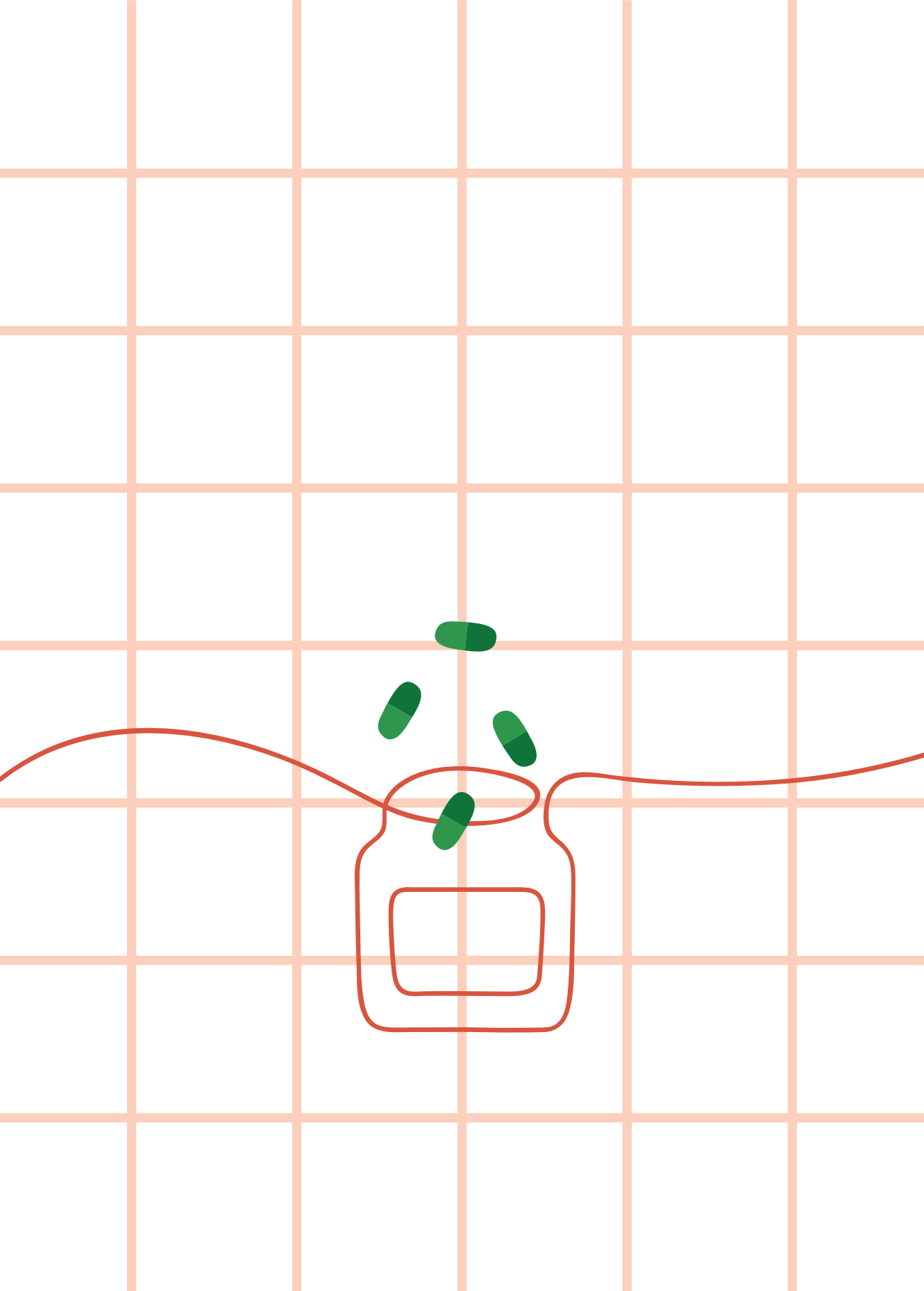
CHAPTER 02

Towards human ex vivo organ perfusion models to elucidate drug pharmacokinetics in health and disease

L.J. Stevens, J.M. Donkers, J. Dubbeld, W.H.J. Vaes, C.A.J. Knibbe, I.P.J. Alwayn*
E. van de Steeg*

*these authors are joint senior authors

Abstract

To predict the absorption, distribution, metabolism and excretion (ADME) profile of candidate drugs a variety of preclinical models can be applied. The ADME and toxicological profile of newly developed drugs need to be available before assessment in humans, which is associated with long time-lines and high costs. Therefore, good predictions of ADME profiles earlier in the drug development process are very valuable. Good prediction of intestinal absorption and renal and biliary excretion remain especially difficult, as there is an interplay of active transport and metabolism involved. To study these processes, including enterohepatic circulation, *ex vivo* tissue models are highly relevant and can be regarded as the bridge between *in vitro* and *in vivo* models. In this review the current *in vitro, in vivo* and in more detail *ex vivo* models for studying pharmacokinetics in health and disease are discussed. Additionally, we propose novel models of which we envision these will generate valuable pharmacokinetic information in the future due to improved translation to the *in vivo* situation. These machine perfused organ models will be particularly interesting when combined with biomarkers for assessing functionality of transporter and CYP450 proteins.

1. Introduction

Upon oral intake of a drug, intestinal absorption is the first barrier affecting the final drug concentration in the circulating blood[1]. Following intestinal absorption, drugs reach the liver via the portal vein, where they can be absorbed, metabolized and/or excreted into the bile. The liver is an important and complex organ, is responsible for the biotransformation of many endogenous and exogenous compounds and involved in the storage and biliary excretion of these compounds and their metabolites. In addition to the liver, extrahepatic tissues significantly contributes to the clearance of drugs as a diverse range of transporters and metabolizing enzymes have been characterized in the GI-tract and the kidneys[1-5]. Influx and efflux transporters, expressed on apical or basolateral membranes of these organs, and cytochrome P450 (CYP450) enzymes regulate the absorption of drugs across the intestinal wall into the portal blood, the clearance of drugs in the liver (and kidneys) and excretion by the biliary and renal pathways[6]. To determine how transporters and enzymes are involved with these processes is challenging as conventional research models are (too) simplified and do not properly reflect the conditions *in vivo*. For example, several studies have characterized the interplay between efflux transporter P-glycoprotein (Pgp) and CYP3A4[7,8]. However, knowledge about the role and contribution of transporters in biliary and renal clearance processes, the involvement of the enterohepatic cycle, and drug-drug interactions (DDI) in healthy and diseased tissues are still poorly understood.

Over the past decade, a variety of *in vitro*, *ex vivo, in vivo* and *in silico* preclinical models have been developed to characterize and predict absorption, distribution, metabolism and excretion (ADME) processes in the human situation. The ability to predict the ADME profile of a candidate drug in the preclinical phase is important to determine whether the drug is safe, effective and can advance to phase I clinical trials. Furthermore, the potential of the drug to interact with the kinetics of other drugs needs to be taken into account as predicting potential DDI is important for the patients health. Concomitant administration of drugs can affect the pharmacokinetic and pharmacodynamic profile of one or both compounds. This can lead to a change in the systemic exposure or site specific concentration of the drug, thereby altering the therapeutic outcome or increasing the risk of serious adverse events[9-11]. Extensive research regarding the potential interactions between drugs is

needed prior to clinical trials, as significant interactions can result in withdrawal of the drug from the market[12]. The impact on the development of new drugs in relation to DDI was shown in a systemic review by the FDA demonstrating that almost all new molecular entities had been found to be perpetrators of metabolic interactions on the basis of *in vitro* tests[12,13]. Therefore, it is important to study the functionality of transporters and enzymes, and their interplay in the liver, kidneys and GI tract as the most dominant organs involved in drug uptake, metabolism and excretion using proper preclinical models[14]. This review describes the current models and novel developments using *ex vivo* tissues to improve the predictions of human ADME profiles and DDIs.

2. *In vitro* and *in vivo* models for the prediction of pharmacokinetics

In vitro DMPK

Multiple preclinical *in vitro* models have been developed to predict the pharmacokinetic profile and metabolic clearance of drugs. These models are mainly based on cell lines (e.g. caco-2, HEK293, MDCKII, HePaRG cells), primary cell cultures (e.g. hepatocytes), and isolated microsomes and vesicles to study organ function, drug metabolism, evaluation of transporter function and drug induced organ toxicity[15]. Genetically modified cell lines overexpressing a specific uptake or efflux transporter allow specific assessment of the interaction between drugs and transporter proteins. A major advantage of *in vitro* models is the possibility to study isolated processes such as phase I and II metabolism or to compare metabolism and transporter affinity across species[16]. The medium- to high throughput nature of *in vitro* models makes them highly attractive in drug development screening processes. However, complex processes such as transporter-enzyme interplay are difficult to evaluate *in vitro* models as transport directionality and transporter-enzyme interactions at the organ level often cannot be established[8]. Additionally, cell based models frequently lack specific aspects of the organ, such as the presence of and interaction between different cell types or the ability to excrete bile or urine[17,18]. An example of an *in vitro* model which overcomes the problem of lacking bile excretion is the sandwich-cultured hepatocyte model. The hepatocytes are cultured between two layers of collagen form canalicular networks so that hepatobiliary disposition of compounds can be studied[19]. A limitation of this model is the use of non-human hepatocytes leading to results that remain

difficult to translate to the human *in vivo* situation due to differences in transporter expression between species[19].

New developments in *in vitro* DMPK

Currently, the development of new predictive preclinical *in vitro* models is a field that attracts a lot of attention. The discovery of organoids, a stem-cell based 3D model derived from patient biopsy material, is generating serious attention especially in the field of disease development modelling[20]. Furthermore, major improvements have been established lately in conventional cell models using a combination of 3D cell models and microfluidic technology, commonly referred to as 'organ-on-a-chip' (OOC). These models incorporate microfluidics and the flow thereby generated induces shear stress and mechanical strain to the cells, with a major effect on cell adhesion, growth rate and differentiation processes[21]. The OOC models can better mimic the complexity of *in vivo* organs and it is expected that they will be more useful than conventional *in vitro* cell lines[14,22,23]. Kim et al., for example reported a gut-on-a-chip model with the incorporation of a cyclic strain mimicking peristaltic motions, important for intestinal absorption processes and the ability to co-culture with intestinal bacteria[24]. An advantage of OOC models is the ability to connect multiple organs cultured on a chip using microfluidics and thereby studying the interconnection between metabolizing organs. Tsamandouras et al., developed a coupled gut-liver-chip model to study PK of multiple organs and the interconnection between the organs using diclofenac and hydrocortisone. A minor but significant difference was the formation of the CYP2C diclofenac metabolite 4-OH-DCF in gut-liver chip compared to the Liver-chip alone[25]. Maschmeyer et al., reported a four-organ-chip including the intestine, liver, kidney and skin which is able to study ADME processes[26]. Although these systems are more complex compared to the conventional *in vitro* models, these systems remain cell based and as such limitations remain.

In vivo animal DMPK models

To study *in vivo* processes in the preclinical phase, a variety of laboratory animal models are used. Laboratoy animals are useful in different stages of drug discovery and development and are systematically used to find bioavailable compounds, compare pharmacokinetics (PK) across species, determine the no-observed-adverse-effect-level (NOAEL), test DDI potential and ensure safety[27]. To study the contribution of specific transporters in absorption or clearance

processes of a drug, knock-in or knock-out mouse models are often used[28]. However, most results obtained in pre-clinical studies using experimental animals do not translate well to the human situation[29]. An important contributor to this loss-in-translation is that PK processes are very different in animals and humans; i.e. the amount of drug that enters the circulation in animals shows little correlation to the relative amount measured in the blood of humans[29]. This is not only a result of different physiology between animals and humans, but also due to differences in transporter expression between species[30]. Humanized mouse models are a step towards human *in vivo* DMPK[31]. Katoh et al., demonstrated the metabolism of CYP2D6 substrate debrisoquin in a humanized liver mouse model and showed the presence of human albumin in the blood of the chimeric mice indicating the presence of human hepatocytes[32]. However the predicting intestinal absorption (or bioavailability) and renal and biliary excretion remain difficult, as there is an interplay of active transport and metabolism involved. Predicting of biliary excretion based on bile cannulation in rats or dogs often fail due to species differences[18,33-35]. The enterohepatic circulation (EHC) adds complexity to predicting biliary excretion. An increasing number of compounds is subjective to EHC, making it difficult to predict plasma profiles after oral or intra venous (iv) administration.

In vivo human DMPK

There are limited methods to study clinical ADME processes in humans early in the drug development phase. One of these methods includes microdosing studies using a microtracer of the newly developed pharmaceutical compound labelled with [^{14}C] radiolabel to characterize the PK of the drug using highly sensitive accelerator mass spectrometry technology[36-39]. There are also some unique examples of studies using human subjects undergoing surgery where it is possible to measure intestinal permeability or biliary clearance. For example, *in vivo* intestinal permeability can be assessed using a Loc-I-Gut perfusion system, placed in the jejunum where during a single-pass perfusion, the permeability of a certain compound can be studied[40]. To date, studying biliary excretion in humans is, up to now only possible in postsurgical patients suffering from hepatobiliary diseases and remains very challenging[41].

3. *Ex vivo* models

By using whole or partial organs and tissues, *ex vivo* models are recognized as the bridge between *in vitro* and *in vivo* models. When studying PK and DDI in health and disease it is important that the complexity of the organ is represented in the preclinical model. It is expected that this will lead to better predictions of DMPK than predictions from more simplified, single cell type *in vitro* systems[42,43]. In *ex vivo* models the tissue morphology is maintained including cell-cell interactions, cell-matrix interactions, the complex efflux/uptake transporters and CYP enzyme expression. In the upcoming section the importance, advantages and limitations of existing *ex vivo* models for applications in preclinical DMPK research will be discussed (Table 2.1) (Figure 2.1).

3.1. Precision cut organ slices

Precision cut organ slices (PCS) are widely used in the field of pharmacology and toxicology research[43-45]. It is an easy and medium throughput technique where drug metabolism in an experimental and controlled situation can be studied with the main advantage that the tissue organization and cell-cell and cell-matrix interaction is maintained[18,46,47]. Multiple studies show the applicability of precision cut slices for metabolic capacity assessment, drug induction, inhibition and drug transport to determine phase I and phase II metabolism and drug uptake by measuring the intracellular concentration in the slices at different time intervals[48-49-51]. The intestines, liver and kidneys are heterogenous organs with regional expression of transporters and enzymes in the intestine, metabolic zonation in the liver and cellular heterogeneity and structural complexity of the kidney. Therefore the PCS technique can be very useful in understanding the heterogeneity of the organ, an advantage over cellular *in vitro* systems[47,52]. Li et al., for example used the precision cut intestinal slices (PCIS) technique to study regional expression of Pgp and the potency of Pgp inhibitors[49]. Recently, Arakawa et al., studied azasetron uptake as substrate drug of efflux transporter mdr1a in rat kidney slices[53]. Additionally, increased accumulation of azasetron was measured in the presences of mdra1 inhibitor zusuquidar showing the ability to use organ slices for DDI studies. However, whether DDI leads to a higher systemic exposure or alters biliary or renal clearance cannot be fully mimicked since the tissue is freely floating in culture medium with direct communication of intraluminal and extraluminal compartments.

Table 2.1 - Overview of the discussed ex vivo models with their advantages and disadvantages.

Model			Reference	Advantages	Disadvantages
Precision cut slices	Intestine (PCIS)		• (van de Kerkhof, de Graaf et al. 2008) • (Possidente et al. 2011)	• High throughput model • Suitable for toxicity assessment • Suitable for human and animal derived tissue	• One-compartmental model; No luminal and serosal compartment • No biliary and renal excretion • Static model
	Liver (PCLS)		• (Renwick et al. 2000) • (De Graaf et al. 2010) • (Berginc et al. 2010)		
	Kidney (PCKS)		• (Arakawa et al. 2017) • (Arakawa et al. 2019)		
Intestinal Two-compartmental models	Ussing Chamber		• (Sjöberg et al. 2013) • (Rozehnal et al. 2012) • (Haslam et al. 2011)	• Intestinal transport from A>B and B<A can be assessed • Assessment of efflux transporters using inhibition studies • Multiple intestinal areas can be applied	• Static model • Limited viability of the model, up to a maximum of 6h of incubation
	InTESTine		• (Westerhout et al. 2014) • (Stevens et al. 2019)		
	Everted gut sac model		• (Alam et al. 2012) • (Barthe et al. 1998)		
Perfusion models	Intestine		• (Lindahl et al. 1998) • (Gandia et al. 2004) • (Burks and Long 1966) • (De Vries MH et al. 1989) • (van Midwoud et al.) • (Dawson et al. 2016)	• Relevant physiological morphology • Able to study biliary and renal excretion	• Difficult laboratory skills involved • Low throughput model • Viable for 3 – 4 hours of incubation
	Liver (IPL) Lobe	Human	• (Melgert et al., 2001) • (Schreiter et al., 2012) • (Schreiter et al., 20160)		
	Whole liver	Animal	• (Villeneue et al., 1996) • (Jablonski et al., 1971) • (Gores et al., 1986)		
	Kidney (IPK)		• (Nishiitsutsuji-Uwo et al. 1967) • (Van Crugten et al. 1991) • (Hori et al. 1993)		

Table 2.1 – (continued)

Model		Reference	Advantages	Disadvantages
Machine perfusion models	Whole Liver	• (Boehnert et al., 2013) • (De Vries et al., 2019) • (Watson et al., 2018) • (Eshmuminov et al. 2020)	• Suitable for (diseased and discarded) human organs to study biliary and renal excretion	• Complex chirurgical skills involved • Low throughput model • Limited to discarded and/or diseased human organs
	Kidney	• (Hosgood S et al. 2015) • (Nicholson and Hosgood 2013)	• Highly translatable to *in vivo* condition • Suitable for human (endogenous) biomarker research	

Organ slices are widely used is still a relevant technique in the field of DMPK. Researchers use PCS to study nanoparticle formulations[54,55], anticancer drugs or molecular transport mechanisms[56,57]. Additionally, the PCS technology and microfluidics can also be combined[58,59]. However, the main limitation of the model is that it is qualitative rather than quantitative as basic pharmacokinetic questions such as prediction of intestinal absorption, biliary and urinary excretion, enterohepatic circulation and the effect of DDI on these processes cannot be studied.

3.2. Intestinal two-compartmental models

As described in section 3.1.1., PCIS are freely floating in culture medium, so that there is no intestinal barrier between the luminal and the serosal compartment. However, to study intestinal absorption it is important to have two separate compartments. Therefore, several dual compartmental *ex vivo* methods have been developed which allow study of intestinal absorption of drugs and nutrients while maintaining barrier integrity.

3.2.1. The ussing system

The Ussing chamber is a model in which excised mucosal intestinal tissue is mounted vertically in the system under continuously oxygenated conditions. Subsequently, vectorial transport and intestinal wall metabolism of drugs can be studied. Several studies have demonstrated the applicability of the Ussing system in determining transporter expression and the transport of different drugs including substrates for efflux transporters[60-62]. For instance, the presence and activity of the efflux transporter Pgp was demonstrated by incubating the Ussing system with the Pgp substrates digoxin, cimetidine, vinblastine, quinidine and verapamil, and a clear efflux effect was demonstrated for the first 4 of the 5 compounds[62]. Hence, the Ussing system is a useful method to predict whether newly developed drugs can affect the intestinal absorption of another compound when dosed at the same time, or if they are a substrate for efflux transporters located in the gut. Unfortunately, the model is limited by its low throughput and the difficult laboratory preparation work involved.

3.2.2. InTESTine system

Based on the Ussing system, Westerhout et al., developed a new intestinal two-compartmental model with easier handling and higher throughput called the

InTESTine system[63]. In this system, segments of the mucosal intestinal layer can be mounted horizontally in a 6-well or a 24-well plate device. Smaller tissue segments and reduced apical and basolateral volumes can be used when compared to the Ussing system[63-65]. Using this model, CYP3A-mediated testosterone metabolism as well as the intestinal permeability of a subset of compounds was determined. Additionally, it demonstrated the suitability of the two-compartmental model to study DDI with PhIP as a BCRP substrate and elacridar as inhibitor[63]. Recently, the same group demonstrated the applicability of the InTESTine system with human intestinal tissue to predict the fraction absorbed (F_a) in humans[64]. Besides determining the transport of a subset of compounds across the intestinal wall, regional differences in transporter activity were assessed following the regional variability in Pgp expression in ileum and mid-colon tissue. This shows the additional value of a two-compartmental intestinal model where drugs can be applied at both sides to study the interaction of the compounds at the transporter levels as well as differential expression transporters along the GI tract[64].

3.3.3. Everted Sac method

In contrast to the Ussing and InTESTine model, the everted sac method uses whole enclosed small parts of the intestines[66-68]. In this model, the excised intestines are inverted, closed at both ends and placed in an oxygenated buffer. Drug metabolism, transport and the contribution of transporters in drug absorption can subsequently be studied[69]. Several studies showed the use of the everted sac method to determine the Pgp activity and to test compounds which are potential Pgp modifiers[70]. For example, Barte et al., assessed the activity of the Pgp transporter by showing an increase in digoxin transport upon co-incubation with Pgp inhibitors verapamil and quinidine[71]. Limitations from this model are that it is restricted to the use of animal tissue, relative large surface area and the presence of the muscularis mucosa layer which can result in an underestimation of drug transport[70]. While the model is very suitable for different animal species, the model is rather low throughput with difficult set-up and preparation work involved and therefore not widely applied.

3.4. Perfusion models

The *ex vivo* tissue models discussed thus far study the fat of a drug in a static environment. However, *in vivo* blood flow continuously stimulates cells with chemical, electrical and mechanical cues which can alter the behavior of a drug[72]. *Ex vivo* perfusion models make use of hemodynamics and therefore

these models are suitable to determine specific functions of the whole organ in an isolated environment in the absence of other systemic effects[69]. In the next section we focus on whole organ (liver and kidney) that have been developed to study biliary and renal excretion, the two most important excretion routes of drugs and tissue (intestine) perfusion models.

3.4.1. Intestinal perfusion models

Multiple intestinal perfusion methods have been developed. For a long time, the incorporation of fluidics into conventional preclinical models using tissue explants has been reported by several research groups[73-75]. For example, the everted sac model has been developed into a perfusion model by Gandia et al.[75]. An advantage of using perfusion in contrast to the static everted gut sac model is that the serosal side is continuously perfused which can affect the kinetics of rapidly absorbed drugs during long term incubations. Additionally, the blood supply, intestinal tissue, innervation and clearance capabilities remain intact[71,76]. The isolated perfused intestine is often used to asses the effect of flow on intestinal permeability and to determine the involvement of transporters and enzymes on drug absorption[77,78]. Many researchers used the isolated perfused intestine technique to study CYP3A4-Pgp interplay or the specific contribution of drug transporters by using knockout animals[76]. A minor limitation of the perfusion technique involves the difficulty to properly measure the disappearance of a compound from the perfusion solution, especially for low permeable compounds[76]. Moreover, although the isolated perfused intestine is very useful for mechanistic evaluation, the limited viability of the tissue restricts the assessment of processes aside from drug transport or the assessment of transporter function[79], such as host-microbe interactions and immune responses which play a significant role in gut health and barrier function but also the absorption and metabolism of drugs[80]. Extending the viability of the tissue would enable to study long-term exposure to drugs, intestinal absorption of low permeable drugs and the potential effects of drugs on the inflammatory state of the tissue. Here lies potential for OOC models that use fluidics to create a more physiologic relevant environment for the tissues. Although many studies show gut-on-a-chip perfusion models using single cell lines (e.g. Caco-2, HT-29 cells) or using intestinal organoids, limited gut-on-a-chip models are known using the perfusion of tissue segments. Dawson et al., showed the perfusion of Inflammatory Bowel Disease (IBD) tissue segments into an in-house developed dual-perfusion 'gut-on-a-chip-model' up to 72 hours of incubation[81]. Proper viability was demonstrated by the presence of the crypts

and goblet cells and also the Ki67 staining showed the proliferative capacity of the tissue after incubation. However barrier function and drug absorption was not studied. Together, these studies demonstrate the beneficial effect of fluidics on tissue viability enabling to study prolonged exposure of compounds on intestinal tissue.

3.4.2. Liver perfusion models

Liver perfusion models have attracted far greater attention than intestinal perfusion models. Using PCLS, various perfusion techniques have been developed; e.g. intra-tissue microneedle flow models, perfusion of the top and bottom of liver slices and flow through models[82-84]. The isolated perfused liver (IPL) model, a preclinical tool used to study the function of the whole liver and hepatobiliary disposition of drugs, utilizes perfusion of both the portal vein and the hepatic artery. Furthermore, IPL can be used to evaluate the physiology and pathophysiology of the liver and to study treatment of acute liver failure[85]. A unique aspect of the model is the close representation to the *in vivo* morphology since the 3D architecture of the tissue is maintained. The control over physiological conditions, and determining specific functions of the whole organ in an isolated environment in the absence of other systemic effects are major advantages over *in vitro* and *in vivo* studies. For example, assessment of the effect of albumin concentration on clearance processes are widely studied using the IPL model. Tsao et al studied warfarin uptake in the IPL in absence and presence of bovine serum albumin (BSA) to clarify the albumin-mediated uptake of warfarin[86,87]. Schary and Rowland found that unbound fraction tolbutamide varied in the perfusate upon varying concentrations of albumin or when using albumin from different species[88]. Shand et al., clearly showed a decrease in hepatic extraction of phenytoin upon increasing the albumin concentration form 0.5 g/dl to 5.0 g/dl[89]. Another physiological condition that can be controlled during perfusion is the applied flow rate. This is especially interesting since the overall hypothesis is that the clearance of drugs is related to the organ perfusion flow and the extraction ratio. Lidocaine, a high hepatic extraction ratio drug is often used as model drug in these studies showing flow dependent extraction, in comparison with the low extraction ratio drug antipyrine which is not affected by hepatic flow[90]. Additionally, the same researchers show in another study that the metabolite of lidocaine, MEGX, appears flow dependent. Showing that the parent drug and metabolites are in equilibrium with the concentration of the drug in the liver demonstrating that the well-stirred model describes the hepatic drug clearance[90]. To study the

physiology of the liver and to understand the metabolic zonation of the liver, experiments have been performed using antegrade and retrograde perfusion directions[91,92]. Livers from different species can be assessed where pig and rat liver are most studied. Furthermore, an advantage of the IPL compared to the *in vivo* situation is the ability to study biliary secretion which is also an important improvement to the sandwich cultured hepatocyte model[18]. As the interaction between two drugs may affect the biliary clearance of a drug, the IPL is an excellent model to study the effect on hepatobiliary clearance and the involvement of uptake and efflux transporters. Pfeifer et al used the IPL to demonstrate the biliary clearance of the rosuvastatin, studying the involvement of basolateral efflux transporters MRP2 and BCRP[93]. Using perfused livers from MRP2 deficient mice in the absence and presence of the BCRP inhibitor elacridar the researchers showed a strong reduction in rosuvastatin excretion of MRP2 deficient mice in the presence of elacridar[93]. Booth et al studied the concentration of Pgp substrate doxorubicin in the presence and absence of Pgp inhibitor quinidine. The biliary clearance was significantly reduced upon inhibition while perfusate and liver concentrations were not altered. The researchers also showed increased intracellular concentration of the metabolite doxorubicin thus showing the added value of using the IPL model since the perfusate, liver and biliary secretion can be studied at the same time[94]. The effect of enzyme-transporter interplay using the IPL was demonstrated by Lau et al., who studied the disposition of digoxin and the effect on the systemic concentration when dosed with organic anion transporting protein 1B1/1B3 (OATP1B1/OATP1B3) inhibitor rifampicin and Pgp inhibitor quinidine[8]. Although the IPL is a standardized and validated model, it is mainly applicable to rodents when studying drug pharmacokinetics. Furthermore, it is labor intensive, has a low throughput and the functional integrity is limited up to a few hours[95]. The model is still used to study liver diseases as the model includes immune cells which are involved in many liver diseases. However, it remains difficult to recapitulate the metabolic and excretion function of the liver in a chip model, therefore the IPL is still the best model[23].

3.4.3. Isolated perfused Kidney (IPK)

Most drugs, and in particular water soluble ones, are eliminated by the kidneys and excreted by the urine[96]. Renal secretion involves several processes such as glomerular filtration, tubular secretion and reabsorption[97]. The current main preclinical kidney models (based on primary cells or cell lines) primarily focus

on the function of proximal tubuli cells. Therefore, *ex vivo* models where all main renal processes can be studied, including urinary excretion, are very valuable. Although isolated perfused kidney (IPK) is an interesting method to predict renal metabolism as well as renal clearance, only a handful of studies used the IPK model to study renal metabolism and excretion. Using IPK, Nishiitsutsji-Uwo et al., demonstrated the clearance of creatinine in the perfused rat kidney showing the function of the multidrug and toxin extrusion protein transporter 1/2K (MATE 1/2K) and the organic anion transporter (OCT)[98]. Although perfusion and the urinary flow remained constant, a decrease in clearance function in time was observed. Crugten et al., used the IPK technique to elucidate the renal mechanism involved in morphine clearance[99]. They showed the additive value of a complex whole organ model since glomerular filtration, active tubular secretion and possibly active reabsorption were processes involved in the metabolism and excretion of morphine. Besides elucidation of clearance mechanisms, also DDI can be predicted using the IPK technique. For instance, the renal tubular secretion of the Pgp substrate digoxin was shown in a study by Hori et al., where the researchers showed the dose-dependent inhibition of urinary secretion of digoxin upon co-incubation with Pgp inhibitor quinidine[100].

4. Novel *ex vivo* perfusion models

Although substantial relevant information regarding PK using the isolated perfused organ method has been obtained, a major limitation of the model is the short viability of 3 to 4 hours, animal origin and the decline in integrity of the perfused organs[18,101]. At present, there is much development in the field of organ transplantation regarding organ preservation techniques using machine perfusion. Clearly, organ preservation is of main importance, but there is also increasing interest in the viability and functional assessment of discarded donor organs which, after machine perfusion, might be used for transplantation when found to be of sufficient quality[102,103]. The use of pressure driven perfusion pumps allows study of the function of a whole organ under conditions that are as close as possible to the *in vivo* situation. Many studies showed viability and functionality of porcine and human livers during machine perfusion under normothermic conditions (37°C) using a red blood cell based perfusate[103-106] even up to 7 days[107] Similar to normothermic machine perfusion (NMP) of the liver, NMP of the kidney is a method for quality assessment of extended criteria

donor kidneys[108]. Porcine organs are often used for method validation and device development and it is shown that normothermic machine perfusion (NMP) of organs is an excellent platform to study hepatic and renal processes[109-113].

4.1 Normothermic machine perfusion for DMPK research

Ex vivo machine perfused whole organs might be an interesting new platform to study pharmacokinetics and DDI in the liver and kidney. The commercially available pressure driven perfusion machines for kidney and liver have the ability to manually apply and adjust pressure to the artery and portal vein[114,115]. Adjusting the pressure will result in an altered flow through the organ and this opens the possibility to study for instance flow dependent clearance of compounds. Additionally, researchers are able to take samples from multiple locations in the circulation (e.g. portal vein and vena cava inferior) in order to study the hepatic first pass effect, or to study IV versus portal dosing and the effect of DDI. Compared to isolated perfused organ systems using rat organs or cannulated animal studies, the human or porcine machine perfusion models have relatively high circulating perfused volume (approximately 2L) and bile and urine output (approximately >10mL). This has several advantages. Collection of perfusate and urine and bile samples over time and to tissue biopsies to study intracellular accumulation is easy which makes these models ideal to study drug pharmacokinetics, metabolism, excretion and potential DDIs in a controlled setting. The applicability of machine perfusion for whole intestines is not (yet) developed, probably because intestinal transplantations are not widely performed.

4.2 Opportunities involved in the perfusion of whole organs for DMPK

The major advantage of using whole organ perfusion models which are perfused with a red blood cell based perfusate is the unique opportunity to study renal and biliary excretion pathways, allowing to study more complex pharmacokinetic processes which leads to a better understanding of *in vivo* processes. Currently, research is focusing on finding novel endogenous biomarkers in bile, urine and blood which reflect the function and the status of organ-specific drug metabolizing enzymes and drug transporters[116,117].

An example of such an endogenous biomarker is bilirubin, a degradation product of heme, which is transported by the hepatic Organic Anion

Transporting Protein 1B1 (OATP1B1) and OATP1B3 into the liver. In the liver, bilirubin is conjugated to bilirubin glucuronide by UGT1A1 and subsequently excreted by MRP2 in the bile or by MRP3 in the blood. This means that potential interaction of drugs with OATP1B1 and/or -1B3 transporter can be assessed by measuring the unconjugated bilirubin concentration in the blood. As OATP1B1 and OATP1B3 are involved in the clearance of a variety of drugs by the liver, applying an endogenous biomarker reflecting the function of these transporters is of major value[118]. The conjugated bilirubin concentration in the bile is reflecting the involvement of MRP2 while conjugated bilirubin in the blood is a biomarker for MRP3. In contrast to the IPL where often radiolabel [^{3}H] bilirubin is used to measure bilirubin in a limited volume, a recent study by Eshmuminov et al., showed the bilirubin levels in the plasma and bile of perfused livers without using [^{3}H] bilirubin[107]. Thereby showing proper OATP1B1/1B3 function during perfusion of the livers. Additionally, coproporphyrin I (CPI) and III (CPIII) (byproduct of the heme synthesis), dehydroepiandrosterone sulfate, conjugated and unconjugated bile acids and fatty acid dicarboxylates can function also as biomarker of OATP1B1 and -1B3 function[116,118,119]. The application of endogenous biomarkers as a useful tool to study transporter involvement in clinical trials was demonstrated by Jones et al.,[120]. The researchers measured the endogenous biomarker CPI and CPIII in a clinical study to elucidate the involvement of OATP1 transporters for DDI of fenebrutinib with midazolam, simvastatin and rosuvastatin[120]. As CPI and CPIII concentrations remained unchanged upon fenebrutinib administration the researchers concluded the observed DDI was due to involvement of CYP3A and BCRP rather than the OATP1B transporters. Likewise, different endogenous biomarkers for transporter functionality have been established for the kidney: hippurate and taurine (for transporter OAT1), 6B-hydroxycortisol (OAT3), thiamine (OCT/MATE1/2K), tryptophan (OCT2) and creatinine (MATE1/2K and OCT2). Besides endogenous biomarkers for transporter function it is found that 4B-hydroxycholesterol (4βHC) is an endogenous metabolite formed by the major hepatic metabolizing enzyme CYP3A4, thus functioning as a marker for CYP3A4 functioning[118]. In a clinical study by Kasichayanula et al., it was shown that upon administration of ketoconazole, an inhibitor of CYP3A4, 4βHC decreased. Subsequently upon administration of rifampicin, increased 4βHC was measured[121]. Endogenous biomarkers can play a significant role in organ perfusion as the biomarkers reflect the condition of the organ during perfusion. The ability to administer victim and perpetrator drugs in a controlled setting and the easy accession to plasma, bile and urine lead to valuable

pharmacokinetic and DDI knowledge. On the other hand, organ perfusion models can contribute to the validation of endogenous biomarkers e.g. the inhibition of specific transporters and studying the effect of a compound on the biomarker profile. Additionally, perfusion models can play a major role by the identification of new endogenous biomarkers.

Moreover, the novel perfusion machines with incorporated pressure, temperature and flow sensors can also be a major advantage for the field of advanced physiologically based pharmacokinetic modelling (PBPK) modeling. PBPK models are mathematical multicompartmental models were assumptions based generated in *in vitro* and also *ex vivo* models regarding transporter abundance, metabolizing enzymes and biliary and urinary excretion are made to predict the clearance of a drug[122,123]. Using these assumptions, simulated profiles are generated and subsequently validated with *in vivo* animal studies to see whether PBPK models match the *in vivo* data. The incorporation of experimental data derived from perfused organs into advanced PBPK models can be highly interesting. Clearance, excretion processes, intracellular concentrations, CYP enzymes and transporter expression can all be determined. At the same time, flow settings can be controlled. Of special interest for PBPK modelling are diseased organs since it is known that in liver disease for instance, different processes as the hepatic blood flow, CYP enzymes and transporter expression are altered as well as changes in liver and renal function[122].

5. Application of *ex vivo* models in disease

Accurate predictions in diseased patients remain difficult as proper preclinical models for human diseases are often lacking. It would be a major advantage if diseased human tissues could be used earlier in the drug development process to assess disease-specific drug efficacy and safety. The challenge of using human tissue is the donor-to-donor variability and differences in disease status. However, this can be seen as an advantage since the use of *ex vivo* models is a step closer to the *in vivo* situation and thus a better prediction of *in vivo* DMPK processes. To measure the disease status or quality of the organs, endogenous biomarkers can play a role. This is currently widely applied in the field of organ transplantation using biomarkers in the bile, urine and blood as quality assessment of perfused organs[103,106].

Ex vivo models in intestinal disease

Inflammatory bowel disease (IBD), which includes ulcerative colitis and Crohn's disease, is a group of intestinal diseases showing increased prevalence numbers[124]. It is reported that the expression of certain transporters is altered in the inflamed intestinal regions of patients suffering from IBD[125,126]. For example, it was shown that in mice with intestinal inflammation, Pgp transporter expression and activity was reduced[127]. Interestingly, in the non-inflamed regions an increased activity of Pgp was detected, showing a possible compensatory mechanism in the intestines. Using inflammatory and non-inflammatory regions from IBD patients, the application of PCIS or tissue segments mounted in a two-compartmental setting can be helpful to determine the F_a of compounds, the effect of drug substrates for certain (efflux) transporters, DDI and the potential altered effect on first-pass metabolism. On the other hand, when specific drugs in the treatment for IBD need to be tested, an intestinal perfusion model using dual fluidics would be crucial to assess the effect of immune modulating drugs on the inflamed intestinal tissue as a longer incubation period is needed and thus extended viability of the tissue needs to be guaranteed.

Ex vivo models in liver disease

Altered hepatobiliary transporter expression as well as affected CYP expression are found in patients suffering from liver diseases such as cirrhosis, nonalcoholic steatohepatitis and primary sclerosing cholangitis[128-130]. This may drastically affect drug treatment and drug efficacy in these patients. The use of PCLS of diseased human liver tissue generated useful information regarding the altered metabolic capacity of the diseased liver[131]. Additionally, using human fibrotic tissue in PCLS has proven to be beneficial when studying potential antifibrotic drugs, DDI and drug induced liver injury (DILI) in fibrotic liver tissue[131]. Despite the fact that perfusion models can be very informative and unravel underlying mechanisms in liver disease, the perfusion of the isolated liver is only limitedly used for studying liver diseases using rodent livers as liver diseases need to be induced. Promising models include diet-induced (genetically modified) murine models of non-alcoholic steatohepatitis, reflecting the key inflammatory and cirrhotic processes involved[132,133].

Machine perfusion of redundant whole human organs would be the holy grail, but obviously the use of this technology for pharmacokinetic application is hampered by the availability of healthy human donor organs. There are

however opportunities when applying this technology (or machine perfusion) to 'diseased' organs which, following a pathological assessment are currently discarded after transplantation. Studying the pathophysiology of diseased livers using human orthotopic tissue is particularly helpful as animal models and human disease remains difficult to compare, however limited studies evaluated PK processes of these redundant human organs. Villeneuve et al., described the use of perfused whole human cirrhotic livers to study drug disposition and metabolism in diseased livers as one of the first[134,135]. Their research showed that the application of diseased liver in a perfusion setting is very useful in studying the clearance function of the liver in healthy and diseased state[134]. As very little is known regarding the uptake of drugs in humans and especially in cirrhotic patients, studying site-specific delivery of drugs in an isolated environment of the other organs is of additional value[136]. Melgert et al., and Schreiter et al., studied the functionality of a liver lobe and resected tissue of cirrhotic and non-cirrhotic livers while being perfused under normothermic conditions. Melgert et al., showed phase I and phase II metabolism of lidocaine and 7-hydroxycoumarin in the liver lobe perfusion model[136], while Schreiter et al., compared the metabolic activity of resected tissue of cirrhotic livers to non-cirrhotic livers[137]. The metabolism of paracetamol, midazolam and diclofenac, metabolized by CYP1A1, CYP3A4 or CYP2C9 respectively, was studied and showed that cirrhotic resected tissue had diminished and slower phase I and phase II transformation of those drugs compared to non-cirrhotic tissue[137]. The same researchers demonstrated acetaminophen-induced liver injury of resected liver tissue as they were able to keep the tissue viable up to 30 hours by making use of NMP. Thereby they show the potential of using diseased perfused livers for the pharmacokinetic application and prolongation of the viability of resected tissue[138].

Ex vivo models in kidney disease

A kidney disease affecting kidney function is polycystic kidney disease (PKD). Patients develop fluid-filled cysts in their kidneys which can affect the PK of drugs. Besides altered kidney function, PKD can also affect other organs like the liver and thereby altering liver transporter expression and function[139]. A case report from 1988 described the association of liver cysts with polycystic kidney disease (PKD) and the relation to MRP2 function[140]. Although the use of human tissue is preferred in the prediction of drug metabolism, the use of animal models can be useful in understanding the development of disease processes or the effect of diseases on the function of other metabolic organs. Benzeçon

et al., used the IPL model using PKD induced rats to determine the effect of PKD on hepatic transporter function and biliary excretion which in this case showed to be a very suitable model for this disease[139]. On the other hand, in patients with liver disease compensatory mechanisms in extrahepatic tissues were observed as a result of the reduced hepatic elimination of drugs. For example, it was studied in humans *in vivo* as well as in rat models that with end-stage liver disease the transporters OATP1 and OATP2 were upregulated in the kidney[141]. This renal compensation mechanism was also found for the clearance of N-methylnicotinamide, which was related to the severity of liver cirrhosis[142]. As a consequence, increased renal exposure can result in a higher risk for renal DDI and drug induced injury showing the difficulty *in vivo* to study DMPK in diseased tissues. Another effect of kidney disease is that it might affect the plasma protein concentration and the ability of plasma proteins to bind to drugs, resulting in a higher unbound fraction of the circulating drug[143]. Kidney machine perfusion models not only create the possibility to assess the functionality of the organ and study the involvement of transporters, also different perfusate compositions can be tested and subsequently the effect on plasma protein binding can be assessed in an experimental environment.

6. Conclusion

This review provides an overview of available experimental predictive models to study drug absorption, metabolism and excretion processes, as well as DDI, in health and disease. The use of *ex vivo* models to predict pharmacokinetics has shown to be very useful and valuable considering the intact morphology and presence of the metabolizing enzymes and transporters in the tissue. A diverse range of *ex vivo* models are nowadays available, each with their own advantages and limitations. Maintenance of the viability and integrity of the tissue is a major challenge observed for every model and tissue type. With increasing complexity also more complicated problems and challenges arise as more factors and unknown processes are involved. However, these complex models are expected to provide better translatability to the *in vivo* situation. The multifactorial and complex development of disease is often not fully characterized and therefore make it a huge challenge to properly predict pharmacokinetic processes in diseased patients. This indicates that improved preclinical models remain needed to generate reliable translational results for both healthy and diseased patients.

References

1. Shitara Y, Sato H, Sugiyama Y. Evaluation of drug-drug interaction in the hepatobiliary and renal transport of drugs. Annu Rev Pharmacol Toxicol. 2005;45:689-723.
2. Müller F, Fromm MF. Transporter-mediated drug–drug interactions. Pharmacogenomics 2011;12:1017-1037.
3. van de Steeg E, Stránecký V, Hartmannová H, Nosková L, Hřebíček M, Wagenaar E, van Esch A, et al. Complete OATP1B1 and OATP1B3 deficiency causes human Rotor syndrome by interrupting conjugated bilirubin reuptake into the liver. The Journal of clinical investigation 2012;122:519-528.
4. Chan LM, Lowes S, Hirst BH. The ABCs of drug transport in intestine and liver: efflux proteins limiting drug absorption and bioavailability. European journal of pharmaceutical sciences 2004;21:25-51.
5. Krishna DR, Klotz U. Extrahepatic metabolism of drugs in humans. Clinical pharmacokinetics 1994;26:144-160.
6. Kusuhara H, Sugiyama Y. Role of transporters in the tissue-selective distribution and elimination of drugs: transporters in the liver, small intestine, brain and kidney. Journal of Controlled Release 2002;78:43-54.
7. Benet L, Cummins C, Wu C. Unmasking the dynamic interplay between efflux transporters and metabolic enzymes. International journal of pharmaceutics 2004;277:3-9.
8. Lau YY, Wu C-Y, Okochi H, Benet LZ. Ex situ inhibition of hepatic uptake and efflux significantly changes metabolism: hepatic enzyme-transporter interplay. Journal of Pharmacology and Experimental Therapeutics 2004;308:1040-1045.
9. Rowland M, Benet LZ, Graham GG. Clearance concepts in pharmacokinetics. Journal of pharmacokinetics and biopharmaceutics 1973;1:123-136.
10. Singh SS. Preclinical pharmacokinetics: an approach towards safer and efficacious drugs. Current drug metabolism 2006;7:165-182.
11. Fagerholm U. Prediction of human pharmacokinetics—biliary and intestinal clearance and enterohepatic circulation. Journal of Pharmacy and Pharmacology 2008;60:535-542.
12. Palatini P, De Martin S. Pharmacokinetic drug interactions in liver disease: An update. World journal of gastroenterology 2016;22:1260.
13. Yu J, Ritchie TK, Mulgaonkar A, Ragueneau-Majlessi I. Drug disposition and drug-drug interaction data in 2013 FDA new drug applications: a systematic review. Drug Metabolism and Disposition 2014;42:1991-2001.
14. Zhu J. Application of Organ-on-Chip in Drug Discovery. Journal of Biosciences and Medicines 2020;8:119-134.
15. Li AP. Human hepatocytes: isolation, cryopreservation and applications in drug development. Chemico-biological interactions 2007;168:16-29.
16. Lipscomb JC, Poet TS. In vitro measurements of metabolism for application in pharmacokinetic modeling. Pharmacology & therapeutics 2008;118:82-103.
17. Fabre G, Combalbert J, Berger Y, Cano J-P. Human hepatocytes as a keyin vitro model to improve preclinical drug development. European journal of drug metabolism and pharmacokinetics 1990;15:165-171.
18. Guillouzo A. Liver cell models in in vitro toxicology. Environmental health perspectives 1998;106:511-532.
19. Swift* B, Pfeifer* ND, Brouwer KL. Sandwich-cultured hepatocytes: an in vitro model to evaluate hepatobiliary transporter-based drug interactions and hepatotoxicity. Drug metabolism reviews 2010;42:446-471.
20. Sato T, Clevers H. Growing self-organizing mini-guts from a single intestinal stem cell: mechanism and applications. Science 2013;340:1190-1194.
21. Yum K, Hong SG, Healy KE, Lee LP. Physiologically relevant organs on chips. Biotechnology journal 2014;9:16-27.

22. Bhise NS, Ribas J, Manoharan V, Zhang YS, Polini A, Massa S, Dokmeci MR, et al. Organ-on-a-chip platforms for studying drug delivery systems. Journal of Controlled Release 2014;190: 82-93.
23. Fowler S, Chen K, Duignan D, Gupta A, Hariparsad N, Kenny JR, Lai G, et al. Microphysiological Systems for ADME-Related Applications: Current Status and Recommendations for System Development and Characterization. Lab on a Chip. 2020;20(3):446-467..
24. Kim HJ, Huh D, Hamilton G, Ingber DE. Human gut-on-a-chip inhabited by microbial flora that experiences intestinal peristalsis-like motions and flow. Lab on a Chip 2012;12:2165-2174.
25. Tsamandouras N, Chen WLK, Edington CD, Stokes CL, Griffith LG, Cirit M. Integrated gut and liver microphysiological systems for quantitative in vitro pharmacokinetic studies. The AAPS journal 2017;19:1499-1512.
26. Maschmeyer I, Lorenz AK, Schimek K, Hasenberg T, Ramme AP, Hübner J, Lindner M, et al. A four-organ-chip for interconnected long-term co-culture of human intestine, liver, skin and kidney equivalents. Lab on a Chip 2015;15:2688-2699.
27. Zhang D, Luo G, Ding X, Lu C. Preclinical experimental models of drug metabolism and disposition in drug discovery and development. Acta Pharmaceutica Sinica B 2012;2:549-561.
28. van de Steeg E, Wagenaar E, van der Kruijssen CM, Burggraaff JE, de Waart DR, Elferink RPO, Kenworthy KE, et al. Organic anion transporting polypeptide 1a/1b–knockout mice provide insights into hepatic handling of bilirubin, bile acids, and drugs. The Journal of clinical investigation 2010;120.
29. Shanks N, Greek R, Greek J. Are animal models predictive for humans? Philosophy, ethics, and humanities in medicine 2009;4:2.
30. Wendler A, Wehling M. The translatability of animal models for clinical development: biomarkers and disease models. Current opinion in pharmacology 2010;10:601-606.
31. Ito R, Takahashi T, Katano I, Ito M. Current advances in humanized mouse models. Cellular & molecular immunology 2012;9:208-214.
32. Katoh M, Sawada T, Soeno Y, Nakajima M, Tateno C, Yoshizato K, Yokoi T. In vivo drug metabolism model for human cytochrome P450 enzyme using chimeric mice with humanized liver. Journal of pharmaceutical sciences 2007;96:428-437.
33. Ito K, Iwatsubo T, Kanamitsu S, Ueda K, Suzuki H, Sugiyama Y. Prediction of pharmacokinetic alterations caused by drug-drug interactions: metabolic interaction in the liver. Pharmacological reviews 1998;50:387-412.
34. Musther H, Olivares-Morales A, Hatley OJ, Liu B, Hodjegan AR. Animal versus human oral drug bioavailability: do they correlate? European Journal of Pharmaceutical Sciences 2014;57: 280-291.
35. Lentz KA. Current methods for predicting human food effect. The AAPS journal 2008;10: 282-288.
36. Lappin G, Noveck R, Burt T. Microdosing and drug development: past, present and future. Expert opinion on drug metabolism & toxicology 2013;9:817-834.
37. Mooij MG, van Duijn E, Knibbe CA, Allegaert K, Windhorst AD, van Rosmalen J, Hendrikse NH, et al. Successful Use of [14 C] Paracetamol Microdosing to Elucidate Developmental Changes in Drug Metabolism. Clinical pharmacokinetics 2017;56:1185-1195.
38. Swart P, Lozac'h F, Simon M, van Duijn E, Vaes WH. The impact of early human data on clinical development: there is time to win. Drug discovery today 2016;21:873-879.
39. van Groen BD, Vaes WH, Park BK, Krekels EH, van Duijn E, Kõrgvee LT, Maruszak W, et al. Dose-linearity of the pharmacokinetics of an intravenous [14C] midazolam microdose in children. British journal of clinical pharmacology 2019;85:2332-2340.
40. Lennernäs H. Animal data: the contributions of the Ussing Chamber and perfusion systems to predicting human oral drug delivery in vivo. Advanced drug delivery reviews 2007;59: 1103 1120.
41. Ghibellini G, Leslie EM, Brouwer KL. Methods to evaluate biliary excretion of drugs in humans: an updated review. Molecular pharmaceutics 2006;3:198-211.
42. Benet L, Cummins C, Wu C. Transporter-enzyme interactions: implications for predicting drug-drug interactions from in vitro data. Current drug metabolism 2003;4:393-398.

43. Vickers AE, Fisher RL. Precision-cut organ slices to investigate target organ injury. Expert opinion on drug metabolism & toxicology 2005;1:687-699.
44. Baverel G, Knouzy B, Gauthier C, El Hage M, Ferrier B, Martin G, Duplany A. Use of precision-cut renal cortical slices in nephrotoxicity studies. Xenobiotica 2013;43:54-62.
45. Troth SP, Simutis F, Friedman GS, Todd S, Sistare FD. Kidney Safety Assessment: Current Practices in Drug Development. In: Seminars in nephrology; 2019: Elsevier; 2019. p. 120-131.
46. De Graaf IA, Olinga P, De Jager MH, Merema MT, De Kanter R, Van De Kerkhof EG, Groothuis GM. Preparation and incubation of precision-cut liver and intestinal slices for application in drug metabolism and toxicity studies. Nature protocols 2010;5:1540.
47. Parrish AR, Gandolfi AJ, Brendel K. Precision-cut tissue slices: applications in pharmacology and toxicology. Life sciences 1995;57:1887-1901.
48. Renwick AB, Watts PS, Edwards RJ, Barton PT, Guyonnet I, Price RJ, Tredger JM, et al. Differential maintenance of cytochrome P450 enzymes in cultured precision-cut human liver slices. Drug Metabolism and Disposition 2000;28:1202-1209.
49. Li M, de Graaf IA, Groothuis GM. Precision-cut intestinal slices: alternative model for drug transport, metabolism, and toxicology research. Expert opinion on drug metabolism & toxicology 2016;12:175-190.
50. Possidente M, Dragoni S, Franco G, Gori M, Bertelli E, Teodori E, Frosini M, et al. Rat intestinal precision-cut slices as an in vitro model to study xenobiotic interaction with transporters. European Journal of Pharmaceutics and Biopharmaceutics 2011;79:343-348.
51. van de Kerkhof EG, de Graaf IA, Ungell A-LB, Groothuis GM. Induction of metabolism and transport in human intestine: validation of precision-cut slices as a tool to study induction of drug metabolism in human intestine in vitro. Drug Metabolism and Disposition 2008;36: 604 613.
52. Kanter R, Monshouwer M, Meijer D, Groothuis G. Precision-cut organ slices as a tool to study toxicity and metabolism of xenobiotics with special reference to non-hepatic tissues. Current drug metabolism 2002;3:39-59.
53. Arakawa H, Kubo H, Washio I, Staub AY, Nedachi S, Ishiguro N, Nakanishi T, et al. Rat Kidney Slices for Evaluation of Apical Membrane Transporters in Proximal Tubular Cells. Journal of pharmaceutical sciences 2019.
54. Bartucci R, Åberg C, Melgert BN, Boersma YL, Olinga P, Salvati A. Time-Resolved Quantification of Nanoparticle Uptake, Distribution, and Impact in Precision-Cut Liver Slices. Small 2020:1906523.
55. Daga SM, de Graaf IA, Argenziano M, Barranco ASM, Loeck M, Al-Adwi Y, Cucci MA, et al. Glutathione-responsive cyclodextrin-nanosponges as drug delivery systems for doxorubicin: Evaluation of toxicity and transport mechanisms in the liver. Toxicology in Vitro 2020;65:104800.
56. Estrada-Ortiz N, Guarra F, de Graaf IA, Marchetti L, de Jager MH, Groothuis GM, Gabbiani C, et al. Anticancer Gold N-Heterocyclic Carbene Complexes: A Comparative in vitro and ex vivo Study. ChemMedChem 2017;12:1429-1435.
57. Spreckelmeyer S, Estrada-Ortiz N, Prins GG, Van Der Zee M, Gammelgaard B, Stürup S, De Graaf IA, et al. On the toxicity and transport mechanisms of cisplatin in kidney tissues in comparison to a gold-based cytotoxic agent. Metallomics 2017;9:1786-1795.
58. Meekel JP, Groeneveld ME, Bogunovic N, Keekstra N, Musters RJ, Zandieh-Doulabi B, Pals G, et al. An in vitro method to keep human aortic tissue sections functionally and structurally intact. Scientific reports 2018;8:1-12.
59. Rodriguez AD, Horowitz LF, Castro K, Kenerson H, Bhattacharjee N, Gandhe G, Raman A, et al. A microfluidic platform for functional testing of cancer drugs on intact tumor slices. Lab on a Chip 2020;20(9):1658-1675.
60. Haslam IS, O'Reilly DA, Sherlock DJ, Kauser A, Womack C, Coleman T. Pancreatoduodenectomy as a source of human small intestine for Ussing chamber investigations and comparative studies with rat tissue. Biopharmaceutics & drug disposition 2011;32:210-221.

61. Rozehnal V, Nakai D, Hoepner U, Fischer T, Kamiyama E, Takahashi M, Yasuda S, et al. Human small intestinal and colonic tissue mounted in the Ussing chamber as a tool for characterizing the intestinal absorption of drugs. European Journal of Pharmaceutical Sciences 2012;46: 367-373.

62. Sjöberg Å, Lutz M, Tannergren C, Wingolf C, Borde A, Ungell A-L. Comprehensive study on regional human intestinal permeability and prediction of fraction absorbed of drugs using the Ussing chamber technique. European Journal of Pharmaceutical Sciences 2013;48:166-180.

63. Westerhout J, van de Steeg E, Grossouw D, Zeijdner EE, Krul CA, Verwei M, Wortelboer HM. A new approach to predict human intestinal absorption using porcine intestinal tissue and biorelevant matrices. European Journal of Pharmaceutical Sciences 2014;63:167-177.

64. Stevens LJ, van Lipzig MM, Erpelinck SL, Pronk A, van Gorp J, Wortelboer HM, van de Steeg E. A higher throughput and physiologically relevant two-compartmental human ex vivo intestinal tissue system for studying gastrointestinal processes. European Journal of Pharmaceutical Sciences 2019;137:104989.

65. Vaessen SF, van Lipzig MM, Pieters RH, Krul CA, Wortelboer HM, van de Steeg E. Regional expression levels of drug transporters and metabolizing enzymes along the pig and human intestinal tract and comparison with Caco-2 cells. Drug Metabolism and Disposition 2017;45:353-360.

66. Bridges JF. A study of macromolecule absorption in vitro by the small intestine of adult rats: Keele University; 1980.

67. Levine RR, McNary WF, Kornguth PJ, LeBlanc R. Histological reevaluation of everted gut technique for studying intestinal absorption. European journal of pharmacology 1970;9: 211-219.

68. Wilson TH, Wiseman G. The use of sacs of everted small intestine for the study of the transference of substances from the mucosal to the serosal surface. The Journal of physiology 1954;123:116-125.

69. Roeselers G, Ponomarenko M, Lukovac S, Wortelboer HM. Ex vivo systems to study host–microbiota interactions in the gastrointestinal tract. Best Practice & Research Clinical Gastroenterology 2013;27:101-113.

70. Alam MA, Al-Jenoobi FI, Al-mohizea AM. Everted gut sac model as a tool in pharmaceutical research: limitations and applications. Journal of Pharmacy and Pharmacology 2012;64: 326-336.

71. Barthe L, Bessouet M, Woodley J, Houin G. The improved everted gut sac: a simple method to study intestinal P-glycoprotein. International journal of pharmaceutics 1998;173:255-258.

72. Bhadriraju K, Chen CS. Engineering cellular microenvironments to improve cell-based drug testing. Drug discovery today 2002;7:612-620.

73. Burks T, Long J. 5-Hydroxytryptamine release into dog intestinal vasculature. American Journal of Physiology-Legacy Content 1966;211:619-625.

74. De Vries MH, Rademaker CM, Geerlings C, Van Duk A, Noordhoek J. Pharmacokinetic modelling of the effect of activated charcoal on the intestinal secretion of theophylline, using the isolated vascularly perfused rat small intestine. Journal of Pharmacy and Pharmacology 1989;41: 528-533.

75. Gandia P, Lacombe O, Woodley J, Houin G. The perfused everted intestinal segment of rat. Arzneimittelforschung 2004;54:467-473.

76. Stappaerts J, Brouwers J, Annaert P, Augustijns P. In situ perfusion in rodents to explore intestinal drug absorption: challenges and opportunities. International journal of pharmaceutics 2015;478:665-681.

77. Prasad N, Bhasker S. Characterization of intestinal transport of Vincristine in rats applying in situ single pass intestinal perfusion. Pharmacologia 2012;3:617-621.

78. Schanker LS, Tocco DJ, Brodie BB, Hogben CAM. Absorption of drugs from the rat small intestine. Journal of Pharmacology and Experimental Therapeutics 1958;123:81-88.

79. Maeng HJ, Durk MR, Chow EC, Ghoneim R, Pang KS. 1α, 25-Dihydroxyvitamin D3 on intestinal transporter function: studies with the rat everted intestinal sac. Biopharmaceutics & drug disposition 2011;32:112-125.

80. van de Steeg E, Schuren FH, Obach RS, van Woudenbergh C, Walker GS, Heerikhuisen M, Nooijen IH, et al. An ex vivo fermentation screening platform to study drug metabolism by human gut microbiota. Drug Metabolism and Disposition 2018;46:1596-1607.

81. Dawson A, Dyer C, Macfie J, Davies J, Karsai L, Greenman J, Jacobsen M. A microfluidic chip based model for the study of full thickness human intestinal tissue using dual flow. Biomicrofluidics 2016;10:064101.

82. Schumacher K, Khong Y-M, Chang S, Ni J, Sun W, Yu H. Perfusion culture improves the maintenance of cultured liver tissue slices. Tissue engineering 2007;13:197-205.

83. van Midwoud PM, Merema MT, Verpoorte E, Groothuis GM. Perifusion of Human Precision-Cut Liver Slices in a Microfluidic Device for Metabolism and Toxicology Studies. An alternative approach based on microfluidics to study drug metabolism and toxicity using liver and intestinal tissue:101.

84. Khong YM, Zhang J, Zhou S, Cheung C, Doberstein K, Samper V, Yu H. Novel intra-tissue perfusion system for culturing thick liver tissue. Tissue engineering 2007;13:2345-2356.

85. Jablonski P, Douglas M, Gordon E, Owen J, McK. Watts J. Studies on the isolated perfused pig liver. British Journal of Surgery 1971;58:129-137.

86. Tsao SC, Sugiyama Y, Sawada Y, Iga T, Hanano M. Kinetic analysis of albumin-mediated uptake of warfarin by perfused rat liver. Journal of pharmacokinetics and biopharmaceutics 1988;16:165-181.

87. Stollman YR, Gärtner U, Theilmann L, Ohmi N, Wolkoff AW. Hepatic bilirubin uptake in the isolated perfused rat liver is not facilitated by albumin binding. The Journal of clinical investigation 1983;72:718-723.

88. Schary WL, Rowland M. Protein binding and hepatic clearance: studies with tolbutamide, a drug of low intrinsic clearance, in the isolated perfused rat liver preparation. Journal of pharmacokinetics and biopharmaceutics 1983;11:225-243.

89. Shand DG, Cotham RH, Wilkinson GR. Perfusion-limited effects of plasma drug binding on hepatic drug extraction. Life sciences 1976;19:125-130.

90. Pang KS, Rowland M. Hepatic clearance of drugs. I. Theoretical considerations of a "well-stirred" model and a "parallel tube" model. Influence of hepatic blood flow, plasma and blood cell binding, and the hepatocellular enzymatic activity on hepatic drug clearance. Journal of pharmacokinetics and biopharmaceutics 1977;5:625-653.

91. O'Sullivan D, Brosnan TJ, Brosnan EM. Hepatic zonation of the catabolism of arginine and ornithine in the perfused rat liver. Biochemical Journal 1998;330:627-632.

92. Pang KS, Koster H, Halsema I, Scholtens E, Mulder GJ, Stillwell R. Normal and retrograde perfusion to probe the zonal distribution of sulfation and glucuronidation activities of harmol in the perfused rat liver preparation. Journal of Pharmacology and Experimental Therapeutics 1983;224:647-653.

93. Pfeifer ND, Yang K, Brouwer KL. Hepatic basolateral efflux contributes significantly to rosuvastatin disposition I: characterization of basolateral versus biliary clearance using a novel protocol in sandwich-cultured hepatocytes. Journal of Pharmacology and Experimental Therapeutics 2013;347:727-736.

94. Booth CL, Brouwer KR, Brouwer KL. Effect of multidrug resistance modulators on the hepatobiliary disposition of doxorubicin in the isolated perfused rat liver. Cancer research 1998;58:3641-3648.

95. Bessems M, 't Hart N, Tolba R, Doorschodt B, Leuvenink H, Ploeg R, Minor T, et al. The isolated perfused rat liver: standardization of a time-honoured model. Laboratory animals 2006;40:236-246.

96. Bekersky I. Use of the isolated perfused kidney as a tool in drug disposition studies. Drug metabolism reviews 1983;14:931-960.

97. Van Ginneken C, Russel F. Saturable pharmacokinetics in the renal excretion of drugs. Clinical pharmacokinetics 1989;16:38-54.

98. Nishiitsutsuji-Uwo J, Ross B, Krebs H. Metabolic activities of the isolated perfused rat kidney. Biochemical Journal 1967;103:852.

99. Van Crugten JT, Sallustio BC, Nation RL, Somogyi AA. Renal tubular transport of morphine, morphine-6-glucuronide, and morphine-3-glucuronide in the isolated perfused rat kidney. Drug metabolism and disposition 1991;19:1087-1092.

100. Hori R, Okamura N, Aiba T, Tanigawara Y. Role of P-glycoprotein in renal tubular secretion of digoxin in the isolated perfused rat kidney. Journal of Pharmacology and Experimental therapeutics 1993;266:1620-1625.

101. Gores GJ, Kost LJ, Larusso NF. The isolated perfused rat liver: conceptual and practical considerations. Hepatology 1986;6:511-517.

102. Vogel T, Brockmann JG, Friend PJ. Ex-vivo normothermic liver perfusion: an update. Current opinion in organ transplantation 2010;15:167-172.

103. Watson CJ, Kosmoliaptsis V, Pley C, Randle L, Fear C, Crick K, Gimson AE, et al. Observations on the ex situ perfusion of livers for transplantation. American Journal of Transplantation 2018;18:2005-2020.

104. Boehnert M, Yeung J, Bazerbachi F, Knaak J, Selzner N, McGilvray I, Rotstein O, et al. Normothermic acellular ex vivo liver perfusion reduces liver and bile duct injury of pig livers retrieved after cardiac death. American Journal of Transplantation 2013;13:1441-1449.

105. Borie DC, Eyraud D, Boleslawski E, Lemoine A, Sebagh M, Cramer DV, Roussi J, et al. Functional metabolic characteristics of intact pig livers during prolonged extracorporeal perfusion: potential for a unique biological liver-assist device. Transplantation 2001;72:393-405.

106. de Vries Y, Matton AP, Nijsten MW, Werner MJ, van den Berg AP, de Boer MT, Buis CI, et al. Pretransplant sequential hypo-and normothermic machine perfusion of suboptimal livers donated after circulatory death using a hemoglobin-based oxygen carrier perfusion solution. American Journal of Transplantation 2019;19:1202-1211.

107. Eshmuminov D, Becker D, Borrego LB, Hefti M, Schuler MJ, Hagedorn C, Muller X, et al. An integrated perfusion machine preserves injured human livers for 1 week. Nature Biotechnology 2020:1-10.

108. Hosgood S, Barlow A, Hunter J, Nicholson M. Ex vivo normothermic perfusion for quality assessment of marginal donor kidney transplants. British Journal of Surgery 2015;102: 1433-1440.

109. Butler AJ, Rees MA, Wight DG, Casey ND, Alexander G, White DJ, Friend PJ. Successful extracorporeal porcine liver perfusion for 72 hr1. Transplantation 2002;73:1212-1218.

110. Yoshikawa R, Matsuno N, Morito N, Gouchi M, Otani M, Takahashi H, Shonaka T, et al. Evaluation Using an Isolated Reperfusion Model for Porcine Liver Donated After Cardiac Death Preserved with Oxygenated Hypothermic Machine Perfusion. Annals of transplantation 2018;23:822.

111. Jamieson RW, Zilvetti M, Roy D, Hughes D, Morovat A, Coussios CC, Friend PJ. Hepatic steatosis and normothermic perfusion—preliminary experiments in a porcine model. Transplantation 2011;92:289-295.

112. Hosgood SA, van Heurn E, Nicholson ML. Normothermic machine perfusion of the kidney: better conditioning and repair? Transplant International 2015;28:657-664.

113. Vogel T, Brockmann JG, Pigott D, Neil DA, Muthusamy ASR, Coussios CC, Friend PJ. Successful transplantation of porcine liver grafts following 48-hour normothermic preservation. PloS one 2017;12:e0188494.

114. OrganAssist. n.d. [accessed]. https://www.organ-assist.nl/products/liver-assist/.

115. Organox. n.d. [accessed]. https://www.organox.com/.

116. Rodrigues A, Taskar K, Kusuhara H, Sugiyama Y. Endogenous probes for drug transporters: balancing vision with reality. Clinical Pharmacology & Therapeutics 2018;103:434-448.

117. Fromm M. Prediction of Transporter-Mediated Drug–Drug Interactions Using Endogenous Compounds. Clinical Pharmacology & Therapeutics 2012;92:546-548.

118. Chu X, Chan GH, Evers R. Identification of endogenous biomarkers to predict the propensity of drug candidates to cause hepatic or renal transporter-mediated drug-drug interactions. Journal of pharmaceutical sciences 2017;106:2357-2367.

119. Shen H, Dai J, Liu T, Cheng Y, Chen W, Freeden C, Zhang Y, et al. Coproporphyrins I and III as functional markers of OATP1B activity: in vitro and in vivo evaluation in preclinical species. Journal of Pharmacology and Experimental Therapeutics 2016;357:382-393.

120. Jones NS, Yoshida K, Salphati L, Kenny JR, Durk MR, Chinn LW. Complex DDI by Fenebrutinib and the Use of Transporter Endogenous Biomarkers to Elucidate the Mechanism of DDI. Clinical Pharmacology & Therapeutics 2020;107:269-277.

121. Kasichayanula S, Boulton DW, Luo WL, Rodrigues AD, Yang Z, Goodenough A, Lee M, et al. Validation of 4β-hydroxycholesterol and evaluation of other endogenous biomarkers for the assessment of CYP3A activity in healthy subjects. British journal of clinical pharmacology 2014;78:1122-1134.

122. Jones H, Rowland-Yeo K. Basic concepts in physiologically based pharmacokinetic modeling in drug discovery and development. CPT: pharmacometrics & systems pharmacology 2013;2: 1-12.

123. Fleishaker JC, Smith RB. Compartmental model analysis in pharmacokinetics. The Journal of Clinical Pharmacology 1987;27:922-926.

124. Bilski J, Mazur-Bialy A, Wojcik D, Surmiak M, Magierowski M, Sliwowski Z, Pajdo R, et al. Role of Obesity, Mesenteric Adipose Tissue, and Adipokines in Inflammatory Bowel Diseases. Biomolecules 2019;9:780.

125. Blokzijl H, Borght SV, Bok LI, Libbrecht L, Geuken M, Van den Heuvel FA, Dijkstra G, et al. Decreased P-glycoprotein (P-gp/MDR1) expression in inflamed human intestinal epithelium is independent of PXR protein levels. Inflammatory bowel diseases 2007;13:710-720.

126. Blokzijl H, Van Steenpaal A, Vander Borght S, Bok LI, Libbrecht L, Tamminga M, Geuken M, et al. Up-regulation and cytoprotective role of epithelial multidrug resistance-associated protein 1 in inflammatory bowel disease. Journal of Biological Chemistry 2008;283:35630-35637.

127. Buyse M, Radeva G, Bado A, Farinotti R. Intestinal inflammation induces adaptation of P-glycoprotein expression and activity. Biochemical pharmacology 2005;69:1745-1754.

128. Czerwinski M, Oberheide B, Hatfield N, Ewy B, Seib C, Gatineau E, Yiannikouris F, et al. Microsomal cytochrome P450 enzyme activities in nonalcoholic steatohepatitis livers. In: Drug Metabolism and Pharmacokinetics; 2019: JAPANESE SOC STUDY XENOBIOTICS INT MED INF CENTER SHINANOMACHI RENGAKAN, 35 …; 2019. p. S25-S25.

129. George J, Murray M, Byth K, Farrell GC. Differential alterations of cytochrome P450 proteins in livers from patients with severe chronic liver disease. Hepatology 1995;21:120-128.

130. Zollner G, Fickert P, Silbert D, Fuchsbichler A, Marschall H-U, Zatloukal K, Denk H, et al. Adaptive changes in hepatobiliary transporter expression in primary biliary cirrhosis. Journal of hepatology 2003;38:717-727.

131. Westra IM. Precision-cut liver slices: an ex vivo model for the early onset and end-stage of liver fibrosis: Rijksuniversiteit Groningen, 2014.

132. Morrison MC, Kleemann R, van Koppen A, Hanemaaijer R, Verschuren L. Key inflammatory processes in human NASH are reflected in Ldlr−/−. Leiden mice: a translational gene profiling study. Frontiers in physiology 2018;9:132.

133. Abe N, Kato S, Tsuchida T, Sugimoto K, Saito R, Verschuren L, Kleemann R, et al. Longitudinal characterization of diet-induced genetic murine models of non-alcoholic steatohepatitis with metabolic, histological, and transcriptomic hallmarks of human patients. Biology open 2019;8:bio041251.

134. Villeneuve JP, Huet PM, Gariepy L, Fenyves D, Willems B, Côté J, Lapointe R, et al. Isolated perfused cirrhotic human liver obtained from liver transplant patients: a feasibility study. Hepatology 1990;12:257-263.

135. Villeneuve J-P, Dagenais M, Huet P-M, Lapointe R, Roy A, Marleau D. Clearance by the liver in cirrhosis. III. Propranolol uptake by the isolated perfused human liver. Canadian journal of physiology and pharmacology 1996;74:1327-1332.

136. Melgert BN, Olinga P, Weert B, Slooff MJ, Meijer DK, Poelstra K, Groothuis GM. Cellular distribution and handling of liver-targeting preparations in human livers studied by a liver lobe perfusion. Drug metabolism and disposition 2001;29:361-367.

137. Schreiter T, Marquitan G, Darnell M, Sowa J-P, Bröcker-Preuss M, Andersson TB, Baba HA, et al. An ex vivo perfusion system emulating in vivo conditions in noncirrhotic and cirrhotic human liver. Journal of Pharmacology and Experimental Therapeutics 2012;342:730-741.
138. Schreiter T, Sowa J-P, Schlattjan M, Treckmann J, Paul A, Strucksberg K-H, Baba HA, et al. Human ex-vivo liver model for acetaminophen-induced liver damage. Scientific reports 2016;6:31916.
139. Bezençon J, Beaudoin JJ, Ito K, Fu D, Roth SE, Brock WJ, Brouwer KL. Altered Expression and Function of Hepatic Transporters in a Rodent Model of Polycystic Kidney Disease. Drug Metabolism and Disposition 2019;47:899-906.
140. Salam M, Keeffe EB. Liver cysts associated with polycystic kidney disease: role of Tc-99m hepatobiliary imaging. Clinical nuclear medicine 1989;14:803-807.
141. Wang L, Zhou M-T, Chen C-Y, Yin W, Wen D-X, Cheung C-W, Yang L-Q, et al. Increased renal clearance of rocuronium compensates for chronic loss of bile excretion, via upregulation of Oatp2. Scientific reports 2017;7:40438.
142. Orlando R, Floreani M, Napoli E, Padrini R, Palatini P. Renal clearance of N1-methylnicotinamide: A sensitive marker of the severity of liver dysfunction in cirrhosis. Nephron 2000;84:32-39.
143. Reidenberg MM, Odar-Cederlöf I, von Bahr C, Borgå O, Sjöqvist F. Protein binding of diphenylhydantoin and desmethylimipramine in plasma from patients with poor renal function. New England Journal of Medicine 1971;285:264-267.

PART II

The liver perfusion model to study drug pharmacokinetic processes and endogenous substrate handling
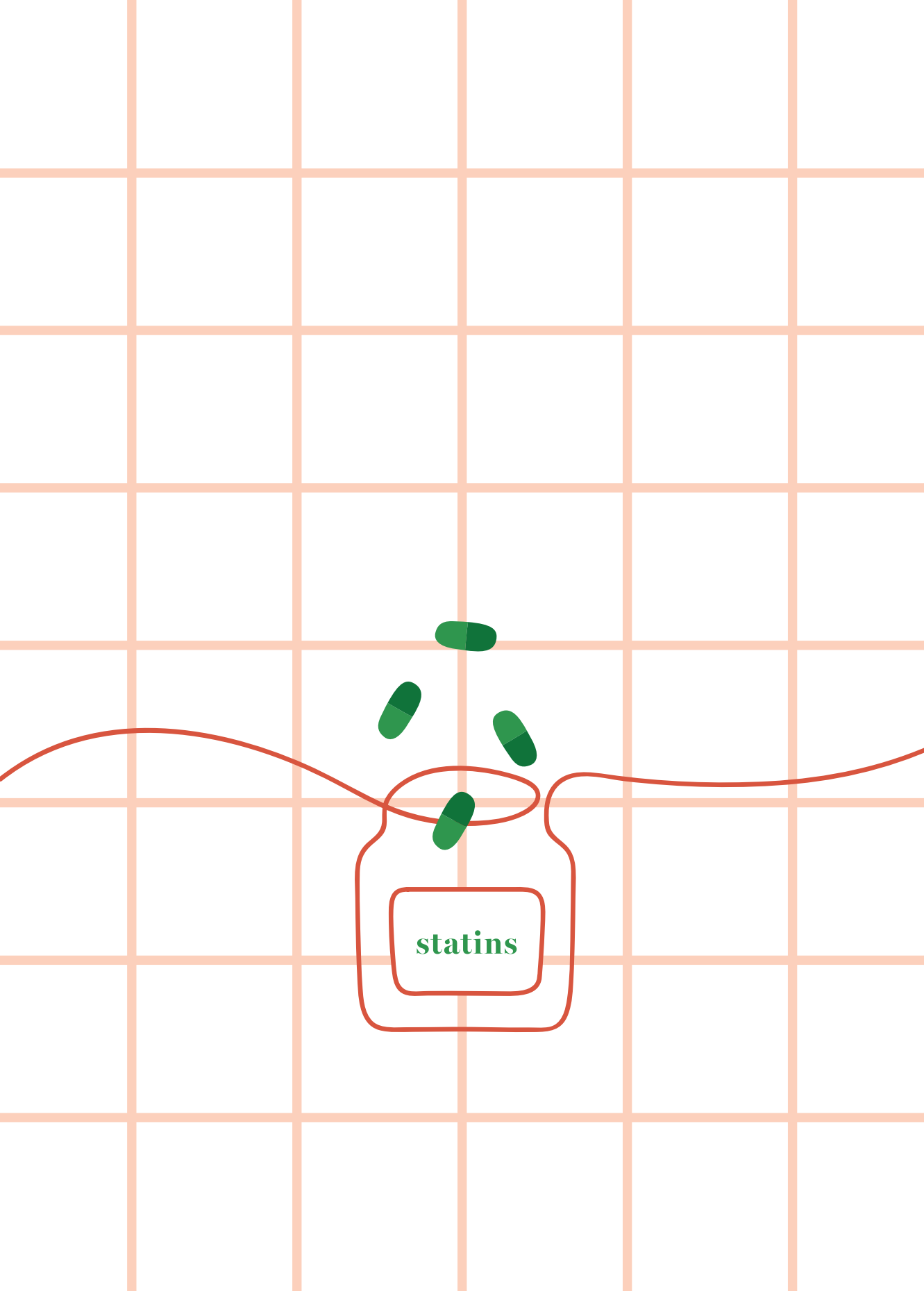
statins

CHAPTER 03

Evaluation of normothermic machine perfusion of porcine livers as a novel preclinical model to predict biliary clearance and transporter-mediated drug-drug interactions using statins

L.J. Stevens, A.Z.X. Zhu, P.P. Chothe, S.K. Chowdhury, J.M. Donkers, W.H.J. Vaes, C.A.J. Knibbe, I.P.J. Alwayn, E. van de Steeg

Abstract

There is a lack of translational preclinical models that can predict hepatic handling of drugs. In this study we aimed to evaluate the applicability of normothermic machine perfusion (NMP) of porcine livers as a novel *ex vivo* model to predict hepatic clearance, biliary excretion and plasma exposure of drugs. For this evaluation we dosed atorvastatin, pitavastatin and rosuvastatin as model drugs to porcine livers and studied the effect of common drug-drug interactions (DDI) on these processes. After 120 min of perfusion, 0.104 mg atorvastatin (n=3), 0.140 mg pitavastatin (n=5) or 1.4 mg rosuvastatin (n=4) was administered to the portal vein, 120 min later followed by a second bolus of the statin co-administered with OATP perpetrator drug rifampicin (67.7 mg). Following the first dose, all statins were rapidly cleared from the circulation (hepatic extraction ratio > 0.7) and excreted into the bile. Presence of human specific atorvastatin metabolites confirmed the metabolic capacity of porcine livers. The predicted biliary clearance of rosuvastatin was found to be closer to the observed biliary clearance. A rank-order of the DDI between the various systems upon co-administration with rifampicin could be observed: atorvastatin (AUC Ratio 7.2)> rosuvastatin (AUC Ratio 3.1)> pitavastatin (AUC Ratio 2.6) which is in good agreement with the clinical DDI data. The results from this study demonstrated the applicability of using NMP of porcine livers as a novel preclinical model to study OATP-mediated DDI and its effect on hepatic clearance, biliary excretion and plasma profile of drugs.

Introduction

The liver is a complex organ involved in the uptake, metabolism and biliary excretion of xenobiotics and endogenous compounds. Transporters located at the basolateral side of the plasma membrane, like the Organic Anion-Transporting Peptides (OATP) 1B1, 1B3, 2B1, Na$^+$-taurocholate cotransporting polypeptide (NTCP) and the Organic Anion Transporter (OAT) 2, are involved in the uptake of drugs and endogenous compounds from the portal and arterial circulation into hepatocytes[1-3]. After uptake, compounds can be metabolized, for example by the cytochrome P450 (CYP450) family of enzymes, and subsequently effluxed into the bile across the canalicular membrane or back into the systemic circulation across the sinusoidal membrane[4]. Several transporters are involved in the hepatic efflux, including multidrug resistance protein 1 (MDR1; P-glycoprotein), breast cancer resistance protein (BCRP), bile salt export pump (BSEP) and multidrug resistance-associated protein 2 (MRP2) at the canalicular membrane and multidrug resistance-associated protein 3 and 4 (MRP3 and MR4) at the basolateral membrane. Concomitant administration of drugs that are substrates for the same transporters and/or metabolizing enzymes can result in a drug-drug interaction (DDI) affecting plasma as well as biliary levels of one of the drugs . As a result, this can change the drug concentration at the target, or it can even lead to toxicity (e.g. drug induced liver injury (DILI)). Therefore, interactions affecting hepatic uptake and biliary excretion are important to characterize in the preclinical phase of drug development[5,6].

To evaluate the potential DDI for newly developed drugs, the FDA stated that it is important to understand the principal route of the drug's elimination and to understand the contribution and effect of the drug on transporters and metabolizing enzymes. Especially DDI at the transporter level is important to characterize since they control the absorption, distribution and elimination of the drug in various organs[7]. When a newly developed drug for example is intended to be used by a population which is likely to also use statins, the sponsor should examine the potential of the investigational drug to interact with OATP1B1/1B3[7].

To study complex processes such as transporter-enzyme interplay, potential DDI and biliary excretion, physiologically relevant models are needed which recapitulate all functions of the liver including the ability to produce bile[8]. The

sandwich cultured hepatocyte and rat liver perfusion models are known to capture these complex processes and are currently used to investigate hepatobiliary disposition of drugs. Unfortunately, these models have their own limitations. *In vitro* to *in vivo* translation often fails due to species differences or due to differences in transporter expression resulting in difficulties in the prediction of plasma profiles after oral and intravenous administration[9]. Therefore, extrapolation of data obtained using rodent models is not feasible for the prediction of human PK and DDI[9-11].

At present, research in the field of organ transplantation is focused on organ preservation techniques using machine perfusion. These pressure driven perfusion machines are able to perfuse human and porcine livers at a physiological pressure under oxygenated and normothermic conditions. Porcine organs are often used for method validation and device development and it has been shown that normothermic machine perfusion (NMP) of the porcine liver is an excellent platform to study hepatic processes[12,13]. The pig model is considered as a proper translational model because of anatomical, physiological and biochemical similarity to humans and nowadays this model is increasingly used in biomedical research[14]. Compared to the rat model, the size of the pig model supports the collection of larger sample volumes and there is the ability to take tissue biopsies in time. Furthermore, an advantage of using livers from pig origin is the similarity of Phase I and Phase II biotransformation reactions[14], which was recently confirmed in a quantitative proteomic analysis comparing transporter and metabolizing enzyme expression in human and porcine liver[15].

In this study, we evaluate using normothermic machine perfusion of porcine livers as a novel preclinical model to predict pharmacokinetic processes. Using three statins as model drug compounds (rosuvastatin, atorvastatin and pitavastatin) we studied the transporter mediated hepatic extraction and biliary excretion. Additionally, we examined the effect of rifampicin on the disposition of these three statins.

Materials and method

Chemicals

Atorvastatin, Pitavastatin and rifampicin were purchased from Bio-Connect (Huissen, the Netherlands). Rosuvastatin calcium, Heparin, taurocholate and insulin were purchased Sigma-Aldrich Chemie B.V. (Zwijndrecht, the Netherlands). Atorvastatin lactone, 2-hydroxy atorvastatin, 2-hydroxy atorvastatin lactone, 4-hydroxy atorvastatin and 4-hydroxy atorvastatin lactone were obtained from Toronto Research Chemicals (Toronto, ON, Canada). Epoprostenol was purchased from R&D systems (Minneapolis, USA). Vitamin solution, L-glutamine, MEM essential acids and glutamax were obtained from Gibco (Paisley, Scotland). Calcium gluconate 10% was obtained from Pharmamarket (Hove, Belgium).

Porcine livers

Livers were obtained from a local slaughterhouse (*Sus scrofa domesticus*, approximately at age of 6 months with body weight between 100 and 120 kg). Pigs were sacrificed by a standardized procedure of electrocution followed by exsanguination. Thereafter, three liters of blood was collected in a container supplemented with 25000 IU of heparin. All abdominal organs were dissected outside the animal and collected. Within 20 min after termination, the *vena porta* was cannulated and directly flushed by gravity with 3L of NaCl 0.9% (Baxter BV, Utrecht the Netherlands) supplemented with 5000 IU of heparin followed by 2L of ice-cold Histidine-Tryptophan-Ketoglutarate (HTK) solution (Plegistore, Warszawa in Poland). In the meantime, the *arteria hepatica* was dissected, cannulated and subsequently flushed with HTK. At the laboratory, side branches were ligated, the common bile duct was cannulated while the *ductus cysticus,* derived from the gall bladder, was ligated.

Normothermic machine perfusion

The porcine livers were perfused using the LiverAssist device (Organ Assist, Groningen, the Netherlands). The machine consists of two rotary pumps that provide a pulsatile flow to the hepatic artery and a continuous flow to the portal vein. The system was filled with 2L perfusion fluid containing red blood cells and plasma (Supplemental Table S3.1). Insulin, taurocholate, heparin and epoprostenol were provided as continuous infusion at a rate of 10U/h, 1041U/h, 10 mL/h (2% w/v) and 8 µg/h, respectively, in order to maintain liver

functioning including bile flow. Additionally, amino acids and vitamins were continuous provided to keep the liver metabolically active (Supplementarl Table S3.1). Gas delivery to the LiverAssist consisted of 95% oxygen and 5% carbon dioxide at 2L/min and the temperature was set at 39°C (body temperature pigs). The livers were perfused with a portal pressure of 11 mmHg and a mean arterial pressure of 50 mmHg. Upon perfusion, additional boluses of sodium bicarbonate and glucose were applied depending on perfusate pH (range 7.35–7.45) and glucose concentration (>5 mmol/L). Arterial blood gas samples were taken hourly to monitor liver viability (pH, glucose, Na, K, lactate etc.) using the i-STAT clinical analyzer (Abbot Point of Care Inc., Princeton, NJ).

Drug administration during perfusion

The plasma and biliary concentration of atorvastatin, rosuvastatin and pitavastatin and rifampicin were determined. Additionally, atorvastatin metabolite formation was determined. The statins and rifampicin were selected based on clinically known DDI and *in vitro* transporter study data and are presented in Table 3.1. Initial portal doses for atorvastatin and rifampicin applied to the system were based on simulations by SimCyp. After pilot experiments, the doses were increased 2x for atorvastatin (0.052 mg to 0.104 mg) and 3x for rifampicin (22.6 mg to 67.7 mg) to facilitate proper detection by LCMS. For the other two statins, rosuvastatin and pitavastatin, the compound profiles were not available in SimCyp. Therefore the portal doses of rosuvastatin and pitavastatin were based on the oral dosage and corrected for the fraction absorbed (F_a), average correction for Fraction escaping the gut (Fg) (0.7) (16) and corrected for the total circulating volume of 2L in the perfusion system (compared to 5L *in vivo*). To study DDI, the set-up as depicted in Figure 1 was applied. After a stabilization period of 120 min, the statin was administered at as a slow bolus at a rate of 1mL/min during 10 min to the portal vein. Time of starting the slow bolus was set at t=0 min. Subsequently, plasma and bile samples were taken for the following 120 min. Arterial blood samples were taken at t=0, 2, 4, 6, 8, 10, 15, 20, 30, 40, 50, 60, 90 and 120 min. Portal samples were taken during the administration of the drug at t=5 and t=10 min to determine the first pass effect. This portal sampling point was ~30cm from the portal dosing point. Bile samples were collected in 10-minute fractions. Blood samples were centrifuged directly after collection at 1.3 *g* for 10 min at 4°C and thereafter plasma (and bile) samples were immediately stored at ≤-70°C until further processed. Drug concentrations in plasma, bile and liver biopsies were determined by LC-MS/MS analysis as described below.

At 120 min, biopsies were taken (n=2) to determine the intracellular concentration in the hepatocytes. After the first 120 min, a slow bolus 10 min (1mL/min) of 67.7 mg rifampicin was administered to the liver and after 5 min (t=125 min), a subsequent slow bolus of the statin was administrated to the portal vein of the liver. The same sampling schedule for the following 120 min was applied. After the last sampling time point of the perfusion experiment, again a biopsy was taken from the liver to determine the intracellular concentration of the substrate and perpetrator. The biopsies were snap frozen and immediately stored at ≤-70°C.

Table 3.1 - General properties on statins and rifampicin as perpetrator drug. mg oral doses applied *in vivo*, fraction absorbed and mg bolus applied to the portal vein of ex vivo perfused livers.

Substrate (victim drug)	Transporters involved	Metabolism	Fraction absorbed (%)	mg oral doses	mg bolus applied to *ex vivo* liver
Atorvastatin	NTCP, OATP1B1, OATP1B3 and OATP2B1[1,2]	CYP3A4[1,2]	12%[3]	10 mg[7]	0.104 mg
Pitavastatin	BCRP, NTCP, OATP1B1 and OATP1B3[1,2]	CYP2C9[3] CYP2C8	60%[3]	2 mg[3]	0.141 mg
Rosuvastatin	OATP1B1, OATP1B3, NTCP, MRP2, BCRP[1,2]	CYP2C9[4]	50%[5]	10 mg[8]	1.400 mg
Perpetrator drug					
Rifampicin			95%[6]	600 mg[1,2]	67.7 mg

[1] (2), [2] (1) , [3] (43), [4] (44), [5] (45) [6] (46), [7] (47), [8] (29)

Bioanalysis

The concentration of atorvastatin and its metabolites, pitavastatin, rosuvastatin and rifampicin in plasma and bile were quantified using LC/MS. Briefly, 20 μL of sample was extracted by adding 100 μL of acetonitrile containing internal standard. Samples were vortexed, centrifuged at 3000 rpm for 5 minutes and 100 μL of supernatant was collected in a clean sample plate. Samples were then mixed with 50 μL of water, vortexed and injected into LC/MS for quantification. The details of LC/MS conditions used for the analysis of each compound are shown in Supplemental Table S3.2. The mass spectrometer (AB Sciex API 5500) was operated in electrospray positive ion mode with the capillary voltage of 5.5 kV and Spray temperature of 550°C. The multiple reaction monitoring transitions used for all the compounds are shown Supplemental Table S3.3.

Liver function assessment

During the perfusion experiment, blood gas analysis was executed every hour by measuring amongst others pH, pO_2, pCO_2, SO_2, glucose and lactate concentrations using a blood gas analyzer (iSTAT Alinity, Abbott). Additionally, hepatic artery and portal vein flow and resistance values were reported from the LiverAssist machine.

Multiple parameters were measured in perfusate and bile samples from the perfused livers to study liver viability. Total bilirubin, alanine transaminase (ALT) and aspartate transaminase (AST) concentration in the plasma and bile samples were measured using a Reflotron (Roche). Additionally, at the end of the perfusion period (360 min of perfusion) a bolus (10 mg) of Indocyanine green (ICG) was applied to the *ex vivo* liver to assess liver functionality by studying the clearance of ICG from the perfusate. Samples were taken at t=0, 1, 2, 4, 6, 8, 10, 15, 20, 30, 40, 50 and 60 min after dosing. Sample were centrifuged to obtain plasma and thereafter, 100 μl was sampled and measured at 788 emission and 813 excitation using a microplate reader (Tecan infinite m200 pro).

Liver perfusion studies were approved when the following acceptance criteria were met: 1) stable bile production and bile flow throughout the whole experiment, with >12 mL/h during 120 after 120 min of perfusion; 2) plasma bilirubin levels <20 μmol/L after 120 min of perfusion; 3) bile bilirubin levels >200 μmol/L after 120 min of perfusion; 4) plateau phase of AST and ALT reached within 60 min of perfusion; 5) plasma ICG reduced by 50% within 40 min after administration of ICG.

In total thirteen livers were perfused for a period of 420 min. Of these livers, three perfusions were excluded from the PK analysis to study DDI: one liver exposed to atorvastatin was excluded due to an experimental dosing error (Figure S3.1 and S3.2) and two livers exposed to pitavastatin showed acute hepatotoxic effects. The PK data of these livers is shown in the supplemental figures (Figure S3.1 and S3.2).
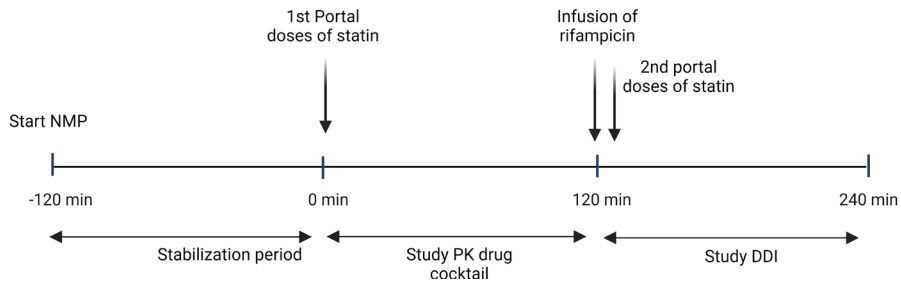
Figure 3.1 - Schematic representation of the experimental set-up. Livers were connected to the perfusion device and after 120 min a 10 min bolus (1mL/min) with a statin was administered to the liver. Plasma and bile samples were taken for 120 min. At t=120, rifampicin was administrated for 10 min at 1mL/min and at t=125 the second bolus of the statin was administrated. Subsequently plasma and bile samples were taken for the following 120 min.
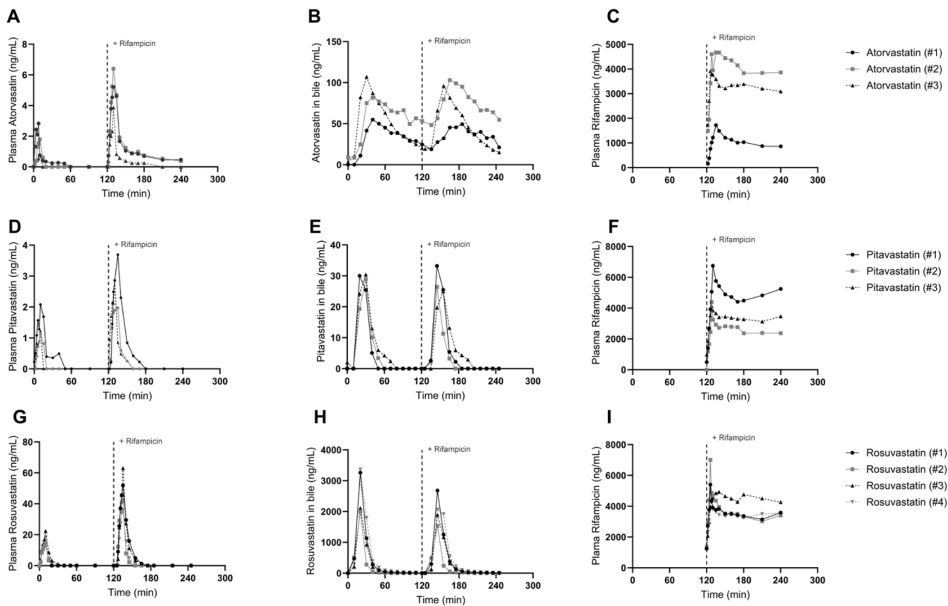

Figure 3.2 - Pharmacokinetic profile of atorvastatin (dosed as slow bolus of 0,104 mg over 10 min to portal vein) in plasma (A) and bile (B), pitavastatin (dosed as slow bolus of 0.141 mg over 10 min to portal vein) in plasma (D) and bile (E), and PK profile of rosuvastatin (dosed as slow bolus of 1.400 mg to portal vein) on plasma(G) and bile (H) Plasma pharmacokinetic profile of rifampicin (dosed as bolus of 67.7 mg to the portal vein) shown for each experiment (C,F and I)

Quantitative LC-MS/MS analysis of hepatic transporters in porcine and human livers

To study transporter and enzyme expression in porcine liver tissue compared to the expression in human liver tissue, from five healthy domestic pigs (*Sus scrofa domesticus*, 2 male and 3 female, age 10–14 weeks and body weight between 15 and 25 kg) was collected. These animals were additionally used for educational purposes at the Utrecht University (Utrecht, The Netherlands). The local animal welfare office approved the use of these animals for these purposes which was in full compliance with the aim to contribute to the reduction, refinement, and replacement of animal experiments. Before termination, pigs had free access to food and water. Liver tissue of domestic pigs was collected only when defined healthy as judged by a veterinarian.

Human liver samples derived from 15 individuals, of which 5 were anonymously collected at the University Medical center of Groningen (UMCG, Groningen, The Netherlands) and were kindly provided by Prof. Dr. G.M.M. Groothuis (University of Groningen, The Netherlands) and 10 were collected at the Department of Surgery, Uppsala University Hospital (Uppsala, Sweden) and were kindly provided by Prof. Dr. P. Artursson (7 male and 3 female donors; human liver specimens also used in previously published study[17]. Collection of redundant tissue from surgeries (collected as waste material) was approved by the Medical Ethical Committee of the UMCG or the Uppsala Ethical Review Board (ethical approval no. 2009/028 and 2011/037). No clinically relevant or identifiable information from the patients was collected.

To determine the protein levels of BCRP, BSEP, MDR1, MRP1, MRP2, OATP2B1, OCT1, GLUT1, MCT1, MRP3, NTCP, OATP1B1, OATP1B3 in porcine and human liver tissue, we followed the protocol of membrane isolation and trypsin digestion as previously described for tissue samples and cell lines ([18,19]). All samples were processed in duplicate. LC-MS/MS settings were as previously described (19). For each peptide 3 transitions were chosen (Q3–1, Q3–2, and Q3–3) for quantitation and confirmation (Supplemental Table S3.4). In case no suitable prototypic peptide could be selected for the human and porcine transporter proteins, two separate peptides were selected and synthesized (Supplemental Table S3.4). Peptides labeled with 15N and 13C (AQUA peptide) were synthesized (Sigma Aldrich Chemie, Steinheim, Germany) and used as an internal standard for quantification. For each peptide, a calibration curve of

0.01–50 ng/ml and quality controls were included in every run. Data are expressed as fmol transporter protein/mg liver.

Data analysis

Data obtained during the perfusion studies was analyzed using Graphpad prism version 8. Values for the area under the concentration time curve (AUC) were calculated using the linear trapezoidal method. The area under the concentration time curve ratio (AUCR) was determined by dividing the $AUC_{120-240\ min}$ / $AUC_{0-120\ min}$. Student's t test was used to analyze differences between two groups.

Results

Assessment of liver functionality during perfusion

During the perfusion of the livers, flow and bile production were monitored. The perfused livers (n=3 for atorvastatin, n=3 for pitavastatin and n=4 for rosuvastatin) included in the PK analysis showing a stable portal and arterial flow of 1548±229 mL/min and 175±67 mL/min respectively and substantial bile production throughout the experiment (on average 79.2±27.6 mL in a period of 360 min) (Figure S3.1). With 57.1±15.7 mL, the livers exposed to pitavastatin produced the least amount of bile during the total perfusion period. For atorvastatin and rosuvastatin exposed livers, bile production was 78.9±24.7 mL and 107.2±12.5 mL respectively.

Plasma concentration profiles and biliary excretion of atorvastatin, pitavastatin and rosuvastatin

In order to study plasma and biliary clearance of the statins, atorvastatin (0.104 mg), pitavastatin (0.141 mg) or rosuvastatin (1.400 mg) was administered via the portal vein in a slow bolus (10 min, 1 mL/min), resulting in initial portal concentrations of 7.02 ng/mL, 8.50 ng/mL and 108.73 ng/mL for atorvastatin, pitavastatin and rosuvastatin respectively. During the dosing period and thereafter, multiple perfusate and bile samples were taken to assess the pharmacokinetic profile of the drugs. Sampling at the portal vein during the 10 min dosing period and simultaneously at the arterial side, enabled us to calculate the hepatic extraction ratio. Table 3.2 and Figure 3.2 show the plasma and biliary profile of the statins and plasma rifampicin concentration. The livers

showed a hepatic extraction ratio of 0.8±0.1 for all statins (Figure 3.2A-B, D-E, G-H, Table 3.2). Within 10 minutes after the start of the bolus administration, atorvastatin was detected in the bile with a T_{max} of 35.0±5.0 min. A total of 13.0±5.6% of the parent compound was secreted into the bile within 120 min of perfusion. Pitavastatin secretion into the bile was slower, and was detected in the bile 20 min after the start of the administration with a substantially lower total biliary excretion of 1.1±0.1% within 120 min. Rosuvastatin was detected in the bile 10 min after the start of the administration, reaching peak levels at 22.5±4.3 min. In total 10.1±2.5% rosuvastatin was excreted into the bile during 120 min of perfusion.

Table 3.2 – Overview of PK of atorvastatin, pitavastatin and rosuvastatin and the effect of rifampicin on the hepatic uptake and biliary clearance of these statins. Values are mean ± SD (n=3 for atorvastatin, n=3 for pitavastatin and n=4 for rosuvastatin).

Statin PK		Plasma			Bile		
		Substrate alone	+ Rifampicin	Fold change	Substrate alone	+ Rifampicin	Fold change
Atorvastatin	C_{max} (ng/mL)	1.79 ± 0.84	5.16 ± 1.03	2.88	216.88 ± 114.98	161.73 ± 86.17	0.75
	$AUC_{0 – 120\ min/\ 120\text{-}240\ min}$ (ng/mL)	18.09 ± 10.73	112.79 ± 46.06	7.24	13517.33 ± 5809.52	7780.25 ± 3676.67	0.58
	% biliary excretion	-	-	-	13.00 ± 5.59	7.48 ± 3.54	0.58
	Biliary clearance (L/h)	-	-	-	87.78 ± 78.42	6.31 ± 6.38	0.07
	Hepatic extraction ratio	0.82 ± 0.08	0.51 ± 0.09	0.62	-	-	-
Pitavastatin	C_{max} (ng/mL)	1.47 ± 0.43	2.43 ± 0.70	3.03	65.07 ± 7.27	72.12 ± 20.35	1.11
	$AUC_{0 – 120\ min/\ 120\text{-}240\ min}$ (ng/mL)	19.51 ± 11.89	32.64 ± 17.62	2.63	1448.33 ± 129.39	1288.33 ± 281.69	0.89
	% biliary excretion	-	-	-	1.03 ± 0.09	0.91 ± 0.20	0.89
	Biliary clearance (L/h)	-	-	-	5.33 ± 2.73	1.16 ± 0.86	0.22
	Hepatic extraction ratio	0.84 ± 0.01	0.72 ± 0.08	0.87	-	-	-
Rosuvastatin	C_{max} (ng/mL)	18.43 ± 3.15	48.28 ± 10.25	2.62	8927 ± 1302	6384.25 ± 207.58	0.72
	$AUC_{0 – 120\ min/\ 120\text{-}240\ min}$ (ng/mL)	186.57 ± 44.90	578.73 ± 152.91	3.10	140123 ± 34948	118572.00 ± 28916.47	0.85
	% biliary excretion	-	-	-	10.01 ± 2.50	8.47 ± 2.07	0.85
	Biliary clearance (L/h)	-	-	-	46.66 ± 13.27	13.18 ± 5.39	0.28
	Hepatic extraction ratio	0.82 ± 0.03	0.71 ± 0.07	0.87	-	-	-

Effect of rifampicin on statin kinetics and biliary clearance

To study the effect of rifampicin on statin plasma kinetics and biliary clearance, a second bolus of the statin was co-administered with a bolus of rifampicin (67.7 mg). Upon co-administration of rifampicin, the plasma C_{max} increased ~3-fold for all statin drugs: from 1.8±0.8 ng/mL to 5.2±1.1 ng/mL for

atorvastatin, from 1.5±0.4 ng/mL to 4.5±1.9 ng/mL for pitavastatin and from 18.4±3.2 ng/mL to 48.3±10.3 ng/mL for rosuvastatin (Figure 3.2, Table 3.2). Additionally, all plasma AUCs of the statins increased upon co-administration of rifampicin: livers exposed to atorvastatin showed the highest AUC ratio (AUCR) of 7.2, followed by rosuvastatin (AUCR 3.1) and pitavastatin (AUCR 2.6) upon rifampicin co-administration (Figure 3.3A). In line with these data, the most profound effect of rifampicin on the hepatic extraction was also observed for atorvastatin that decreased from 0.8±0.1 to 0.5±0.1, while it decreased from 0.8±0.1 to 0.7±0.1 for both pitavastatin and rosuvastatin. The addition of rifampicin resulted in a biliary secretion of 6.80±3.85% of administered atorvastatin corresponding to 0.47-fold reduction in biliary clearance. Interestingly, a more profound reduction in biliary excretion was observed for rosuvastatin and pitavastatin upon co-administration with rifampicin, i.e., 0.15-fold and 0.11-fold, respectively.
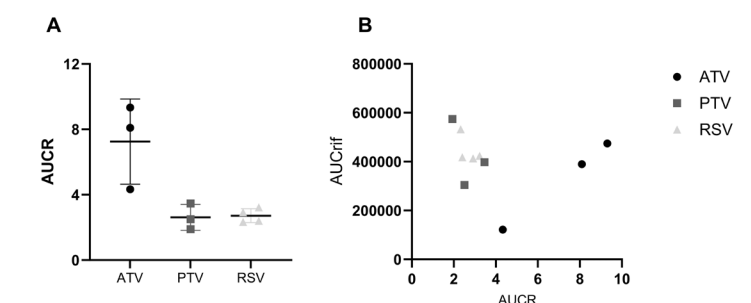

Figure 3.3 - (A) Showing the rank-order of DDI in AUCR for atorvastatin (ATV), pitavastatin (PTV) and rosuvastatin (RSV) (B) Relation of AUCR to $AUC_{rifampicin}$.

Pharmacokinetics of rifampicin

Figures 3.2C, F and I show the concentration time profile of the perpetrator rifampicin in the three statin groups. The livers exposed to atorvastatin showed the lowest C_{max}, 3.4± 1.3 µg/mL for rifampicin compared to livers exposed to pitavastatin (5.1± 1.2 µg/mL) and rosuvastatin (5.3±1.0 µg/mL; Figure 3.2C,F and I, Table 3.3). After administration, rifampicin was rapidly detected in the bile with a T_{max} of 46.7±4.7 min, 30.0±0.0 min and 35.0±11.2 min for livers exposed to atorvastatin, pitavastatin, and rosuvastatin respectively. The biliary clearance of rifampicin was 6.7±4.8%, 5.7±2.5%, 10.9±1.6% respectively in livers treated with atorvastatin, pitavastatin and rosuvastatin livers.

Table 3.3 - Overview of PK of rifampicin during ex vivo liver perfusion. Values are mean ± SD (n=3 for Atorvastatin, n=3 for pitavastatin and n=4 for rosuvastatin).

		Plasma	Bile
Atorvastatin	C_{max} (µg/mL)	3.43 ± 1.25	63.27 ± 31.08
	T_{max} (min)	15.33 ± 3.68	46.67 ± 4.71
	AUC $_{120-240min}$ (µg/mL)	328.58 ± 150.18	5622.59 ± 2934.09
	% biliary excretion	-	8.39 ± 4.38
Pitavastatin	C_{max} (µg/mL)	5.09 ± 1.18	64.96 ± 1.92
	T_{max} (min)	10.33 ± 2.05	30.00 ± 0.00
	AUC $_{120-240min}$ (µg/mL)	425.32 ± 111.98	4690.66 ± 1066.66
	% biliary excretion	-	7.00 ± 1.59
Rosuvastatin	C_{max} (µg/mL)	5.53 ± 0.95	88.18 ± 7.56
	T_{max} (min)	12.00 ± 1.00	35.00 ± 11.20
	AUC $_{120-240min}$ (µg/mL)	446.61 ± 49.48	7284.19 ± 1053.33
	% biliary excretion	-	10.87 ± 1.57

Metabolism of atorvastatin and the effect of rifampicin on metabolism

Since atorvastatin is subjected to CYP3A4 mediated hepatic metabolism, we also investigated the presence of its known metabolites (atorvastatin lactone, 2-OH atorvastatin, 2-OH atorvastatin lactone, 4-OH atorvastatin and 4-OH atorvastatin lactone) in plasma and bile samples obtained from the perfused livers exposed to atorvastatin (Figure 3.4, Table 3.3). All five clinically known metabolites were detected in the bile, but no metabolites were detected in plasma. For all metabolites, the biliary secretion was decreased upon the co-administration of rifampicin (Table 3.4). Main inhibition was shown for the metabolites atorvastatin lactone (AUCR of 0.1), followed by 2-OH atorvastatin (AUCR of 0.8) and 4-OH atorvastatin (AUCR of 0.7).
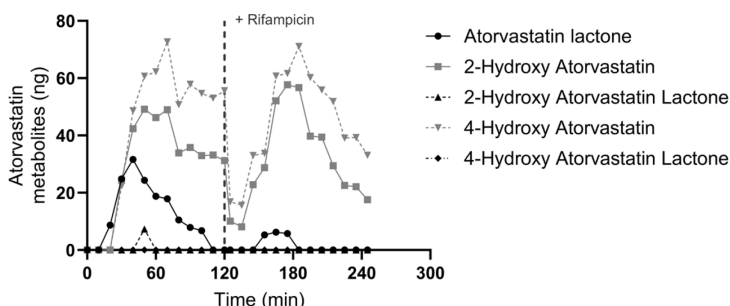

Figure 3.4 - Atorvastatin metabolite excretion into the bile (n=1) upon dosing atorvastatin (0,104 mg) to the portal vein of perfused porcine liver, before (0-120 min) and after co-administration with perpetrator rifampicin (125-245 min).

Table 3.4 - % Biliary excretion of atorvastatin (0.104 mg) metabolites for atorvastatin alone and atorvastatin + rifampicin n=1.

% biliary clearance of metabolites	Atorvastatin	Atorvastatin+ Rifampicin	AUCR
Atorvastatin lactone	1.45	0.17	0.11
2-hydroxy atorvastatin	3.49	2.64	0.76
2-hydroxy atorva lactone	0.07	0.00	0.00
4-hydroxy atorvastatin	4.91	3.33	0.68
4-hydroxy atorvastatin lactone	0.00	0.00	0.00

Bilirubin as potential endogenous biomarker for OATP function

Total bilirubin levels were measured in plasma and bile samples of the perfused livers (Figure 3.5), as bilirubin was recently recommended as an endogenous biomarker for OATP1B1/1B3 function[3,20]. Rifampicin, an inhibitor of multiple transporters including OATP1B1/1B3, should therefore also block the (re)uptake of (glucuronidated) bilirubin from the plasma. During the first 120 min of perfusion, when only the statins were administered to the livers, a stable concentration of plasma bilirubin was measured (Figure 3.5A). Upon rifampicin exposure (120-240 min of perfusion), an increase in total plasma bilirubin was measured in all livers. For all three statins, the AUC $_{120-240}$/AUC $_{0-120}$ ratio showed an mean ratio of 1.6 indicating interference of rifampicin on the hepatic uptake of (glucuronidated) bilirubin. Total bilirubin concentration in the bile decreased upon rifampicin exposure and a mean AUCR of 0.5±0.14 was measured (Figure 3.5B).
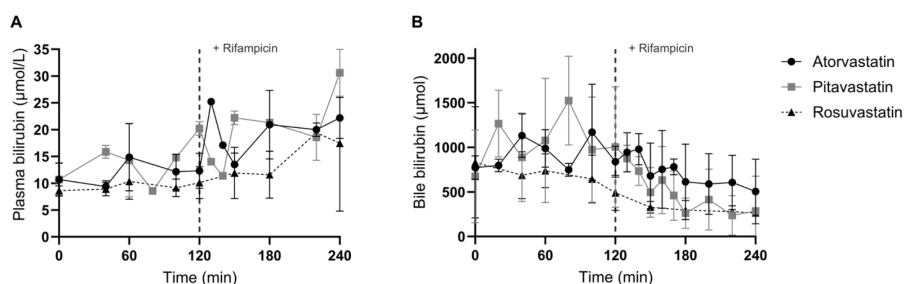
Figure 3.5 - Total bilirubin levels in plasma (A) en bile (B) of all liver perfusion experiments, discriminating atorvastatin (closed circles), pitavastatin (closed squares), and rosuvastatin (closed triangles), before (0-120 min) and after co-administration with perpetrator rifampicin (125-245 min).

First signs of drug induced toxicity by pitavastatin

Two out of 5 livers exposed to pitavastatin co-administrated with rifampicin were excluded from the PK analysis. Compared to the other three livers exposed to pitavastatin, these two livers demonstrated a delay in plasma clearance of pitavastatin and rifampicin with a plasma AUCR of 19.8 and 11.8 after the second bolus of pitavastatin (Figure 3.6A,C) and a lower hepatic extraction ratio of 0.5 for both affected livers (Figure 6H). Immediately after the second administration of pitavastatin, a reduction in the bile flow was observed for these two livers and the bile production completely stopped after 360 min of perfusion (Figure 3.6G). Upon the addition of rifampicin, these same livers showed an increase in plasma bilirubin compared to all the other perfused livers (60.1 µmol/L and 62.9 µmol/L at 360 min of perfusion) compared to the atorvastatin and rosuvastatin perfused livers (23.2±7.4 µmol/L at 360 min of perfusion) (Figure 6D). Plasma rifampicin concentrations were also elevated compared to the other livers exposed to pitavastatin (Figure 3.6C). To verify liver toxicity, plasma alanine aminotransferase (ALT) and aspartate transaminase (AST) levels were assessed (Figure 3.6E-F). The 2 livers showed increasing AST levels indicating induced liver toxicity. No effect on ALT was measured as all livers showed stable ALT levels reaching a plateau phase after 60 min (Figure 3.6F). Altogether, these results indicate a potential (start of) pitavastatin-induced hepatotoxicity in the form of impaired drug and bilirubin clearance and compromised bile production.

Protein expression of hepatic transporters

Figure 3.7 shows the absolute expression of drug transporters in liver tissue of porcine (domestic pig) and human origin. While the expression of the main transporter proteins BCRP, MDR1, MRP1, MRP2, GLUT1 and MCT1 was similarly abundant in porcine and human livers, the expression of OCT1 was approximately 1.8-fold higher in human livers compared to porcine livers ($P<0.001$). In contrast, the expression of BSEP, MRP3, NTCP, and OATP2B1 was 1.9, 1.7, 1.7 and 2.6 fold higher respectively in porcine livers than in human livers ($P<0.01$). OATP1B4 is the porcine ortholog for OATP1B1 and OATP1B3. The expression of OATP1B1 and OATP1B3 in human liver together, was significantly lower ($P<0.05$) to the protein expression level of OATP1B4 in porcine livers (2.8±1.0 fmol/mg tissue in human livers 5.8±1.8 fmol/mg tissue in porcine liver).
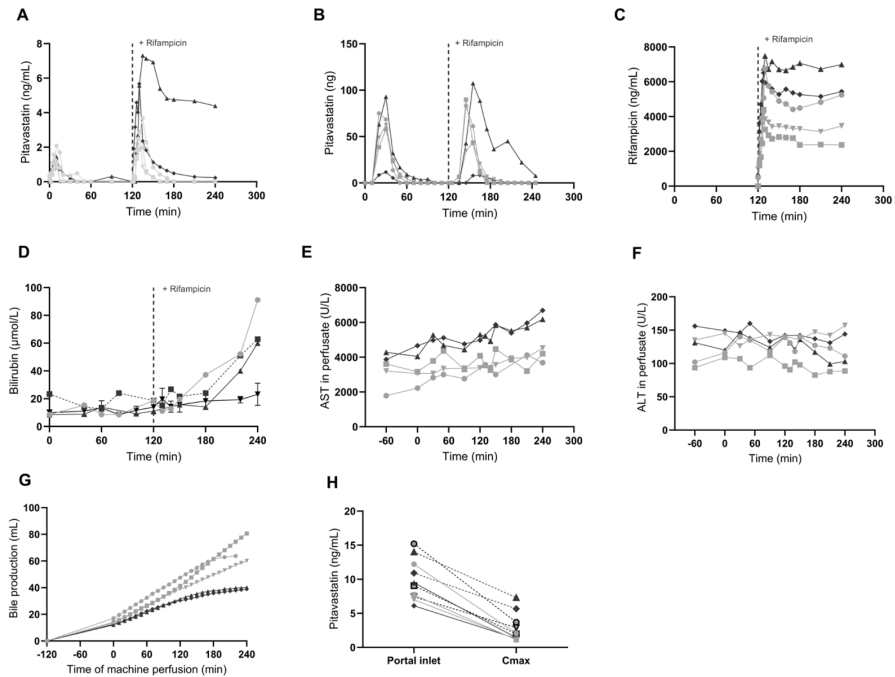
Figure 3.6 - First signs of drug induced liver toxicity in 2 of 5 livers exposed to pitavastatin (0.141 mg). These 2 livers are indicated with red lines, compared to the other three livers in grey. (A) plasma pitavastatin levels of 2 livers which showed signs of pitavastatin induced liver toxicity by the disability to take up pitavastatin compared to the other livers (B) biliary clearance of pitavastatin (C) plasma rifampicin concentration (D) plasma bilirubin increases dramatically after rifampicin co-administration compared to the atorvastatin and rosuvastatin perfused livers (black line) (E) plasma AST levels (F) plasma ALT levels and (G) total bile production during 360 min of perfusion (H) hepatic extraction during dosing *ex vivo* perfused livers (dotted lined represents the co-administration of rifampicin)
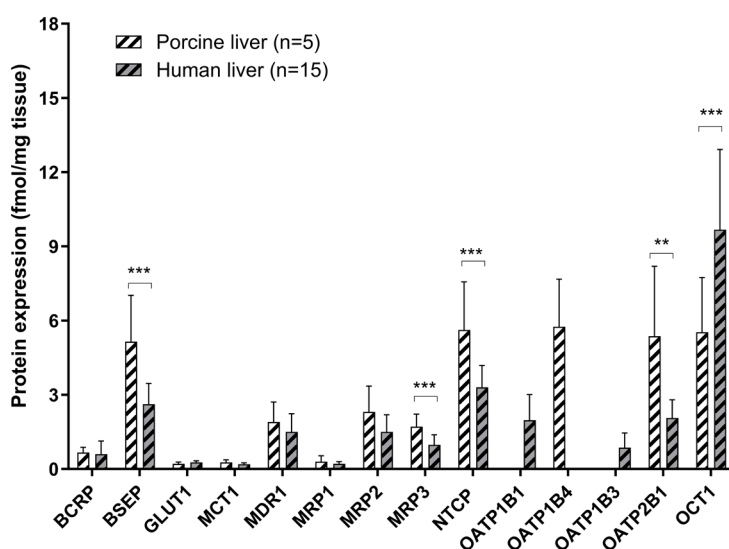
Figure 3.7 - Absolute expression (fmol/mg tissue) of various uptake and efflux transporter proteins within the plasma membrane of porcine livers (n=5) compared to the protein expression in human liver (n=15). Significant differences are denoted as asterisks (Students t-test * $P<0.05$, ** $P<0.01$, ***$P<0.001$).

Discussion

The ability to study biliary excretion and intracellular concentrations provides valuable information regarding metabolism and excretion of the drug. Thus far, to predict the hepatobiliary disposition of drugs, experimental studies have been performed using sandwich cultured hepatocytes, isolated perfused organ systems with rat livers or cannulated animal studies. In this study we perfused porcine livers using a novel advanced pressure driven perfusion machine, with a red blood cell-based perfusate which is suitable for normothermic and oxygenated conditions[12,21,22]. We describe for the first time the use of NMP of porcine livers to predict human hepatobiliary disposition – and DDI of drugs as demonstrated by using known OATP substrate drugs such as atorvastatin, pitavastatin and rosuvastatin with known OATP inhibitor, rifampicin as a perpetrator drug. Hepatobiliary toxicity in humans is poorly predicted from animal studies, primarily due to the fact that many animals differ markedly from humans in response to pharmacological agents[14]. In contrast to dogs, mice and rats, there is not much data on pigs in preclinical testing. Nevertheless, for

more complex research questions, *ex vivo* models from pig origin are regularly used to study intestinal absorption or the hepatic and biliary disposition of drugs[23-27]. In a comprehensive overview, Vaessen and co-workers provided protein and mRNA expression in human and pig intestinal tissues for a variety of transporters and enzymes. In general the protein and mRNA expression were well comparable between humans and pigs[19]. Furthermore, Elmorsi and co-workers recently showed a proteomic characterization of drug metabolizing enzymes and transporters in the pig liver showing the high resemblance with humans[15]. These data on transporters are in line with the proteomic data we show here comparing transporter protein expression in pig livers to the expression in human liver tissue. Except for the expression of BSEP, MRP3, NTCP, OATP2B1 and OCT1, no significant differences were observed in the expression of other transporter proteins. There is no porcine homologue for the human OATP1B1 however, porcine livers shown to express OATP1B4, which is the homologue of OATP1B3 showing 84% similarity ([15,28]).Although an almost 2-fold difference in human OATP1B1/1B3 vs pig OATP1B4 protein expression was observed, the obtained AUCR's were comparable to the human in vivo condition. Despite these differences, we here provide evidence that AUCR can be predicted by making use of ex vivo porcine NMP. The compounds tested are very good OATP (and NTCP) substrates and the results suggest that the hepatic uptake contributes to a similar percentage to the total clearance in humans and pigs. Other factors such as permeability differences between species and Km differences (for OATP-mediated uptake transporters) may compensate for the protein expression differences.

For this study, three statins were selected to study transporter-mediated DDI at the hepatic level. These statins, atorvastatin, rosuvastatin and pitavastatin, are listed as clinical substrates for the assessment of OATP1B1 and OATP1B3[2]. Additionally, the clearance of these drugs is mediated via diverse mechanism: CYP3A4 and OATP for atorvastatin, MRP2 and BCRP for rosuvastatin and BCRP for pitavastatin. All three statins showed to be good substrates for the uptake transporters, since a hepatic extraction ratio of >0.7 was observed. This is in line with clinically observed data[29,30] demonstrating that the experimental set-up is sufficient to predict the hepatic extraction ratio in humans.

In previous studies, statins have been applied to several preclinical models to predict rifampicin induced DDI. Bergman et al. performed an *in vivo* human study where rosuvastatin was administered into the jejunum via a Loc-I-Gut-

catheter[29]. The biliary clearance of rosuvastatin was measured after intestinal administration[29]. The C_{max} of rosuvastatin was detected 40 min after administration with a total biliary secretion of 11%; these data correspond very well to that from our experiments, showing a biliary secretion of 10%. Using the IPRL model, Lau et al. studied the interplay between transporters and enzymes in the disposition of atorvastatin (Lau et al. 2005). Compared to our porcine perfusion model, the IPRL model showed an extensively reduced interaction between atorvastatin and rifampicin. The biliary secretion in the IPRL model of atorvastatin was 7.4% while in our model the biliary clearance was 13.0±5.6%. Also, the effect of rifampicin on the inhibition of the biliary clearance was remarkably lower (21% in the IPRL vs. 50% in our model). The IPRL may therefore underpredict the DDI for atorvastatin and rifampicin. Together, these data show the IPRL model underpredicts the biliary clearance whereas a good comparability is observed between the porcine and human *in vivo* situation to the *ex vivo* perfused pig liver model. The metabolic activity of porcine livers during perfusion was shown by the presence of five different atorvastatin metabolites in the bile. The presence of all these metabolites in our study indicates that CYP3A4, CYP2C8 and UGT1A3 are metabolically active in the perfused pig liver[31-33].

In the experiments with atorvastatin, variability in AUCR was observed between replicates. Although rifampicin was administered in a similar slow bolus in each experiment, variability in plasma rifampicin concentrations were observed, possibly due to experimental handling and difference in total perfusate volume. Additionally, in clinical studies, the highest variation in AUCR is also observed for atorvastatin compared to the pitavastatin and rosuvastatin groups[1,2,34]. Our results showed a relation between plasma rifampicin AUC and AUCR for atorvastatin, while minor variation was observed for the pitavastatin and rosuvastatin group (Figure 3.3B). A comparable concentration-dependent inhibition effect of rifampicin on atorvastatin clearance was previously shown *in vivo* by Takehara et al. 2018 and Mori et al. 2019 and in vitro by Lau et al.[35]. Upon co-administration with rifampicin, the most profound effect was observed for atorvastatin (AUCR of 7.24), followed by rosuvastatin (AUCR of 3.07) and pitavastatin (AUCR of 3.03). As can be observed in Table 3.5, this same absolute AUCR as well as rank order of DDI magnitude was observed in studies with healthy volunteers[1,2,34].

Table 3.5 - Comparison of plasma AUCR between the NMP porcine liver model and in vivo studies. In all three clinical studies, the statins were dosed as a cocktail in healthy volunteers.

	NMP porcine liver model (current study)	Mori et al. 2019[1]	Takehara et al. 2018[2]	Prueksaritanont et al. 2016[34]
Atorvastatin	7.24	7.29	6.1	10.01
Pitavastatin	2.63	4.01	2.8	4.45
Rosuvastatin	3.10	2.48	2.4	5.38

In this study, pitavastatin exposure showed to affect hepatic function in 2 out of 5 perfused livers. Pitavastatin is one of the least prescribed statins[36] and although there are infrequent cases known of pitavastatin induced liver injury, it is known that pitavastatin can increase plasma AST, ALT and bilirubin concentration in the clinic[37-40]. Here, increased plasma AST was observed in 2 out of 5 livers exposed to pitavastatin. These same livers also showed the lowest bile production, the lowest bile bilirubin AUCR, the most profound effect on the hepatic extraction ratio and a prolonged ICG half-life (Figure S3.3). Together, these results indicate the first signs of acute drug-induced hepatoxicity. The therapeutic dose of pitavastatin is between 1–4 mg daily. However, the FDA prescribes not to exceed 2 mg once daily when patients also take rifampicin. Rifampicin significantly increases the Cmax of pitavastatin and therefore also increases the risk of rhabdomyolysis and myopathy[41]. In our study, the repeated dosing of pitavastatin could have resulted in hepatic injury due to affecting the ATP levels of the liver. Viola et al. showed a dramatic depletion of ATP in keratinocyte-irradiated cells which were exposed to pitavastatin[42]. Since the uptake and excretion of pitavastatin, bilirubin and rifampicin are ATP dependent processes, depletion of ATP resulted in a deteriorated functioning of these processes. A decrease in ATP levels may result in apoptosis and eventually necrosis[42]. This might be an explanation of our observations. To our knowledge, there is no other preclinical model which showed these acute adverse effects of pitavastatin in the liver.

Lately, the interest in endogenous biomarkers reflecting transporter involvement has increased. An example of such an endogenous biomarker is bilirubin. Due to the role of OATP1B1 and OATP1B3 in bilirubin uptake, bilirubin could serve as an endogenous biomarker for OATP1B1 and -1B3 related DDIs in the liver[3,20]. In our model, after administration of rifampicin, a direct increase in plasma bilirubin concentration was measured (AUCR 1.89) showing the direct inhibition of OATP-mediated hepatic uptake of (glucuronidated) bilirubin.

Furthermore, a decrease in biliary total bilirubin concentration was measured after the addition of rifampicin reflecting the inhibition of MRP2 and possibly UGT1A1. Unfortunately, no good correlation between plasma rifampicin concentration and plasma and bile bilirubin AUCR was observed, indicating that bilirubin fits more as a control marker rather than a precise biomarker. The current practice involves the use of CP-I, CP-III and conjugated bile salts as clinical biomarkers for OATP's[1]. Therefore, studies should incorporate these suggested biomarkers upon assessing DDI potential of drugs.

Conclusion

In conclusion, we have demonstrated that NMP of porcine livers is a potential novel and reliable model to study OATP-mediated DDI and its effect on hepatic clearance, biliary excretion and plasma (metabolite) profile of statins. Overall, the rank order of DDI severity indicated in our experiments is in good agreement with clinical data, the lowest DDI for pitavastatin and the highest for atorvastatin, indicating the potential importance of this new *ex vivo* model in early drug discovery.

Acknowledgement

References

1. Mori D, Kashihara Y, Yoshikado T, Kimura M, Hirota T, Matsuki S, Maeda K, et al. Effect of OATP1B1 genotypes on plasma concentrations of endogenous OATP1B1 substrates and drugs, and their association in healthy volunteers. Drug metabolism and pharmacokinetics 2019;34:78-86.
2. Takehara I, Yoshikado T, Ishigame K, Mori D, Furihata K-i, Watanabe N, Ando O, et al. Comparative study of the dose-dependence of OATP1B inhibition by rifampicin using probe drugs and endogenous substrates in healthy volunteers. Pharmaceutical research 2018;35: 1-13.
3. Chu X, Chan GH, Evers R. Identification of endogenous biomarkers to predict the propensity of drug candidates to cause hepatic or renal transporter-mediated drug-drug interactions. Journal of pharmaceutical sciences 2017;106:2357-2367.
4. Yang X, Gandhi YA, Duignan DB, Morris ME. Prediction of biliary excretion in rats and humans using molecular weight and quantitative structure–pharmacokinetic relationships. The AAPS journal 2009;11:511-525.
5. Fagerholm U. Prediction of human pharmacokinetics—biliary and intestinal clearance and enterohepatic circulation. Journal of Pharmacy and Pharmacology 2008;60:535-542.
6. Ito K, Iwatsubo T, Kanamitsu S, Ueda K, Suzuki H, Sugiyama Y. Prediction of pharmacokinetic alterations caused by drug-drug interactions: metabolic interaction in the liver. Pharmacological reviews 1998;50:387-412.
7. FDA. In Vitro Drug Interaction Studies — Cytochrome P450 Enzyme- and Transporter-Mediated Drug Interactions Guidance for Industry. In; 2020.
8. Stevens LJ, Donkers JM, Dubbeld J, Vaes WH, Knibbe CA, Alwayn IP, van de Steeg E. Towards human ex vivo organ perfusion models to elucidate drug pharmacokinetics in health and disease. Drug metabolism reviews 2020;52:438-454.
9. Guillouzo A. Liver cell models in in vitro toxicology. Environmental health perspectives 1998;106:511-532.
10. Chu X, Bleasby K, Evers R. Species differences in drug transporters and implications for translating preclinical findings to humans. Expert opinion on drug metabolism & toxicology 2013;9:237-252.
11. Gores GJ, Kost LJ, Larusso NF. The isolated perfused rat liver: conceptual and practical considerations. Hepatology 1986;6:511-517.
12. Borie DC, Eyraud D, Boleslawski E, Lemoine A, Sebagh M, Cramer DV, Roussi J, et al. FUNCTIONAL METABOLIC CHARACTERISTICS OF INTACT PIG LIVERS DURING PROLONGED EXTRACORPOREAL PERFUSION: POTENTIAL FOR A UNIQUE BIOLOGICAL LIVER-ASSIST DEVICE1. Transplantation 2001;72:393-405.
13. Eshmuminov D, Becker D, Borrego LB, Hefti M, Schuler MJ, Hagedorn C, Muller X, et al. An integrated perfusion machine preserves injured human livers for 1 week. Nature biotechnology 2020;38:189-198.
14. Helke KL, Swindle MM. Animal models of toxicology testing: the role of pigs. Expert opinion on drug metabolism & toxicology 2013;9:127-139.
15. Elmorsi Y, Al Feteisi H, Al-Majdoub ZM, Barber J, Rostami-Hodjegan A, Achour B. Proteomic characterisation of drug metabolising enzymes and drug transporters in pig liver. Xenobiotica 2020;50:1208-1219.
16. Varma MV, Obach RS, Rotter C, Miller HR, Chang G, Steyn SJ, El-Kattan A, et al. Physicochemical space for optimum oral bioavailability: contribution of human intestinal absorption and first-pass elimination. Journal of medicinal chemistry 2010;53:1098-1108.
17. Wegler C, Gaugaz FZ, Andersson TB, Wiśniewski JR, Busch D, Gröer C, Oswald S, et al. Variability in mass spectrometry-based quantification of clinically relevant drug transporters and drug metabolizing enzymes. Molecular pharmaceutics 2017;14:3142-3151.

18. Bosgra S, van de Steeg E, Vlaming ML, Verhoeckx KC, Huisman MT, Verwei M, Wortelboer HM. Predicting carrier-mediated hepatic disposition of rosuvastatin in man by scaling from individual transfected cell-lines in vitro using absolute transporter protein quantification and PBPK modeling. European Journal of Pharmaceutical Sciences 2014;65:156-166.
19. Vaessen SF, van Lipzig MM, Pieters RH, Krul CA, Wortelboer HM, van de Steeg E. Regional expression levels of drug transporters and metabolizing enzymes along the pig and human intestinal tract and comparison with Caco-2 cells. Drug Metabolism and Disposition 2017;45:353-360.
20. Fromm M. Prediction of Transporter-Mediated Drug–Drug Interactions Using Endogenous Compounds. Clinical Pharmacology & Therapeutics 2012;92:546-548.
21. Boehnert M, Yeung J, Bazerbachi F, Knaak J, Selzner N, McGilvray I, Rotstein O, et al. Normothermic acellular ex vivo liver perfusion reduces liver and bile duct injury of pig livers retrieved after cardiac death. American Journal of Transplantation 2013;13:1441-1449.
22. Watson CJ, Kosmoliaptsis V, Randle LV, Gimson AE, Brais R, Klinck JR, Hamed M, et al. Normothermic perfusion in the assessment and preservation of declined livers before transplantation: hyperoxia and vasoplegia—important lessons from the first 12 cases. Transplantation 2017;101:1084.
23. Anzenbacher P, Soucek P, Anzenbacherová E, Gut I, Hruby K, Svoboda Z, Kvetina J. Presence and activity of cytochrome P450 isoforms in minipig liver microsomes: comparison with human liver samples. Drug Metabolism and Disposition 1998;26:56-59.
24. Bergman E, Lundahl A, Fridblom P, Hedeland M, Bondesson U, Knutson L, Lennernäs H. Enterohepatic disposition of rosuvastatin in pigs and the impact of concomitant dosing with cyclosporine and gemfibrozil. Drug metabolism and disposition 2009;37:2349-2358.
25. Kararli TT. Comparison of the gastrointestinal anatomy, physiology, and biochemistry of humans and commonly used laboratory animals. Biopharmaceutics & drug disposition 1995;16:351-380.
26. Stevens LJ, van Lipzig MM, Erpelinck SL, Pronk A, van Gorp J, Wortelboer HM, van de Steeg E. A higher throughput and physiologically relevant two-compartmental human ex vivo intestinal tissue system for studying gastrointestinal processes. European Journal of Pharmaceutical Sciences 2019;137:104989.
27. Westerhout J, van de Steeg E, Grossouw D, Zeijdner EE, Krul CA, Verwei M, Wortelboer HM. A new approach to predict human intestinal absorption using porcine intestinal tissue and biorelevant matrices. European Journal of Pharmaceutical Sciences 2014;63:167-177.
28. Dalgaard L. Comparison of minipig, dog, monkey and human drug metabolism and disposition. Journal of pharmacological and toxicological methods 2015;74:80-92.
29. Bergman E, Forsell P, Tevell A, Persson EM, Hedeland M, Bondesson U, Knutson L, et al. Biliary secretion of rosuvastatin and bile acids in humans during the absorption phase. European journal of pharmaceutical sciences 2006;29:205-214.
30. Elsby R, Hilgendorf C, Fenner K. Understanding the critical disposition pathways of statins to assess drug–drug interaction risk during drug development: it's not just about OATP1B1. Clinical Pharmacology & Therapeutics 2012;92:584-598.
31. Lau Y, Huang Y, Frassetto L, Benet L. Effect of OATP1B transporter inhibition on the pharmacokinetics of atorvastatin in healthy volunteers. Clinical Pharmacology & Therapeutics 2007;81:194-204.
32. Riedmaier S, Klein K, Winter S, Hofmann U, Schwab M, Zanger UM. Paraoxonase (PON1 and PON3) polymorphisms: impact on liver expression and atorvastatin-lactone hydrolysis. Frontiers in Pharmacology 2011;2:41.
33. Lau YY, Okochi H, Huang Y, Benet LZ. Pharmacokinetics of atorvastatin and its hydroxy metabolites in rats and the effects of concomitant rifampicin single doses: relevance of first-pass effect from hepatic uptake transporters, and intestinal and hepatic metabolism. Drug metabolism and disposition 2006;34:1175-1181.
34. Prueksaritanont T, Tatosian D, Chu X, Railkar R, Evers R, Chavez-Eng C, Lutz R, et al. Validation of a microdose probe drug cocktail for clinical drug interaction assessments for drug transporters and CYP3A. Clinical Pharmacology & Therapeutics 2017;101:519-530.

35. Lau YY, Okochi H, Huang Y, Benet LZ. Multiple transporters affect the disposition of atorvastatin and its two active hydroxy metabolites: application of in vitro and ex situ systems. Journal of Pharmacology and Experimental Therapeutics 2006;316:762-771.
36. Amiri M. Worldwide statins prescription pattern: is it similar. Biom Biostat Int J 2020;9:194.
37. Kumar P, Mangla B, Singh S. Pitavastatin: A Potent Drug. Int J Pharma Res Health Sci 2018;6:2070-2074.
38. Teramoto T, Shimano H, Yokote K, Urashima M. New evidence on pitavastatin: efficacy and safety in clinical studies. Expert opinion on pharmacotherapy 2010;11:817-828.
39. Bhatti H, Tadi P. Pitavastatin. StatPearls [Internet] 2020.
40. Thapar M, Russo MW, Bonkovsky HL. Statins and liver injury. Gastroenterology & hepatology 2013;9:605.
41. FDA. LIVALO (pitavastatin) tablets, for oral use. In; 2009.
42. Viola G, Grobelny P, Linardi MA, Salvador A, Dall'Acqua S, Sobotta Ł, Mielcarek J, et al. Pitavastatin, a new HMG-CoA reductase inhibitor, induces phototoxicity in human keratinocytes NCTC-2544 through the formation of benzophenanthridine-like photoproducts. Archives of toxicology 2012;86:483-496.
43. Mukhtar R, Reid J, Reckless J. Pitavastatin. International journal of clinical practice 2005;59: 239-252.
44. Schneck DW, Birmingham BK, Zalikowski JA, Mitchell PD, Wang Y, Martin PD, Lasseter KC, et al. The effect of gemfibrozil on the pharmacokinetics of rosuvastatin. Clinical Pharmacology & Therapeutics 2004;75:455-463.
45. Sjöberg Å, Lutz M, Tannergren C, Wingolf C, Borde A, Ungell A-L. Comprehensive study on regional human intestinal permeability and prediction of fraction absorbed of drugs using the Ussing chamber technique. European Journal of Pharmaceutical Sciences 2013;48:166-180.
46. Zwolska Z, Niemirowska-Mikulska H, Augustynowicz-Kopec E, Walkiewicz R, Stambrowska H, Safianowska A, Grubek-Jaworska H. Bioavailability of rifampicin, isoniazid and pyrazinamide from fixed-dose combination capsules. The International Journal of Tuberculosis and Lung Disease 1998;2:824-830.
47. Lennernäs H. Clinical pharmacokinetics of atorvastatin. Clinical pharmacokinetics 2003;42:1141-1160.
48. Kamiie J, Ohtsuki S, Iwase R, Ohmine K, Katsukura Y, Yanai K, Sekine Y, et al. Quantitative atlas of membrane transporter proteins: development and application of a highly sensitive simultaneous LC/MS/MS method combined with novel in-silico peptide selection criteria. Pharmaceutical research 2008;25:1469-1483.
.

Supplementary materials

Table S3.1 - Perfusate composition.

Components	Quantity
Red blood cells	1000 mL
Plasma	1000 mL
Calcium gluconate (10%)	10 mL
Sodium bicarbonate 8.4% solution	To pH of 7.4
Heparin	1000 IU
Fast-acting insulin	**Continuous infusion**
	(10 U/mL; 1mL/h)
Taurocholate	**Continuous infusion**
	(2% w/v; 10 mL/h)
Epoprostenol	**Continuous infusion**
	(80 µg in 100 mL; 10mL/h)
Heparin	**Continuous infusion**
	1041 U/h (1mL/h)
	Continuous infusion
Vitamin solution,	(1 mL/hr)
L-glutamine,	(1 mL/hr)
MEM essential acids and	(2 mL/hr)
Glutamax	(1 mL/hr)

Table S3.2 - Details of the LC/MS conditions used for the analysis of atorvastatin and atorvastatin metabolites, pitavastatin, rosuvastatin and rifampicin.

Compound	Column	Mobile Phase A	Mobile Phase B	Time (sec)	Mobile Phase B (%)	Flow (ml/min)
Atorvastatin, atorvastatin lactone, 2-hydroxy atorvastatin, 4-hydroxy-atorvastatin, 4-hydroxy atorvastatin lactone	Macmod; ACE 3 C18-AR; 30x2.1 mm	0.1% Formic Acid in 95:5 Water:Acetonitrile	0.1% Formic Acid in 50:50 Acetonitrile:Methanol	15 (Step) 60 (Ramp) 5 (Ramp) 30 (Step)	45 95 95 95	0.800
Pitavastatin				15 (Step) 60 (Ramp) 5 (Ramp) 30 (Step) 40 (Step)	30 70 95 95 30	
Rosuvastatin				15 (Step) 60 (Ramp) 30 (Step) 40 (Step)	40 80 95 40	
Rifampicin	Waters; Xbridge C8; 50x2.1 mm			30 (Step) 120 (Ramp) 50 (Step) 40 (Step)	30 70 95 30	0.700

Table S3.3 - The Multiple Reaction Monitoring Transition (MRM) of Compounds.

Compound	MRM Transition(m/z)
Atorvastatin	559.30→466.00
Atorvastatin lactone	541.30→448.10
2-hydroxy atorvastatin	575.40→440.00
2-hydroxy atorvastatin lactone	557.30→448.10
4-hydroxy atorvastatin	575.30→440.20
4-hydroxy atorvastatin lactone	557.40→448.10
Pitavastatin	422.20→318.10
Rosuvastatin	482.10→258.20
Rifampicin	823.50→399.20
Glyburide (internal standard)	494.20→369.10
Carbamazepine (internal standard)	237.10→194.10
Rifampicin_d3 (internal standard)	826.50→794.70
Chrysin (internal standard)	255.10→153.00

Table S3.4 - Multiple reaction monitoring (MRM) transitions of the various peptides and the corresponding internal standard (AQUA) used. The peptide sequences were chosen according to the in silico peptide criteria defined by Kamiie et al.[48] and are exclusively present in the selected protein of interest.

Name	Labelled	Peptide sequence[a]	MW	Q1	Q3-1	Q3-2	Q3-3
BCRP	unlabelled	SSLLDVLAAR	1.044.2	522.8	644.3	757.5	529.4
	AQUA	SSLLDV**L**AAR	1.060.2	526.3	651.3		
BSEP	unlabelled	STALQLIQR	1.029.2	515.3	657.4	841.6	529.4
	AQUA	STALQ**L**IQR	1.045.2	518.8	664.3		
GLUT-1	unlabelled	VTILELFR	990.2	495.8	790.5	677.4	201.2
	AQUA	VTILELFR	1.00.2	500.8	800.5		
MCT-1	unlabelled	SITVFFK	841.0	421.2	173.3	641.3	201.1
	AQUA	SITVFFK	851.0	426.2	651.3		
MDR1	unlabelled	AGAVAEEVLAAIR	1269.5	467.7	719.4	216.1	618.4
	AQUA	AGAVAEEV**L**AAIR	1276.5	471.2	726.5		
MRP-1	unlabelled	TPSGNLVNR	957.1	479.2	428.8	759.4	672.4
	AQUA	TPSGNLVNR	973.1	482.7	432.3		
MRP2	unlabelled	VLGPNGLLK	910.1	455.8	698.5	185.3	213.3
	AQUA	VLGPNGL**L**K	926.1	459.2	705.4		
MRP3	unlabelled	ALVITNSVK	944.1	472.8	760.4	661.4	548.4
	AQUA	ALVITNS**V**K	950.1	475.8	766.5		
NTCP-pig	unlabelled	GIYDGTLK	866.0	433.7	696.3	143.2	171.2
	AQUA	GIYDGT**L**K	882.0	437.2	703.4		
NTCP-human	unlabelled	GIYDGDLK	880.0	440.7	710.3	143.2	171.2
	AQUA	GIYDGDLK	896.0	444.2	717.3		
OATP-1B1	unlabelled	LNTVGIAK	815.0	408.2	399.4	588.3	288.2
	AQUA	LNTVG**I**AK	831.0	411.7	402.9		
OATP-1B3	unlabelled	IYNSVFFGR	1.102.3	551.8	826.5	249.1	526.2
	AQUA	IYNSVF**F**GR	1.112.3	556.8	836.4		
OATP-1B4-pig	unlabelled	LTLVGIAK	816.0	408.2	399.4	588.3	288.2
	AQUA	LTLVG**I**AK	832.0	411.7	402.9		
OATP-2B1	unlabelled	SSISTVEK	849.9	425.7	563.3	676.3	175.1
	AQUA	SSIST**V**EK	855.9	428.7	569.3		
OCT-1	unlabelled	LPPADLK	752.9	377.2	543.3	183.3	260.3
	AQUA	LPPAD**L**K	768.9	380.7	550.4		

Table S3.5 - Absolute expression (fmol/mg tissue) of various uptake and efflux transporter proteins within the plasma membrane of porcine livers (n=5) compared to the protein expression in human liver (n=15). Values are mean ± SD. (ND = non detected).

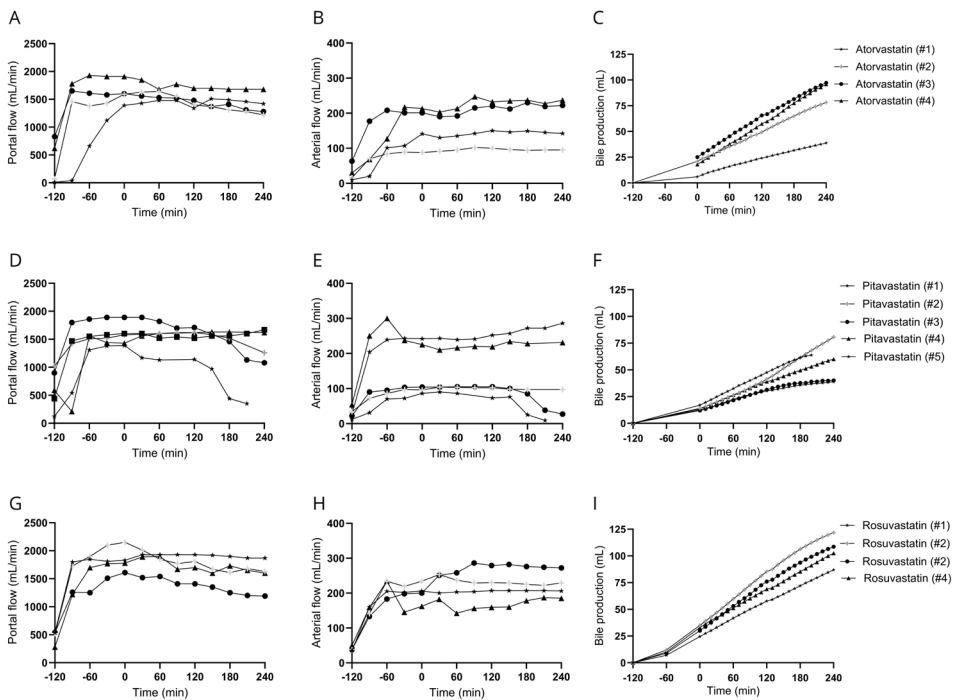|	Porcine livers (n=5)	Human livers (n=15)
BCRP	0.66 ±0.20	0.60 ±0.52
BSEP	5.15 ±1.77	2.62 ±0.82
GLUT-1	0.20 ±0.08	0.27 ±0.06
MCT1	0.27 ±0.09	0.19 ±0.05
MDR1	1.90 ±0.76	1.50 ±0.71
MRP1	0.30 ±0.23	0.21 ±0.09
MRP2	2.31 ±0.99	1.50 ±0.68
MRP3	1.71 ±0.48	0.98 ± 0.39
NTCP	5.62 ±1.82	3.30 ±0.86
OATP1B1	ND	1.97 ±1.01
OATP1B4	5.76 ±1.79	ND
OATP1B3	ND	0.86 ±0.58
OATP2B1	5.37 ±2.68	2.06 ±0.71
OCT1	5.53 ± 2.09	9.68 ±3.16

Figure S3.1 - Flow characteristics of all porcine livers during 360 min of normothermic perfusion, showing portal flow (A, D and G), arterial flow (B, E and H) and the cumulative bile production (C,F and I) livers exposed to atorvastatin, pitavastatin and rosuvastatin, respectively.
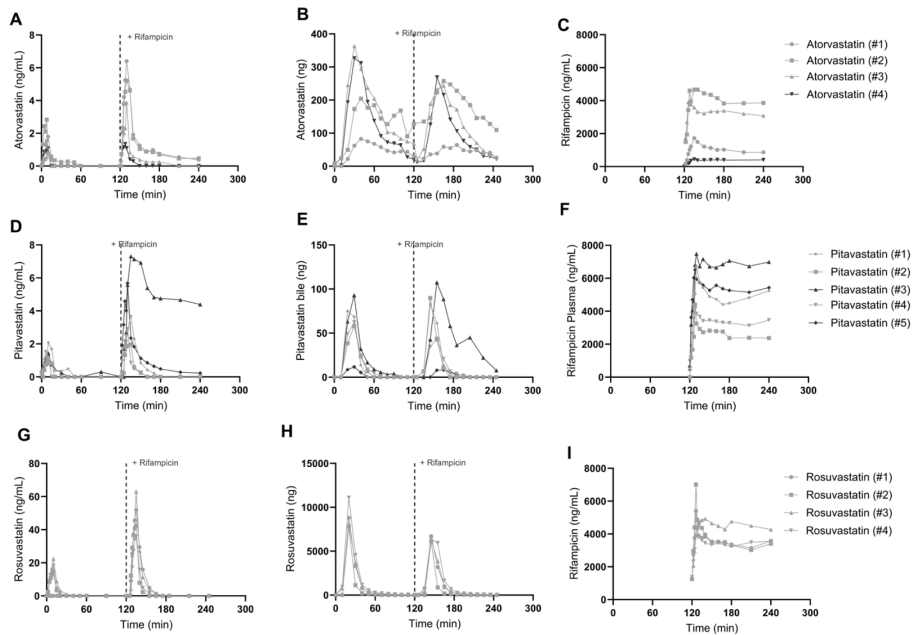
Figure S3.2 – Plasma en bile pharmacokinetic profiles of all perfused livers (n=14). Data excluded from PK analysis are represented with a black line, included data are presented in grey. PK of atorvastatin in (A) plasma and (B) bile, (C) showing the plasma rifampicin concentration of the livers exposed to atorvastatin, (D) PK of pitavastatin in plasma and (E) bile and (F) the plasma profile of rifampicin in livers exposed to pitavastatin. (G) PK of rosuvastatin in plasma and (H) bile and the plasma concentration of rifampicin in livers exposed to rosuvastatin
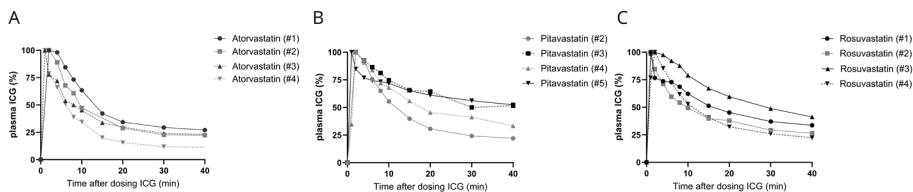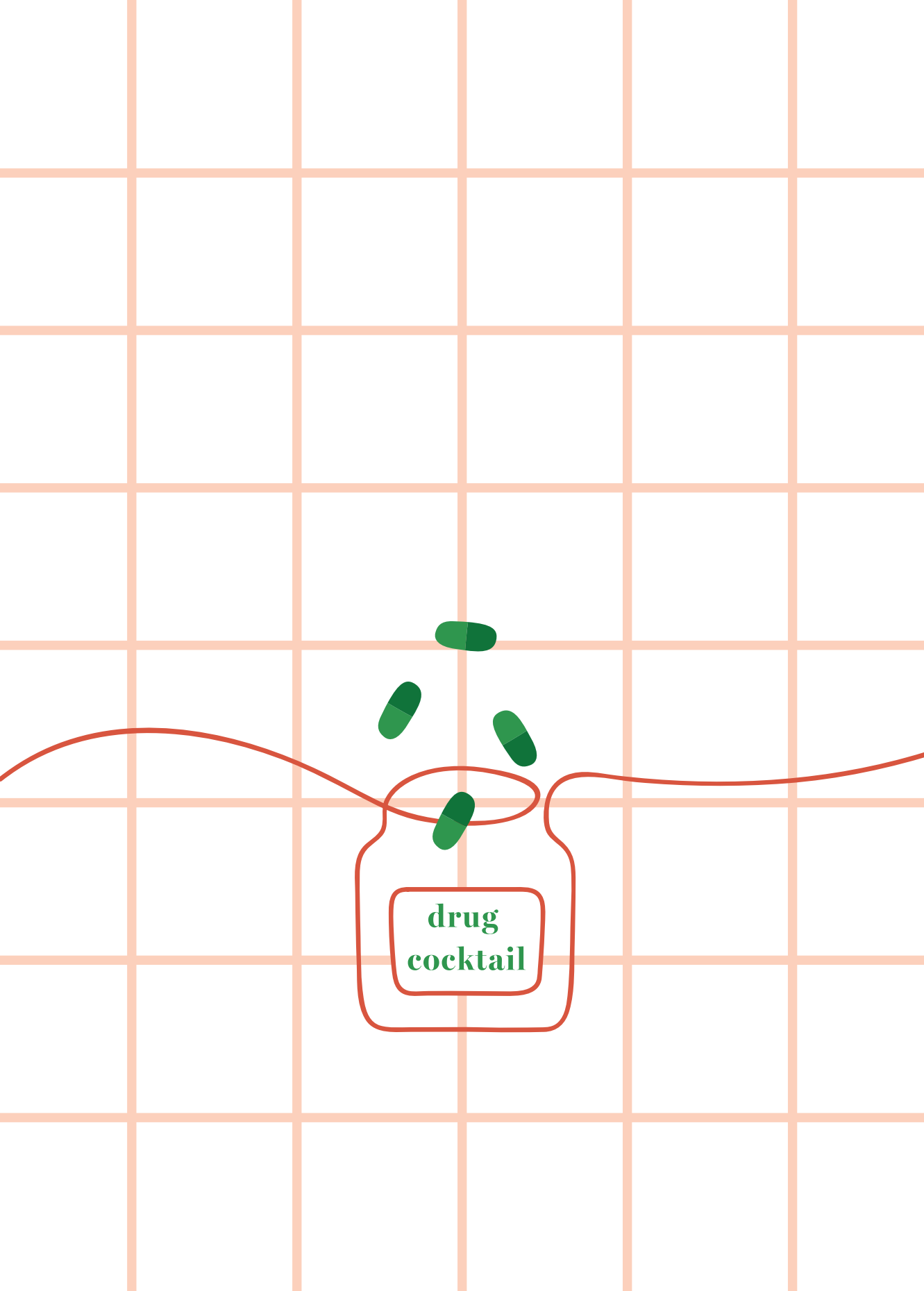

Figure S3.3 – indocyanine green (ICG) clearance from plasma upon dosing ICG as an IV bolus (10 mg) to the perfusate 360 min after starting the liver perfusion and exposing livers to atorvastatin 1-4 (A), pitavastatin 2-5 (pitavastatin 1 NA: due to decrease in portal and arterial and bile flow) (B) and rosuvastatin (C).

drug
cocktail

CHAPTER 04

Novel explanted human liver model to assess hepatic extraction, biliary excretion and transporter function

L.J. Stevens, J. Dubbeld, J.B. Doppenberg, B. Van Hoek, A.L. Menke, J.M. Donkers, A. Alsharaa, A. De Vries, W.H.J. Vaes, C.A.J. Knibbe, E. van de Steeg, I.P.J. Alwayn

Abstract

Realistic models predicting hepatobiliary processes in health and disease are lacking. We therefore aimed to develop a physiologically relevant human liver model consisting of normothermic machine perfusion (NMP) of explanted diseased human livers that can assess hepatic extraction, clearance, biliary excretion and drug-drug interaction

Eleven livers were included in the study, seven with a cirrhotic and four with a non-cirrhotic disease background. After explantation of the diseased liver, NMP was initiated. After 120 minutes of perfusion, a drug cocktail (rosuvastatin, digoxin, metformin and furosemide; OATP1B1/1B3, Pgp, BCRP and OCT1 model compounds) was administered to the portal vein and 120 minutes later, a second bolus of the drug cocktail was co-administered with perpetrator drugs to study relevant drug-drug interactions.

The explanted livers showed good viability and functionality during 360 minutes of NMP. Hepatic extraction ratios close to *in vivo* reported values were measured. Hepatic clearance of rosuvastatin and digoxin showed to be the most affected by cirrhosis with an increase in Cmax of 11.50 and 2.89 times, respectively, compared to non-cirrhotic livers. No major differences were observed for metformin and furosemide. Interaction of rosuvastatin or digoxin with perpetrator drugs were more pronounced in non-cirrhotic livers compared to cirrhotic livers.

Our results demonstrated that NMP of human diseased explanted livers is an excellent model to assess hepatic extraction, clearance, biliary excretion and drug-drug interaction. Gaining insight into pharmacokinetic profiles of OATP1B1/1B3, Pgp, BCRP and OCT1 model compounds is a first step towards studying transporter functions in diseased liver.

Introduction

Accurate prediction of drug disposition in patients with and without hepatic diseases remains difficult, as appropriate models are lacking. The liver plays an important role in drug handling and impairment or alteration of its function may greatly affect multiple processes. Upon first liver pass, after oral administration, drug bioavailability as well as drug clearance may be altered thereby affecting the drug's efficacy. Studies in liver cirrhosis have shown that increased bioavailability as well as reduced clearance lead to a higher prevalence of adverse drug reactions and drug-drug interactions which can result in safety issues and ultimately an increased risk for hospital admission[1,2]. Therefore, drug dosing should be tailored according to the varying degree of liver dysfunction among patients with liver diseases. However, with the currently available preclinical and clinical models, it remains difficult to quantify the required tailoring of the dose related to the degree and type of liver dysfunction[3].

Established *in vitro* and animal models are often used to study the pathology and pharmacological characteristics of drugs of varying diseases. However, translation of these findings to clinical practice remains challenging due to, among others, species differences in transporter expression and the difficulty to mimic dynamic liver processes[4,5]. Novel 3D models like liver-on-a-chip and bile duct-on-a-chip models have gained significant interest as a predictive platform to study liver processes due to the incorporation of haemodynamics[6,7]. Although these organ-on-a-chip models hold much promise, they are still in their infancy owing to the difficulty of mimicking (patho)physiological processes in the liver such as portal and arterial blood flow and biliary excretion[7]. Normothermic machine perfusion (NMP) systems using human *ex vivo* whole organs overcome this problem since hepatic architecture is combined with (near) physiological hemodynamics. Thereby, use of human explanted liver whole organ enables to study hepatobiliary processes as well as liver disease specific pharmacokinetics[8-10].

In this study we developed a novel hepatic model using diseased explanted human livers. Four model drugs (rosuvastatin, digoxin, furosemide and metformin) with and without perpetrator drugs were used to study hepatic extraction, clearance, biliary excretion and drug-drug interaction. These model

drugs are known substrates for different important hepatic uptake and efflux transporters and enabled comparison of the model to *in vivo* reported data.

Materials and methods

Human livers

Patients undergoing liver transplantation were included in this study. After providing informed consent, the patients approved the usage of the explanted liver for experimental study (Figure 4.1). The use of explanted liver tissue was approved by the medical ethical committee of the Leiden University Medical Center (B19.040). Patients with polycystic liver disease, with a transjugular intrahepatic portosystemic shunt, or waitlisted for recurrent- orthotopic liver transplantation were excluded from participation. Eleven human livers were included in the study. The underlying disease processes of these livers were primary biliary cholangitis (PBC, n=1), non-alcoholic fatty liver disease (NAFLD, n=2), alcoholic liver disease (ALD, n=3), hepatocellular carcinoma in the context of Hepatitis B viral disease (HBV+HCC, n=2). In addition, three discarded non-cirrhotic livers which were declined for transplantation were included in this study. The reasons for decline were; steatosis (n=2) and an occlusion of right hepatic artery (n=1). Immediately following explantation of the recipient diseased liver, a portal and arterial flush with cold Histidine-tryptophan-ketoglutarate (HTK) (Carnamedica, Warsaw, Poland) preservation solution was performed. The period between explantation (i.e. clamping and transection of the portal and hepatic veins as final step of the hepatectomy) and cold flush of the explanted liver (*ex vivo*), is described as the warm ischemia time (WIT). After a clean effluent flush, the liver was transported in cold preservation solution to the Organ Preservation and Regeneration room in the OR complex. Here, under sterile conditions, a back table reconstruction of the right and left hepatic artery and portal vein was performed using surplus donor blood vessels, in order to facilitate cannulation (portal vein- 25Fr cannula, hepatic artery – 12Fr cannula) and connection to the machine perfusion device (Liver Assist™ device, XVIVO, Groningen, the Netherlands). Thereafter, the bile duct was cannulated.

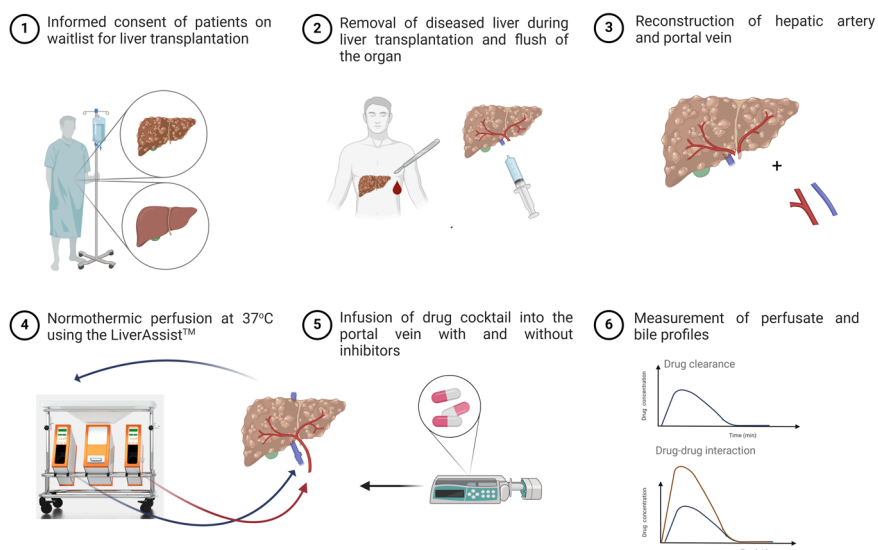**Ex vivo human explanted liver perfusion**

1. Informed consent of patients on waitlist for liver transplantation
2. Removal of diseased liver during liver transplantation and flush of the organ
3. Reconstruction of hepatic artery and portal vein
4. Normothermic perfusion at 37°C using the LiverAssist™
5. Infusion of drug cocktail into the portal vein with and without inhibitors
6. Measurement of perfusate and bile profiles

Figure 4.1 - Schematic representation of normothermic explanted human liver perfusion set-up.

Normothermic machine perfusion

All human livers were perfused using the Liver Assist™ device. The machine consists of two centrifugal pumps which provide a pulsatile flow to the hepatic artery and a continuous flow to the portal vein[11]. The system reservoir was filled with 2L perfusion fluid containing 1:1 ratio of human red blood cells and fresh frozen plasma (Sanquin, Amsterdam, the Netherlands). Insulin, sodium taurocholate, heparin and epoprostenol were provided as continuous infusion at a rate of 10U/h, 1041U/h, 10 mL/h (2% w/v) and 8 μg/h, respectively, in order to maintain liver functioning and to facilitate bile flow. Additionally, nutrients (aminoplasmal 10E (B Braun Melsungen AG, Melsungen, Germany) and cernevit (Baxter BV, Utrecht, the Netherlands) were continuously provided (23mL/hr) to keep the liver metabolically active (Supplemental Table S4.1). Gas delivery to the Liver Assist™ consisted of 95% oxygen and 5% carbon dioxide at 1.5 L/min and the temperature was set at 37°C. The non-cirrhotic livers were perfused with a portal pressure of 11 mmHg and the cirrhotic livers required perfusion at 14 mmHg to generate a sufficient portal flow. Mean arterial pressure was set at 50 mmHg. After 360 minutes of perfusion, the livers were submerged in

formaldehyde and transported the pathology department and were examined according to the institution's clinical guidelines dependent on the patient's underlying pathophysiology.

Drug administration during perfusion

Drug clearance in perfusate and bile of the drug cocktail (rosuvastatin, metformin, furosemide and digoxin) were determined in the absence and presence of perpetrator drugs (quinidine, rifampicin, cimetidine and probenecid)[12]. The dosage applied to the system were based on clinically prescribed oral dosage and calculated as previously described in Stevens et al. 2021[13]. In short, portal doses of the drug cocktail compounds and inhibitors were calculated based on the fraction absorbed in the intestine to the portal vein, fraction of metabolism and circulating volume (Supplemental Table S4.2). After 120 min. of perfusion, a slow bolus for 10 min of the drug cocktail was administered via the portal vein at 1 mL/min to mimic oral absorption through the gut. Subsequently, perfusate and bile samples were taken for the following 120 min. Arterial samples were taken at t=120, 122, 124, 126, 128, 130, 135, 140, 150, 160, 170, 180, 210, and 240 min. Additional portal samples were taken during the administration of the drug at t=126 and t=130 min to determine the hepatic extraction. Bile samples were collected in 10 minute fractions from 120 min onwards. After 240 min., first a slow bolus 10 min (1 mL/min) of perpetrator drugs (quinidine, cimetidine, rifampicin and probenecid) was administered to the liver and after 5 min (at t=245 min.), again, a subsequent slow bolus of the drug cocktail was administered via the portal vein. Biopsies were taken at the end of the first dose (t=240 min) and second dosing with inhibitors (t=360 min). The same sampling schedule for arterial samples and bile samples was followed. Perfusate and bile samples were immediately stored at ≤-70°C until further processing.

Liver function assessment

Hepatic artery and portal vein flow were recorded from the Liver Assist™ machine. Perfusate samples and bile samples (collected under mineral oil to prevent bile exposure to ambient air[14]) were taken hourly to monitor liver viability (pH, glucose, lactate etc.) using a RapidPoint 500 blood gas analyzer (Siemens, Germany). Alanine aminotransferase (ALT) concentration in the perfusate samples was measured by reflectance photometry (Reflotron-Plus system, Roche diagnostics, Almere, the Netherlands). Perfusate and bile

parameters were compared to defined criteria used in clinical transplantation studies; perfusate ALT <6000 and lactate <2.5 mmol/L after 120 min of perfusion, biliary pH >7.5 (15-17).

Histological analysis

Pre-perfusion (n=2) and post-perfusion (n=2) biopsies were taken for each liver, fixed in 10% formalin and subsequently embedded in paraffin. Slices of 4 µm were cut and stained with hematoxylin & eosin (H&E) for examination using light microscopy.

Bioanalysis

The concentration of the drug cocktail was quantified using LC-MS/MS (Waters, Etten-Leur, the Netherlands). Perfusate and bile sample (10 µL) were deproteinized with 100 µL acetonitrile (ACN) with the addition of 10 of µL the isotopically labelled internal standards (1 µg/mL). Thereafter samples were vortexed, centrifuged and supernatant was transferred to 96 well plate and dried under nitrogen. Thereafter, samples were dissolved in 100 µL 10% ACN + 0,1% formic acid and injected in to LC-MS/MS for quantification. Details of the LC-MS/MS conditions used are shown in Supplemental Table S4.3 and S4.4.

Chemicals

Rosuvastatin, digoxin, furosemide, quinidine were obtained from Sigma-Aldrich (Zwijndrecht, the Netherlands). Metformin and rifampicin and cimetidine were obtained from Bioconnect (Huissen, the Netherlands). Heparin, sodium taurocholate (Sigma-Aldrich, Zwijndrecht, the Netherlands), insulin (Novo Nordisk, Alphen aan den Rijn, the Netherlands) and epoprostenol (Flolan; GlaxoSmithKline Inc, Mississauga, ON, Canada) were obtained as indicated.

Data analysis and statistics

Data obtained during the perfusion studies was analyzed using Prism version 8 (GraphPad, California, USA). Values for the area under the concentration time curve 0 -120 min (AUC_{0-tau}) were calculated using the linear trapezoidal method. The area under the concentration time curve ratio (AUCR) was determined by dividing the $AUC_{125-245\ min}$ (with inhibitors) by the $AUC_{0-120\ min}$ (without inhibitors). The hepatic extraction ratio was calculated during the 10 min dosing period as following: concentration entering the liver (portal vein) - concentration leaving

the liver / concentration entering the liver. Significance of differences between the cirrhotic and non-cirrhotic livers was tested using the Mann-Whitney U test. Data is presented as median and inter-quartile range (IQR) for non-parametric distributed data. P-value below 0.05 was considered significant.

Results

Explanted livers showed good viability during perfusion

Both cirrhotic (n=7, characteristics Table 4.1) and non-cirrhotic (n=4, characteristics Table 4.1) livers had a stable arterial flow with minimal variation during perfusion; 235 mL/min (IQR:214.7-249) in cirrhotic livers vs. 230 mL/min (IQR:21.3-239.5) in non-cirrhotic livers (Figure 4.2A). A significant lower portal flow in cirrhotic livers was observed compared to non-cirrhotic livers of 523 mL/min (IQR:489-557) vs. 1678 mL/min (IQR:1596-1710)), respectively, p<0.001 (Figure 4.2B). Figure 4.2C demonstrates perfusate lactate, which is a marker of liver function. Lactate clearance was observed after 30 min of perfusion in the non-cirrhotic liver group and remained low (1.39 mmol/L (IQR:0.48-.29)), while cirrhotic livers showed higher levels of perfusate lactate (13.25 mmol/L (IQR:3.20-22.91) after 360 min of NMP). As marker of hepatocellular injury, release of ALT was measured throughout the perfusion (Figure 4.2D). Levels of ALT reached a plateau after 60 min of perfusion and remained stable until 360 min of perfusion. ALT levels were significantly higher in the non-cirrhotic livers compared to the cirrhotic livers (p=0.017). All livers produced bile during perfusion, but significantly more bile was produced by the cirrhotic livers 55 mL (IQR:37-61) vs. 28 mL (IQR:22-60)) p=0.034 (Figure 4.2E). The pH of produced bile during perfusion showed to be >7.5 in cirrhotic as well as non-cirrhotic livers (Figure 4.2F), demonstrating good cholangiocyte viability and meeting the defined viability criteria. To investigate the effect of perfusion on the integrity of the livers, biopsies of the livers pre-, and post-perfusion were stained with H&E. Figure 4.2G shows a representative example of a non-cirrhotic liver and a cirrhotic liver, before perfusion and post-perfusion (t=360 min). The histopathological analysis indicated that the perfusion did not have obvious detrimental morphological effects on the liver tissue. Additional markers of hepatocellular injury and function and cholangiocyte viability can be found in Supplemental Figure S4.1. Gene expression data of housekeeping genes, transporters and enzymes can be found in Supplemental Figure S4.2.
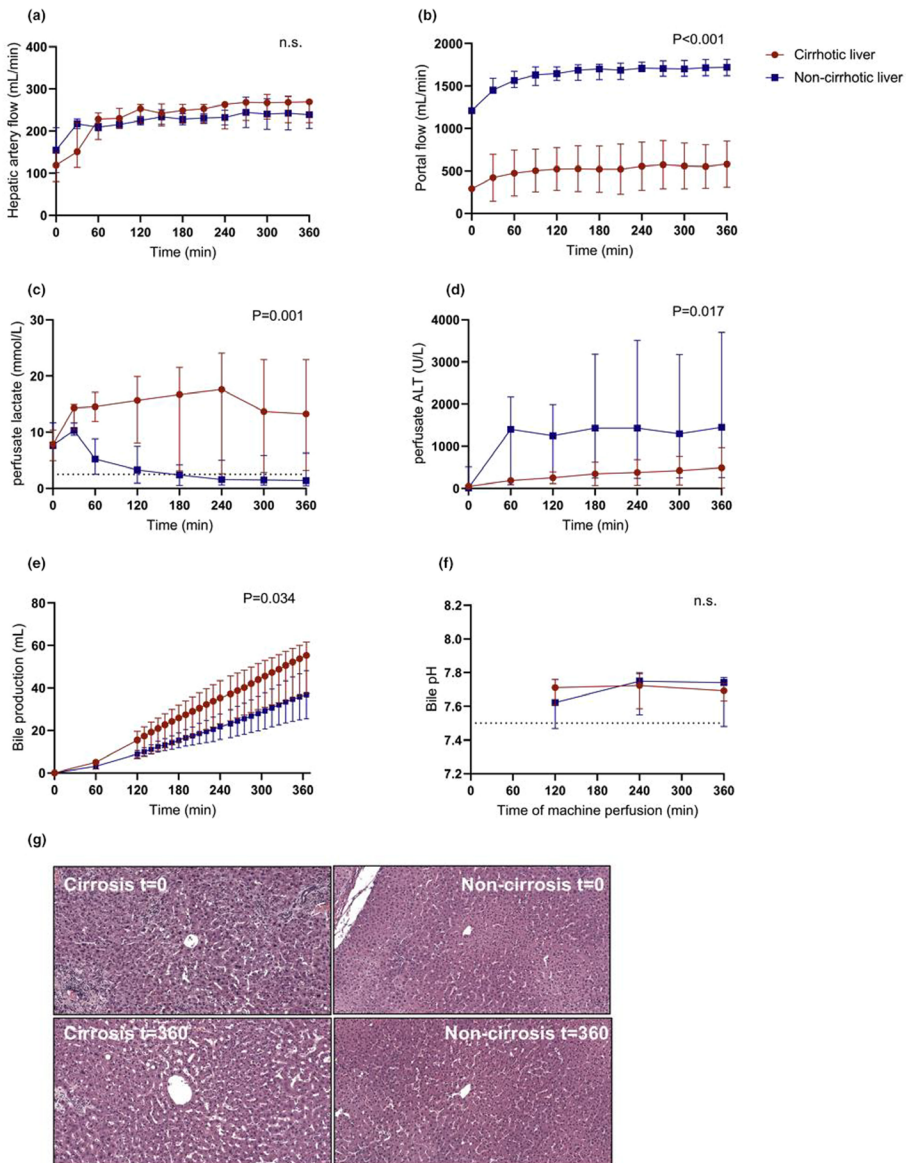
Figure 4.2 - Liver functionality, viability, and injury markers measured in perfusate, bile, and tissue of normothermic perfused cirrhotic and noncirrhotic livers. (a) hepatic artery flow, (b) portal flow, (c) perfusate lactate, (d) perfusate ALT levels (e) bile production (f) biliary pH and of cirrhotic and noncirrhotic livers measured during 360 minutes of normothermic perfusion. (g) H&E staining of a cirrhotic liver and noncirrhotic liver, before perfusion (t=0) and after perfusion (360 minutes; 200×). Data represent median and interquartile range in cirrhotic (n=7) and noncirrhotic livers (n=4). Differences between groups were analyzed using the Mann–Whitney U test; P value is presented in the right corner of each graph. ALT, alanine aminotransferase; H&E, hematoxylin and eosin; n.s., not significant.

Table 4.1 - Liver characteristics and ischemic times of cirrhotic and non-cirrhotic livers.

	Cirrhotic livers N=7	Noncirrhotic livers N=4	P values
Underlying disease	ALD (n=3) NAFLD (n=2) HBV+HCC (n=1) PBC (n=1)	Discarded liver (n=3) HBV+HCC (n=1)	n.a.
Age, years	59 (54–69)	63 (30–67)	0.545
Gender			
Male	6	4	
Female	1	0	
BMI, kg/m^2	29.4 (23.8–31.4)	26.8 (26.0–28.8)	>0.99
WIT, minutes	5 (4–6)	12 (5–14)	0.067
CIT, minutes	80 (71–99)	270 (105–507)	0.070
Weight of the liver, g	1,507 (1,297–2,005)	1,975 (1,394–2,008)	0.648
MELD	11 (9–23)	6 (6–6)	0.006

Differences between groups were analyzed using the Mann–Whitney U test. ALD, alcoholic liver disease; BMI, body mass index; CIT, cold ischemia time; HBV, hepatitis B virus; HCC, hepatocellular carcinoma; MELD, model of end stage liver disease; n.a., not applicable; NAFLD, nonalcoholic fatty liver disease; PBC, primary biliary cholangitis; WIT, warm ischemia time..

Hepatic clearance and biliary excretion of rosuvastatin and digoxin are affected by cirrhosis

To assess hepatic clearance and biliary excretion, a drug cocktail was infused to the portal vein (Figure 4.3, Supplemental Figure S4.3, Supplemental Table S4.1). Perfusate concentrations of rosuvastatin appeared to be the most affected by liver cirrhosis, with an approximate 11.5-fold increased Cmax in cirrhotic livers compared to the perfused non-cirrhotic livers (463.3 ng/mL (IQR: 243.2-555.2) vs. 41.10 ng/mL (IQR: 7.01-71.02), p=0.024) and 190-fold increased AUC$_{0-tau}$ of 20.96 µg/mL (IQR: 11.61-29.98) vs. 0.11 µg/mL (IQR:0.10-5.15, p<0.001) (Figure 4.4A). A comparable effect was observed for digoxin, with a perfusate Cmax that was more than 3-fold higher in cirrhotic livers (10.03 ng/mL (IQR:7.75-11.78)) compared to non-cirrhotic livers (3.46 ng/mL ng/mL (IQR:2.33-7.80, p=0.038)) and an AUC$_{0-tau}$ that was almost 3-fold higher; 629 ng/mL (IQR:282-746) in cirrhotic livers versus 222 ng/mL (IQR:171-503) in non-cirrhotic livers, p=0.003 (Figure 4.4D). Biliary excretion of rosuvastatin and digoxin was higher in cirrhotic livers (66% and 51% respectively) compared to non-cirrhotic livers (47% and 17%, respectively), however not significant (Figure 4.4B,E). Figure 4.4C and 4.4F show lower intrahepatic levels of rosuvastatin and digoxin respectively in cirrhotic livers compared to non-cirrhotic livers which is in line with the biliary excretion. As can be observed in Figure 4.4G-L, cirrhosis had a minor effect on furosemide and metformin concentrations as Cmax was 1.19 and 1.13 times higher in cirrhotic livers compared to non-cirrhotic livers (not significant). Metformin and furosemide were only minimally cleared through biliary

excretion (in the range of 1-3%) which was not affected by the cirrhosis (Figure 4.4H,K) and also intrahepatic levels were comparable between cirrhotic and noncirrhotic livers (Figure 4.4I,L).
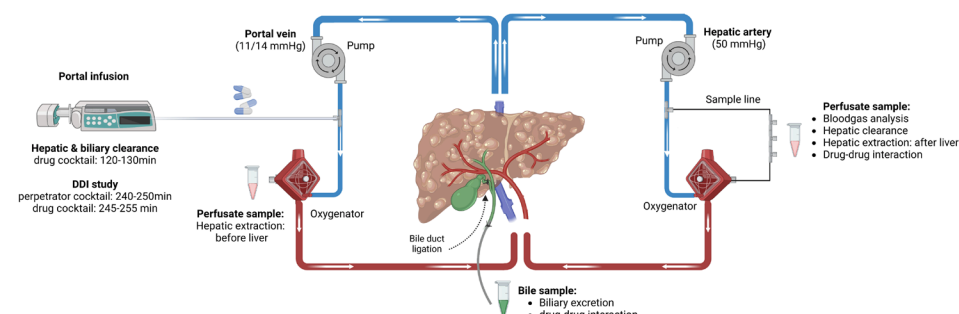

Figure 4.3 - Schematic representation of normothermic machine perfusion setup of the liver to study drug hepatobiliary processes. DDI, drug-drug interaction.

Hepatic extraction of rosuvastatin affected by cirrhosis

A unique application of the perfusion model is to sample from the portal vein (before the liver) and hepatic artery (after liver sample) during the dosing period (Figure 4.5A), enabling to determine the hepatic extraction ratio (Figure 4.5B). A high hepatic extraction by the non-cirrhotic livers of rosuvastatin was measured; 0.70 (IQR:0.69-0.83), which showed to be affected by cirrhosis (0.57 (IQR:0.42-0.67)). The hepatic extraction of digoxin, furosemide and metformin, which are low hepatic extraction ratio drugs, did not show to be affected by cirrhosis.
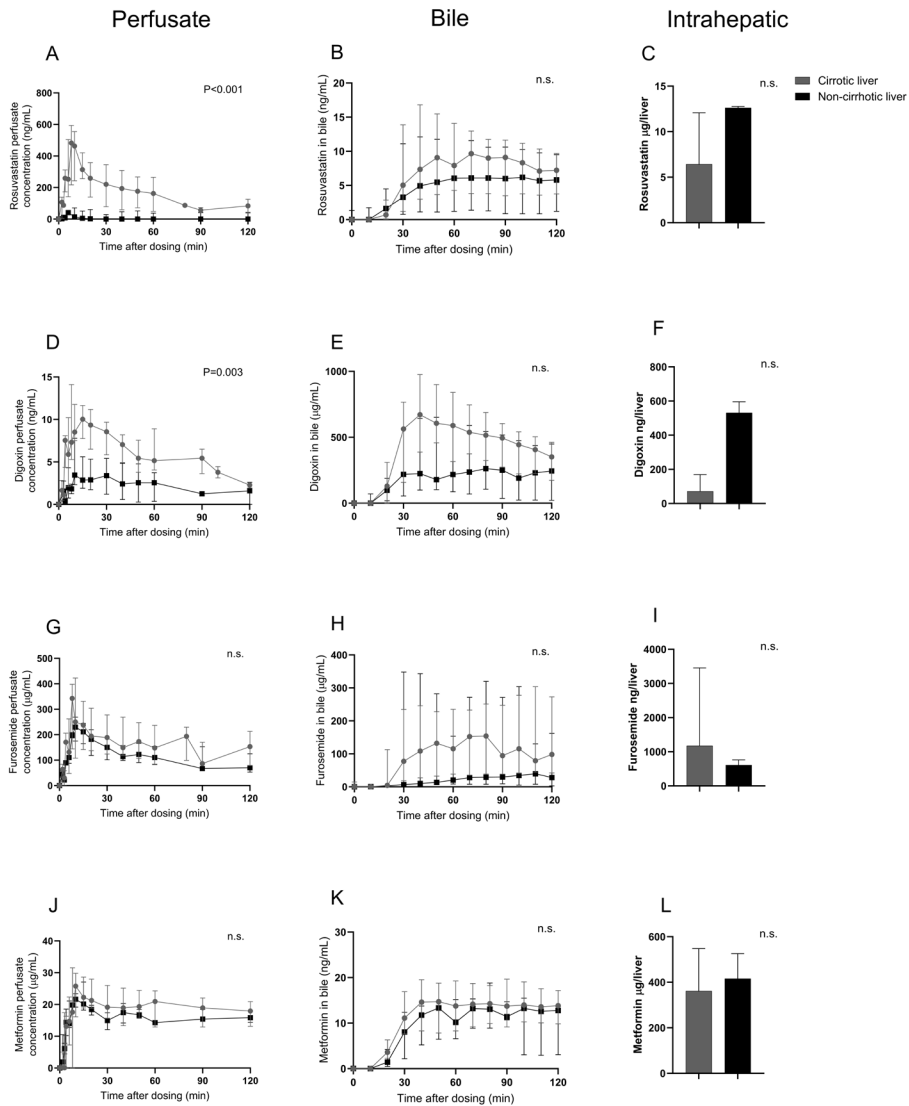
Figure 4.4 - Pharmacokinetic profiles of rosuvastatin, digoxin, metformin, and furosemide in cirrhotic and noncirrhotic perfused livers. Rosuvastatin (applied dose of 1.80 mg) (a) perfusate levels, (b) biliary excretion of rosuvastatin, and (c) intrahepatic rosuvastatin levels. Digoxin (applied dose of 0.11 mg) (d) perfusate levels, (e) biliary excretion of digoxin, and (f) intrahepatic digoxin levels. Furosemide (applied dose of 0.77 mg) (g) perfusate levels, (h) biliary excretion of furosemide, and (i) intrahepatic furosemide levels. Metformin (applied dose of 74.40 mg) (j) perfusate levels, (k) biliary metformin excretion, and (l) intrahepatic metformin levels. Data represent median and interquartile range in cirrhotic (*n*=7) and noncirrhotic livers (*n*=4) for perfusate and bile. There were five in the cirrhotic and three in noncirrhotic livers for intrahepatic data. Differences in AUC between groups were analyzed using the Mann–Whitney *U* test; *P* value is presented in the right corner of each graph. AUC, area under the concentration time curve; n.s., not significant.
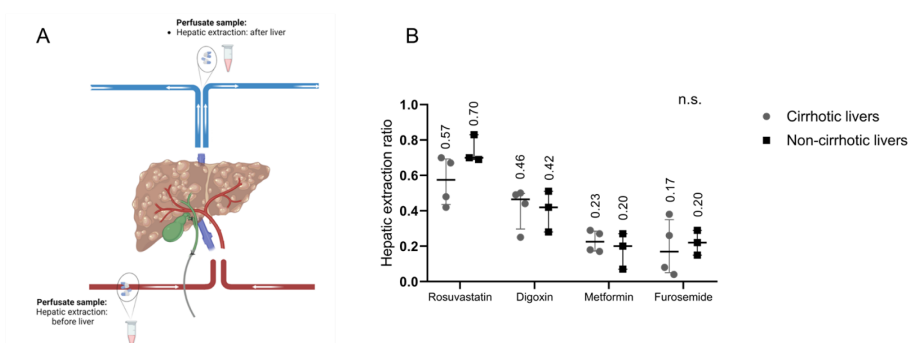
Figure 4.5 - Hepatic extraction of drug cocktail compounds. (a) Schematic representation of sample points before and after liver (b) hepatic extraction ratio of rosuvastatin, digoxin, metformin, and furosemide (*n*=3 noncirrhotic livers and *n*=4 cirrhotic livers). Differences between groups were analyzed using the Mann–Whitney *U* test; *P* value is presented in the right corner of each graph. n.s., not significant.

Increased risk of drug-drug interaction for rosuvastatin and digoxin

Figure 4.6 shows the results of the studies in which different drugs were used to inhibit the uptake and /or excretion of the drug cocktail from the previous section (Figure 6A). In both cirrhotic and non-cirrhotic livers, rosuvastatin and digoxin $AUC_{0\text{-tau}}$ and Cmax were increased upon co-administration of a perpetrator cocktail (Figure 4.6B,C). However, the drug-drug interaction, expressed as an increase in Cmax, and increase in AUCR (i.e. ratio AUC of victim drug with and without inhibitors over 120 min) was more profound but not significant in the non-cirrhotic livers than the cirrhotic livers. More specifically, the AUCR for rosuvastatin and digoxin was 5.6 (IQR: 3.1-13.3) and 8.1 (IQR: 4.6-20.5) respectively in non-cirrhotic livers compared to 1.4 (IQR: 0.9-1.9) and 2.2 (IQR: 1.3-3.5) respectively in cirrhotic livers. No increase in $AUC_{0\text{-tau}}$ and Cmax was observed for the low-hepatic extraction ratio drugs furosemide and metformin. The inhibition of biliary excretion (expressed in AUC ratio) of rosuvastatin and digoxin which are highly biliary excreted is shown in Figure 4.6D. The Pgp mediated biliary excretion of digoxin is shown to be inhibited as demonstrated by an AUCR ratio of 0.28 (IQR: 0.11-0.52) in cirrhotic livers and 0.66 (IQR: 0.12-1.14) in non-cirrhotic livers. Intrahepatic levels, demonstrated in Figure 4.6F, showed to be 6-fold increased in cirrhotic livers and 1.6-fold increased in non-cirrhotic livers upon co-administration of the inhibitors, which is in line with the inhibition of the biliary excretion.
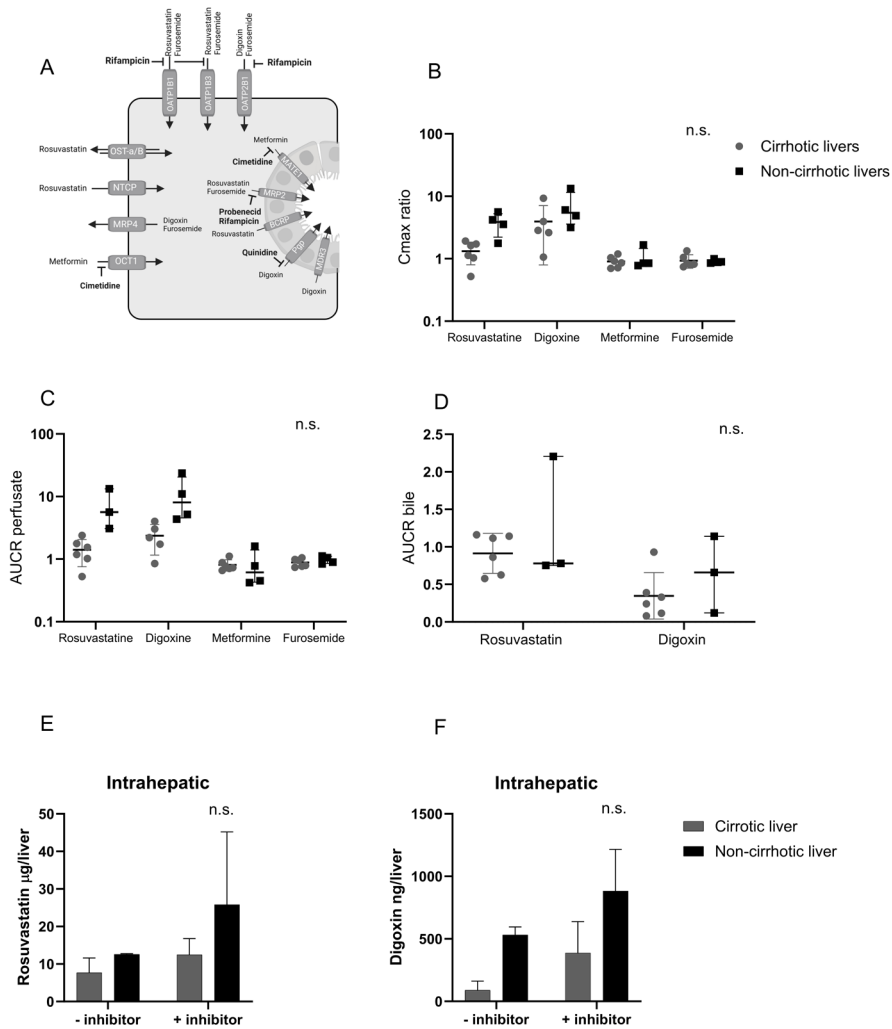
Figure 4.6 - Effect of drug inhibitor mix on hepatic clearance of rosuvastatin, digoxin, metformin, and furosemide. (a) Graphical representation of relevant hepatic drug transporters for the victim drugs (rosuvastatin, digoxin, metformin, and furosemide) and the applied perpetrators (quinidine, rifampicin, cimetidine, and probenecid). (b) Ratio of perfusate Cmax and (c) perfusate AUCR with and without applied perpetrator drugs for the cirrhotic and noncirrhotic livers. (d) Bile AUCR of digoxin and rosuvastatin with and without applied perpetrator drugs for the cirrhotic and non-cirrhotic livers. (e) Intrahepatic levels upon dosing inhibitor mix on rosuvastatin and (f) intrahepatic digoxin levels. Data represent median and interquartile range in cirrhotic (n=7) and noncirrhotic livers (n=4) for perfusate and bile, five in cirrhotic and three in noncirrhotic livers for intrahepatic data. Differences between groups were analyzed using the Mann–Whitney U test; P value is presented in the right corner of each graph. AUCR, area under the concentration time curve ratio; Cmax, maximum plasma concentration; n.s., not significant.

The BCRP mediated biliary excretion of rosuvastatin showed to be inhibited in the non-cirrhotic livers (0.78 (IQR:0.75-2.20)) while on average no inhibition of rosuvastatin in bile produced by cirrhotic livers was measured (0.98 (IQR:0.61-1.15)). Co-administration of the inhibitor mix showed to mildly increase the intrahepatic accumulation by 1.6-fold and 2-fold in cirrhotic and non-cirrhotic livers (Figure 4.6E). Metformin and furosemide showed to be minimally biliary excreted (range 1-3%), therefore no interaction in bile was presented here.

Discussion

Here we show for the first time the use of explanted human diseased livers as a model to assess hepatic extraction, biliary clearance and transporter function. We successfully perfused 7 cirrhotic livers and 4 non-cirrhotic livers for a period of 360 min, maintaining liver viability and functionality, as indicated by stable flow, bile production, proper histology pre- and post-perfusion, stable ALT values and stable gene expression throughout the perfusion.

The use of NMP has proven to be beneficial for organ transplantation[11,18] and NMP has become a widely accepted method to assess viability of the donor liver prior to transplantation[19,20]. Many criteria of hepatocellular and cholangiocellular function have been described (e.g. lactate clearance, perfusate ALT and biliary pH) to establish liver viability based on perfusion results and post-transplantation outcomes, demonstrating the robustness of the model in perfusion research[14-18]. The explanted cirrhotic livers perfused in this study met most of the criteria for hepatocellular function, except for lactate clearance and portal flow whereas other hemodynamic parameters did not show significant changes. As expected, portal flow was lower in cirrhotic livers compared to non-cirrhotic livers as a result of portal hypertension[21].

Unique advantages of the whole organ perfusion model is the dynamic environment; enabling to measure the hepatic extraction and the preservation of the biliary excretion route, thus allowing for the assessment of biliary excretion. The non-cirrhotic livers showed to rapidly take up rosuvastatin and digoxin from the perfusate with a hepatic extraction ratio of 0.70 and 0.42 respectively which are close to *in vivo* reported measures of 0.63 and 0.3 respectively[22,23]. In this study, hepatic extraction and clearance of rosuvastatin showed to be the most affected by cirrhosis as hepatic extraction decreased to

0.57 and a 190-fold AUC difference was observed. Rane et al.[24] reported that the clearance of hepatically cleared drugs with a high extraction ratio are related to blood flow and thus a major decrease in portal flow as in cirrhosis can dramatically affect the first passage across the liver[25,26]. However, changes in portal flow alone do not explain the 190-fold difference. Reduced uptake (C_{max}: 11.5-fold higher), as well as delayed elimination was observed. We hypothesize that decreased transporter abundance of OATP1B1/1B3 as reported in literature also contributed to the delayed elimination as we observed in the cirrhotic livers[27-29]. Hardly any studies are known regarding the effect of liver cirrhosis on for instance rosuvastatin pharmacokinetics. Only Simonson et al. 2003 reported the effect of advanced liver cirrhosis on rosuvastatin Cmax and AUC values for 2 patients[30]. This is substantiating the need for more knowledge regarding the role of cirrhosis in hepatic handling of drugs. *In vivo* studies demonstrated a high biliary excretion of rosuvastatin of approximately 76.8% as measured by fecal excretion[31]. The *ex vivo* non-cirrhotic livers showed a biliary excretion of 37% in 120 min, extrapolation of the data resulted in 77% total excretion of rosuvastatin which is in line with *in vivo* data. Interestingly, digoxin showed a relative high biliary clearance in cirrhotic (51%) and non-cirrhotic (17%) livers during 120 min of perfusion. *In vivo* studies have shown that digoxin is extensively renally eliminated (75%)[32]. However, multiple studies demonstrated that digoxin is highly involved in the enterohepatic circulation, thereby decreasing the *in vivo* fecal excretion of digoxin[33,34]. The two other compounds used in this study, furosemide and metformin, which are mainly renally cleared, showed a low hepatic extraction ratio and minor biliary excretion (≤3%) in both cirrhotic and non-cirrhotic which is in line with human *in vivo* data which showed that biliary eliminated was limited[35,36]. By showing the biliary excretion of two compounds which are mainly biliary excreted and two that are not/minorly excreted via the biliary route we demonstrated that the perfused liver retained its function while in the ex vivo environment. Interestingly, the percentage of biliary clearance was higher, for all compounds, in the cirrhotic perfused livers and lower intrahepatic levels of digoxin and rosuvastatin were measured. This might be due to an elevated bile flow which has been observed in patients cirrhosis and is confirmed in our model, resulting in a more efficiency biliary clearance[37]. Also, it has been reported for digoxin that Pgp levels are significantly elevated in cirrhosis which can contribute to a more efficient biliary clearance of digoxin[27].

The effect of drug-drug interactions in cirrhotic and non-cirrhotic livers was subsequently determined by using a cocktail of perpetrator drugs. The non-cirrhotic livers showed an increased AUCR for a drug-drug interaction with rosuvastatin (3.52) where values between 2.48–5.38 for rosuvastatin with rifampicin as inhibitor have been observed[38-40], showing good agreement with clinical data. Although it is observed that rifampicin can inhibit MRP2 and thereby limiting biliary excretion of rosuvastatin[41] we observed minimal inhibition at the biliary level. It is possible that the observed results are a consequence of inadequate portal dosing of rifampicin, as the perfusate concentration likely did not reach the desired levels. In our porcine perfusion we have measured C_{max} levels of 7.3 µM (n=10)[13], which is lower than 20 µM plasma levels in other clinical studies[38]. Digoxin, showed a high increase in AUCR upon dosing with inhibitors, which is potentially the result of inhibiting uptake via OATP (rifampicin as inhibitor) as described by Lau and co-authors[42]. A decrease in Pgp mediated biliary excretion was observed to an average inhibition of 0.64 in non-cirrhotic livers. This is the same inhibition we have observed in our porcine experiments. Since there is some variation between the human livers, we do recommend more replicates for future experiments. It remains difficult to compare to *in vivo* observations since a major part of the drug-drug interaction takes place at the intestinal level, when orally absorbed, thereby affecting the portal vein concentration. Still, the observations from this study showed that we could mimic a drug-drug interaction with digoxin in this perfusion model leading to an increased Cmax and AUCR.

Explanted livers obtained during orthotopic liver transplantation are currently only used for pathological assessment and subsequently discarded. While many preclinical and laboratory animal models try to mimic liver diseases as best as possible, many models fail due to a lack of translation to the human situation. This model can be widely applied in a variety of research settings, however implementation will only be feasible in a limited number of centers were liver transplantations are regularly performed. Considering the scarcity of explanted human livers for research purposes the utilization of porcine livers in early stages of drug development can prove to be a valuable approach as we have previously shown[13]. Although we have used a limited time-window perfusion, recent studies have shown the possibility to prolong organ perfusion duration even up to 7 days[19] which will broaden the applicability of liver perfusion.

Liver disease can affect the abundance of transporter proteins and/or metabolizing enzymes. In fact, multiple studies have analyzed liver biopsies from patients with liver disease showing alterations in expression of specific proteins relevant for pharmacokinetics[27-29,43]. For instance, Drozdzik et al., showed an increase in Pgp and multidrug resistance protein 4 (MRP4) and decreases in NTCP, OCT1 and OATP1B1 in patients with severe liver disease[27]. Although these studies already provided some hints towards altered pharmacokinetics and metabolism of drugs in patients with liver diseases, ex vivo perfusion of diseased livers offers a unique opportunity to directly study the effect of altered expression levels of transporter proteins and metabolizing enzymes. In this study we used known drug substrates for different important hepatic uptake and efflux transporters. Gaining insight into pharmacokinetic profiles of OATP1B1/1B3, Pgp, BCRP and OCT1 model compounds is a first step towards studying transporter functions in diseased liver. Additionally, for many drugs, dosing advice is currently incomplete for patients with cirrhosis because of lacking evidence or showing major interindividual differences. Studying drug pharmacokinetics using explanted human livers can serve as a basis to explore the differences in hepatic handling of drugs for patients with hepatic impairment even though to date it is yet too early to know what the exact place of this model is for clinical practice or drug development[44].

In conclusion, we demonstrated for the first time NMP of diseased human livers explanted during liver transplantation and discarded donor livers to study hepatic extraction, clearance, biliary excretion and drug-drug interactions. The ability to sample perfusate, bile and tissue during- and after dosing is a unique approach to gain insights into hepatobiliary processes, transporter function and transporter abundance.

Acknowledgements

References

1. Franz CC, Egger S, Born C, Rätz Bravo AE, Krähenbühl S. Potential drug-drug interactions and adverse drug reactions in patients with liver cirrhosis. European journal of clinical pharmacology 2012;68:179-188.
2. Franz CC, Hildbrand C, Born C, Egger S, Rätz Bravo AE, Krähenbühl S. Dose adjustment in patients with liver cirrhosis: impact on adverse drug reactions and hospitalizations. European journal of clinical pharmacology 2013;69:1565-1573.
3. Rodighiero V. Effects of liver disease on pharmacokinetics. Clinical pharmacokinetics 1999;37:399-431.
4. Nevzorova YA, Boyer-Diaz Z, Cubero FJ, Gracia-Sancho J. Animal models for liver disease–A practical approach for translational research. Journal of hepatology 2020;73:423-440.
5. Guillouzo A. Liver cell models in in vitro toxicology. Environmental health perspectives 1998;106:511-532.
6. Du Y, Polacheck WJ, Wells RG: Bile Duct-on-a-Chip. In: Organ-on-a-Chip: Springer, 2022; 57-68.
7. Hassan S, Sebastian S, Maharjan S, Lesha A, Carpenter A-M, Liu X, Xie X, et al. Liver-on-a-chip models of fatty liver disease. Hepatology (Baltimore, Md.) 2020;71:733.
8. Melgert BN, Olinga P, Weert B, Slooff MJ, Meijer DK, Poelstra K, Groothuis GM. Cellular distribution and handling of liver-targeting preparations in human livers studied by a liver lobe perfusion. Drug metabolism and disposition 2001;29:361-367.
9. Schreiter T, Marquitan G, Darnell M, Sowa J-P, Bröcker-Preuss M, Andersson TB, Baba HA, et al. An ex vivo perfusion system emulating in vivo conditions in noncirrhotic and cirrhotic human liver. Journal of Pharmacology and Experimental Therapeutics 2012;342:730-741.
10. Villeneuve JP, Huet PM, Gariepy L, Fenyves D, Willems B, Côté J, Lapointe R, et al. Isolated perfused cirrhotic human liver obtained from liver transplant patients: a feasibility study. Hepatology 1990;12:257-263.
11. van Rijn R, Schurink IJ, de Vries Y, van den Berg AP, Cortes Cerisuelo M, Darwish Murad S, Erdmann JI, et al. Hypothermic machine perfusion in liver transplantation—a randomized trial. New England Journal of Medicine 2021;384:1391-1401.
12. Stopfer P, Giessmann T, Hohl K, Hutzel S, Schmidt S, Gansser D, Ishiguro N, et al. Optimization of a drug transporter probe cocktail: potential screening tool for transporter-mediated drug–drug interactions. British journal of clinical pharmacology 2018;84:1941-1949.
13. Stevens LJ, Zhu AZ, Chothe PP, Chowdhury SK, Donkers JM, Vaes WH, Knibbe CA, et al. Evaluation of normothermic machine perfusion of porcine livers as a novel preclinical model to predict biliary clearance and transporter-mediated drug-drug interactions using statins. Drug Metabolism and Disposition 2021;49:780-789.
14. de Vries Y, Matton AP, Nijsten MW, Werner MJ, van den Berg AP, de Boer MT, Buis CI, et al. Pretransplant sequential hypo-and normothermic machine perfusion of suboptimal livers donated after circulatory death using a hemoglobin-based oxygen carrier perfusion solution. American journal of transplantation 2019;19:1202-1211.
15. Brüggenwirth IM, van Leeuwen OB, Porte RJ, Martins PN. The emerging role of viability testing during liver machine perfusion. Liver Transplantation 2021.
16. Mergental H, Stephenson BT, Laing RW, Kirkham AJ, Neil DA, Wallace LL, Boteon YL, et al. Development of clinical criteria for functional assessment to predict primary nonfunction of high-risk livers using normothermic machine perfusion. Liver Transplantation 2018;24: 1453-1469.
17. van Leeuwen OB, de Vries Y, Fujiyoshi M, Nijsten MW, Ubbink R, Pelgrim GJ, Werner MJ, et al. Transplantation of high-risk donor livers after ex situ resuscitation and assessment using combined hypo-and normothermic machine perfusion: a prospective clinical trial. Annals of surgery 2019;270:906-914.
18. Boteon YL, Laing RW, Schlegel A, Wallace L, Smith A, Attard J, Bhogal RH, et al. Combined hypothermic and normothermic machine perfusion improves functional recovery of extended criteria donor livers. Liver transplantation 2018;24:1699-1715.

19. Eshmuminov D, Becker D, Bautista Borrego L, Hefti M, Schuler MJ, Hagedorn C, Muller X, et al. An integrated perfusion machine preserves injured human livers for 1 week. Nature biotechnology 2020;38:189-198.

20. Op den Dries S, Karimian N, Sutton M, Westerkamp A, Nijsten M, Gouw A, Wiersema-Buist J, et al. Ex vivo normothermic machine perfusion and viability testing of discarded human donor livers. American Journal of Transplantation 2013;13:1327-1335.

21. Bosch J, García-Pagán JC. Complications of cirrhosis. I. Portal hypertension. Journal of hepatology 2000;32:141-156.

22. Bergman E, Forsell P, Tevell A, Persson EM, Hedeland M, Bondesson U, Knutson L, et al. Biliary secretion of rosuvastatin and bile acids in humans during the absorption phase. European journal of pharmaceutical sciences 2006;29:205-214.

23. Hebert MF. Impact of pregnancy on maternal pharmacokinetics of medications. Clinical pharmacology during pregnancy 2013:17-39.

24. Rane A, Wilkinson G, Shand D. Prediction of hepatic extraction ratio from in vitro measurement of intrinsic clearance. Journal of Pharmacology and Experimental Therapeutics 1977;200: 420-424.

25. Delco F, Tchambaz L, Schlienger R, Drewe J, Krähenbühl S. Dose adjustment in patients with liver disease. Drug safety 2005;28:529-545.

26. Johnson TN, Boussery K, Rowland-Yeo K, Tucker GT, Rostami-Hodjegan A. A semi-mechanistic model to predict the effects of liver cirrhosis on drug clearance. Clinical pharmacokinetics 2010;49:189-206.

27. Drozdzik M, Szelag-Pieniek S, Post M, Zeair S, Wrzesinski M, Kurzawski M, Prieto J, et al. Protein abundance of hepatic drug transporters in patients with different forms of liver damage. Clinical Pharmacology & Therapeutics 2020;107:1138-1148.

28. Thakkar N, Slizgi JR, Brouwer KL. Effect of liver disease on hepatic transporter expression and function. Journal of pharmaceutical sciences 2017;106:2282-2294.

29. Wang L, Collins C, Kelly EJ, Chu X, Ray AS, Salphati L, Xiao G, et al. Transporter expression in liver tissue from subjects with alcoholic or hepatitis C cirrhosis quantified by targeted quantitative proteomics. Drug Metabolism and Disposition 2016;44:1752-1758.

30. Simonson S, Martin P, Mitchell P, Schneck D, Lasseter K, Warwick M. Pharmacokinetics and pharmacodynamics of rosuvastatin in subjects with hepatic impairment. European journal of clinical pharmacology 2003;58:669-675.

31. Martin PD, Warwick MJ, Dane AL, Hill SJ, Giles PB, Phillips PJ, Lenz E. Metabolism, excretion, and pharmacokinetics of rosuvastatin in healthy adult male volunteers. Clinical therapeutics 2003;25:2822-2835.

32. Iisalo E. Clinical pharmacokinetics of digoxin. Clinical pharmacokinetics 1977;2:1-16.

33. Doherty JE, Flanigan W, Murphy M, Bulloch R, Dalrymple G, Beard O, Perkins W, et al. Tritiated digoxin: XIV. Enterohepatic circulation, absorption, and excretion studies in human volunteers. Circulation 1970;42:867-873.

34. Ben-Itzhak J, Bassan HM, Shor R, Lanir A. Digoxin quinidine interaction: a pharmacokinetic study in the isolated perfused rat liver. Life sciences 1985;37:411-415.

35. Beermann B, Dalen E, Lindström B, Rosen A. On the fate of furosemide in man. European journal of clinical pharmacology 1975;9:57-61.

36. Graham GG, Punt J, Arora M, Day RO, Doogue MP, Duong J, Furlong TJ, et al. Clinical pharmacokinetics of metformin. Clinical pharmacokinetics 2011;50:81-98.

37. Erlinger S. Bile secretion. British medical bulletin 1992;48:860-876.

38. Mori D, Kashihara Y, Yoshikado T, Kimura M, Hirota T, Matsuki S, Maeda K, et al. Effect of OATP1B1 genotypes on plasma concentrations of endogenous OATP1B1 substrates and drugs, and their association in healthy volunteers. Drug metabolism and pharmacokinetics 2019;34:78-86.

39. Prueksaritanont T, Tatosian D, Chu X, Railkar R, Evers R, Chavez-Eng C, Lutz R, et al. Validation of a microdose probe drug cocktail for clinical drug interaction assessments for drug transporters and CYP3A. Clinical Pharmacology & Therapeutics 2017;101:519-530.

40. Takehara I, Yoshikado T, Ishigame K, Mori D, Furihata K-i, Watanabe N, Ando O, et al. Comparative study of the dose-dependence of OATP1B inhibition by rifampicin using probe drugs and endogenous substrates in healthy volunteers. Pharmaceutical research 2018;35: 1-13.

41. Kaneko K-i, Tanaka M, Ishii A, Katayama Y, Nakaoka T, Irie S, Kawahata H, et al. A clinical quantitative evaluation of hepatobiliary transport of [11C] dehydropravastatin in humans using positron emission tomography. Drug Metabolism and Disposition 2018;46:719-728.

42. Lau YY, Wu C-Y, Okochi H, Benet LZ. Ex situ inhibition of hepatic uptake and efflux significantly changes metabolism: hepatic enzyme-transporter interplay. Journal of Pharmacology and Experimental Therapeutics 2004;308:1040-1045.

43. Billington S, Ray AS, Salphati L, Xiao G, Chu X, Humphreys WG, Liao M, et al. Transporter expression in noncancerous and cancerous liver tissue from donors with hepatocellular carcinoma and chronic hepatitis C infection quantified by LC-MS/MS proteomics. Drug Metabolism and Disposition 2018;46:189-196.

44. Weersink RA, Bouma M, Burger DM, Drenth JP, Hunfeld NG, Kranenborg M, Monster-Simons MH, et al. Evaluating the safety and dosing of drugs in patients with liver cirrhosis by literature review and expert opinion. BMJ open 2016;6:e012991.

Supplementary materials

Table S4.1 - Composition of perfusate and continuous infusions.

Components	Quantity
Red blood cells (Sanquin)	4x 250 mL
Fresh Frozen plasma	4x 250 mL
Calcium gluconate (10%)	10 mL
Sodium bicarbonate 8.4% solution	To pH of 7.4
Heparin	1000 IU
Continuous infusion	
Fast-acting insulin	(10 U/mL; 1mL/h)
Taurocholate	(2% w/v; 10 mL/h)
Flolan	0.026mg/mL/h
Heparin	1041 U/h (1mL/h)
Aminoplasmal (B. Braun)	23 mL/h
Cernevit (Baxter)	22.5 mg/mL/h

Table S4.2 - General properties of drug cocktail (rosuvastatin, digoxin, metformin and furosemide) and drug cocktail inhibitor mix. Oral doses applied *in vivo* (mg), fraction absorbed and mg bolus applied to the portal vein of ex vivo perfused livers.

Substrate (victim drug)	Transporters involved	Metabolism	Fraction absorbed (%)	mg oral doses	mg bolus applied to *ex vivo* liver
Rosuvastatin	OATP1B1, OATP1B3, NTCP, MRP2, BCRP, OST-α/β	CYP2C9	50%	10 mg	1.80 mg
Digoxin	OATP2B1, Pgp MDR3	CYP3A4	81%	0.50 mg	0.11 mg
Metformin	OCT1, MATE1		53%	500 mg	74.20 mg
Furosemide	OATP2B1, OATP1B1, OATP1B3 MRP2		55%	5 mg	0.77 mg
Inhibitor mix					
Rifampicin	OATP1B1 OATP1B3 OATP2B1		95%	600 mg	67.7 mg
Quinidine	Pgp		80%	100 mg	22.4 mg
Cimetidine	OCT1 MATE1		72%	300 mg	59.89 mg
Probenecid	MRP2		50%	250 mg	25 mg

Table S4.3 - Details of the LC/MS conditions used for the analysis of digoxin, rosuvastatin, metformin and furosemide in perfusate and bile matrix.

Compound	Column	Mobile Phase		Time (min)	Mobile Phase B (%)		Flow (mL/min)
		A	B				
Perfusate and Tissue							
Digoxin	Waters	0.1%	0.1% Formic	0	100	0	0.6
Rosuvastatin	Acquity	Formic	Acid	0.50	100	0	
Metformin	UPLC BEH	Acid in	in	1.00	50	50	
Furosemide	C18; 2.1x50	MiliQ	Acetonitrile	1.50	5	95	
	mm, 1.7 µm;	water		2.20	5	95	
	art.nr			2.30	100	0	
	186002350			3.20	100	0	
Bile matrix							
Digoxin	Waters	0.1%	0.1% Formic	0	100	0	0.6
Rosuvastatin	Acquity	Formic	Acid	0.50	100	0	
Metformin	UPLC BEH	Acid in	in	6.50	40	60	
Furosemide	C18; 2.1x50	MiliQ	Acetonitrile	6.60	5	95	
	mm, 1.7 µm;	water		7.30	5	95	
	art.nr			7.40	100	0	
	186002350			8.30	100	0	

Table S4.4 - Details of the LC/MS conditions; Quantification of masses and retention times.

| Compound	Rt (min) Perfusate/tissue	Rt (min) Bile	Exact mass	Polarity	Fragment	m/z
Metformin	0.27	0.28	129.1014	Pos	[M+H]+	130.1087
Metformin ISTD	0.27	0.27	135.1391	Pos	[M+H]+	136.1464
Digoxin	1.34	3.98	780.4296	Neg	[M+HCOOH-H]-	825.4284
Digoxin ISTD	1.34	3.97	783.4484	Neg	[M+HCOOH-H]-	828.4472
Furosemide	1.42	4.07	330.0077	Neg	[M-H]-	329.0004
Furosemide ISTD	1.42	4.04	335.0391	Neg	[M-H]-	344.0318
Rosuvastatin	1.48	4.83	481.1683	Neg	[M-H]-	480.1610
Rosuvastatin ISTD	1.57	5.41	468.1862	Neg	[M+HCOOH-H]-	513.1850
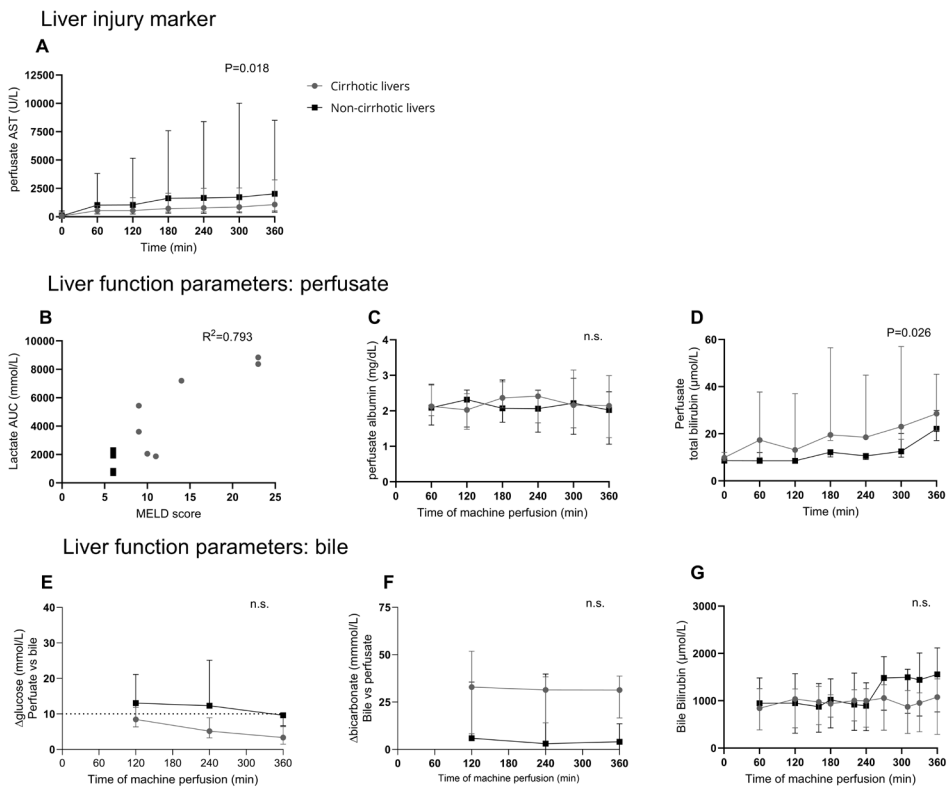
Figure S4.1 - Liver injury and liver function markers, measured in perfusate and bile during normothermic machine perfusion. Liver injury maker (A) Perfusate AST. Liver function parameters measured in perfusate, including; (B) relation of perfusate lactate AUC and MELD score, (C) albumin and (D) total bilirubin. Liver function parameters measured in bile; (E) Δglucose perfusate vs bile, (F) Δbicarbonate bile vs perfusate and (G) bile bilirubin levels during 360 min of perfusion. Data represents median and interquartile range in cirrhotic (n=7). and non-cirrhotic livers (n=4). Differences in AUC between groups were analyzed using the Mann-Whitney U test; p value is presented in right corner of each graph
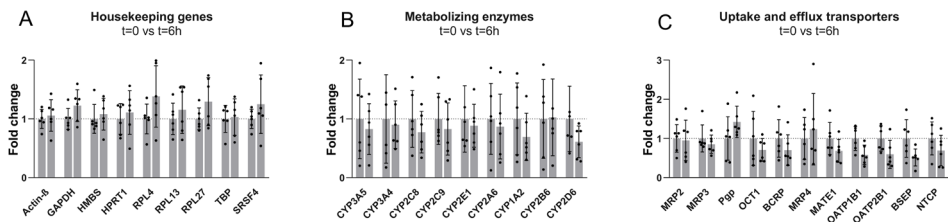
Figure S4.2 - mRNA expression of (A) housekeeping genes (B) CYP450 and (B) transporters during ex vivo normothermic perfusion. Tissue biopsies taken at t=0 hour were compared to t=6 hour. Data represents mean ±SD (n=6; cirrhotic/non-cirrhotic).
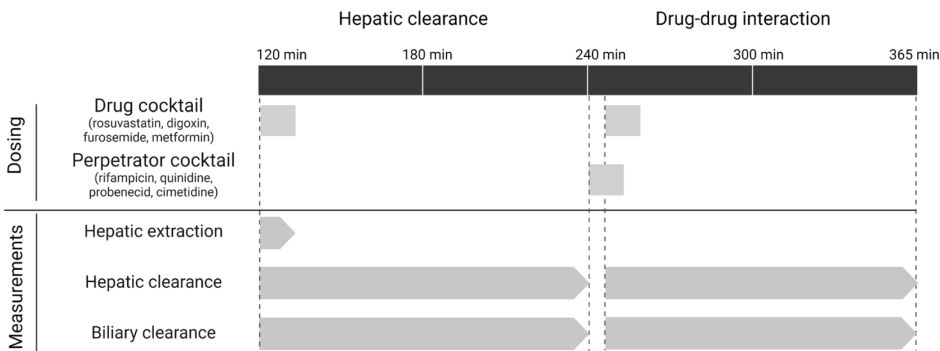

Figure S4.3 - Schematic representation of the experimental set-up for studying pharmacokinetics of a cocktail of drugs and the effects of drug-drug interactions. Stable liver perfusion was maintained in the first 120 min of perfusion. Between 120-130 min, the drug cocktail was infused into the portal vein (1mL/min), during this time the hepatic extraction of the drugs was measured. Hepatic clearance as well as biliary clearance was measured for 120 min (120 -240 min). Thereafter, at t=240 min, drug inhibitors were infused into the portal vein for 10 min (240–250). Between 245-255 the drug cocktail was infused into the portal vein to study drug-drug interactions. Perfusate and bile samples studying the extent of drug-drug interactions were taken between 245 and 365 min
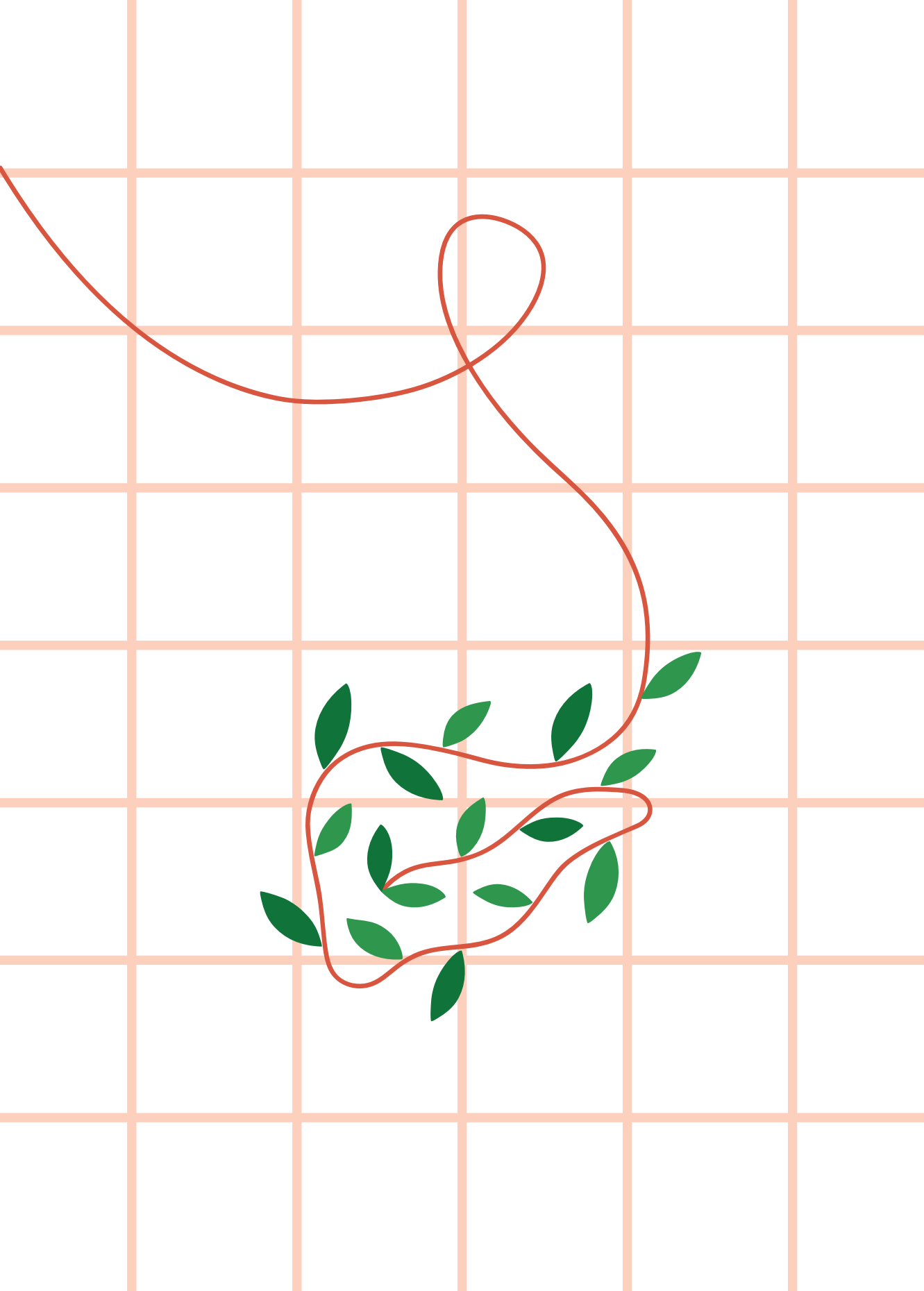
CHAPTER 05

Unraveling and enhancing the dynamics of hepatic bile acid and cholesterol metabolism during ex vivo normothermic machine perfusion; a path to improved liver function through conjugated bile acid infusion

L.J. Stevens, J.M. Donkers, J.B. Doppenberg, M. Caspers, J. Dubbeld, B. Heming, N.A.E. Tramper, L.E.C Kleinjan, D.R. de Waart, R.P.J. Oude Elferink, E. van de Steeg, I.P.J. Alwayn

Abstract

Ex vivo liver normothermic machine perfusion (NMP) does not fully recapitulate physiological liver function due to the absence of the enterohepatic circulation as only infusion of the bile acid taurocholate (TCA) is applied in most protocols. In this study we characterized the *de novo* bile acid synthesis and cholesterol homeostasis during liver NMP. We hypothesized that addition of a more diverse pool of (conjugated)bile acids during liver NMP would decrease the metabolic burden of *de novo* synthesis and thereby improve liver function during NMP.

First, human and porcine livers were perfused for 360 min at 37°C and perfusate containing TCA. Next, the infusion of different conjugated bile acid mixes was assessed during porcine and human liver perfusion. Perfusate, bile and tissue samples were obtained to study liver viability, functionality, gene expression, cholesterol and bile acid levels.

During human and porcine perfusions with TCA infusion, composition of bile was comparable to literature however, synthesis rates were above physiological average and a decrease over time in cholesterol perfusate levels was observed. Additionally, over time a decreased expression of bile acid synthesis related genes, increased gene expression of cholesterol metabolism related genes and decreased expression in bile acid-dependent uptake and efflux transporters were detected. Upon infusion of a conjugated bile acid mix lower AST and ALT values and stable cholesterol homeostasis was observed after 720 min of perfusion. Perfused human livers showed appropriate function and good functioning livers showed rapid bile acid clearance from the perfusate into the bile.

In this study we reveal new insights that infusion of (un)conjugated bile acids in NMP alleviated the burden of the *de novo* bile acid synthesis and improved liver function.

Introduction

Ex vivo normothermic machine perfusion (NMP) of the liver is a well-known technique in the field of organ transplantation to assess metabolic processes and liver function[1,2]. Additionally, NMP can be used as a platform for drug intervention studies, drug pharmacokinetics and disease modelling[3-7]. During NMP, livers are perfused with a red-blood cell based perfusate through the hepatic artery and the portal vein under oxygenated conditions at 37°C. Many protocols depend on infusion of taurocholate (TCA) to induce bile flow[8,9] as current liver viability assessment is partly focused on bile production and bile composition as well as biliary pH, glucose and bicarbonate levels[10,11]. However, TCA is only one of many bile acids found in the bile acid pool which encompasses a variety of (conjugated) bile acids, each with a specific function and contribution to the overall bile metabolism[12-14].

Under physiological conditions the liver synthesizes bile acids from cholesterol through either the classic or alternative pathway, initiated by cholesterol 7α-hydroxylase (CYP7A1) or sterol 27-hydroxylase (CYP27A1), respectively[15]. The synthesized primary bile acids cholic acid (CA) and chenodeoxycholic acid (CDCA) are subsequently conjugated with glycine (G) or taurine (T). After synthesis, conjugated primary bile acids are excreted across the canalicular membrane and drained via the biliary tree into the gall bladder, from where the bile acids are subsequently secreted into the duodenum upon a postprandial signal[13]. In the intestinal tract, bile acids are transformed by intestinal bacteria into secondary bile acids such as deoxycholic acid (DCA), reabsorbed by the intestinal cells and are transported back to the liver via the portal vein[12,15,16]. In the portal vein, the bile acid composition predominantly comprises of GCA, GCDCA and GDCA[17]. This efficient recirculation of bile acids is known as the enterohepatic circulation, where approximately 95% of the total amount of bile acids recirculates between the intestine and the liver[18,19]. The loss of bile acids is mainly due to excretion of bile acids via the feces. As a consequence, the loss of bile acids is compensated by *de novo* synthesis in the liver to maintain homeostasis and a constant bile acid pool[13] in which bile acids regulate their own homeostasis by providing a negative feedback on bile acid biosynthesis genes such as CYP27A1, CYP7A1 and sterol 12α-hydroxylase (CYP8B1). This downregulation is mediated by activation of farnesoid X receptor (FXR) by bile acids, which upon activation also prevents toxic intracellular accumulation of bile acids by inhibiting bile acid uptake and stimulating bile acid export out of

the liver[20,21]. Thus, FXR activation suppresses gene expression of hepatocyte bile acid influx transporters such as sodium taurocholate co-transporting polypeptide (NTCP), organic anion transporter 2 (OAT2), and the organic anion-transporting polypeptides (OATP) 1B1, 1B3 (humans) and 1B4 (pigs)[22]. Concomitantly, FXR activation increases gene expression of canalicular efflux transporters such as bile salt export pump (BSEP) and multidrug resistant-related protein (MRP) 2, which secrete divalently conjugated bile acids into bile and is bile acids are subsequently stored in the gallbladder[21]. Alternatively, bile acids can be exported basolaterally in the systemic circulation via MRP3, which is also upregulated upon FXR activation[23]. As this hepatobiliary transporter system is also responsible for the transport of other substances such as nutrients, endogenous compounds and drugs, is tightly regulated[24,25].

Current clinical and lab-based NMP protocols recreate physiological perfusate compositions in order to maintain and assess liver vitality and functionality thereby only including TCA as bile acid[26]. Here we hypothesize that this imposes a substantial burden on the liver during NMP as it is forced to engage in the *de novo* bile acid synthesis without the support of endogenous bile acids. The *de novo* bile acid synthesis is an energy consuming process using ATP[13]. However given the importance of maintaining optimal organ viability and functionality during *ex vivo* liver perfusion prior to transplantation, it is critical to prevent the depletion of ATP reserves which is essential for various other physiological processes[27]. In our study, we addressed this issue and aimed to characterize the *de novo* bile acid synthesis by profiling the biliary bile acid excretion, cholesterol homeostasis and transporter expression during *ex vivo* liver NMP. We hypothesized that introduction of a variety of bile acids during liver NMP would alleviate the strain of the *de novo* synthesis by the liver and improve the physiological resemblance.

Methods

Procurement, preservation and perfusion of porcine livers

Porcine livers were procured, preserved and perfused as previously published[28]. Standard perfusion protocol consisted of infusion with TCA at a fixed rate of 0.2 g/hr.

Porcine liver perfusion bile acid infusion studies

Porcine liver perfusions were performed using varying compositions of bile acid mixes, summarized in Table 5.1:

- **Standard protocol**
  The standard protocol consisted of infusion of TCA at 0.2 g/hr (0.39 mmol/hr), n=5 studies up to 360 min and n=2 up to 720 min of perfusion.

- **Simple conjugated bile acid mix**
  A bile acid mixture was continuously infused in the portal vein during porcine liver NMP at a rate of 0.15 g/hr (0.41 mmol/hr)[8] (n=2). The bile acid mixture consisted of GCDCA, 40%, GCA, 40%, CDCA 10% and CA 10%, representing the two most prevalent human bile acids supplemented with unconjugated primary bile acids to alleviate the strain of the *de novo* synthesis. Livers were perfused for a total time of 720 minutes.

- **Complete conjugated bile acid mix**
  To study the effect of a more completed conjugated bile acid mix was continuously infused in the portal vein at a rate of 0.15 g/h (0.35 mmol/hr) (n=3). This mixture consisted of GCA, 24%, GCDCA, 24%, GDCA, 24%, TCA, 11%, tCDCA, 11%, DCA, 5%, CA, 0.6% and CDCA, 0.6%, more closely resembling human *in vivo* conditions[17]. Additionally, 3 mL/hr of omegaven (Fresenius, 's Hertogenbosch, the Netherlands) was infused. Livers were perfused for a total time of 660 minutes.

Table 5.1 - Composition of bile acid mixes.

Standard protocol	Conjugated simple bile acid mix	Conjugated complete bile acid mix
TCA (100%)	GCDCA (40%)	GCA (24%)
	GCA (40%)	GCDCA (24%)
	CDCA (10%)	GDCA (24%)
	CA (10%)	TCA (11%)
		TCDCA (11%)
		DCA (5%)
		CA (0.6%)
		CDCA (0.6%)

Human liver perfusion

Human explanted and discarded livers were perfused as previously published[6]. Standard perfusion protocol consisted of infusion with TCA at a fixed rate of 0.2 g/hr. The samples (perfusate, bile and tissue) used in this research with TCA infusion were derived from a study which was previously published[6].

Human liver perfusion bile acid infusion studies

Livers were perfused with the simple conjugated bile acid mix consisting of GCDCA, (40%), GCA, (40%), CDCA (10%) and CA (10%). An overview of the condition and characteristics of the liver is shown in Table 5.2. Continuous bile acid infusion was applied at 0.15 g/hr.

Table 5.2 - Donor characteristics and ischemic times of human and porcine livers.

	Liver #1	Liver #2	Liver #3	Porcine livers
Reason for decline	Declined after 13h of NMP Necrotic artery patch	Alcohol and smoking history	Choledocholithiasis	-
DBD/DCD	DCD	DBD	DCD	DCD
Age (years)	51	63	51	~ 6 months
Gender	Female	Female	Male	Male
BMI (kg/m^2)	19.9	28	23	-
WIT (min)	16	0	14	9 - 15
CIT (min)	387	226	318	180-210
Weight of the liver (g)	2025	1877	2177	2100 - 2500

Liver #1: Liver was perfused using the OrganOx machine (OrganOx, Oxford, UK), with a perfusate of red blood cells and gelofusine. Continuous bile acid infusion was given from t=15 hours till t=20 hours at 0.15 g/hr. To study clearance capacity, indocyanine green (ICG) was added to the reservoir at t=19h and subsequently, perfusate and bile sample were taken. Infusion speed was increased after 20 hours to 0.3g/hr. An additional bolus (0.2 g) was given at 20.5 hours to study the effect of high bile acids concentrations on liver function.

Liver #2 - #3: Livers were perfused using the Liver Assist device, with a perfusate of red blood cells and plasma. Continuous bile acid infusion was given from t=0 hours till t=12 hours at 0.15 g/hr. ICG was dosed to the reservoir at t=120 min to study liver clearance capacity. During perfusion of liver #2 a bile acid bolus of 0.2 g was given after 6 hours of perfusion to study the effect of high bile acids concentrations on liver function.

Liver function assessment

Several parameters were measured to assess liver viability and functionality. Aspartate transaminase (AST) and alanine transaminase (ALT) and ICG concentrations were measured as previously published. Data of ALT and AST

was expressed as a percentage of AST (U/L) and ALT (U/L), where the highest level of the control study was set at 100%.

Bile acid analysis

Bile acid composition was measured by reverse-phase high performance liquid chromatography (HPLC) as described previously[29]. Total bile acids levels in perfusate and bile were measured by the Total Bile Acid Assay kit (Diazyme Laboratories, Poway, USA) using a microplate reader set at 405 nm.

Cholesterol assay

Cholesterol levels were quantified using the enzymatic CHOD-PAP assay (Roche Diagnostics, Basel, Switzerland). Perfusate total cholesterol was measured spectrophotometrically using an enzymatic assay (Roche diagnostics, Almere, the Netherlands) according to the manufacturer's instructions.

RT-qPCR analysis

RNA was extracted from liver tissue using the RNeasy Mini Kit (Qiagen) according to manufacturer's instructions. cDNA was synthesized from RNA using the iScript™ Reverse Transcription Supermix (Bio-Rad, Hercules, California, USA) according to manufacturer's description. Forward and reverse primers, of which details can be found in Supplementary Table S5.1 and S5.2, were designed for both human and porcine tissue. An Applied Biosystems™ 7500 Fast Real-Time PCR System (Fisher Scientific) was used to run the RT-qPCR using SYBR green (Bio-Rad, Hercules, California, USA).

RNA sequencing

After RNA isolation, RNA quality was evaluated using a Fragment Analyzer (tot.RNA conc. & RQN). Total RNA was processed into tagged random sequence libraries (NEBNext Ultra II Directional RNA Library Prep Kit for Illumina, NEB #E7760S/L, Biolabs) and sample quality was checked for proper size distribution (300-500 bp peak, Fragment Analyzer). The mixed (multiplex) sample libraries were sequenced on an Illumina NovaSeq6000 sequencer with a paired-read 150-cycle sequencing protocol at GenomeScan BV (Leiden, the Netherlands), resulting in ~18-26 million read counts per sample. Clustering and DNA sequencing using the NovaSeq6000 was performed according to manufacturer's protocols. A concentration of 1.1 nM of DNA was used yielding

paired end reads (2x 150bp). NovaSeq control software NCS v1.7 was used. Image analysis, base calling, and quality check was performed with the Illumina data analysis pipeline RTA3.4.4 and Bcl2fastq v2.20. Trimmed Fastq files (Trimmomatic software) were merged (in case of Paired-end reads) and aligned to the reference genomes (Human: Homo_sapiens.GRCh38.gencode.v29; Pig: GCF_000003025.6_Sscrofa11.1_genomic) using the STAR 2.5 algorithm with default settings (https://github.com/alexdobin/STAR). Based on the mapped read locations and the gene annotation, Htseq-count 0.6.1p1 was used to count the read mapping frequency/gene (transcript region) resulting in read mapping frequency per gene. Expression was normalized based on total counts per sample and corrected for GAPDH expression.

Data analysis

Data was analyzed and visualized using GraphPad Prism 8.0.1 (GraphPad Inc., La Jolla, California, USA). Statistics were performed as indicated in figure legends. Values for the area under the concentration time curve (AUC) were calculated using the linear trapezoidal method. Significance of differences between the intervention and standard protocol was tested using the Mann-Whitney U test. Data is presented as median and range for non-parametric distributed data. P-values below 0.05 were considered significant.

Results

Characterization of the *de novo* bile acid synthesis

To study the *de novo* bile acid synthesis in the standard protocol with the infusion of TCA, the produced bile during NMP of human and porcine livers was characterized. TCA was not presented in the graphs since TCA was administrated and the measured output was in line with the administration. In human bile, GCA, GCDCA and TCDCA were the three most abundant bile acids, followed by tauroursodeoxycholic acid (UDCA), taurohyodeoxycholic acid (THDCA) and glycohyodeoxycholic acid (GHDCA) the least (Figure 5.1A). Porcine bile showed the highest abundance of GHC, gHDC and GCDCA but with minimal detection of TUDCA, HCA and GDCA (Figure 5.1B). Figure 5.1C-D show the bile composition of hourly fractions from human and porcine bile. For human bile, the bile acid GCDCA decreased significantly over time (36% at t=60 min, to 20% at t=360 min compared to t=0). Porcine bile composition showed no significant

changes and remained stable over time. The total bile acid excretion was calculated and expressed as cumulative bile acid excretion in grams over time to illustrate the total synthesis of bile acids during NMP (Figure 5.1E). The total bile acid excretion showed to be higher in porcine bile compared to in human bile during 360 minutes of perfusion with values of 0.67±0.22g in porcine bile versus 0.14+0.04 in human bile. Figure 5.1F shows the biliary excretion of TCA which is a marker for NTCP (uptake) and BSEP (excretion) function. The dotted line shows the administrated TCA dose during *ex vivo* liver perfusion (0.2g/hr). In human as well as porcine livers, the excretion of TCA was linear and constant in time indicating proper NTCP as well as BSEP function. We also investigated bile acid conjugation to glycine as main conjugated product (Figure 5.1G). Human bile conjugation to glycine increased during perfusion from 76±11% to 82±7% after 240 minutes of perfusion, whereafter it remained stable thereafter until 360 minutes of perfusion. In contrast, glycine conjugation in porcine livers was stable over time, with 88±3% conjugation at t=60 min versus 84±1% conjugation after 360 min of perfusion, showing no significant change. Lastly, the perfusate cholesterol levels were quantified as cholesterol is the precursor of bile acid synthesis. During human liver perfusion, perfusate cholesterol levels remained stable until 240 minutes after perfusion, whereafter a decreasing trend was observed (Figure 5.1H) whereas in pigs, perfusate levels of cholesterol decreased throughout the perfusion, starting at 80 mg/dL at t=60 min and with a final concentration of 50 mg/dL after 360 min of perfusion.
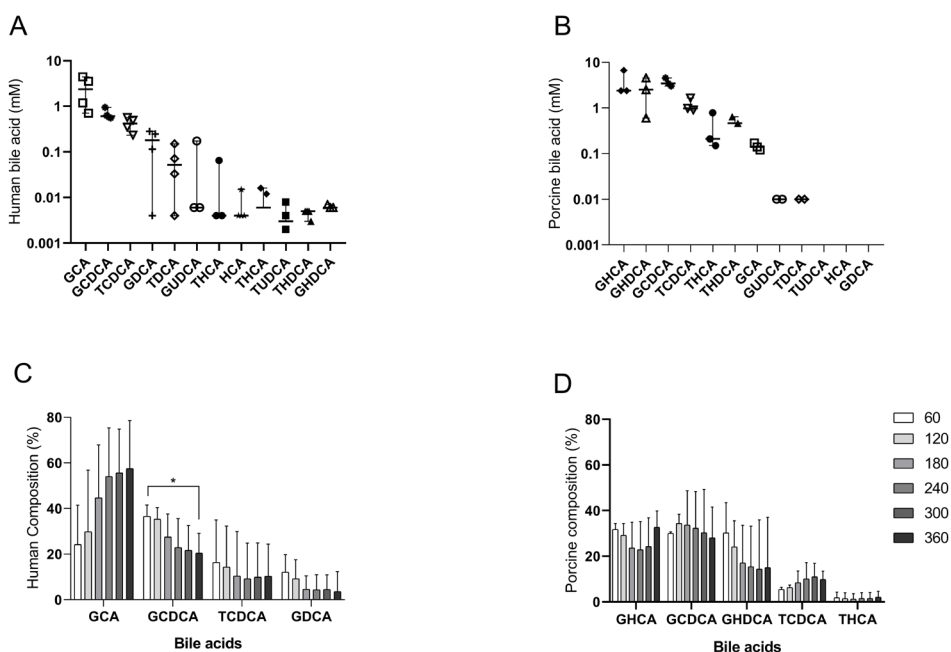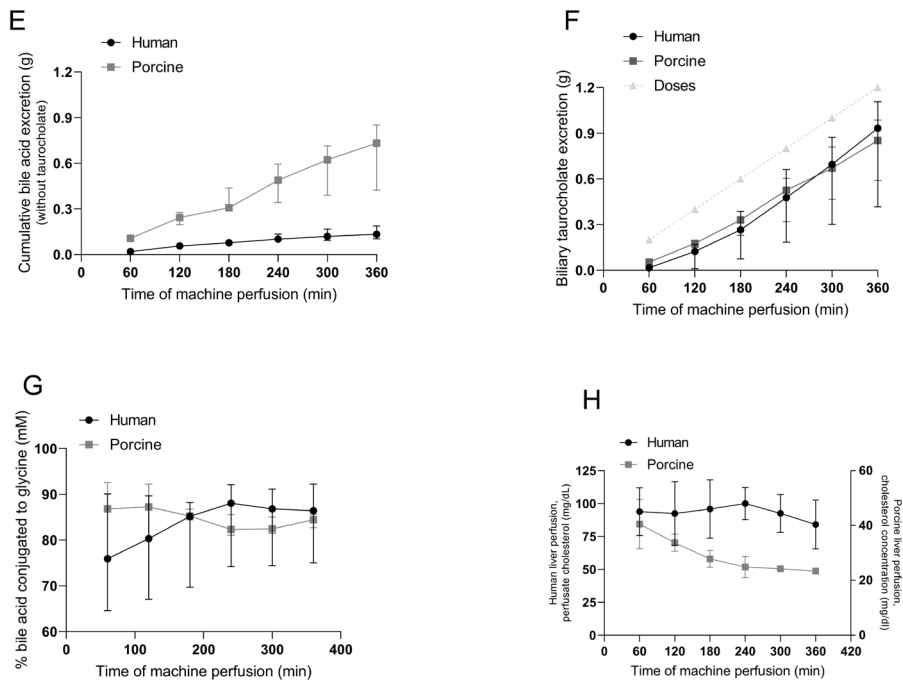
Figure 5.1 - Characterization of human and porcine de novo bile acid synthesis and cholesterol metabolism (A) average human bile acid composition (t=60-360min), (B) average porcine bile acid composition (t=60-360min), (C) human bile acid composition over time and (D) porcine bile acid composition over time, (E) Cumulative bile acid excretion in grams during NMP for human and porcine livers, (F) biliary excretion of taurocholate in human and porcine livers versus the administered taurocholate dose, (G) % bile acids conjugated to glycine in human and porcine bile and (H) perfusate cholesterol concentration during 360 min of perfusion. Data represents median ± range of n=4 human livers and n=3 porcine livers. Differences between groups were analyzed using the Mann-Whitney U test

Dysregulated cholesterol- and bile acid gene expression during NMP with TCA

RNA sequencing was performed on tissue biopsies taken at t=0 min and t=360 min of perfusions using the standard protocol with TCA. Genes involved in cholesterol synthesis, cholesterol import and export, bile acid synthesis, bile acid conjugation, and bile acid transporter expression were analyzed since bile acid transporter gene expression is regulated through bile acid signaling[30] (Figure 5.2). The genes LDL-r, HMG-CoA and NPC1, responsible for cholesterol uptake, cholesterol synthesis and intracellular transport, respectively, exhibited increased expression in human liver biopsies at t=360 min. Notably, NPC1 demonstrated a significant 1.8-fold upregulation (p<0.05) (Figure 5.2A),

indicating the intracellular need for cholesterol. The genes ABCA1 and ABCG8, involved in cholesterol efflux, showed a 0.8- and 0.3-fold decrease, however not significant. In pig liver tissues the genes involved in cholesterol uptake and synthesis showed a strong upregulation of which LDL-r (fold change of 3.4, p<0.05), NPC1L1 (fold change of 4.5, p<0.05) and NPC1 (fold change of 4.5 p<0.01) (Figure 5.2B). Additionally, ABCG8 strongly decreased to 0.3 fold change (p<0.01). Regarding cholesterol metabolism, the effect on gene expression were comparable, however, it was more pronounced in pig liver tissues. Figure 2C-D demonstrates the expression of bile acid synthesizing enzymes in human and pig liver biopsies. In human liver biopsies, CYP27A1 and CYP8B1, and bile acid conjugating enzymes (bile acid:amino acid transferase, BAAT [human] and bile acid:CoA synthase, BACS) in general had a decreased gene expression following 360 min liver NMP, though only CYP27A1 (p<0.05) and CYP8B1 (p<0.05) were statistically significant in human liver tissues. In pig liver biopsies, CYP27A1 (P<0.05) and CYP7A1 (P<0.05) were significantly decreased after 360 min of liver NMP and CYP8B1 and BACS showed decreasing trend over time. Figure 5.2E and 5.2F present data on bile acid uptake and efflux transporter expression showing that a decrease for all measured bile acid transporters was observed over time. For example, in human liver biopsies, OAT2 (fold change of 0.43, p<0.05) and BSEP (fold change of 0.45, p<0.05) significantly decreased and in porcine liver tissue, OATP1B4 (fold change of 0.41, p<0.01) and BSEP (fold change of 0.32, p<0.05) showed a significant decrease. Together, similar trends in gene expression were observed between porcine and human livers, however, effects on cholesterol uptake, intracellular transport and synthesis were more uniform in pig liver biopsies. These results combined with the bile acid synthesis and cholesterol data strongly suggest that bile acid homeostasis is dysregulated during liver NMP using current standard protocol of TCA infusion.
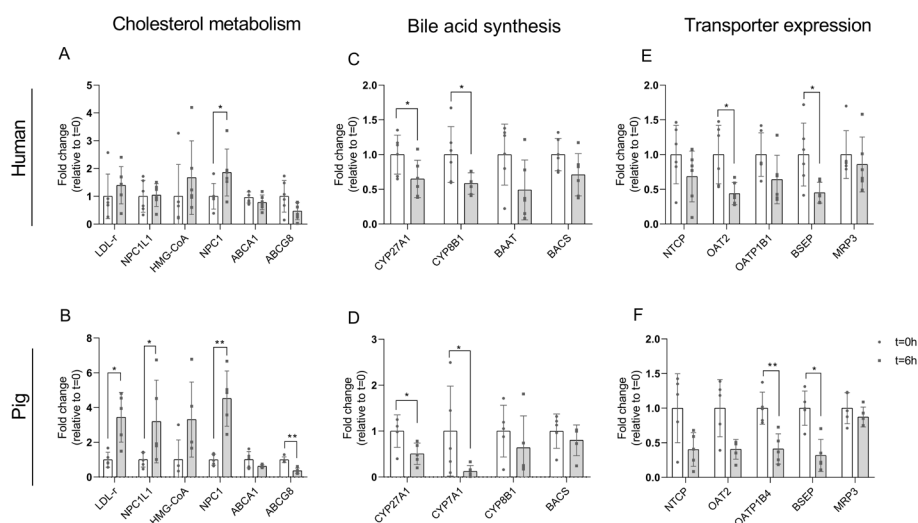
Figure 5.2 - Gene expression pattern before and after 360 min of human and porcine liver NMP (A) gene expression pattern of various genes in cholesterol metabolism such as influx transporters (LDL-r, NPC1L1), cholesterol biosynthetic enzyme (HMG-CoA reductase), intracellular cholesterol transporter (NPC1) and efflux transporters (ABCA1, ABCG8) before and after 360 minutes of NMP in human and (B) pig livers. (C) Gene expression pattern of enzymes involved in bile acid biosynthesis (CYP27A1, CYP7A1, CYP8B1) and conjugation (BACS, BAAT) before and after 360 minutes of human and (D) pig livers. (E) gene expression pattern of uptake and efflux transporters involved in bile acid uptake and excretion before and after 360 min of NMP in human and (F) pig livers. Data was expressed as FC relative to expression at t=0. Bars represent the mean of n=5 (porcine) or n=6 (human) independent experiments whereas lines represent individual livers. Differences between groups were analyzed using the Mann-Whitney U test

Infusion of conjugated bile acid mix enhances liver viability and function during NMP

After the observed increase in cholesterol-related gene expression and decrease in bile acid transporter gene expression in livers during NMP, we aimed to study the effect and addition of unprocessed bile on cholesterol and bile acid transporter gene expression during NMP of the liver. Case studies were performed by infusing unprocessed bile (10 mL/hr) during NMP, showing stimulated expression of several genes (Supplemental Figure S5.1). Since the use of unprocessed bile will never be applicable in the clinical setting, we aimed to investigate whether infusion of a variety of specific bile acids during liver NMP would alleviate the burden of the *de novo* synthesis by the liver and improve organ physiology. Various combinations of bile acids, both conjugated and unconjugated, were tested and compared to the standard protocol with TCA only. First attempts to perfuse porcine livers with primary bile acids only

(CDCA +CA) resulted in elevated ALT levels by potentially direct toxic effects of these primary bile acids (Supplemental Figure S5.2). Thus different strategies were explored. Figure 5.3 shows the liver viability and functionality parameters of upon infusion of a simple conjugated bile acid mix and a complete conjugated bile acid mix with Figure 5.3A showing the cumulative bile production during 720 minutes of perfusion. All livers produced consistent amounts of bile during 720 min of perfusion and no significant differences were observed between the groups. Perfusate ALT and AST were measured to study liver injury (Figure 5.3B-C). Figure 5.3B shows the AST release during 720 minutes of perfusion. Compared to the standard protocol using TCA, both the simple conjugated- and complete conjugated bile acid mix tended to show lower AST (average 56.3±9.9% and 63.5±10.8% respectively) and ALT levels (average 57.1±10.1% and 84.7±17.5% respectively). To study liver clearance capacity, a bolus of ICG was administered after 120 minutes of perfusion, as ICG is cleared through transporter-mediated mechanisms (OATP, NTCP, MRP2)[31] (Figure 5.3D-E). Efficient ICG clearance from the perfusate was observed in all livers, which was comparable to standard perfusions. The biliary excretion on ICG into bile tended to be faster for the simple conjugated bile acid mix, showing a steeper elimination curve compared to the standard and complete conjugated bile acid mix, however this difference was not significant (Figure 5.3E).
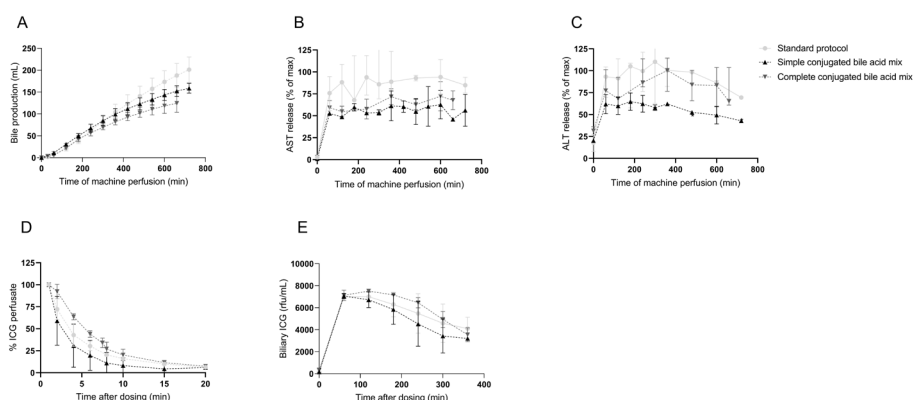

Figure 5.3 - Liver functionality during porcine liver NMP comparing the standard protocol versus continuous infusion with a simple conjugated bile acid mix versus continuous infusion with a complete conjugated bile acid mix. (A) Bile production during 720 min of perfusion, (B) AST release in the perfusate and expressed as % of highest AST release observed in the standard protocol, (C) ALT release in the perfusate and expressed as % of highest AST release observed in the standard protocol, (D) ICG elimination from the perfusate after a single bolus administration expressed as % of highest observed concentration (Cmax) and (E) biliary excretion of ICG studies over 360 min after administration. Data represents median ± range of standard protocol n=2, conjugated simple bile acid mix n=2, conjugated complete bile acid mix n=3.

Conjugated bile acid mix moderates *de novo* bile acid synthesis in porcine livers

Next, bile acid concentration in the perfusate and bile were determined of the perfusion with simple-, complete conjugated bile acid and TCA infusion. Figure 5.4A demonstrates the perfusate total bile acid concentration. In the standard protocol (TCA infusion), an increase in perfusate bile acid concentration was observed at t=60 min of perfusion whereas the simple conjugated- as well as complete conjugated bile acid mix showed lower perfusate bile acid levels indicating the ability of the perfused liver to efficiently clear the infused bile acids from the perfusate. Figure 5.4B shows the excreted bile acid concentration in bile over time demonstrating no differences in the excretion of total bile acids between protocols. The cumulative total bile acid output, visualized in Figure 5.4C, also showed no significant differences among the protocols. The total bile acid output was 4.18 mmol in 12h (4.8 mmol was infused in 12h) for standard protocol, 3.9 mmol in 12h (4.9 mmol was infused in 12h) for the conjugated simple bile acid mix and 3.0 in 11h (3.9 mmol was infused in 11hr). Cholesterol, which is the precursor of bile acids, remained at higher concentrations in the perfusate throughout the perfusions when bile acid mixes were supplemented, suggesting a reduced need for the intrahepatic conversion of cholesterol into bile acids. This is visualized in Figure 5.4D by the delta cholesterol (t=end - t=60 min of the perfusion), showing a drop of 25.9±4.4 mg/dL in perfusate levels of cholesterol in the standard protocol group. That result likely indicates a high consumption of cholesterol by the liver, needed for bile acid synthesis. The simple conjugated bile acid mix showed a subtle increase in cholesterol perfusate (Δ 5.3±1.3 mg/dL, p<0.05) and the complete conjugated bile acid mix demonstrated a small (not significant) reduction in cholesterol consumption compared to the standard protocol (Δ 12.8±15.2 mg/dL). Biopsies of the liver were taken at several time points during perfusion to study gene expression (Figure 5.4E-J). The simple conjugated bile acid mix increased the FXR gene expression to some extent at 360 and 540 min of perfusion (fold change 1.5), thereafter FXR expression returned to baseline (Figure 5.4E). In the complete conjugated bile acid mix FXR expression was stable over the length of the perfusion. HMG Co-A reductase as well as LDL-r gene expression increased upon the infusion of the different bile acid mixtures, in a similar manner compared to the standard protocol (Figure 5.4F-G). The expression of OATP1B4 showed a delayed decrease (after 360 min of perfusion) compared to the standard protocol showing a decrease after 240 min (Figure 5.4H). BSEP and NTCP (Figure 5.4I-J) both showed a fluctuating gene

expression profile, however after 720 min of perfusion, a decrease was observed in all protocols.
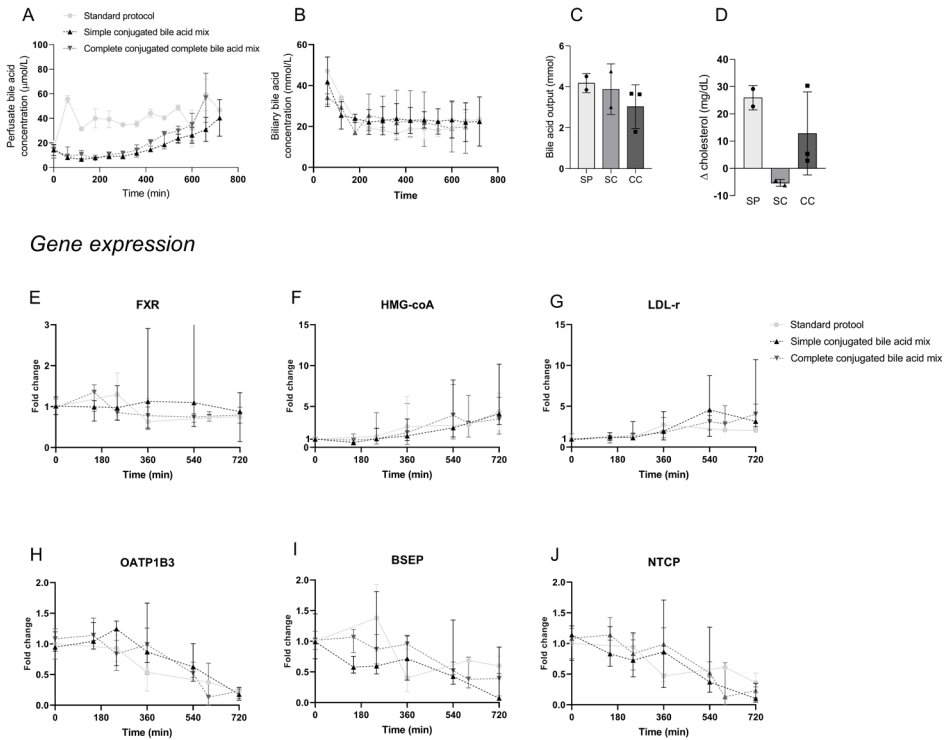
Bile and perfusate bile acid profiles

Gene expression

Figure 5.4 - Bile and perfusate bile acid profiles and corresponding gene expression characterization during 720 min of perfusion in the standard protocol versus continuous infusion with a conjugates simple bile acid mix versus continuous infusion with a conjugated complete bile acid mix. (A) perfusate bile acid concentration during NMP, (B) biliary bile acid concentration during NMP, (C) total bile acid output during NMP as corrected for total bile flow, SP=standard protocol, CS=conjugated simple bile acid mix, CC=conjugated complete bile acid mix, (D) delta cholesterol: end of perfusate – t=60 min. Gene expression profile during porcine liver NMP of (E) FXR, (F) HMG-CoA, (G) LDL-r, (H) OATP1B4, (I) BSEP and (J) NTCP. Data represents median ± range of standard protocol n=2 (n=8: 0-360 min, n=2: 360-720 min), conjugated simple bile acid mix n=2, conjugated complete bile acid mix n=3.

Bile acid challenge as hepatobiliary function assessment in human livers

The simple conjugated bile acid mix was chose to be applied during 3 independent human liver perfusions (referred to as liver #1, #2 and #3)

because of its positive effects on ALT AST release and ICG clearance observed in the porcine liver experiments. Donor characteristics are presented in Table 5.2 and set-up of the liver perfusion is illustrated in Figure 5.5A. Human liver perfusion demonstrated a proper bile flow during the infusion of the simple conjugated bile acid mix in all three livers (Figure 5.5B). Human livers were able to rapidly clear lactate, of which the subsequent levels remained stable during the perfusion duration demonstrating appropriate hepatocellular function (Figure 5.5C). ALT and AST levels in liver #1 and #2 remained low and stable during the perfusion whereas liver #3 had relatively high ALT levels (1800 U/L) from the start of the perfusion, likely relating to the presence of a pre-existing pathological condition (including choledocholithiasis). Bile pH was alkalotic (>7.5) from all three livers and remained stable throughout the perfusion (Figure 5.5E). The plasma cholesterol levels were stable over time (Figure 5.5F). The functionality of the livers was assessed by studying ICG clearance from the perfusate after 4h and 2h for liver #1 and #2-#3 respectively (Figure 5.5G). Overall, rapid elimination of ICG from the perfusate was observed with subsequent biliary elimination detected 20 min after administration. Additionally during perfusion, a bile acid challenge was performed to liver #1 and #2 by providing a bolus of simple conjugated bile acids (0.2g) to the perfusate and assessing clearance of these bile acids as a functional parameter. Prior to the bile acid bolus in liver #1 and #2, perfusate and biliary bile acid concentrations remained stable over time (5.5±1.4 μmol/L in perfusate, 15.3±2.1 mmol/L in bile in #1, 4.3±2.2 μmol/L in perfusate, 16.3.7±1.5 mmol/L in bile in #2). Upon administration of a bile acid bolus, the perfusate levels showed to peak and rapidly decline indicating the ability to efficiently clear bile acids from the circulation. This was also illustrated by an increase in bile acid concentration in bile. Liver #3 suffered from choledocholithiasis as is visualized by the limited bile acid output and decreased bile acid absorption from the perfusate (Figure 5.5I). The data shows that the simple conjugated bile acid mix supports proper liver function and is safe to use however did not have pronounced effects on bile acid-regulated genes (Supplemental Figure S5.3, supplemental Figure S5.4).
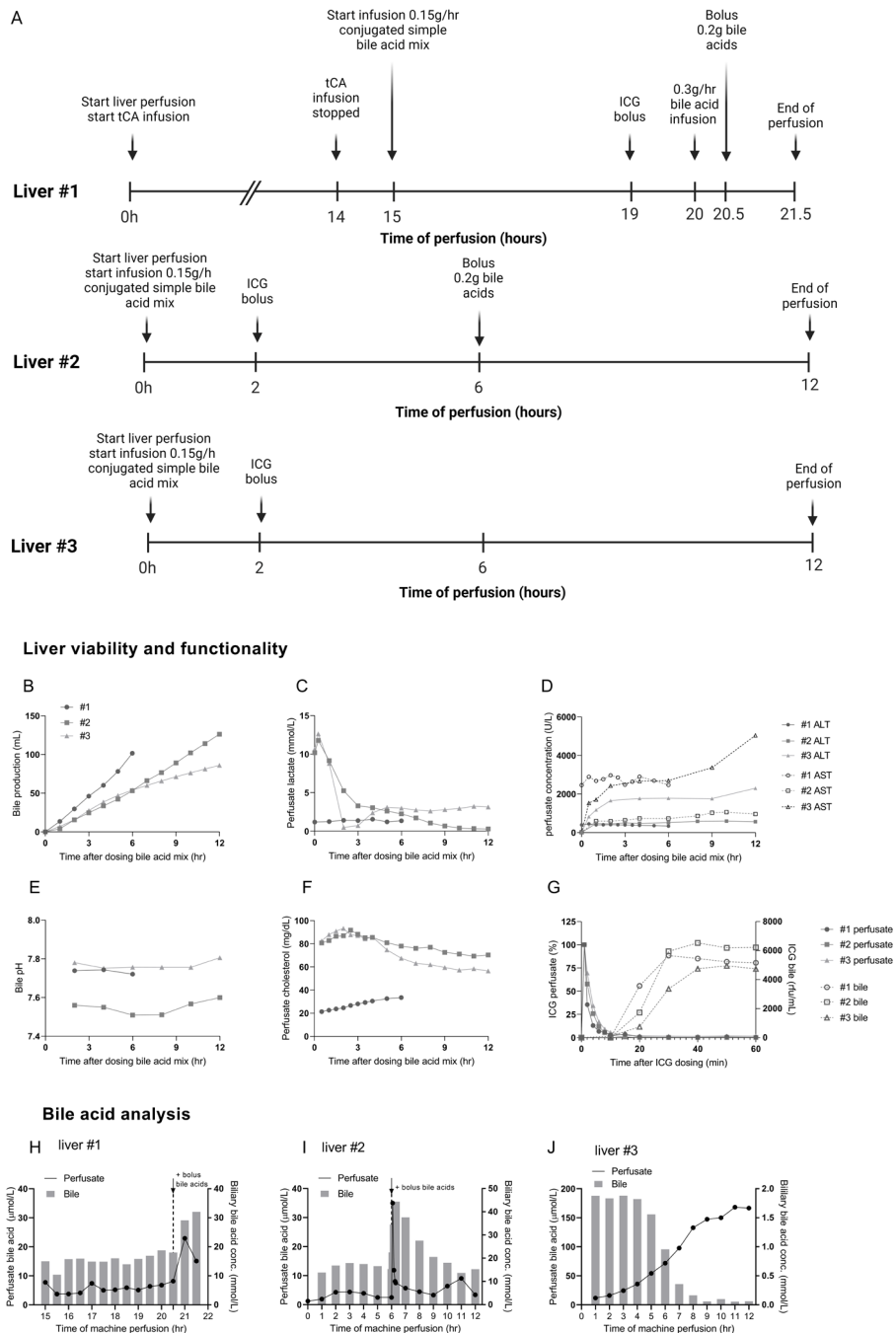
Figure 5.5 - Human liver perfusion with administration of conjugated simple bile acid mix. (A) schematic overview of the study set-up (B) Cumulative bile production, (C) perfusate lactate

concentration, (D) perfusate ALT and AST concentration, (E) Bile pH, (F) cholesterol perfusate concentration, (G) ICG perfusate and ICG biliary excretion measured after 4 hours of perfusion liver #1, 2 hours of perfusion liver #2 and #3, (H) perfusate bile acid concentration during 15-20 hours and 20 – 21,5 with increased bile acid infusion + additional bolus liver #1, (I) perfusate and biliary bile acid concentration in liver #2 with a bile acid bolus at t=360 min and (J) perfusate and biliary bile acid concentration in liver #3 min. Data represents mean ± SD n=3 individual experiments.

Discussion

Bile acid metabolism, is a complex phenomenon in our body and often not taken into account during *ex vivo* liver perfusion as standard protocols only apply TCA. In the first part of this study, applying the standard protocol with TCA only, we showed that during *ex vivo* liver NMP bile acid and cholesterol homeostasis was dysregulated. In the second part of this study, we described that infusion of a (un)conjugated bile acid mixture alleviated the burden of the *de novo* bile acid synthesis in the liver by showing decreased ALT and AST levels while retaining appropriate liver functions. These finding provide valuable new insights for improving the physiological resemblance of bile acids (and cholesterol) metabolism during NMP and thereby improving organ viability and functionality.

The human body is a complex biological system with continuous feedback systems and a dynamic interplay between organs, which is essential for maintaining homeostatic processes. Interestingly, the perfused livers in the first part of the study with TCA infusion appeared to be comparable to biliary drainage models where the EHC is interrupted[32-34]. During NMP, a decrease in perfusate cholesterol was observed accompanied by an increase in HMG-CoA reductase expression and altered cholesterol gene expression profile, similar to biliary drainage models. Kuipers et al.[32] and Smit et al.[34] demonstrated in rats that interruption of the EHC rapidly reduced plasma cholesterol and biliary bile acid output, and interestingly, increased food intake[32]. Additionally, a rapid decrease in bile flow was observed in the first hours after cannulation[32-34]. In humans, a similar phenomenon was observed, with Shoda et al.[35] reporting the low biliary secretion of bile acids just after biliary drainage. These findings indicate that the absence of EHC *in vivo* profoundly impacts bile acid and cholesterol homeostasis, suggesting that incorporating EHC during liver perfusion could enhance liver function and homeostasis.

The intervention studies with (un)conjugated bile acids indicated that cholesterol consumption in the liver was equivalent to cholesterol synthesis, since cholesterol perfusate levels remained more stable compared to control perfusions with TCA only. Supplementation of an (un)conjugated bile acid mixture reduced the requirement for *de novo* bile acid synthesis, demonstrated by the reduced cholesterol consumption while retaining similar bile acid output. Furthermore, peak bile acid concentration was observed in the standard protocol at t=60 min, which was absent during the perfusions with conjugated bile acid infusion. Higher levels of ALT and AST at t=60 were observed for the standard protocol compared to the intervention protocols possibly attributed to the elevated perfusate bile acid levels[13]. After static cold storage, the liver is subjected to a sudden increase in temperature when connected to the perfusion device resulting in a rapid increase in metabolic rate. The (un)conjugated bile acid mix may support this recuperation phase as evidenced by efficient bile acid clearance during the first hours of perfusion. However, more research is needed to study the optimal bile acid infusion composition especially given the potential for prolonged *ex vivo* liver perfusion. Current studies show prolonged *ex vivo* liver perfusion duration up to 7 days or longer[8,36] and thus the need for bile acid supplementation will become more substantial. Eshmuminov highlighted the utilization of UCDCA in-stead of TCA, based on UCDCA's epithelial protection properties[11]. Yet, using a single bile acid during perfusion does not replicate the diverse pool normally synthesized and excreted by the liver. Infusing a pool of (un)conjugated bile acid could efficiently extend perfusion duration by reducing the necessity for *de novo* synthesis, thus resulting in reduced energy requirement as the *de novo* synthesis of bile acids is an energy demanding process[12,13].

In the human liver perfusions using supplementation of the simple conjugated bile acid mix, stable cholesterol perfusate levels were observed, indicating reduced use of cholesterol for the conversion to bile acids. Good liver function and safe use of the simple conjugated bile acid mix was observed by showing lactate clearance, alkalotic bile pH and ICG clearance. In 2 out of 3 human livers efficient removal of the bile acid bolus from the perfusate was observed and subsequent increased excretion of total bile acids was measured as well as an increase in bile production. This indicates presence and appropriate function of the transporters NTCP and BSEP, highlighting the potential utility of a bile acid challenge as a tool to assess viability and/or quality during NMP. Notable, one of the livers (liver #3) from a patient with underlying pathology of gall

stones, showed diminished clearance of bile acids, potentially explained by the lower abundance of the transporters NTCP and BSEP in this donor[37].

In this study it was hypothesized that bile acid signaling would be one of the main mechanism in regulating stable (ADME) gene expression during NMP. However, the gene expression profile in pigs following intervention with the (un)conjugated bile acid pools continued to exhibit effects on bile acid-regulated genes. It is important to acknowledge that the porcine bile acid composition differs from that of humans, showing higher presence of hyocholic acid and its conjugates. The most optimal scenario would have been to mimic porcine bile acids however obtaining hyocholic acids in mg scale was economically unfeasible[38]. Although to a lesser and more delayed extent, also a decreasing trend in relevant gene expression was observed during the human liver perfusion. It could be that other mechanisms such as circadian rhythm overpowered gene regulation. It is known that genes involved in bile acid metabolism are regulated by central and hepatic circadian clock genes in addition to the timing of food intake, which was not taken into account in this study[18,39]. Therefore, longer term perfusion of the livers (>24 hours) is needed to study potential fluctuation in gene expression regulated by circadian clock genes.

Conclusion

In conclusion, replacing standard TCA infusion during liver NMP with a more physiologically representative bile acid pool to stimulate the enterohepatic recirculation of bile acids has yielded promising results. The infusion of a more physiologically relevant bile acid mixture containing a variety of (un)conjugated bile acids showed a decreased release of hepatic injury markers and better maintenance of stable cholesterol levels in the perfusate, compared to standard NMP. Moreover, the results demonstrated that the infusion of (un)conjugated bile acids may enhance liver function during NMP, thereby pointing towards potential advancements in liver preservation during the and transplantation process.

References

1. de Vries Y, Matton AP, Nijsten MW, Werner MJ, van den Berg AP, de Boer MT, Buis CI, et al. Pretransplant sequential hypo-and normothermic machine perfusion of suboptimal livers donated after circulatory death using a hemoglobin-based oxygen carrier perfusion solution. American journal of transplantation 2019;19:1202-1211.
2. Watson CJ, Kosmoliaptsis V, Randle LV, Gimson AE, Brais R, Klinck JR, Hamed M, et al. Normothermic perfusion in the assessment and preservation of declined livers before transplantation: hyperoxia and vasoplegia—important lessons from the first 12 cases. Transplantation 2017;101:1084.
3. Bonaccorsi-Riani E, Gillooly AR, Iesari S, Brüggenwirth IM, Ferguson CM, Komuta M, Xhema D, et al. Delivering siRNA compounds during HOPE to modulate organ function: a proof-of-concept study in a rat liver transplant model. Transplantation 2022;106:1565-1576.
4. Dengu F, Abbas SH, Ebeling G, Nasralla D. Normothermic machine perfusion (NMP) of the liver as a platform for therapeutic interventions during ex-vivo liver preservation: a review. Journal of clinical medicine 2020;9:1046.
5. Gillooly AR, Perry J, Martins PN. First report of siRNA uptake (for RNA interference) during ex vivo hypothermic and normothermic liver machine perfusion. In: LWW; 2019.
6. Stevens LJ, Dubbeld J, Doppenberg JB, van Hoek B, Menke AL, Donkers JM, Alsharaa A, et al. Novel explanted human liver model to assess hepatic extraction, biliary excretion and transporter function. Clinical Pharmacology & Therapeutics 2023.
7. Krüger M, Ruppelt A, Kappler B, Van Soest E, Samsom RA, Grinwis GC, Geijsen N, et al. Normothermic Ex Vivo Liver Platform Using Porcine Slaughterhouse Livers for Disease Modeling. Bioengineering 2022;9:471.
8. Eshmuminov D, Becker D, Bautista Borrego L, Hefti M, Schuler MJ, Hagedorn C, Muller X, et al. An integrated perfusion machine preserves injured human livers for 1 week. Nature biotechnology 2020;38:189-198.
9. Javitt NB, Emerman S. Effect of sodium taurolithocholate on bile flow and bile acid excretion. The Journal of clinical investigation 1968;47:1002-1014.
10. Brüggenwirth IM, de Meijer VE, Porte RJ, Martins PN. Viability criteria assessment during liver machine perfusion. Nature biotechnology 2020;38:1260-1262.
11. Eshmuminov D, Schuler MJ, Becker D, Borrego LB, Mueller M, Hagedorn C, Häusler S, et al. Bile formation in long-term ex situ perfused livers. Surgery 2021;169:894-902.
12. Chiang JY. Bile acids: regulation of synthesis: thematic review series: bile acids. Journal of lipid research 2009;50:1955-1966.
13. Chiang JY. Bile acid metabolism and signaling. Comprehensive physiology 2013;3:1191.
14. Chen M-j, Liu C, Wan Y, Yang L, Jiang S, Qian D-w, Duan J-a. Enterohepatic circulation of bile acids and their emerging roles on glucolipid metabolism. Steroids 2021;165:108757.
15. Chiang JY. Targeting bile acids and lipotoxicity for NASH treatment. Hepatology communications 2017;1:1002.
16. Mertens KL, Kalsbeek A, Soeters MR, Eggink HM. Bile acid signaling pathways from the enterohepatic circulation to the central nervous system. Frontiers in neuroscience 2017:617.
17. Eggink HM, van Nierop FS, Schooneman MG, Boelen A, Kalsbeek A, Koehorst M, Ten Have GA, et al. Transhepatic bile acid kinetics in pigs and humans. Clinical Nutrition 2018;37:1406-1414.
18. Eggink HM, Oosterman JE, de Goede P, de Vries EM, Foppen E, Koehorst M, Groen AK, et al. Complex interaction between circadian rhythm and diet on bile acid homeostasis in male rats. Chronobiology international 2017;34:1339-1353.
19. Sips FL, Eggink HM, Hilbers PA, Soeters MR, Groen AK, Van Riel NA. In silico analysis identifies intestinal transit as a key determinant of systemic bile acid metabolism. Frontiers in Physiology 2018;9:631.

20. De Fabiani E, Mitro N, Gilardi F, Caruso D, Galli G, Crestani M. Coordinated control of cholesterol catabolism to bile acids and of gluconeogenesis via a novel mechanism of transcription regulation linked to the fasted-to-fed cycle. Journal of Biological Chemistry 2003;278:39124-39132.
21. Halilbasic E, Claudel T, Trauner M. Bile acid transporters and regulatory nuclear receptors in the liver and beyond. Journal of hepatology 2013;58:155-168.
22. Staudinger JL, Woody S, Sun M, Cui W. Nuclear-receptor–mediated regulation of drug–and bile-acid–transporter proteins in gut and liver. Drug metabolism reviews 2013;45:48-59.
23. Zollner G, Fickert P, Fuchsbichler A, Silbert D, Wagner M, Arbeiter S, Gonzalez FJ, et al. Role of nuclear bile acid receptor, FXR, in adaptive ABC transporter regulation by cholic and ursodeoxycholic acid in mouse liver, kidney and intestine. Journal of hepatology 2003;39: 480-488.
24. Chu X, Chan GH, Evers R. Identification of endogenous biomarkers to predict the propensity of drug candidates to cause hepatic or renal transporter-mediated drug-drug interactions. Journal of pharmaceutical sciences 2017;106:2357-2367.
25. Petzinger E, Geyer J. Drug transporters in pharmacokinetics. Naunyn-Schmiedeberg's archives of pharmacology 2006;372:465-475.
26. Eshmuminov D, Leoni F, Schneider MA, Becker D, Muller X, Onder C, Hefti M, et al. Perfusion settings and additives in liver normothermic machine perfusion with red blood cells as oxygen carrier. A systematic review of human and porcine perfusion protocols. Transplant International 2018;31:956-969.
27. Rui L. Energy metabolism in the liver. Comprehensive physiology 2014;4:177.
28. Stevens LJ, Zhu AZ, Chothe PP, Chowdhury SK, Donkers JM, Vaes WH, Knibbe CA, et al. Evaluation of normothermic machine perfusion of porcine livers as a novel preclinical model to predict biliary clearance and transporter-mediated drug-drug interactions using statins. Drug Metabolism and Disposition 2021;49:780-789.
29. Slijepcevic D, Kaufman C, Wichers CG, Gilglioni EH, Lempp FA, Duijst S, de Waart DR, et al. Impaired uptake of conjugated bile acids and hepatitis b virus pres1-binding in na+-taurocholate cotransporting polypeptide knockout mice. Hepatology 2015;62:207-219.
30. Chiang JY. Bile acid regulation of gene expression: roles of nuclear hormone receptors. Endocrine reviews 2002;23:443-463.
31. de Graaf W, Häusler S, Heger M, van Ginhoven TM, van Cappellen G, Bennink RJ, Kullak-Ublick GA, et al. Transporters involved in the hepatic uptake of 99mTc-mebrofenin and indocyanine green. Journal of hepatology 2011;54:738-745.
32. Kuipers F, Havinga R, Bosschieter H, Toorop G, Hindriks F, Vonk R. Enterohepatic circulation in the rat. Gastroenterology 1985;88:403-411.
33. Myant N, Eder HA. The effect of biliary drainage upon the synthesis of cholesterol in the liver. Journal of Lipid Research 1961;2:363-368.
34. Smit M, Temmerman AM, Havinga R, Kuipers F, Vonk R. Short-and long-term effects of biliary drainage on hepatic cholesterol metabolism in the rat. Biochemical Journal 1990;269:781-788.
35. Shoda J, Kano M, Oda K, Kamiya J, Nimura Y, Suzuki H, Sugiyama Y, et al. The expression levels of plasma membrane transporters in the cholestatic liver of patients undergoing biliary drainage and their association with the impairment of biliary secretory function. The American journal of gastroenterology 2001;96:3368-3378.
36. Lau YY, Okochi H, Huang Y, Benet LZ. Pharmacokinetics of atorvastatin and its hydroxy metabolites in rats and the effects of concomitant rifampicin single doses: relevance of first-pass effect from hepatic uptake transporters, and intestinal and hepatic metabolism. Drug metabolism and disposition 2006;34:1175-1181.
37. Stanca C, Jung D, Meier PJ, Kullak-Ublick GA. Hepatocellular transport proteins and their role in liver disease. World Journal of Gastroenterology 2001;7:157.
38. Imber CJ, Peter SDS, De Cenarruzabeitia IL, Lemondea H, Rees M, Butlera A, Clayton PT, et al. Optimisation of bile production during normothermic preservation of porcine livers. American Journal of Transplantation 2002;2:593-599.

39. Sukumaran S, Almon RR, DuBois DC, Jusko WJ. Circadian rhythms in gene expression: Relationship to physiology, disease, drug disposition and drug action. Advanced drug delivery reviews 2010;62:904-917.

Supplementary materials

Table S5.1 - Human primer sequences.

Species	Gene/protein	Primer sequences forward (FW) and reverse (REV) '5-3'
Human	*GAPDH*/GAPDH	FW: ATGGAAATCCCATCACCATCTT
		REV: CGCCCCACTTGATTTTGG
	ACTB/ACTB	FW: GCTGCCCTGAGGCACTCTT
		REV: GGATGCCACAGGACTCCATG
	ABCB11/BSEP	FW: AAAGCACTCATTTGCCCCTG
		REV: TCTTGTAGATTCCTGCCGCC
	NR1H4/FXR	FW: TGTGAGGGGTGTAAAGGTTTCT
		REV: GCCAACATTCCCATCTCTTTGC
	HMGCR/HMG-CoA reductase	FW: TACCATGTCAGGGGTAC
		REV: CAAGCCTAGAGACATAAT
	LDLR/LDLR	FW: GTGCTCCTCGTCTTCCTTTG
		REV: GCAAATGTGGACCTCATCCT
	SLC10A1/NTCP	FW: CTTCTGCCTCAATGGACGGT
		REV: AGGCCACATTGAGGATGGTG
	SLCO1B3/OATP1B3	FW: GGGTGAATGCCCAAGAGATA
		REV: ATTGACTGGAAACCCATTGC

Table S5.2 - Porcine primer sequences.

| Species	Gene/protein	Primer sequences forward (FW) and reverse (REV) '5-3'
Porcine	*GAPDH*/GAPDH	FW: ATCGTCAGCAATGCCTCCTG
		REV: ACCGTGGTCATGAGTCCCTC
	ABCB11/BSEP	FW: GGATTCATGTGGTGTCTCATCTTT
		REV: ACAAGGGTTCCTGCTGTGTATTC
	ABCG8/ABCG8	FW: AGACGCAATCCTCAATGCCA
		REV: GCAGGAGTCTGGGCTTGAAT
	CYP27A1/CYP27A1	FW: TTGAGAAACGCATTGGCTGC
		REV:ATCCAGGTATCGCCTCCAGT
	NR1H4/FXR	FW: ATGGGAATGTTGGCTGAATGT
		REV:TGTTGAGGTCACTTGTCGCA
	HMGCR/HMG-CoA reductase	FW: GACTCCGTTGACTGGAGACG
		REV: AAAGAGGCCATGCATTCGGA
	ABCC2/MRP2	FW: TCACCTGCAACTTGGGTTGT
		REV: GTCTCTAGATCCACCGCAGC
	SLC10A1/NTCP	FW: TTACCCCCAAAAGCCTCACC
		REV: TTTTATGCCTGTGGGGCACT
	SLC22A7/OAT2	FW: CTGGGAATACGACCACTCGG
		REV: GGCTCTGTTCAGGCCTTTCT
	SLCO1B4/OATP1B4	FW: CCTCTTCATTGGGAACCATCTC
		REV: GAATTCCTCCTAGCGTTCGAATAGT
	*ABCB1/*P-gp	FW: AAATTGTGTGAATTGCCCAGATAAC
		REV: GCCACAGTAATAATAGGCGTACACTG
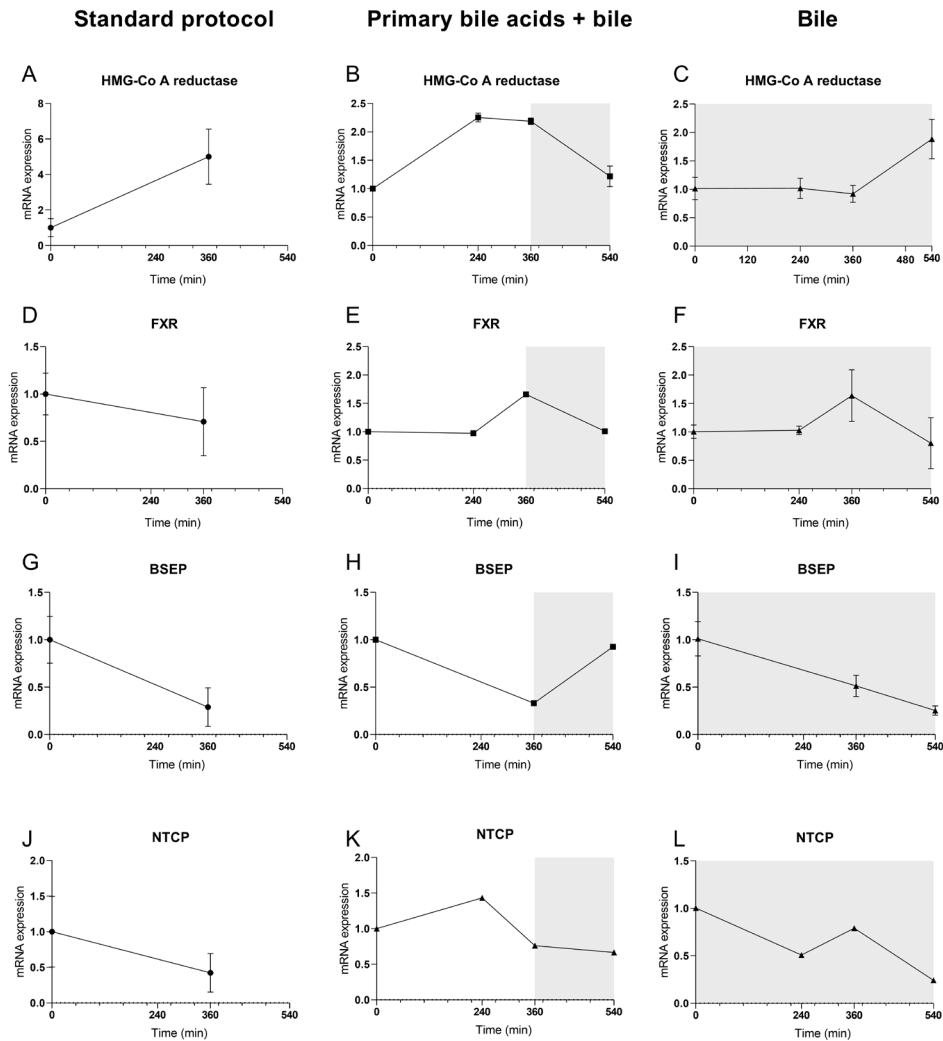
Figure S5.1 - Case studies showing gene expression profile upon standard protocol, infusion with primary bile acids + unprocessed bile or continuous infusion of unprocessed bile during NMP in porcine livers. (A-C) Gene expression of HMG-CoA, (D-F) FXR, (G-I) BSEP and (J-L) NTCP. Data represents median ± + IQR, n=5 for the standard protocol and n=1 for primary bile acids + bile and n=1 for bile condition. Primary bile acid infusion: To study the effect of primary bile acids and porcine bile, tCA was replaced by the primary bile acids CDCA and CA (total rate of 0.2g/hr (0.37mmol/hr)) (n=1). Liver was perfused for 360 minutes, thereafter bile from the gall bladder was infused at a rate of 10mL/hr from 360 minutes until 540 minutes. Continuous bile infusion: To study the effect of continuous bile infusion, tCA was replaced by porcine bile (pooled from n=5 pig gall bladders) (n=1). Bile was infused at a rate of 10 mL/hr. Livers were perfused for a total time of 540 minutes.
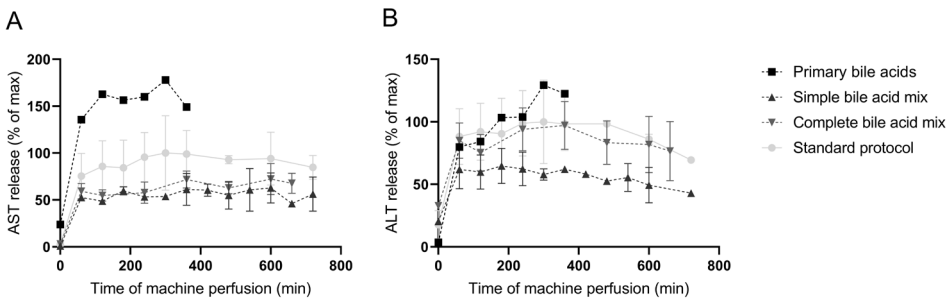
Figure S5.2 - AST and ALT levels during infusion of different bile acid mixes. Livers were perfused and continuous infusion of primary bile acids (CDCA+CA), conjugated simple bile acid mix, conjugated complete bile acid mix or with tCA (standard protocol). (A) perfusate AST and (B) perfusate ALT release. Data represents mean with range (min-max).
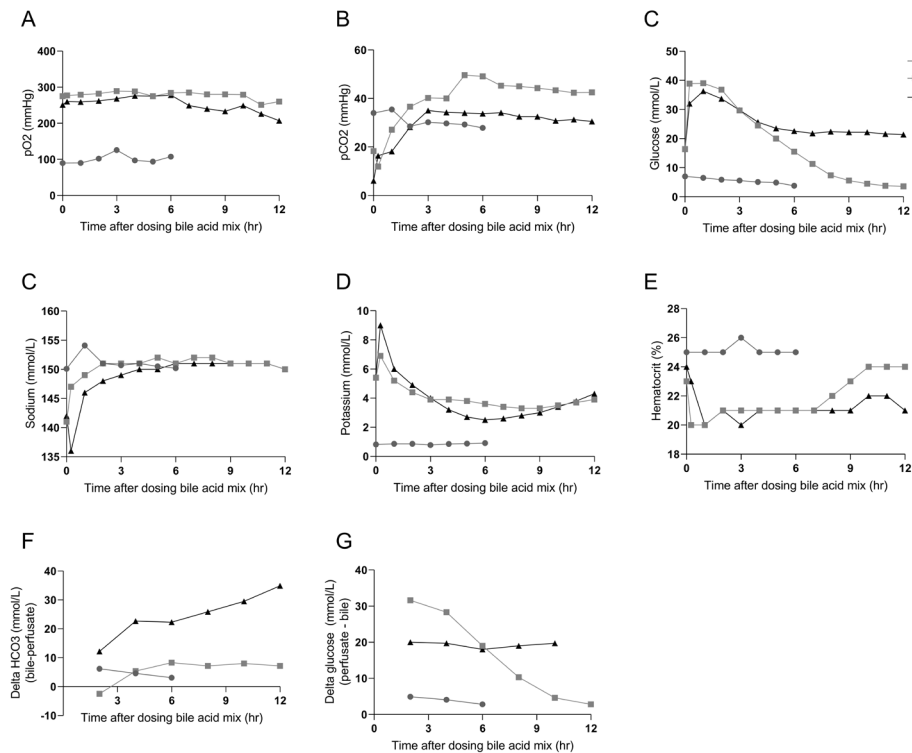

Figure S5.3 - Bloodgas analysis data of human liver perfusions with continuous infusion of conjugated simple bile acid mix. (A) pO2, (B) pCO2, (C) perfusate glucose, (D) perfusate sodium, (E) perfusate potassium, (F) perfusate hematocrit level (G) delta HCO3 (bile-perfusate) and (I) delta glucose (perfusate-bile). Data represents individual data of n=3 experiments.
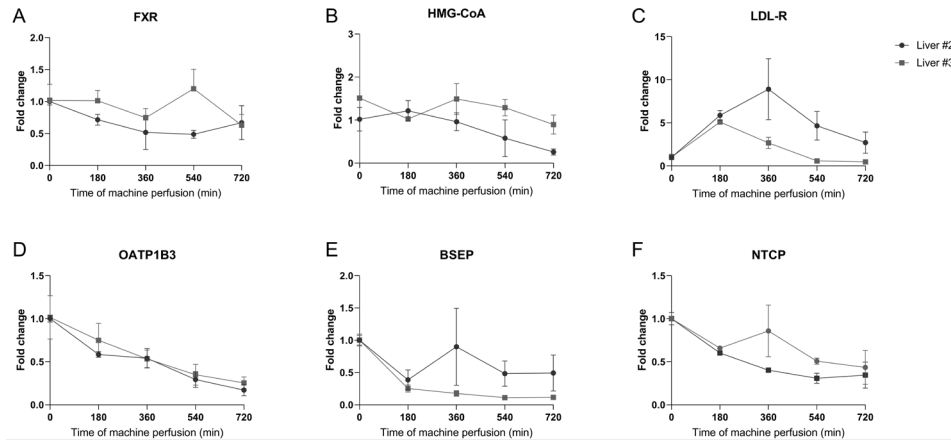
Figure S5.4 - Gene expression profile of human liver #2 and #3 during 720 min of perfusion. Gene expression profile during human liver NMP of (A) FXR, (B) HMG-CoA, (C) LDL-r, (D) OATP1B3, (E) BSEP and (F) NTCP. Data represents n=2. No biopsies were taken from liver #1 which perfused using the OrganOx system due to inability of the closed system

PART III

Unraveling pharmacokinetics through multi-organ perfusion
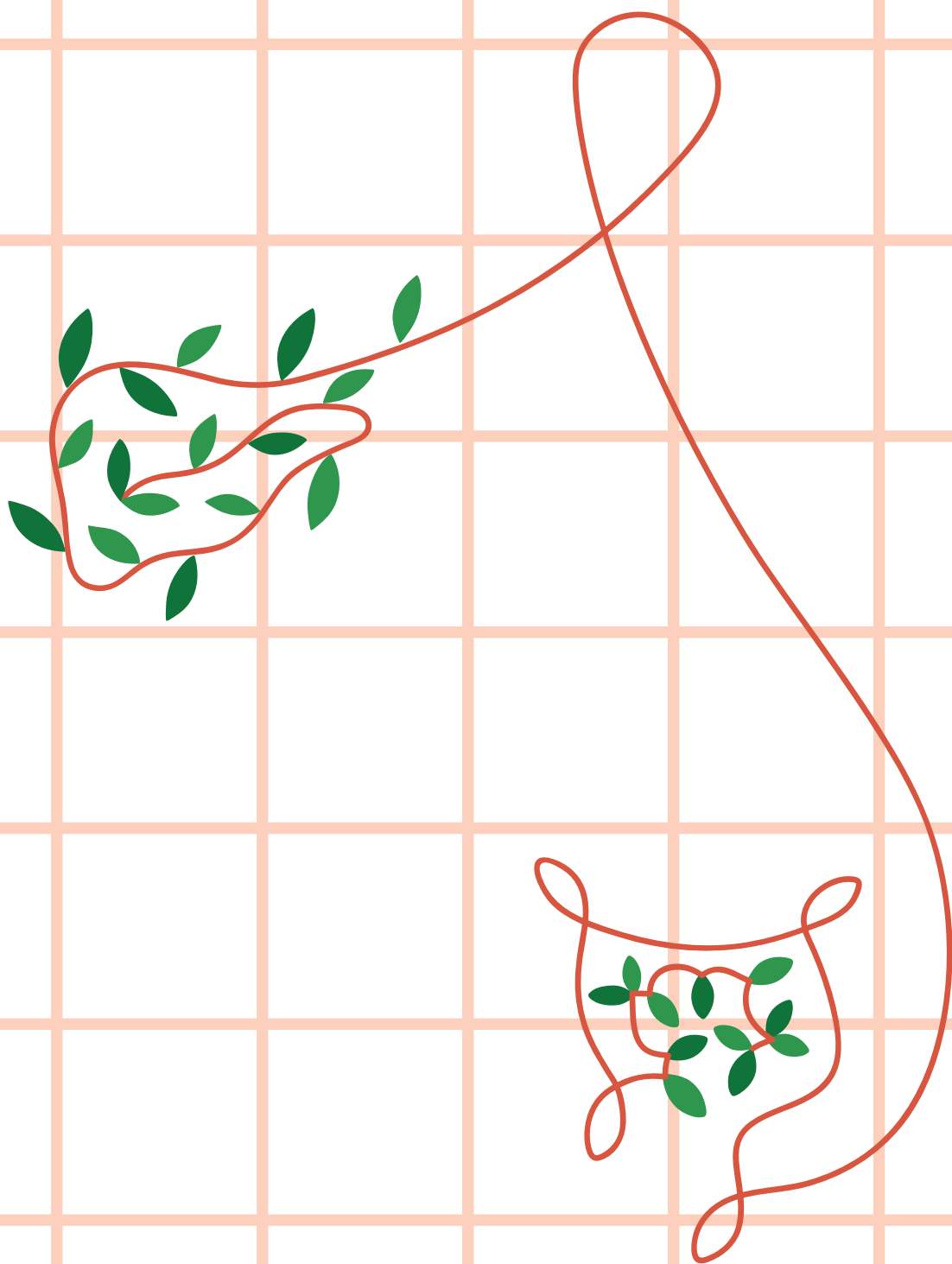
CHAPTER 06

Ex vivo Gut-Hepato-Biliary organ perfusion model to characterize oral absorption, gut-wall metabolism, pre-systemic hepatic metabolism and biliary excretion; application to midazolam

L.J. Stevens, E. van de Steeg, J.B. Doppenberg, I.P.J. Alwayn, C.A.J. Knibbe, J. Dubbeld

Abstract

To date, characterization of the first-pass effect of orally administered drugs consisting of local intestinal absorption and metabolism, portal vein transport and hepatobiliary processes remains challenging. Aim of this study was to explore the applicability of a porcine ex-vivo perfusion model to study oral absorption, gut-hepatobiliary metabolism and biliary excretion of midazolam.

Slaughterhouse procured porcine *en bloc* organs (n=4), were perfused via the aorta and portal vein. After 120min of perfusion, midazolam, atenolol, antipyrine and FD4 were dosed via the duodenum and samples were taken from the systemic- and portal vein perfusate, intestinal faecal effluent and bile to determine drug and metabolite concentrations.

Stable arterial and portal vein flow was obtained and viability of the perfused organs was confirmed. After intraduodenal administration, midazolam was rapidly detected in the portal vein together with 1-OH midazolam (E_{G-pv} of 0.16±0.1) resulting from gut wall metabolism through oxidation. In the intestinal faecal effluent, 1-OH midazolam and 1-OH midazolam glucuronide ($E_{G-intestine}$ 0.051±0.03) was observed resulting from local gut glucuronidation. Biliary elimination of midazolam (0.04±0.01%) and its glucuronide (0.01±0.01%) only minimally contributed to the enterohepatic circulation. More extensive hepatic metabolism (F_H 0.35±0.07) over intestinal metabolism (F_G 0.78±0.11) was shown, resulting in oral bioavailability of 0.27±0.05.

Ex vivo perfusion demonstrated to be a novel approach to characterize pre-systemic extraction of midazolam by measuring intestinal as well as hepatic extraction. The model can generate valuable insights into the absorption and metabolism of new drugs.

Introduction

In order to determine the oral bioavailability of a drug, characterization of gut-wall, liver and biliary processes is of great importance[1]. Insight into the extent of intestinal absorption and metabolism, portal venous blood concentrations and hepatic metabolism and biliary excretion is crucial in the early stages of drug development to understand the pharmacokinetics (PK) and select compounds that achieve a desirable systemic exposure. This is especially the case for compounds prone to CYP3A metabolism which reduce the oral bioavailability due to first-pass metabolism in both the gut wall and liver. Oral bioavailability, determined by the fraction absorbed (F_a), fraction escaping gut-wall elimination (F_G) and fraction escaping hepatic elimination (F_H) show the importance of the intestine and liver in this process[2].

However, the assessment of F_a, F_G and F_H is extremely challenging and rarely performed due to ethical and technical reasons[3,4]. Therefore, preclinical evaluation is needed to assess the oral absorption and concentrations of drug and metabolite in the systemic circulation. The possibility to study F_G and F_H in a preclinical *in vitro* model is also limited as it remains difficult to recapitulate complete organ function behaviour within a single model. Such a single model could provide highly relevant information in early drug development for several fields of research, for example, in physiologically based pharmacokinetic (PBPK) modelling prediction. This is especially crucial as precise predictions can effectively reduce attrition and failure rates within the drug development process, while also aiding in the determination of initial starting dosages of compounds[5]. Recent advancements in organ perfusion techniques have created new opportunities for studying physiological processes in an *ex vivo* setting. Normothermic machine perfusion (NMP) has been demonstrated in numerous studies to maintain *ex vivo* liver, kidney, pancreas and even intestinal function for several hours[6-9]. In the field of pharmacology, NMP has proven to be advantageous for determining the hepatic and biliary clearance as well as renal clearance[10-13]. The intact vasculature and presence of the elimination routes of these whole-organ models offers greater potential of studying absorption, distribution, metabolism and elimination (ADME) process compared to cellular preclinical systems[14]. While the majority of studies focus on perfusion with a single organ, a few studies have investigated the possibility of a multi-organ perfusion model to study physiological processes[15-18]. These studies, combining liver and kidneys in one circuit, show that combination of organs is

beneficial for the biochemical environment and as well can reduce the impact of warm ischemia and reperfusion injury[16,19]. Together, the option to perfuse multiple organs allows in-depth analysis of ADME processes like gut wall metabolism, portal vein concentrations, hepatic uptake and biliary excretion. Simultaneously, it maintains a favourable biochemical environment through the inclusion of homeostatic organs.

The aim of the study was to explore the applicability of a porcine *ex vivo* perfusion model to characterize oral absorption, gut wall metabolism, first pass hepatic metabolism and biliary excretion by pre-systemic measurements of midazolam and metabolite concentrations in portal vein, intestinal faecal effluent and systemic and bile measurement.

Materials and methods

Chemicals

Heparin, sodium taurocholate, insulin, dexamethasone, atenolol, antipyrine and FD4 were purchased from Sigma-Aldrich, Zwijndrecht, the Netherlands. Epoprostenol was purchased from R&D systems (Minneapolis, USA). Calcium gluconate 10% was obtained from Pharmamarket (Hove, Belgium). Aminoplasmal 10E was obtained from (B Braun Melsungen AG, Melsungen, Germany). Midazolam was obtained from Spruyt Hillen (Ijsselstein, the Netherlands).

Organ procurement

En bloc organs were obtained from a local slaughterhouse, in compliance with the guidelines of the Dutch food safety authority. Pigs (*Netherlands Landrace*, approximately 6 months of age with body weight between 100 and 120 kg) were anesthetized by a standardized procedure of electrocution followed by exsanguination (termination). Three liters of blood was collected during exsanguination in a container supplemented with 25000 IU of heparin. Per industry guidelines, carcasses were cleaned in a pig washing & whipping machine using 70°C water for approximately 3-5 minutes and dehaired through scalding. Slaughter offal was dissected from the carcasses, keeping all organs and vascular structures intact.

Porcine *en bloc* organ preservation and model development

After receiving the organ package, the heart, lungs and esophagus were dissected. Thereafter the abdominal aorta was proximally cannulated (25 Fr). In order to create a closed abdominal compartment for arterial perfusion, the abdominal aorta was ligated distal from the renal arteries. The lumbar arteries were separately ligated. A cold flush was initiated within ~15 min after termination (warm ischemic time), using Histidine-Tryptophan-Ketoglutarate (HTK) solution (Plegistore, Warszawa in Poland) by applying a pressure of 80 mmHg (pressure bag Endomed, Uden, the Netherlands). During the flush, the entire colon was dissected from the organ package. After approximately 7L of HTK solution, an additional portal flush was performed. The portal vein was partially dissected and cannulated at both ends (Supplemental Figure S6.1) resulting in 1) portal vein – intestinal side cannulation (25 Fr) (efferent), and 2) a portal vein – liver side (afferent), (25 Fr). Additional flush at the portal vein – liver side was applied with 2L of HTK. Thereafter, the organs were transported on static cold storage. At the laboratory, the stomach was removed and the small intestine was shortened to approximately 2 meters preserving the duodenum and the proximal part of the jejunum (~1.5 meter). A cannula was placed in the orifice of the duodenum to allow for administration of (dissolved) compounds. A clamp was placed on the cannula before and after administration of compound(s) in order to prevent backflow. To make intestinal outflow possible at the jejunal side, a second cannula was inserted. Thereafter the common bile duct was cannulated to the liver side, while the *cystic duct,* derived from the gall bladder, was ligated to restrict bile flow to the gall bladder. Lastly, the ureters were cannulated which was the final step before initiation of normothermic perfusion.

Normothermic machine perfusion

The porcine organs (n=4) were perfused using the Liver Assist™ device (XVIVO, Groningen, the Netherlands) (Figure 6.1A-B). The reservoir included in the disposable set was too small to fit the organs, therefore a custom made organ reservoir was made. The newly developed reservoir consisted of a box (60x40x20 cm box) with a built in drain connecting the box with the Liver Assist reservoir. An mesh basket (60x40x15 cm) was suspended in the box. The organs were placed in the mesh basket, enabling the venous outflow of the organs flowing in the box and subsequently to the Liver Assist reservoir via the drain. The system was filled with 3 liter perfusion fluid containing autologous

red blood cells and plasma (ratio 1:1), supplemented with 10 mL (10%) mannitol and 18 mg dexamethasone, 75µg epoprostenol and 10 mL 10% calcium gluconate. Insulin, taurocholate, heparin, epoprostenol and aminoplasmal 10E were provided as continuous infusion at a rate of 10 U/h, 1041 U/h, 10 mL/h (2% w/v), 8 µg/h and 10 mL/hr respectively to keep the liver metabolically active[13]. Gas delivery to the Liver Assist™ device consisted of 40% oxygen at 1.5 L/min and the temperature was set at 39°C. An arterial pressure was set at 60-80 mmHg. Due to reduction in the intestinal length and thereby reduction in the vascular bed, the portal vein flow could result in an insufficient flow. Therefore, portal perfusion was applied via the portal vein-liver side (Supplemental Figure S6.1), with a pressure between 8-11 mmHg. The aorta and portal vein received perfusate from the reservoir, venous outflow of the organs was open and flowed back to the reservoir (Figure 6.1B). Continuous recirculation of the perfusate was applied. During normothermic perfusion, absorption of fluid into the intestine was observed. To retain a sufficient perfusate level, red blood cells and plasma of a blood type-matched pig was used when a decrease in hematocrit was observed (<20% hematocrit), otherwise ringers lactate was used to replenish the perfusate level. The *en bloc* organs were perfused for a total time of 420 minutes.

Drug administration during normothermic perfusion

20 mg midazolam, 25 mg atenolol, 50 mg antipyrine and 1 mL of 10 mM FITC-Dextran 4000 (FD4) were dissolved in Williams E medium (50 mL) and dosed via the cannula in the duodenum. Exact luminal concentration of the compounds is not known since luminal fluid was already present in the intestine resulting in further dilution of the compounds. T=0 min was defined as time of starting the bolus into the duodenum. Subsequently, intestinal faecal effluent, portal vein perfusate, systemic perfusate and bile samples were taken for the following 240 min at time points t=0, 15, 30, 45, 60, 90, 120, 150, 180, 210 and 240 min after dosing. Samples were centrifuged directly after collection and immediately stored at ≤-70°C until further processing. Drug concentrations of midazolam, 1-OH midazolam, 1-OH midazolam glucuronide, atenolol and antipyrine in the portal vein perfusate, systemic perfusate, intestinal faecal effluent, bile and tissue were determined by LC-MS/MS and UPLC analysis as described below.
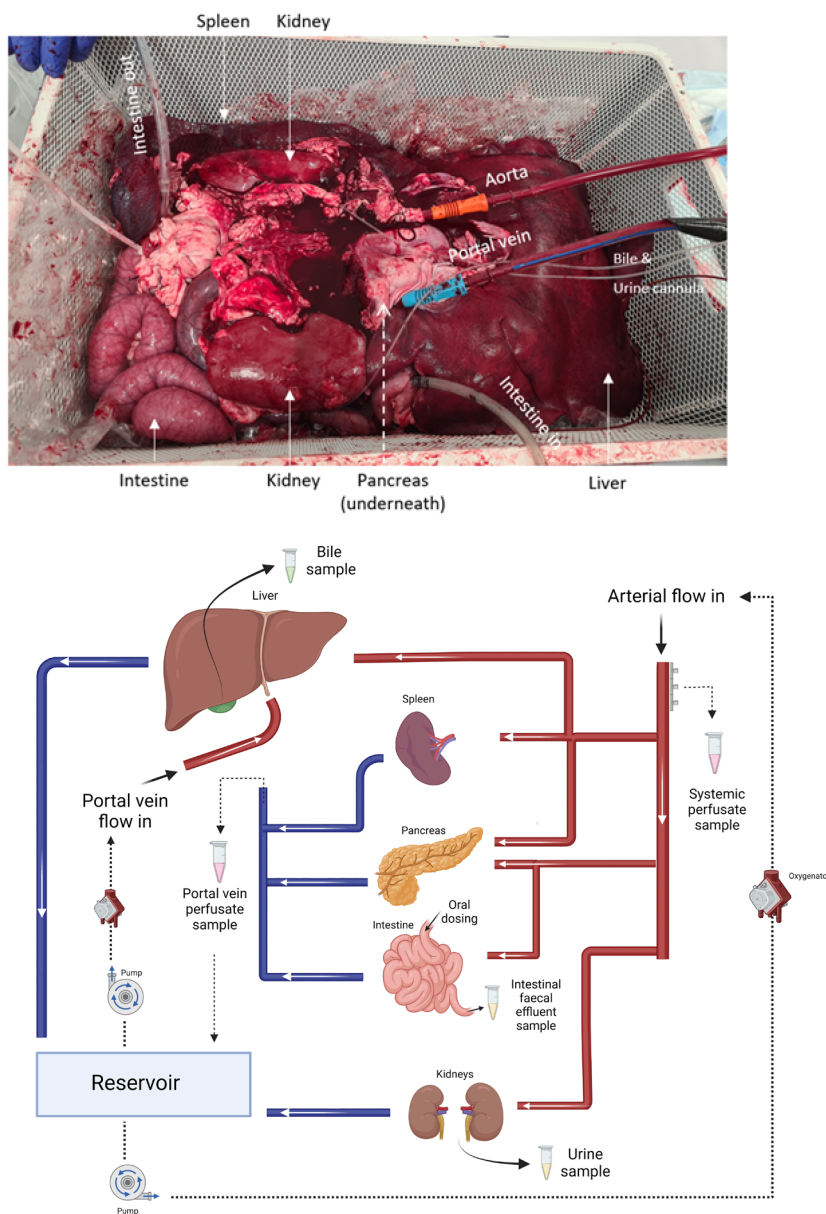
Figure 6.1 - Representation of the ex vivo perfusion model including liver, spleen, pancreas, intestine and kidneys. (A) Visual appearance of the model during normothermic machine perfusion in one of the experiments. Organs and cannulas are indicated, pancreas is indicated since it is not visible. (B) Simplified schematic representation of the gut-hepatobiliary perfusion model. Sample points are indicated by the eppendorfs including the systemic perfusate, portal vein perfusate, bile, urine and intestinal fecal effluent. Drug was dosed in the duodenum mimicking the oral dosing pathway indicated by the arrow towards the intestine 'oral dosing'.

Organ function assessment

During the perfusion experiment, blood gas analysis was executed every hour by measuring a blood gas panel, electrolytes and a hematology panel using a blood gas analyzer (iSTAT Alinity, Abbot Point of Care Inc., Princeton, NJ). Additionally, arterial and portal vein flow and resistance values were reported from the Liver Assist™ device. Next to blood gas analysis, the following parameters were measured in systemic perfusate and bile samples to study viability of the organs. Intestine: Intestinal barrier integrity was characterized by measuring FD4 and atenolol and antipyrine. FD4 was analyzed using a BioTek Synergy HT microplate reader (BioTek Instruments Inc., Winooski, VT) with an excitation/emission wavelength of 485 nm and 528 nm. FD4 concentration were determined by measuring the fluorescence in relative fluorescence units (rfu). Bioanalysis of atenolol and antipyrine is described below. Liver: lactate concentrations in the perfusate were measured by bloodgas analysis, bile production was collected in fractions and volume was measured from the collection tubes throughout the perfusion. Total bilirubin, alanine transaminase (ALT) and aspartate transaminase (AST) concentration were determined in the systemic perfusate (Reflotron-Plus system, Roche diagnostics, Almere, the Netherlands). Pancreas: C-peptide levels were measured using an ELISA (Sigma Aldrich, Zwijndrecht, the Netherlands) according to manufactures description and amylase in intestinal faecal effluent was measured (Reflotron-Plus system, Roche diagnostics, Almere, the Netherlands). Kidney: systemic perfusate sodium, potassium and blood urea nitrogen (BUN) were determined using bloodgas analysis. No assessments were performed to study the viability of the spleen.

Bioanalysis

The concentration of midazolam in systemic perfusate, portal vein perfusate, bile and tissues was quantified using LC-MS/MS (Waters, Etten-Leur, the Netherlands). Atenolol and Antipyrine in the different matrixes were measured using UPLC (Waters, Etten-Leur, the Netherlands). Perfusate, bile and tissue samples were deproteinized with acetonitrile (1:3) with the addition of 10 of µL the isotopically labelled internal standards midazolam (1 µg/mL). Thereafter samples were vortexed, centrifuged and supernatant was transferred to 96 well plate and dried under nitrogen. Samples were then dissolved in 100 µL 10% ACN + 0,1% formic acid and injected in to LC-MS/MS for quantification of midazolam, 1-OH midazolam and 1-OH midazolam glucuronide (Supplemental

Table S6.1 and S6.2) and UPLC for quantification of antipyrine and atenolol (Supplemental Table S6.3 and S6.4). Chromatograms of midazolam, atenolol and antipyrine are shown in Supplemental Figure S6.2.

Data analysis

Data obtained during the perfusion studies was analyzed using Graphpad prism version 8 (Graphpad, California, USA). Values for the area under the concentration time curve (AUC) were calculated using the linear trapezoidal method. Oral bioavailability was calculated based on F_G and F_H:

$$(1)\ F = F_a * F_G * F_H = F_a * (1 - E_G) * (1 - E_H)$$

To calculate intestinal gut-wall extraction of midazolam (E_G), midazolam metabolism into 1-OH midazolam in the intestinal lumen ($E_{G\text{-intestinal}}$ lumen) and in the portal vein ($E_{G\text{-pv}}$) was calculated[3]

$$(2)\ Intestinal\ extraction\ (E_{G-intestine}) = \frac{AUC_{Intest.effluent}^{mdz-metab.}}{AUC_{intest.effluent}^{mdz-metab.} - AUC_{Intest.effluent}^{mdz}}$$

$$(3)\ Intestinal\ extraction\ (E_{G-pv}) = \frac{Q_{pv} * (AUC_{pv}^{1-OH} - AUC_{pv}^{1-OH-calc*})}{Q_{pv} * (AUC_{pv}^{1-OH} - AUC_{pv}^{1-OH-calc*}) + Q_{pv} * (AUC_{pv}^{mdz} - AUC_{pv}^{mdz-calc*})}$$

Where Q_{pv} is the portal vein flow, superscripts mdz and mdz-metab. refer to the parent drug and metabolites (Supplemental Figure S6.3). Subscripts pv, s and intest. effluent refer to portal vein perfusate, systemic perfusate and intestinal faecal effluent respectively. AUC represents the area under the plasma concentration time curve. To determine E_G in the portal vein, a systemic sample (without contribution of the liver is needed[3], here considered as pv[1-mdz-calc*] and pv[1-OH-calc*] (Supplemental Figure S6.3). The $AUC_{pv}^{1-OH-calc*}$ was considered the systemic circulation without liver, calculated as followed:

The portal vein - liver in concentrations of midazolam and metabolites were calculated based on FD4 measurements. Since FD4 is not metabolized by the liver, a dilution factor could be calculated based on FD4 portal vein perfusate concentration and FD4 systemic perfusate concentration. Using the FD4 data,

the pre liver in concentrations and subsequent AUC ($AUC_{pv}^{1-OH-calc*}$) was calculated.

$$(4)\ Portal\ vein^{1-OH-calc*} = \frac{Portal\ vein_{intestinal\ side}^{1-OH}}{\dfrac{FD4_{portal\ side}}{FD4_{systemic\ circulation}}}$$

Where Portal vein intestinal side sample (Supplemental Figure S6.1) is the portal vein blood flow directly coming from the intestine. The midazolam concentration in the portal vein ($AUC_{pv}^{mdz-calc*}$) as calculated in a similar fashion as the 1-OH concentration in the portal vein.

Fraction escaping gut wall (F_G) metabolism was defined by intestinal gut-wall extraction (E_G) of midazolam:

$$(5)\ F_G = (1 - E_G)$$

Hepatic extraction ratio (E_H) of midazolam was determined using portal vein (based on FD4 diluted calculation) and perfusate samples.

$$(6)\ Hepatic\ extraction\ (E_H) = \frac{Conc.\ midazolam_{pv}^{mdz-calc*} - Conc.\ midazolam_{systemic\ circulation}}{Conc.\ midazolam_{pv}^{mdz-calc*}}$$

Based on the hepatic extraction ratio, the fraction escaping hepatic elimination could be calculated:

$$(7)\ F_H = (1 - E_H)$$

Results

Organs show proper viability and function during perfusion

Figure 6.2A - N show organ specific viability and injury markers for the intestine, liver, pancreas and kidney. The intestinal barrier function was assessed by measuring the permeability FD4 and of atenolol, and antipyrine. Varying but high levels of FD4 were collected from the intestinal faecal effluent ($1.2*10^8 \pm 1.0*10^8$ rfu/mL perfusate) while detection of FD4 in the portal vein perfusate and systemic perfusate remained low ($0.03*10^8 \pm 0.03*10^8$ rfu/mL perfusate vs $0.02*10^8 \pm 0.02*10^8$ rfu/mL perfusate respectively) indicating

minimal leakage of FD4 into the perfusate and thus a proper intestinal barrier (Figure 6.2A). Besides FD4, the permeability of atenolol and antipyrine was measured. Atenolol has a moderately permeability and translocates via the paracellular route while antipyrine is a high permeable drug which translocates via the transcellular route. Atenolol was, on average, detected at slightly lower concentrations in the portal vein perfusate compared to antipyrine (Supplemental Figure S6.4), indicating proper preservation of transcellular and paracellular transport routes (Figure 6.2B-C). Additionally, intestinal peristalsis was observed in all experiments between 30-120 min after start of the perfusion and intestinal peristalsis remained throughout the whole length of the experiment (Supplemental Video S6.1). Regarding liver viability, lactate levels showed to remain stable throughout the perfusion with a small decline observed for 2 out of 4 experiments (Figure 6.2D). Figure 6.2E shows the bile production of the livers. Bile production was very consistent throughout the perfusion time with an average bile production of 148.42±36.81 mL after 420 min of perfusion. ALT and AST increased 60 min after starting perfusion and remained stable throughout the perfusion (Figure 6.2F-G). Bilirubin showed to be very stable in experiment 3 and 4 (9.1 and 9.3 µmol/L respectively), however in experiment 1 and 2, increase in perfusate bilirubin was observed (23.1 and 35 µmol/L respectively at t=420 min) (Figure 6.2H). As a marker of endocrine and exocrine pancreas viability, C-peptide secretion and intestinal amylase concentration were measured in systemic perfusate and intestinal faecal effluent respectively. C-peptide was detected in the systemic perfusate in all experiments at t=60 min with a concentration of 8.47±1.38 ng/mL and remained stable throughout the whole perfusion (Figure 6.2I). The intestinal faecal effluent showed to contain high concentrations of amylase (AUC 49472 ±17565 U/L) indicating active secretion by the pancreas (Figure 6.2J). Figure 6.2K demonstrates the glucose kinetics during organ perfusion. In two the of the multi-organ perfusion studies (study 1 and 4) stable glucose levels throughout the perfusion were observed with a maximum glucose peak of 11mmol/L at 30 min indicating possible glucose regulation by the pancreas. The other perfusions showed a peak glucose levels of ~39 mmol/L 60 min after perfusion, whereafter linear glucose uptake was observed indicating glucose consumption by the various organs. In the absence of a kidney function biomarker, systemic perfusate levels of sodium, potassium and blood urea nitrogen (BUN) were measured (Figure 6.2L-N). Sodium and potassium levels remained stable throughout the perfusion duration and minimally increased, indicating maintenance of a proper biochemical environment. BUN increased

during the perfusion reaching a final concentration of 38.75±5.90 mmol/L at 420 min of perfusion, retaining relatively low levels of perfusate BUN levels to single organ perfusion (Supplemental Figure S6.5). Minimal urine output (0-10 mL) was observed during perfusion. Together, these data shown proper viability as well as functionality up to 420 min of perfusion of different organs involved in the perfusion model (Supplemental Figure S6.6).
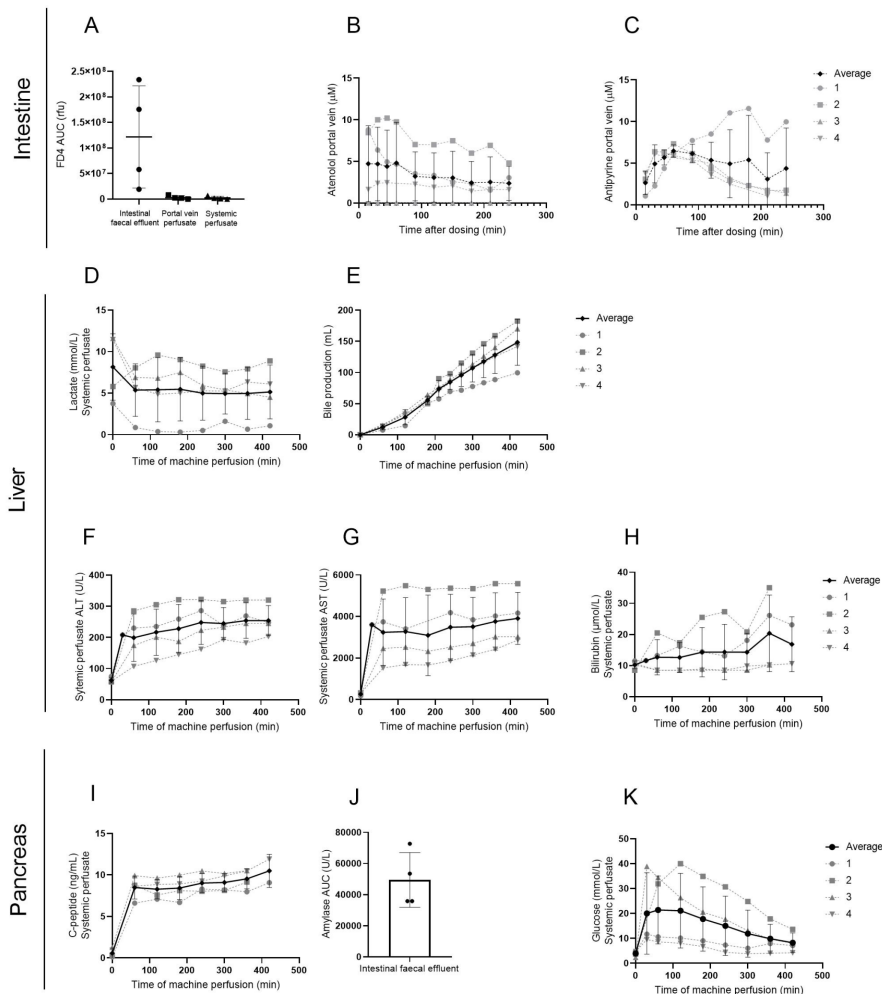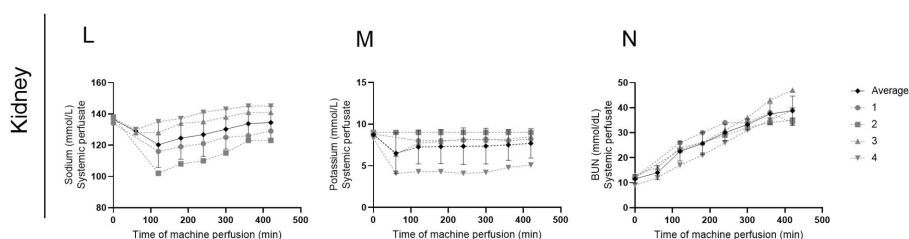
Figure 6.2 - General viability, functionality and injury markers of the intestine (A-C), liver (D-H), pancreas (I-J) and kidney (L-M). (A) Area under the curve (AUC) of FD4 measured in the intestinal faecal effluent, portal vein perfusate and systemic perfusate. (B-C) Concentration of Atenolol and Antipyrine measured in the portal vein perfusate as markers for paracellular and transcellular transport respectively. (D) systemic perfusate lactate concentration (E) cumulative bile production during 420 min of perfusion, (F) ALT concentration measured in the systemic perfusate, (G) AST concentration measured in the systemic perfusate, (H) bilirubin concentration measured in the systemic perfusate. (I) C-peptide concentration was measured in the systemic perfusate, (J) AUC of amylase measured in the intestinal fecal effluent and (K) systemic perfusate glucose concentrations . (L) Systemic perfusate levels of sodium (M) Systemic perfusate levels of potassium and (n) systemic perfusate levels of BUN. Data represents mean ± SD of 4 individual experiments. Individual experiments are presented by the dotted lines.

Active midazolam absorption, metabolism and excretion

Absorption and metabolism of midazolam was studied to characterize the viability of the intestine and liver. Figure 6.3A-C illustrate the role of the intestine (and liver) in midazolam metabolism. After an intraduodenal dose, midazolam was detected in the portal vein perfusate to a higher extent than the systemic perfusate indicating active midazolam absorption. The C_{max} concentration in the portal vein was 426.47 nM, 90 min after administration. Corresponding C_{max} in systemic perfusate was 80.16 nM at 90 min after administration. Portal vein concentration decreased over time to 117.60 nM at 240 min after dosing, with a perfusate concentration of 36.01 nM. Figure 6.3B shows the 1-OH midazolam concentrations in the portal vein and systemic perfusate. 1-OH midazolam concentrations showed to be higher in the portal vein compared to the perfusate indicating active gut wall metabolism of midazolam to its metabolite. Samples from the intestinal faecal effluent were taken to assess midazolam and metabolite concentrations (Figure 6.3C). Midazolam was detected at higher levels compared to the metabolites 1-OH midazolam and 1-OH midazolam glucuronide (2889±2321 vs. 111.59±86.22 vs. 1.31±1.06 µM/0-240min respectively) showing incomplete absorption of midazolam as well as gut-wall metabolism and interestingly, excretion to the luminal side. Figure 6.3D and 6.33E demonstrates the liver contribution to the metabolism of midazolam. 1-

OH midazolam glucuronide was measured at slightly higher levels in the systemic perfusate compared to the portal vein perfusate. Biliary excretion of midazolam was demonstrated with a C_{max} at 90 min (46.78 ng), and total biliary excretion of 0.04% (±0.01%) of the administered dose. The metabolite 1-OH midazolam glucuronide was also detected in the bile, however only in 1 out of 4 experiments, at minimal output (0.02% of administered dose). Figure 6.3F shows the systemic midazolam profile. The metabolite, 1-OH midazolam was detected in the perfusate 30 min after dosing and linearly increased throughout the perfusion with a C_{max} of 57.20 nM at 210 min whereafter a decrease was observed. The midazolam metabolite 1-OH midazolam glucuronide was detected in the perfusate 30 min after perfusion. The glucuronide demonstrated a more rapid increase in its detection in the systemic perfusate over time (117.99 nM at 240 min) compared to 1-OH midazolam. The relative slight increase in the detection of 1-OH midazolam with the steep increase in the detection of 1-OH glucuronide suggest metabolism of 1-OH into its glucuronide.
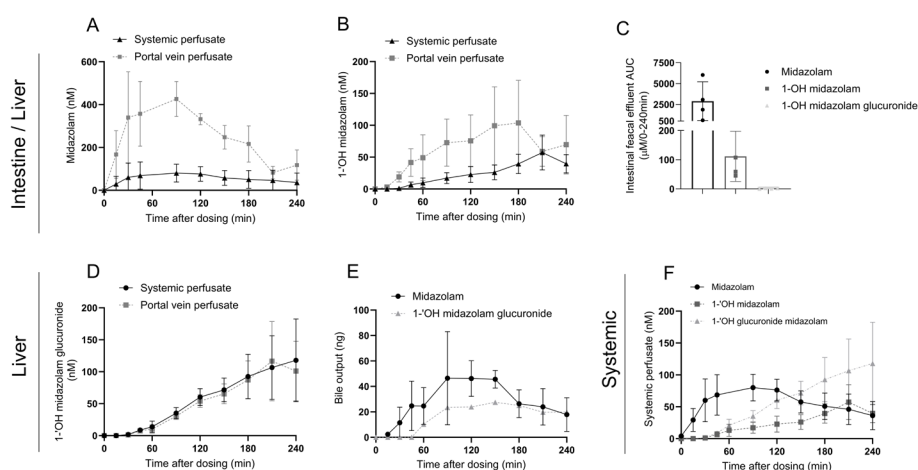

Figure 6.3 - Midazolam absorption, metabolism and elimination categorized for the contribution of the intestine/liver (A-C), liver (D-E and systemic profile (F) measured in the ex vivo perfusion model after duodenal administration of 20mg midazolam. Intestinal absorption and metabolism is shown in: (A) midazolam concentration in the systemic and portal vein perfusate (B) 1-OH midazolam concentration in the systemic and portal vein perfusate and (C) midazolam, 1-OH midazolam and 1-OH midazolam glucuronide concentrations (AUC) detected in the intestinal faecal effluent. Liver metabolism and elimination is shown in: (D) 1-OH midazolam glucuronide in the systemic and portal vein perfusate, (E) biliary elimination of midazolam and 1-OH midazolam glucuronide and (F) midazolam, 1-OH midazolam and 1-OH midazolam glucuronide PK profile measured in the systemic perfusate. Data represents mean ± SD of 4 individual experiments.

High tissue levels of midazolam in the intestine

The concentration of midazolam, 1-OH midazolam and 1-OH midazolam glucuronide after 240 min of perfusion were determined in intestine, liver and kidney tissue (Figure 6.4A-B). Concentration of 1-OH midazolam showed to be below the limit of quantification in all the organs. Compared to kidney (0.12±0.08 nM/mg tissue) and liver (0.10±0.03 nM/mg tissue), high concentrations of midazolam were observed in the intestine (5.20±3.97 nM/mg tissue) (Figure 6.4A). The conjugated metabolite, 1-OH midazolam glucuronide, tended to show higher tissue levels in the liver (0.06±0.08 nM/mg tissue) compared to intestine (0.02±0.01 nM/mg tissue) and kidney (0.03±0.02 nM/mg tissue). However this was mainly observed in 1 out of 3 studies.
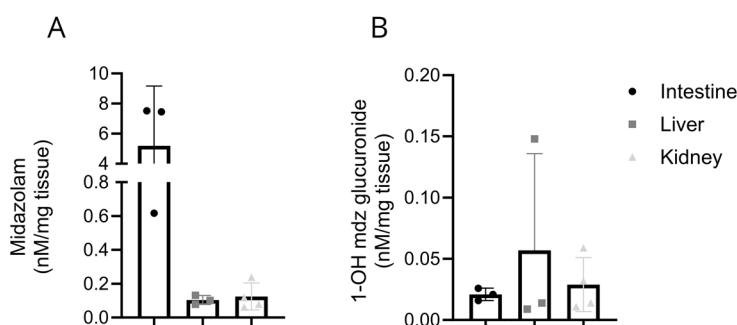

Figure 6.4 - Tissue concentrations of midazolam and 1-OH midazolam glucuronide measured at the end of the perfusion in the ex vivo perfusion model after duodenal administration of 20mg midazolam. (A) tissue concentration of midazolam and (B) tissue concentration of 1-OH midazolam glucuronide in intestine (n=3), liver (n=3) and kidney (n=4). Data represents mean ± SD of 3-4 individual experiments. Multiple biopsies per experiment were taken (n=2-3)

Determination of the oral bioavailability

Based on the measured concentrations in the perfusate, portal vein and intestinal lumen the E_H, E_G, F_G, F_H and subsequently F_{oral} was calculated. The E_G, metabolite formation to the gut lumen showed to be less than the metabolite formation in the portal vein (0.051±0.03 vs. 0.16±0.10 respectively). Together, an E_G of 0.21±0.11 was measured in our model (Figure 6.5A). The E_H varied between 0.55-0.74 with an average of 0.65±0.07. The F_G and F_H showed a value of 0.78±0.11 and 0.35±0.07 respectively, indicating more extensive hepatic metabolism than through intestinal metabolism. Assuming a fraction absorbed of 1, the F_{oral} was calculated to be 0.27±0.05.
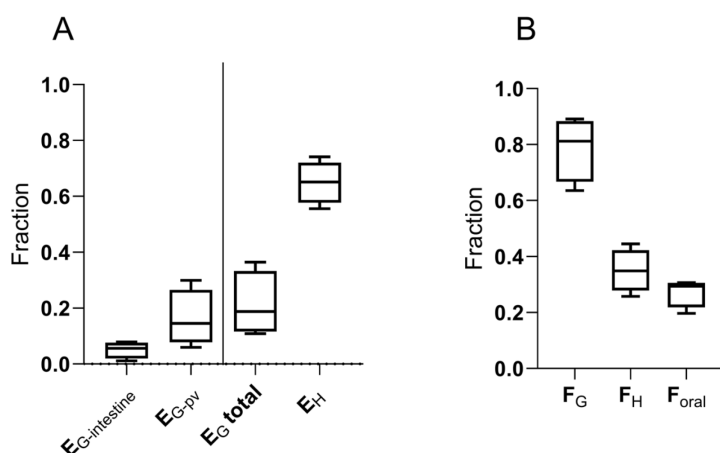
Figure 6.5 - Oral bioavailability of midazolam (A) Gut wall extraction of midazolam, determined in the intestinal faecal effluent (E_G-intestine), portal vein and systemic perfusate (E_G-pv), combined showing the E_G total, and hepatic extraction of midazolam measured in the portal vein and systemic perfusate. (B) Fraction escaping gut wall metabolism, fraction escaping hepatic extraction and oral bioavailability of midazolam. Data represents mean ± SD of 4 individual experiments.

Discussion

To date, complete ADME profiles with a focus on oral bioavailability can only be studied in *in vivo* models as it remains difficult to recapitulate all organ functions within a single *in vitro* model. However, with the innovations into state-of-the-art perfusion devices we have demonstrated the ability to perfuse multiple abdominal organs *en bloc* in an *ex vivo* setting. The model showed a stable flow, intestinal peristalsis was observed throughout the experiment and viability of the organs was demonstrated by bloodgas analysis, specific viability assays and by showing absorption, metabolism and excretion of midazolam.

Although *ex vivo* NMP is typically conducted with a single organ, the simultaneous perfusion of multiple organs occurs less frequently. Our data indicates that the inclusion of multiple homeostatic organs (e.g. liver, kidneys and pancreas) holds significant advantages, especially in maintaining the acid-base balance and glucose regulation of the perfusate. This is also observed by Chung et al.,[15,19] and He et al.,[16] showing the addition of a kidney to the liver circuit improved the biochemical environment. During liver perfusion, a spike in glucose concentration is typical[20]. Interestingly, in two out of four perfusions

only a slight increase occurred. We hypothesize that the addition of the pancreas to the circuit was beneficial for the glucose regulation and homeostasis, as evidenced by a concurrent production of C-peptide. Moreover, no additional glucose infusion was needed, suggesting effective glucose regulation by the pancreas. Delayed warm-up of organs in two of the perfusions might explain the glucose rise at t=60 min, affecting the pancreas functionality and viability. Using a multi-organ perfusion approach, including homeostatic organs, achieving prolonged perfusion will become more feasible. Previous studies demonstrated prolonged abdominal organ perfusion, with viability up to 24 hours[21] and 45 hours[18]. Both above mentioned studies used organs obtained before sacrificing the animal, allowing for minimal warm ischaemic time before preservation. To our knowledge, no other previous studies demonstrated a multi-organ model using slaughterhouse organs, in which warm ischemia times are inherent. With this study we show the possibility to use slaughterhouse material (waste material), contributing to the 3R principle of reduction in the use of animal testing[22]. Additionally, the availability of slaughterhouse organs is a significant advantage allowing for experimentation without the need for an animal laboratory[23]. However, good agreements with the slaughterhouse is essential to ensure proper quality of the organs during resection of the *en bloc* organs out of the carcass. The complexities encountered in small intestinal and multivisceral organ transplantation show similarities to our developed *ex vivo* model[24]. We observed extensive fluid secretion into the small intestines. It is known that the small intestine secretes 8-9 liters water including electrolytes per day which is reabsorbed by the ileum and the colon tissue[25,26]. Extensive excretion is a phenomena known in small intestine transplantation; colectomy patients suffer from severe diarrhea after surgery indicating the inability to reabsorb the secreted fluid. Furthermore, in a rat intestine-transplant model obtained after circulatory death, abnormalities were shown in intestinal secretion[27,28]. Also Pang et al.[29] reported the hypersecretion into the lumen of the intestine in a gut-liver in situ rat perfusion model, however this could be overcome by the infusion of norepinephrine and dexamethasone. This strategy limiting hypersecretion is promising for future multi-organ experiments and would possibly enable to include the whole small intestine allowing for even better absorption studies.

To demonstrate the applicability of the perfusion model to study the first pass effect and oral bioavailability, the metabolism of midazolam was studied. Since

midazolam is metabolized by the intestine as well as the liver by CYP3A in both of these organs, valuable insight can be generated regarding the extent of involvement of the organs into the first-pass metabolism. Intestinal absorption of midazolam was observed followed by detection of 1-OH midazolam and 1-OH midazolam glucuronide in the portal vein and systemic perfusate indicating CYP3A metabolism and UGT1A4 and UGT2B4/2B7 activity in the intestine and liver. Additionally, the presence of these metabolites in the intestinal faecal effluent suggest gut wall metabolism and intestinal glucuronidation to some extent. High levels of 1-OH midazolam in the portal vein perfusate indicate gut-wall metabolism, while extensive hepatic glucuronidation was observed. This was evidenced by increasing levels of the glucuronide in the systemic perfusate assuming a higher expression of UGT enzymes in the liver compared to intestinal UGT expression. Minor urine excretion was observed during the perfusion and thus urinary elimination of midazolam and the metabolites could not be studied. We hypothesize that the limited urine production could be due to perfusate conditions, ischemia reperfusion injury or the water flux from the perfusate to the intestinal lumen, limiting the 'need' to produce urine for the kidneys.

The hepatic extraction ratio calculated in the multi-organ model showed to be 0.65 (±0.07). Although minor to no hepatic extraction data of midazolam in pigs is known, the reported human hepatic extraction ratio showed to be slightly lower (0.44±0.14)[30]. Midazolam extraction is affected by the blood flow and the activity of metabolizing enzymes[31]. Multiple studies have demonstrated that porcine liver microsomes possess a higher CYP3A4 activity compared to human liver microsomes[32,33]. Also our lab demonstrated a higher activity of porcine liver microsomes compared to human liver microsomes (Supplemental Figure S6.7). A higher activity of CYP3A can result in a higher hepatic extraction ratio and thus a higher first-pass effect, confirming the results observed in our perfusion model. Ochs et al.,[34] demonstrated the intestinal and hepatic extraction of midazolam in pigs by comparing oral administration versus iv administration. The systemic venous / portal venous ratio of midazolam showed to be 0.15 indicating extensive hepatic extraction. IV administration showed almost similar AUC values in systemic venous and portal venous samples suggesting minimal intestinal extraction. This study showed that the extraction of midazolam after duodenal administration could be contributed to almost entirely hepatic metabolism. In humans, intestinal extraction plays a more dominant role since extraction values of 0.43-0.44 have been reported

for the intestine, indicating substantial involvement of the intestine in the extraction process[3,30]. Thummel et al.,[30] demonstrated a large variation within the intestinal extraction (0.0–0.77), as also shown by Brill et al.,[35] predicting extraction values between 0.05–0.8 in morbidly obese patients. One possible explanation for the disparity in observed intestinal extraction data between humans and pigs could be variations in the abundance of CYP3A4 enzymes. Schelstraete et al.,[36] compared the CYP450 enzymatic status in porcine livers and intestine to human enzymatic status. Duodenal relative quantitative results showed to be remarkably similar between pigs and men (CYP3A4 88% in pig vs 82% in humans). However, intestinal CYP450 microsomal activity was significantly lower in porcine microsomes for CYP3A, even up to 6-10 times lower as reported in human[37]. Subsequently, the overall oral bioavailability showed to be 27% in our model. Only two *in vivo* studies using pigs (micro minipigs and Gottinger minipigs) reported the bioavailability of midazolam after oral intake, showing values between 3.0% and 14%[32,34,38]. Although our reported oral bioavailability data is close to the reported *in vivo* data, slight underprediction of the intestinal metabolism in our model could affect the F_G and thus affect the oral bioavailability. The slight underprediction of the intestinal metabolism could be due to the inclusion of only ~2 meter of small intestinal tissue. Although the highest expression of CYP3A4 is detected in the duodenum and gradually decreases along the intestinal tract, metabolism further along the intestine could have contributed to a higher intestinal metabolism[3,39-41]. Moreover, temperature of the ex vivo organs might have influenced the metabolism of midazolam. Despite maintaining the perfusate temperature at 38°C which was monitored at the arterial and venous flow, the ex vivo organs placed in a box were susceptible to cooling down. This could result in lower tissue temperature that could have impacted the (intestinal) absorption and metabolism of midazolam and be a reason for variation in the results[42,43]. Besides detection of 1-OH midazolam and 1-OH midazolam glucuronide, we observed multiple hydroxy and glucuronide metabolites (Supplemental Figure S6.8) however, not quantified. This could also partly account for the slight underprediction of metabolism. Also differences in pig species used in these studies compared to our study can affect the F_G and F_H and thus affect the oral bioavailability. Clinical studies using human subjects show a higher midazolam bioavailability; between 29-44%[3,30,44]. Taking into account the higher CYP3A4 activity in the liver in pig studies, human *in vivo* studies show lower F_H values resulting in a higher oral bioavailability which is in line with our data. In summary, the generated hepatic and intestinal extraction

data is in line with *in vivo* pig data. To translate this data to humans, the use of physiologically based pharmacokinetic (PBPK) modeling with allometric scaling could be applied. Multiple pig PBPK models have been developed since there is a growing use of pigs as preclinical species[45]. On the other hand, multi-organ perfusions can generate novel insights and input for these PBPK modelling exercises. One of the challenges in PBPK modeling is to dissect out the contributions of the intestines and liver, two serially arranged organs in first-pass metabolism[46]. Studying PK processes of organs involved in ADME in an isolated environment gives the ability to control the process. The ability to take (unlimited) samples from different locations (e.g. different venous outflows) and tissues over time can generate valuable information regarding the contribution of each organ into the metabolism of a drug. Especially sampling from the intestinal faecal effluent and the portal venous blood generating insight into gut-wall metabolism is very unique. The model presents numerous future perspectives; it offers the potential for studying regional absorption as the expression of transporters like Pgp, OATP and CYP enzymes varies along the intestinal tract[47]. Since the model closely resembles physiology, including intact intestinal tissue and peristalsis the model could be used to study formulation effects since sampling from the intestinal faecal effluent and portal venous blood stream is feasible and dosing at a physiological pH can be applied as the tissue is able to handle the enzymatic and pH environment. A pre-digestion protocol designed to mimick stomach digestion can even more accurately stimulate gastrointestinal conditions, thus better simulate in vivo conditions. This is particularly important as the stomach's acidic environment aids in solubilizing and dissolving drugs[48]. Furthermore, the gut-hepatobiliary model offers an excellent opportunity to study drug-drug interactions (DDI) as DDI can occur at the intestinal as well as the hepatic level as currently a combination of both models is needed in order to properly predict the magnitude of DDI.

Conclusion

We have successfully developed a porcine *ex vivo* perfusion model of multiple abdominal organs and demonstrated its capabilities and potential use in studying ADME processes. Using this model we were able to characterize pre-systemic extraction of midazolam by measuring the intestinal as well as hepatic extraction. As a result, oral bioavailability could be determined. F_H, F_G and oral bioavailability findings were in line with pig *in vivo* data. This model,

complemented with physiologically based pharmacokinetic modelling is a valuable approach to investigate the first-pass effect and oral bioavailability of novel pharmaceutical compounds. By employing this approach, valuable insights can be generated into the absorption and metabolism of new drugs, thereby facilitating the development and optimization of drug candidates for human use.

Acknowledgement

References

1. Alqahtani S, Mohamed LA, Kaddoumi A. Experimental models for predicting drug absorption and metabolism. Expert Opinion on Drug Metabolism & Toxicology 2013;9:1241-1254.
2. Varma MV, Obach RS, Rotter C, Miller HR, Chang G, Steyn SJ, El-Kattan A, et al. Physicochemical space for optimum oral bioavailability: contribution of human intestinal absorption and first-pass elimination. Journal of medicinal chemistry 2010;53:1098-1108.
3. Paine MF, Shen DD, Kunze KL, Perkins JD, Marsh CL, McVicar JP, Barr DM, et al. First-pass metabolism of midazolam by the human intestine. Clinical Pharmacology & Therapeutics 1996;60:14-24.
4. Peters SA, Jones CR, Ungell A-L, Hatley OJ. Predicting drug extraction in the human gut wall: assessing contributions from drug metabolizing enzymes and transporter proteins using preclinical models. Clinical pharmacokinetics 2016;55:673-696.
5. Heikkinen AT, Baneyx G, Caruso A, Parrott N. Application of PBPK modeling to predict human intestinal metabolism of CYP3A substrates–an evaluation and case study using GastroPlus™. European journal of pharmaceutical sciences 2012;47:375-386.
6. Eshmuminov D, Becker D, Bautista Borrego L, Hefti M, Schuler MJ, Hagedorn C, Muller X, et al. An integrated perfusion machine preserves injured human livers for 1 week. Nature biotechnology 2020;38:189-198.
7. Hamed M, Barlow A, Dolezalova N, Khosla S, Sagar A, Gribble F, Davies S, et al. Ex vivo normothermic perfusion of isolated segmental porcine bowel: a novel functional model of the small intestine. BJS open 2021;5:zrab009.
8. Nicholson M, Hosgood S. Renal transplantation after ex vivo normothermic perfusion: the first clinical study. American Journal of Transplantation 2013;13:1246-1252.
9. Ogbemudia AE, Hakim G, Dengu F, El-Gilani F, Dumbill R, Mulvey J, Sayal K, et al. Development of ex situ normothermic reperfusion as an innovative method to assess pancreases after preservation. Transplant International 2021;34:1630-1642.
10. Clark T, Bau L, Dengu F, Voyce D, Carlisle R, Friend P, Coussios C. Predicting clinical pharmacokinetics and toxicity of current and emerging oncology therapeutics by normothermic perfusion of isolated human-sized organs. Cancer Research 2021;81: 1369-1369.
11. Posma RA, Venema LH, Huijink TM, Westerkamp AC, Wessels AMA, De Vries NJ, Doesburg F, et al. Increasing metformin concentrations and its excretion in both rat and porcine ex vivo normothermic kidney perfusion model. BMJ Open Diabetes Research and Care 2020;8:e000816.
12. Stevens LJ, Dubbeld J, Doppenberg JB, van Hoek B, Menke AL, Donkers JM, Alsharaa A, et al. Novel explanted human liver model to assess hepatic extraction, biliary excretion and transporter function. Clinical Pharmacology & Therapeutics 2023;114(1):137-147.
13. Stevens LJ, Zhu AZ, Chothe PP, Chowdhury SK, Donkers JM, Vaes WH, Knibbe CA, et al. Evaluation of normothermic machine perfusion of porcine livers as a novel preclinical model to predict biliary clearance and transporter-mediated drug-drug interactions using statins. Drug Metabolism and Disposition 2021;49:780-789.
14. Rowland M, Benet LZ, Graham GG. Clearance concepts in pharmacokinetics. Journal of pharmacokinetics and biopharmaceutics 1973;1:123-136.
15. Chung WY, Gravante G, Al-Leswas D, Arshad A, Sorge R, Watson CC, Pollard C, et al. The development of a multiorgan ex vivo perfused model: results with the porcine liver-kidney circuit over 24 hours. Artificial Organs 2013;37:457-466.
16. He X, Ji F, Zhang Z, Tang Y, Yang L, Huang S, Li W, et al. Combined liver-kidney perfusion enhances protective effects of normothermic perfusion on liver grafts from donation after cardiac death. Liver Transplantation 2018;24:67-79.
17. Li J, Jia J, He N, Jiang L, Yu H, Li H, Peng Y, et al. Combined kidney-liver perfusion enhances the proliferation effects of hypothermic perfusion on liver grafts via upregulation of IL-6/Stat3 signaling. Molecular medicine reports 2019;20:1663-1671.

18. Chen C, Chen M, Lin X, Guo Y, Ma Y, Chen Z, Ju W, et al. En bloc procurement of porcine abdominal multiple organ block for ex situ normothermic machine perfusion: a technique for avoiding initial cold preservation. Annals of Translational Medicine 2021;9(14):1116.

19. Chung WY, Gravante G, Al-Leswas D, Alzaraa A, Sorge R, Ong SL, Pollard C, et al. The autologous normothermic ex vivo perfused porcine liver-kidney model: improving the circuit's biochemical and acid-base environment. The American journal of surgery 2012;204:518-526.

20. Watson CJ, Jochmans I. From "gut feeling" to objectivity: machine preservation of the liver as a tool to assess organ viability. Current transplantation reports 2018;5:72-81.

21. Chien S, Diana JN, Oeltgen PR, Todd EP, O'Connor WN, Chitwood Jr WR. Eighteen to 37 hours' preservation of major organs using a new autoperfusion multiorgan preparation. The Annals of thoracic surgery 1989;47:860-867.

22. Han JJ. FDA Modernization Act 2.0 allows for alternatives to animal testing. In: Wiley Online Library; 2023.

23. Dengu F, Neri F, Ogbemudia E, Ebeling G, Knijff L, Rozenberg K, Dumbill R, et al. Abdominal multiorgan procurement from slaughterhouse pigs: A bespoke model in organ donation after circulatory death for ex vivo organ perfusion compliant with the 3 Rs (reduction, replacement & refinement). Annals of translational medicine 2022;10(1).

24. Abu-Elmagd KM, Costa G, Bond GJ, Soltys K, Sindhi R, Wu T, Koritsky DA, et al. Five hundred intestinal and multivisceral transplantations at a single center: major advances with new challenges. Annals of surgery 2009;250:567-581.

25. Donohoe CL, Reynolds JV. Short bowel syndrome. The surgeon 2010;8:270-279.

26. Field M. Intestinal secretion. Gastroenterology 1974;66:1063-1084.

27. Goulet O, Colomb-Jung V, Joly F. Role of the colon in short bowel syndrome and intestinal transplantation. Journal of pediatric gastroenterology and nutrition 2009;48:S66-S71.

28. Teitelbaum DH, Sonnino RE, Dunaway DJ, Stellin G, Harmel RP. Rat jejunal absorptive function after intestinal transplantation: effects of extrinsic denervation. Digestive diseases and sciences 1993;38:1099-1104.

29. Pang KS, Cherry W, Ulm E. Disposition of enalapril in the perfused rat intestine-liver preparation: absorption, metabolism and first-pass effect. Journal of Pharmacology and Experimental Therapeutics 1985;233:788-795.

30. Thummel KE, O'Shea D, Paine MF, Shen DD, Kunze KL, Perkins JD, Wilkinson GR. Oral first-pass elimination of midazolam involves both gastrointestinal and hepatic CYP3A-mediated metabolism. Clinical Pharmacology & Therapeutics 1996;59:491-502.

31. Dundee J, Collier P, Carlisle R, Harper K. Prolonged midazolam elimination half-life. British journal of clinical pharmacology 1986;21:425-429.

32. Mogi M, Toda A, Iwasaki K, Kusumoto S, Takehara H, Shimizu M, Murayama N, et al. Simultaneous pharmacokinetics assessment of caffeine, warfarin, omeprazole, metoprolol, and midazolam intravenously or orally administered to Microminipigs. The Journal of toxicological sciences 2012;37:1157-1164.

33. Thörn HA, Lundahl A, Schrickx JA, Dickinson PA, Lennernäs H. Drug metabolism of CYP3A4, CYP2C9 and CYP2D6 substrates in pigs and humans. European journal of pharmaceutical sciences 2011;43:89-98.

34. Ochs H, Greenblatt D, Eichelkraut W, Bakker C, Göbel R, Hahn N. Hepatic vs. gastrointestinal presystemic extraction of oral midazolam and flurazepam. Journal of Pharmacology and Experimental Therapeutics 1987;243:852-856.

35. Brill MJ, Välitalo PA, Darwich AS, van Ramshorst B, Van Dongen H, Rostami–Hodjegan A, Danhof M, et al. Semiphysiologically based pharmacokinetic model for midazolam and CYP3A mediated metabolite 1-OH-midazolam in morbidly obese and weight loss surgery patients. CPT: pharmacometrics & systems pharmacology 2016;5:20-30.

36. Schelstraete W, Clerck L, Govaert E. Characterization of porcine hepatic and intestinal drug metabolizing CYP450. comparison with human orthologues from A quantitative, activity and selectivity perspective 2019;2019:9.

37. Galetin A, Houston JB. Intestinal and hepatic metabolic activity of five cytochrome P450 enzymes: impact on prediction of first-pass metabolism. Journal of Pharmacology and Experimental Therapeutics 2006;318:1220-1229.
38. Lignet F, Sherbetjian E, Kratochwil N, Jones R, Suenderhauf C, Otteneder MB, Singer T, et al. Characterization of pharmacokinetics in the Göttingen minipig with reference human drugs: an in vitro and in vivo approach. Pharmaceutical research 2016;33:2565-2579.
39. Berggren S, Gall C, Wollnitz N, Ekelund M, Karlbom U, Hoogstraate J, Schrenk D, et al. Gene and protein expression of P-glycoprotein, MRP1, MRP2, and CYP3A4 in the small and large human intestine. Molecular pharmaceutics 2007;4:252-257.
40. Bruyere A, Decleves X, Bouzom F, Ball K, Marques C, Treton X, Pocard M, et al. Effect of variations in the amounts of P-glycoprotein (ABCB1), BCRP (ABCG2) and CYP3A4 along the human small intestine on PBPK models for predicting intestinal first pass. Molecular pharmaceutics 2010;7:1596-1607.
41. Nishi K, Ishii T, Wada M, Amae S, Sano N, Nio M, Hayashi Y. The expression of intestinal CYP3A4 in the piglet model. In: Transplantation proceedings; 2004: Elsevier; 2004:361-363.
42. Tortorici MA, Kochanek PM, Poloyac SM. Effects of hypothermia on drug disposition, metabolism, and response: a focus of hypothermia-mediated alterations on the cytochrome P450 enzyme system. Critical care medicine 2007;35:2196-2204.
43. van den Broek MP, Groenendaal F, Egberts AC, Rademaker CM. Effects of hypothermia on pharmacokinetics and pharmacodynamics: a systematic review of preclinical and clinical studies. Clinical pharmacokinetics 2010;49:277-294.
44. Allonen H, Ziegler G, Klotz U. Midazolam kinetics. Clinical Pharmacology & Therapeutics 1981;30:653-661.
45. Henze LJ, Koehl NJ, O'Shea JP, Kostewicz ES, Holm R, Griffin BT. The pig as a preclinical model for predicting oral bioavailability and in vivo performance of pharmaceutical oral dosage forms: a PEARRL review. Journal of pharmacy and pharmacology 2019;71:581-602.
46. Pang KS, Yang QJ, Noh K. Unequivocal evidence supporting the segregated flow intestinal model that discriminates intestine versus liver first-pass removal with PBPK modeling. Biopharmaceutics & Drug Disposition 2017;38:231-250.
47. Vaessen SF, van Lipzig MM, Pieters RH, Krul CA, Wortelboer HM, van de Steeg E. Regional expression levels of drug transporters and metabolizing enzymes along the pig and human intestinal tract and comparison with Caco-2 cells. Drug metabolism and disposition 2017;45:353-360.
48. Mitra A, Kesisoglou F. Impaired drug absorption due to high stomach pH: a review of strategies for mitigation of such effect to enable pharmaceutical product development. Molecular pharmaceutics 2013;10:3970-3979.

Supplementary materials

Table S6.1 - Details of the LC/MS conditions; Quantification of masses and retention times.

Compound	Rt (min)	Exact mass	Polarity	Fragment	m/z
Midazolam	14.81	326.0855	Positive	tbd	tbd
1-OH midazolam	16.66	342.0804	Positive	tbd	tbd
1-OH midazolam glucuronide	10.36	518.1125	Positive	tbd	tbd

Table S6.2 - Details of the LC/MS conditions used for the analysis midazolam and metabolites.

Compound	Column	Mobile Phase A	Mobile Phase B	Time (min)	Mobile Phase A (%)	Mobile Phase B (%)	Flow (mL/min)
Midazolam	Waters Acquity	5mM	Acetonitrile	0	100	0	0.4
1-OH	HSS-c18(100 x 2.1	ammonium		1.11	85	15	
midazolam	mm i.d., 1.8 µm),	formate in		16.00	75	25	
(glucuronide)	serial no.	water pH		16.50	0	100	
	#01593022418354	4.0		20.00	0	100	

Table S6.3 - Details of the UPLC conditions; Quantification of masses and retention times of atenolol and antipyrine.

Compound	Rt (min)	Exact mass	Polarity
Atenolol	3.81	266.336	positive
Antipyrine	7.01	188.226	positive

Table S6.4 - Details of the UPLC conditions used for the analysis atenolol and antipyrine.

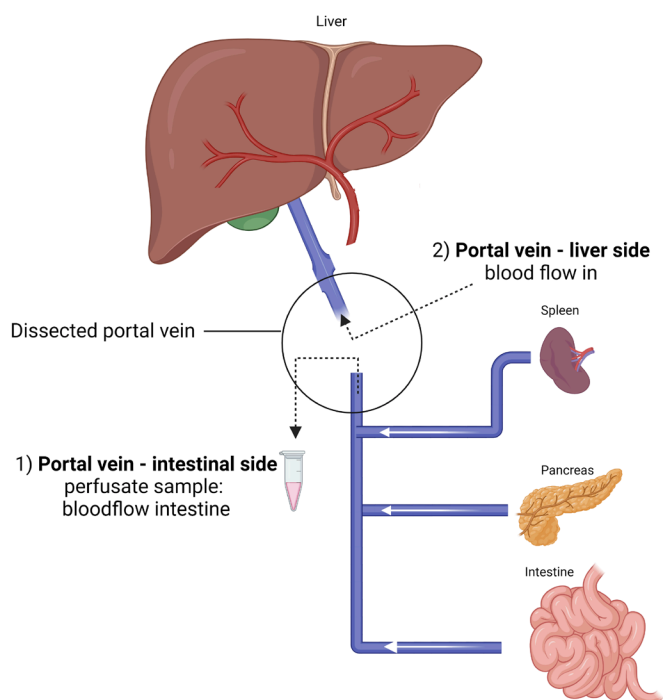| Compound	(pre) Column	Mobile Phase A	Mobile Phase B	Time (min)	Mobile Phase A (%)	Mobile Phase B (%)	Flow (mL/min)
Atenolol	Waters	0.1% FA	0.1% FA in	0.00	100	0.0	0.6
Antipyrine	VanGuard BEH	in MilliQ	ACN	1.11	100	0.0	
	C-			6.00	90	10	
	18 (2.1x 5 mm;			8.00	74	26	
	1.7 µm			9.00	0.0	100	
				10.00	0.0	100	
	Water Acquity-			10.10	100	0	
	BEH C-18 (2.1x			12.00	100	0	
	100mm; 1.7)						

Figure S6.1 - Schematic representation of the dissected portal vein. By dissecting the portal vein, cannulation of the portal vein to the intestinal side is visualized allowing for collection of the portal venous outflow. The portal vein – liver side is also cannulated for an additional flush of the liver during the isolation procedure and to apply a portal flow during NMP.
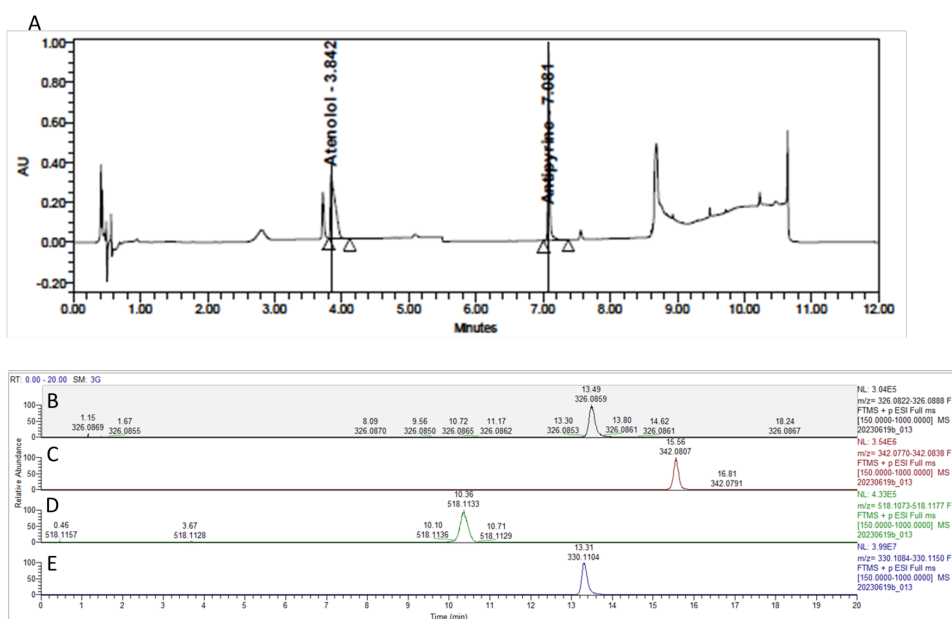
Figure S6.2 - Chromatograms of antipyrine, atenolol, midazolam and midazolam metabolites. (A) Detection of atenolol and antipyrine, (B) midazolam, (C) midazolam 1-OH, (D) midazolam 1-OH glucuronide and (D) midazolam internal standard.
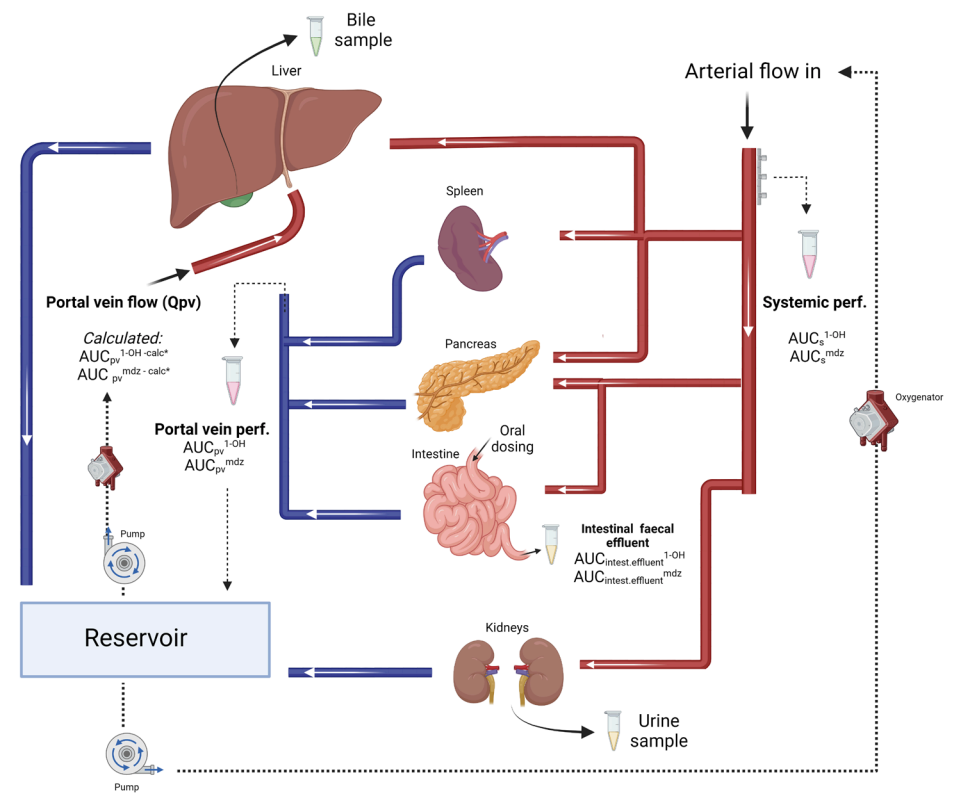
Figure S6.*3* - Schematic representation of concentration measurements of midazolam and metabolites.
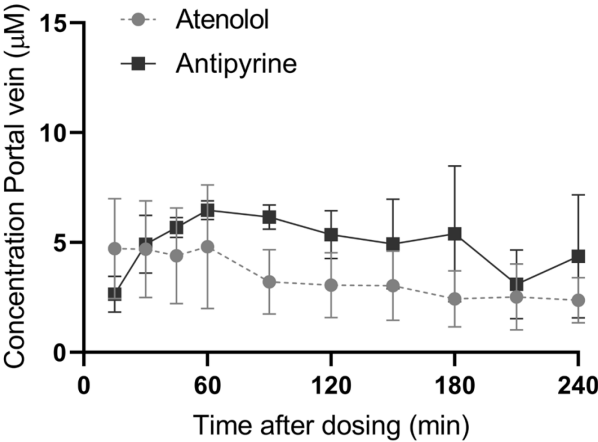

Figure S6.4 - Concentration of Atenolol (µM) and Antipyrine (µM) measured in the portal vein. Data shows average concentration of n=4 experiments ± SEM
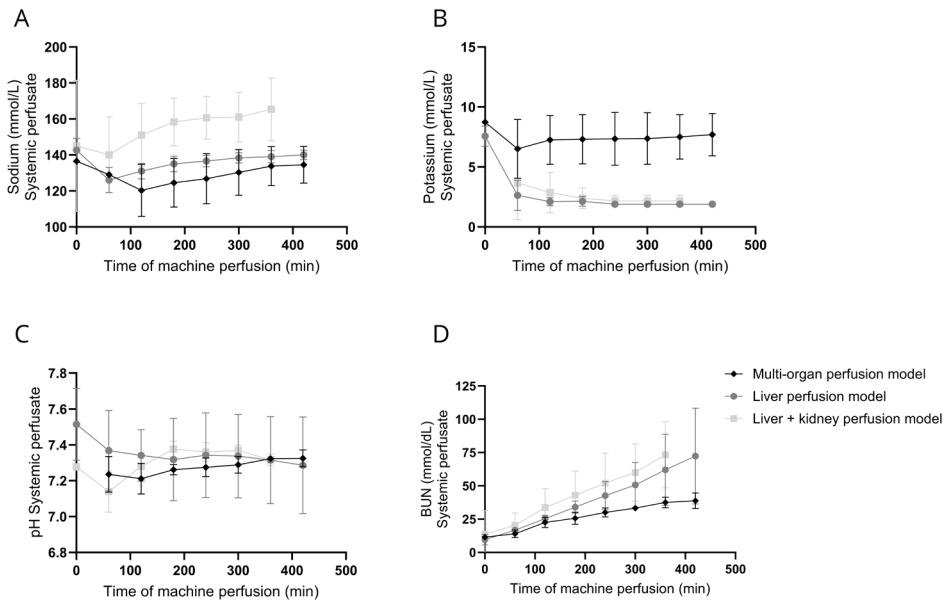
Figure S6.5 - Comparison of systemic perfusate levels of sodium, potassium, pH and BUN between multi-organ perfusion model, liver only and liver+kidney combined perfusion. (A) sodium levels in the systemic perfusate are relatively lower throughout the perfusion compared to liver only and combined liver+kidney perfusion. (B) Potassium levels in the systemic perfusate remain constant and measurable. Both the liver and combined liver+kidney perfusion model show a rapid decline in potassium levels which are <2 after 180 min of perfusion. (C) pH levels in systemic perfusate remain constant throughout the perfusion without the need for bicarbonate supply. (D) Blood urea nitrogen (BUN) levels measured in the systemic perfusate increase in all conditions however remain the lowest in the multi-organ model compared to the liver only and combined liver+kidney perfusion model.
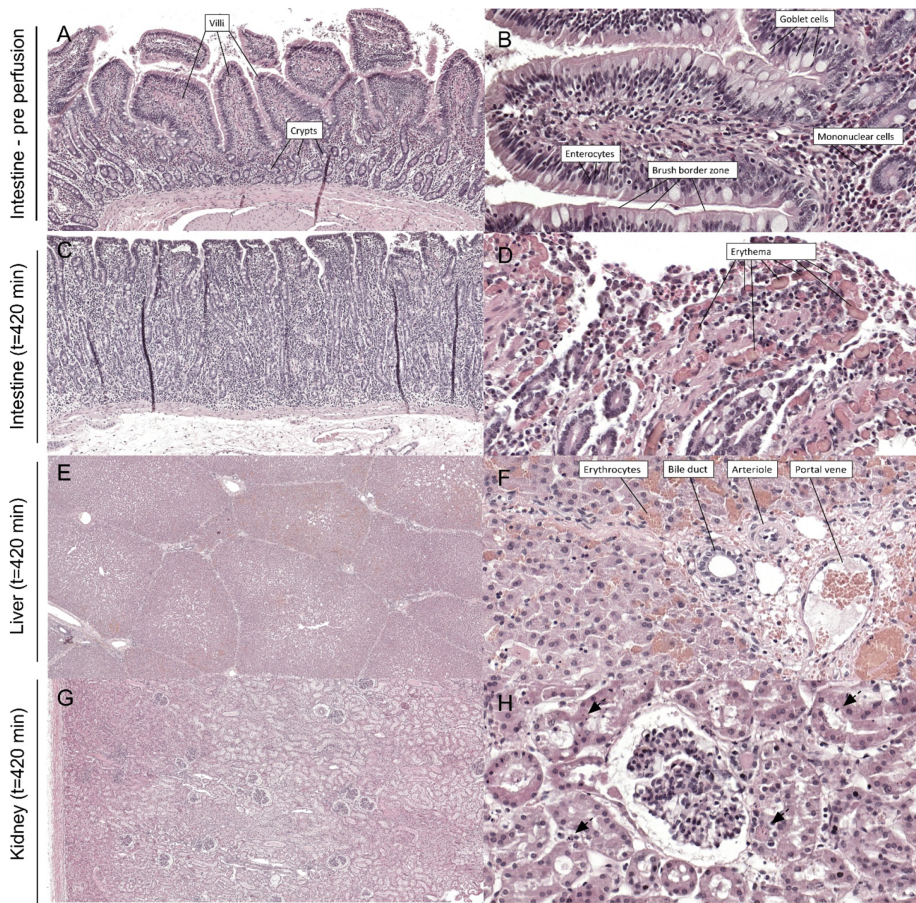
Figure S6.6 - Histological overview of intestine, liver and kidney. (A) H&E staining of the small intestine, taken after flush and before the start of the perfusion of the excised small intestinal tissue, showed intact palisade enterocytes at the villi (40x), (B) visibility of the enterocytes and goblet cells (200x). (C) After 420 min of perfusion partly intact epithelial layer of the intestine was observed, including presence of the villi with enterocytes and goblet visible (40x). (D) In 3 out of 4 studies vessel dilation (erythema) was observed (200x). (E) Morphology of the liver; chord structure was maintained with minimal to mild multifocal hepatocellular single cell necrosis associated with dilated sinusoids (E) Presence of erythrocytes in the portal venous area (200x) (G) Morphology of the kidney; Intact glomeruli were detected in all kidney slices (40x) (G) mild to moderate tubular single cell necrosis was present as indicated by the arrows (200x).
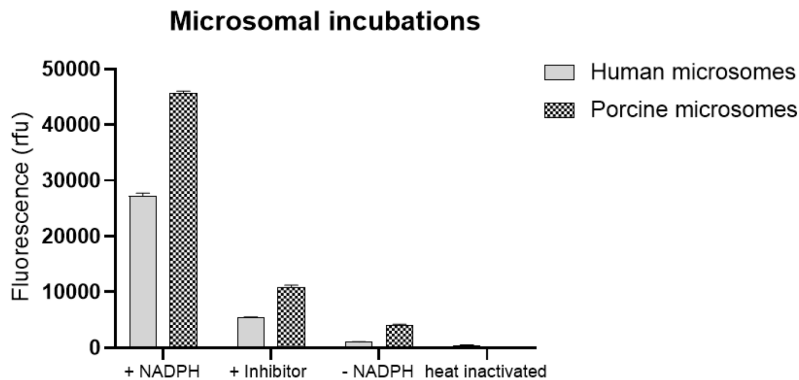
Figure S6.7 - CYP3A4 activity assessment in human and porcine microsomal fractions. CYP3A4 activity was measured using the VIVID red CYP3a4 activity kit with different conditions. To study CYP3A4 activity microsomes were incubated +NADPH. As control conditions, CYP3a4 activity in combination with: + 10 μM inhibitor (ketoconazole), -NADPH and heat inactivated microsomes was determined. Data shows mean ± SD n=3 (one individual experiment).
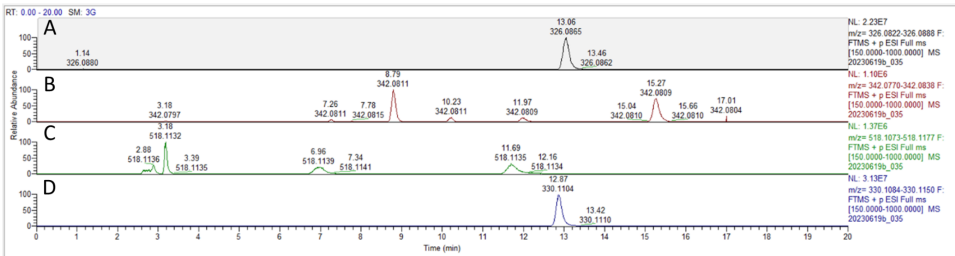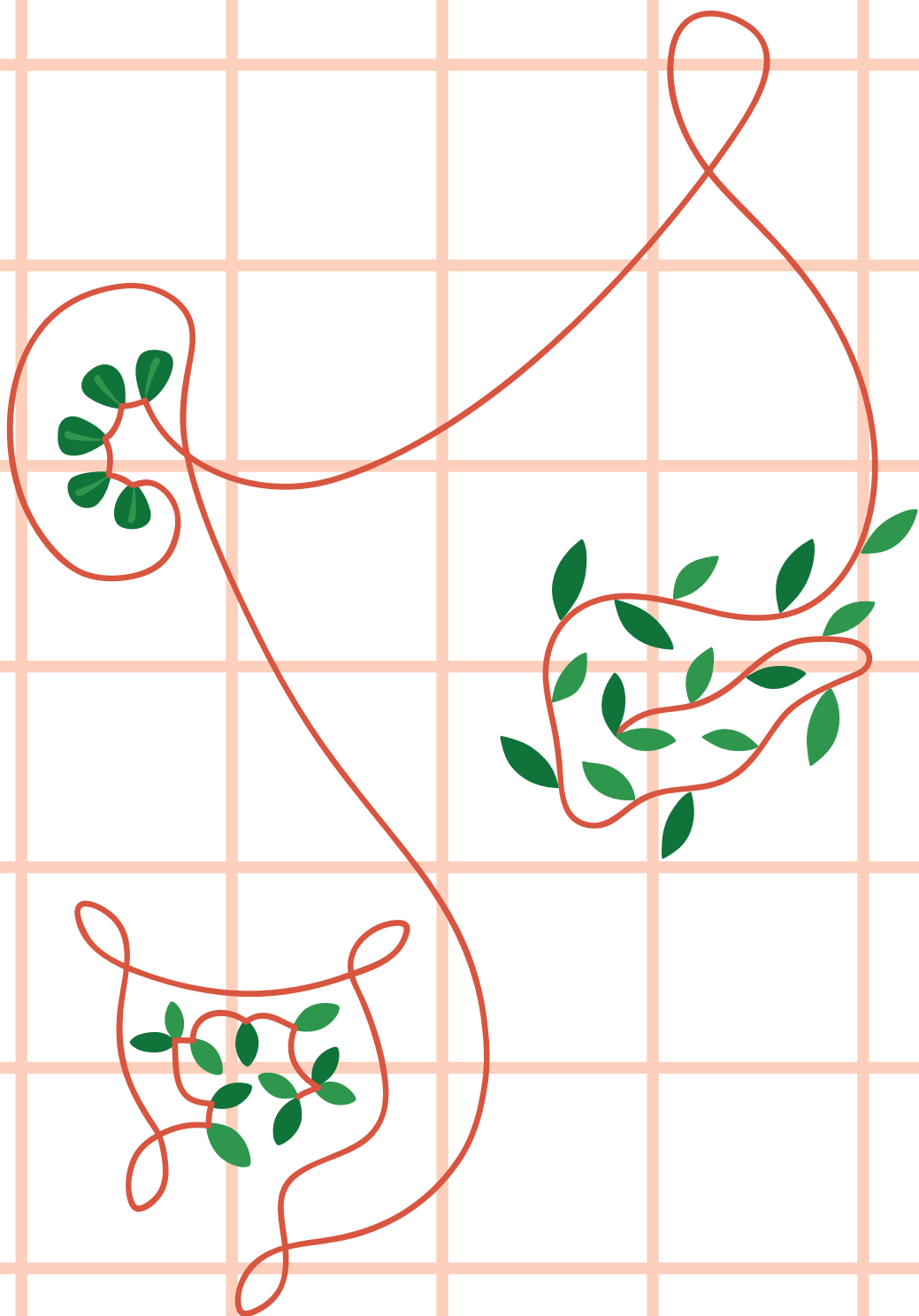

Figure S6.8 - Chromatogram of portal vein sample, 120 min after intraduodenal dose of midazolam (20 mg) showing multiple midazolam metabolites. (A) midazolam, (B) 1-OH midazolam, (C), 1-OH midazolam glucuronide and (D) midazolam internal standard.

PART IV

Summary, future perspectives and conclusions

CHAPTER 07

Summary, future perspectives and conclusions

Summary

The ability to predict the PK profile of drugs in development remains a challenging process with a very poor success rate[1]. Preclinical studies are an important part of the drug discovery process, which aim to provide information regarding the efficacy and safety of the drug[2]. To this end, a comprehensive understanding of the ADME and PK profile is essential. To study ADME processes, *ex vivo* preclinical models can be regarded as the bridge between *in vitro* and *in vivo* models which is discussed in Part I of this thesis. In **chapter 2** we provided an overview of the experimental predictive *ex vivo* models available to study drug ADME processes as well as DDI, in health and disease. The use of normothermic machine perfusion facilitates to study organ function under dynamic and as close as possible to the *in vivo* setting. The intact morphological structure, application of physiological blood flow rates and presence of intact elimination pathways are important characteristics in the field of pharmacology. These aspects, which cannot be adequately simulated in simplified *in vitro* models, provide valuable insights into substrate affinity for transporters, DDI and elimination routes. The objective of this thesis was to explore the applicability of pressure driven normothermic organ perfusion to study pharmacological processes in liver, intestine and kidney. In the different chapters we have shown the use of liver perfusion and the multi-organ model to characterize pharmacokinetic processes like DDI, endogenous substrate handling, pre-systemic intestinal and hepatic metabolism and excretion profiles.

In part II, we studied the applicability of normothermic machine perfusion of the liver to study drug pharmacokinetics and endogenous substrate handling. As a first step, in **chapter 3**, we used the porcine NMP model to investigate whether the perfusion model is a suitable platform to mimic clinical observed OATP mediated DDI[3,4]. We have demonstrated that NMP of porcine livers is a potential novel and reliable model to study OATP-mediated DDI and we showed its effect on hepatic clearance, biliary excretion and perfusate (metabolite) profile of statins. Overall, the rank order of DDI magnitude indicated in our experiments was in good agreement with clinical data. The lowest DDI for pitavastatin (AUC ratio 2.6) and the highest for atorvastatin (AUC ratio 7.2), indicating the potential importance of this new *ex vivo* model in early drug discovery.

Translation of preclinical findings using animal derived tissue like the porcine liver model to clinical practice remains challenging due to, among others, species differences in transporter expression[5,6]. On top of this, liver disease in humans leading to cirrhosis can affect liver morphology and transporter expression thereby affecting drug PK profiles. However, with the currently available preclinical and clinical models, it continues to be difficult to study the effect of these pathological changes on drug PK. In **chapter 4** we showed for the first time the use of explanted human diseased livers as a model to assess the effect of liver cirrhosis on drug PK by measuring hepatic extraction, biliary clearance, DDI transporter function using 4 model drugs. We successfully perfused 7 cirrhotic livers and 4 non-cirrhotic livers for a period of 360 min, maintaining liver viability and functionality. Hepatic clearance of rosuvastatin and digoxin showed to be the most affected by cirrhosis with an increase in C_{max} of 11.5 and 2.9 times, respectively, compared to non-cirrhotic livers. No major differences were observed for metformin and furosemide. Interaction of rosuvastatin or digoxin with perpetrator drugs were more pronounced in non-cirrhotic livers (AUC ratio of 5.6 and 8.1 respectively) compared to cirrhotic livers (AUC ratio of 1.4 and 2.2 respectively). Studying drug pharmacokinetics using explanted human livers can serve as a basis to explore the differences in hepatic handling of drugs for patients with different types of hepatic impairment.

An advantage of the perfusion model is to determine specific functions of the whole organ such as the hepatic first pass effect and biliary excretion in an isolated environment in the absence of other systemic effects. However, the liver is a central organ in the human body and is in close connection to the intestines linked by the portal blood flow receiving nutrients, bile acids and hormones which activate or inhibit certain pathways[7-9]. Bile acids regulate their own homeostasis by providing negative feedback on bile acid biosynthesis. Bile acids inhibit CYP27A1, CYP7A1 and CYP8B1 by activating FXR, which upon activation also prevents toxic intracellular accumulation of bile acids by inhibiting bile acid uptake and stimulating bile acid export[10,11]. The currently used NMP protocols, which are widely applied in clinical as well as research settings, fall short of mimicking the natural functioning of the liver. This limitation arises from the absence of a recirculating bile acid pool as they rely solely on the infusion of taurocholic acid. This places a substantial burden on the liver during NMP as it is forced to engage in the *de novo* synthesis without the support of endogenous bile acids. In **chapter 5**, we addressed this gap and

aimed to characterize the *de novo* bile acid synthesis by profiling the biliary bile acid excretion, cholesterol homeostasis and transporter expression during *ex vivo* liver NMP. We showed that in porcine and human perfused livers, bile acid synthesis rates were above average reported values *in vivo* and decreased cholesterol perfusate levels were observed. Additionally, a decreased expression of bile acid synthesis related genes, increased gene expression of cholesterol metabolism related genes and a decreased expression in bile acid-dependent uptake and efflux transporters was observed after 360 min of human and porcine liver perfusion. Replacing taurocholate infusion with a more representative bile acid pool for the enterohepatic circulation has yielded promising results. The infusion of a bile acid mixture containing (un)conjugated bile acids showed a decreased release of hepatic injury markers and the maintenance of stable cholesterol levels in the perfusate. This approach has also shown that the infusion of (un)conjugated bile acids enhanced liver function pointing towards potential advancements in liver preservation and transplantation techniques.

In Part III, we studied PK processes through the perfusion of en-bloc porcine *ex vivo* abdominal organs. Real time characterization of the first-pass effect of orally administered drugs consisting of local intestinal absorption and metabolism, portal vein transport and hepatobiliary processes remains challenging[12]. In **chapter 6**, we showed the development of a porcine *ex vivo* perfusion model consisting of multiple abdominal organs and demonstrated its capabilities and potential use in studying ADME processes. Using this model, we were able to characterize pre-systemic extraction of midazolam by measuring the intestinal (E_G of 0.22) as well as hepatic extraction (E_H 0.65). As a result, oral bioavailability showed to be 0.27±0.05 which is in line with pig *in vivo* data. By employing this approach, valuable insights can be generated into the absorption and metabolism of new drugs, thereby facilitating the development and optimization of drug candidates for human use.

Future perspectives

NMP holds major potential for the field of pharmacology and drug development. Besides offering the opportunity to enhance the mechanistic understanding of ADME and PK processes of known and marketed drugs, it may also serve a platform to study the PK and efficacy of novel types of drugs.

The close to physiology representation and ability to control experimental settings is a hugh asset over conventional preclinical models. *However, can ex vivo models, particularly normothermic machine perfusion, provide a better understanding of DDI?* In this thesis, we showed the development and application of novel perfusion models like the human explanted liver model and the multi-organ perfusion model. *How can multi-organ perfusion models enhance our understanding of drug pharmacokinetics?* And *the future potential of explanted human diseased organs for ex vivo perfusion resear*ch will be discussed. Finally, the key question remains; *How do ex vivo models translate to in vivo PK profiles?*

Better understanding of DDI through *ex vivo* perfusion models?

In chapter 3 and 4 of this thesis, the applicability to study DDI in perfused porcine and human livers was studied. The FDA guidance for industry, for *in vitro* and *in vivo* drug interaction studies, states that it is important to determine if a new drug is a substrate for Pgp, BCRP, OATP1B1/1B3, MATE and/or OCT2 since these transporters interact with drugs in clinical use[13,14]. In chapter 3, we showed that it was possible to mimic DDI at the transporter level and showed that the rank-order of DDI between statins was in good agreement with clinical data[4,15]. The porcine liver model showed to be a suitable platform to study transporter mediated hepatic uptake and/or transporter mediated biliary excretion. This is particularly valuable for drugs in development that are suspected to have the potential to induce or inhibit transporters or face other potential transporter mediated challenges. To illustrate, compound X, a drug in development, showed non-linear kinetics upon increasing dose levels in a phase I study. The underlying mechanism was suspected to be Pgp mediated saturation of biliary excretion. This was evaluated in our normothermic perfusion model using pig livers (Figure 7.1). Upon a step wise 3-fold increasing dose levels (0.56 mg, 1.67 mg, 5.0 mg, and 15.0 mg), we demonstrated that the AUC increased 3.3, 3.9, and 7.1 times, respectively (Figure 7.1A). This non-linearity effect was observed at dose levels >1.67 mg of compound X. Additionally, an increase in T_{max} from 6 to 15 min was observed in this study, also pointing towards decreased excretion rate at higher dose levels. The excretion of compound X into the bile decreased upon increasing the dose level from 0.56 mg (26% of dose excreted into bile) to 15.0 mg (15% of dose excreted into bile) (Figure 7.1B). Additionally, compound X showed to accumulate in the liver upon higher dose levels (Figure 7.1C). These results

indicated saturation of biliary excretion of compound X at dose levels >1.67 mg, which might be caused by transporter mediated saturation of biliary excretion.
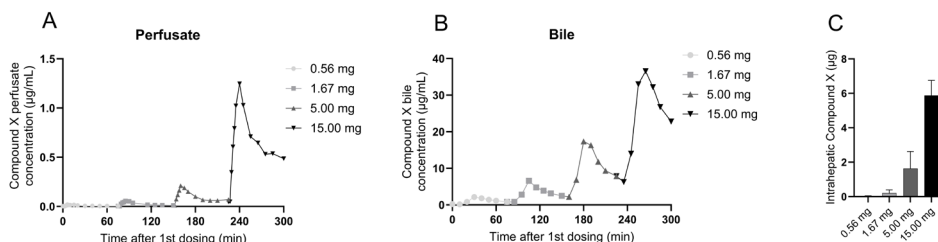

Figure 7.1 - Studying increasing dose levels to determine non-linear kinetics in the ex vivo porcine liver perfusion model. Increasing dose levels of 0.56 mg, 1.67 mg, 5.00 mg and 15.00 mg in (A) perfusate, (B) Biliary excretion of compound X upon increasing dose levels and (C) intrahepatic accumulation of compound X in biopsies taken at the end of each dosing.

To confirm Pgp mediated biliary efflux of compound X, a DDI experiment was designed like in chapter 3 was performed of this thesis. The Pgp inhibitor quinidine was applied as perpetrator drug and upon co-infusion with compound X a potential DDI was simulated (Figure 7.2A-C). Upon co-administration of Pgp inhibitor quinidine (22.4 mg), the plasma AUC increased 1.37-fold (Figure 7.2A) compared to the PK profile of compound X alone. The increased plasma AUC can be explained by diminished biliary excretion of compound X in the presence of Pgp inhibitor quinidine, resulting in 44% decrease in biliary excretion (AUC ratio 0.56) (Figure 7.2B). These results suggest that Pgp is actively involved as a biliary efflux transporter for clearance of compound X upon hepatic uptake. The results were also in line with digoxin, which was used as a positive control and known Pgp substrate (data not shown). After assessing Pgp involvement, in a follow up study also the OATP1B1/1B3 involvement was studied as OATP1B1/1B3 was suspected to be the main hepatic uptake transporter. In a separate study, this was studied by applying cyclosporin as inhibitor for OATP1B/1B3 (Figure 7.2D). Upon co-administration of cyclosporin A, the plasma AUC increased 1.27 times, demonstrating a slight inhibition of OATP-mediated hepatic uptake of compound X. To give more insight into OATP1B/1B3 involvement, bilirubin, the endogenous biomarker for OATP1B1/1B3 function was measured in perfusate (Figure 7.2G-H). The results illustrate that following each administration of compound X, there was a noticeable increase in bilirubin levels, indicating competition for hepatic uptake of bilirubin through the OATP transporter.
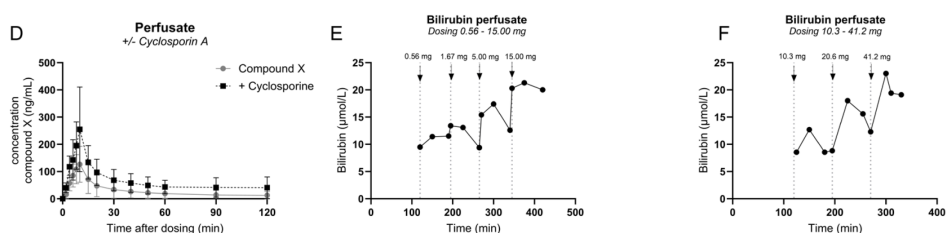
Pgp involvement
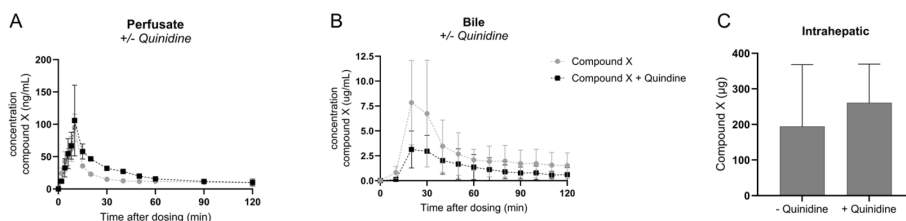
OATP involvement

Figure 7.2 - Determination of Pgp and OATP involvement with the use of inhibitor dosing using the ex vivo porcine liver perfusion model. (A) perfusate (B) biliary excretion and (C) intrahepatic accumulation of compound X (dosed 1.67 mg) in the absence and presence of P-gp inhibitor quinidine dosed at 22.4 mg. Studying OATP involvement in (D) perfusate of compound X (dosed 1.67 mg) in the absence and presence of OATP inhibitor Cyclosporin A (22.4 mg). Bilirubin in perfusate was assessed as endogenous biomarker for OATP in (E) studies with infusion of 0.56 – 15.00 mg and (F) 10.3-41.2 mg.

Together these data clearly show that the porcine liver perfusion model holds great potential to study transporter involvement in a DDI design, which helps towards a better understanding of the uptake and excretion of drugs. Moreover, the ability to study DDI is crucial because it helps to ensure safe and effective medication use, minimizing potential risk and optimizing patient outcomes.

During the liver perfusion studies we infused the perpetrator drug, 5 minutes prior to the victim drug thereby simulating DDI. This setup has been employed in various other isolated liver perfusion studies as well[16]. However, *in vivo*, following oral administration of a drug, the rate and extent of intestinal absorption determines the portal vein concentration which differs between drugs. Bioavailability of a drug is therefore also affected by factors as dissolution, intestinal transit time and permeability, biotransformation by the

intestinal flora and gut wall metabolism[17]. Consequently, measuring DDI in a multi-organ perfusion model approach by dosing both drugs via the duodenum would result in an even more physiological representation of the biology. As demonstrated in chapter 3, varying perfusate rifampicin levels were observed in the condition with atorvastatin, leading to variation in the degree of DDI. The intestine thus plays a crucial role in the regulating the portal vein concentration and thus regulating the magnitude of hepatic DDI[18].

Besides DDI at the transporter level, the interaction can also occur at the (metabolizing) enzyme level as drugs can be an inhibitor or an inducer of these enzymes[13]. Rifampicin, for instance, showed to interact with the PK of several statins via interaction with drug transporters, while long term rifampicin administration (>7 days) results in the induction of the metabolizing CYP3A4 enzyme, thereby also showing that studying long-term effects can be crucial[19]. Interestingly, the first few reports in literature demonstrated the ability to extent normothermic perfusion times which offer a promising avenue to investigate drug induced CYP450 modulation over time[20-22]. Bridging the field of transplantation and pharmacology highlights the importance of long-term liver perfusion as a valuable approach to study CYP450 modulation. To take it one step further, several publications now report the possibility to perfuse split livers[21,23-25] which is an interesting and safe approach for studying drug induced CYP450 enzyme expression. Splitting the liver into two parts enables exposure of one half to the drug while the other half serves as a control. The use of for instance the 'Basel cocktail' containing specific substrates for: CYP1A2 (caffeine), CYP2B6 (Efavirenz), CYP2C9 (Flurbiprofen), CYP2C19 (omeprazole), CYP2D6 (metoprolol) and CYP3A4 (midazolam) can be applied to determine effects on the PK of these certain compounds[26].

Next to the potential that drugs can modulate drug metabolizing enzymes, some drugs have the potential to modulate cytokine release and induce an inflammatory environment which subsequently can suppress of elevate CYP450 enzymes which is known as a drug-biologic interaction. These type of drugs are commonly used for the treatment of cancer as well as inflammatory and immunologic diseases indicating a broad therapeutic range and use[27]. Drug-biological interactions are currently being studied in primary hepatocyte cultures, which are treated with different concentrations of cytokines to study the effect on CYP450 activity and mRNA/protein expression[28-30]. To illustrate, multiple *in vitro* studies show effects of IL-6, IL-1β, TNF-α and IFN-y on the

expression of different CYP450 enzymes in primary hepatocytes[28,31-34]. Klein et al.[35] showed a significant reduction in the formation of the CYP3A4-derived atorvastatin metabolite after 48h and 72h incubation upon dosing 10 ng/mL of IL-6 in HepaRG cells. Additionally, a significant reduction was shown in the CYP3A4 gene expression. The liver perfusion model described in this thesis would be an interesting platform to study whether certain biologics modulate cytokine levels and subsequently alter CYP450 status and function. However, crucial in these studies is the understanding that the cytokine releasing effect of the biologic drug comes specifically from the drug itself and is not elicited by the perfusion process. Conducting a literature search on cytokine release during *ex vivo* organ perfusion highlighted the complexities inherent in this process, revealing that this subject is more challenging than initially anticipated. In a study by Gravante et al.[36], the researchers studied the potential cytokine response to ischemia reperfusion injury in an *ex vivo* porcine liver perfusion model. Significant elevation of IL-6 and IL-8 was observed after 6 hours of perfusion. Additionally, Chung et al.[37], Weissenbacher et al.[38] and Hosgood et al.[39] also showed release of a subset of cytokines (e.g. IL-6, IL-8, IFN-y) during liver and/or kidney perfusion[40]. In healthy individuals, baseline IL-6, IL-8 and IFN-y concentrations are around 5, 12 and 50 pg/mL respectively[41]. IL-6 levels reported in perfusion studies are in the range of ng/mL showing a thousand-fold difference between *in vivo* conditions and *ex vivo* perfusion studies[36,38,39]. To put this in perspective, IL-6 levels in the ng/mL range have been reported for critically ill patients with severe infections like sepsis[42]. This indicates ongoing cytokine release and inflammatory environment which could also influence the CYP450 expression. The use of a hemoadsorption filter has been recommended for eliminating cytokines in the treatment of severe inflammatory driven medical conditions. Hosgood et al.[43] showed that the use of a hemoadsorption filter during kidney perfusion resulted in lower and stable cytokine levels during 6 hours of perfusion. The addition of the cytosorb filter reduced the IL-6 and IL-8 concentration by 87% and 59% respectively[43]. From a pharmacological perspective and for future PK perfusion studies, it would be recommended to include an adsorbent membrane to diminish the inflammatory environment and thereby not affecting the CYP450 enzyme abundance and activity.

How can multi-organ perfusion models enhance our understanding of drug pharmacokinetics?

In chapter 6, we showed the possibility to perfuse multiple organs and subsequently study the ADME profile of midazolam. The ability to study the gut-liver axis offers a unique opportunity to unravel the dynamic interplay between gut-wall metabolism and hepatic uptake and metabolism. We showed the ability to measure pre-systemic intestinal and hepatic metabolism for midazolam, a widely applied CYP3A4 substrate model compound. Up to now, no preclinical models have been developed which directly give insight into the gut wall absorption and metabolism. This is mainly because the intestine is a heterogenous organ and therefore difficult to capture all its function into one *in vitro* model[44,45]. Therefore, PBPK modeling is often needed to generate insight into the extent of the fraction escaping first pass gut wall metabolism, the F_G. Gertz et al.[46] did build a PBPK model to predict the F_G, using microsomal fractions as input data. The authors showed that drugs with a low intestinal extraction could in general be well predicted, however the prediction of high intestinal extraction drugs was less accurate[46]. Current assessment of the F_G is based on plasma concentration time profiles of IV versus oral dosing or concentration time profiles after dosing an inhibitor[18,46,47]. Although the abundance of CYP3A4 in the intestine is around 1% of the abundance in liver, CYP3A4 substrate drugs as midazolam show extensive intestinal wall metabolism[48]. The lower blood flow in the intestinal mucosa compared to the liver blood flow, results in an extended duration of a compounds presence in the intestinal tissue and thereby increasing the likelihood of CYP450 mediated metabolism in the intestine compared to the liver which underscores the difficulty to predict CYP450 mediated metabolism in *in vitro* models[18]. The utilization of the multi-organ perfusion model can provide helpful insights into determination of the F_G since it allows the opportunity to collect samples from, among others, the portal vein. The ability to take portal vein samples has only been described by Paine et al.,[47] who studied the intestinal midazolam metabolism in patients undergoing liver transplant surgery in the anhepatic phase. Interestingly, the researchers demonstrated that after IV dosing, there is a higher concentration of the midazolam metabolite 1-OH midazolam in the portal vein compared to the systemic circulation. This indicates that there is basolateral uptake of midazolam with subsequent midazolam oxidation to 1-OH midazolam which is transported back to the portal vein. Studies comparing IV versus oral dosing, like those exemplified here, represent a future application

of the multi-organ model. Such investigations offer valuable insights into the precise metabolism of (new) drugs and serve as input for PBPK modeling.

Besides phase I metabolism, the liver and intestine are also involved in phase II metabolism e.g. glucuronidation and sulfation[49]. After CYP450 mediated metabolism, compounds can undergo further biotransformation, for instance by glucuronidation, whereafter the glucuronidated product can be excreted via the biliary system. Interestingly, it is observed in *ex vivo* fermentation platforms that the gut microbiota also can also contribute to metabolism[50]. An example is the metabolism of irinotecan. Irinotecan is a pro-drug and is metabolized by the liver to SN-38 and subsequently glucuronidated to SN38-glucuronide and eliminated via biliary excretion[51]. After biliary excretion, the intestinal microbiota can deconjugate the SN38-G to SN-38. This is followed by intestinal absorption of SN38 to the portal venous blood, whereafter again glucuronidation can occur, thereby resulting in a prominent secondary plasma peak. This process involving phase I, phase II metabolism, biliary excretion and intestinal absorption is extremely difficult to capture in *in vitro* models as well as via PBPK modelling. Nevertheless, its significance is exemplified by Gupta et al.,[51] who showed that patients with lower rates of hepatic glucuronidation would have higher concentrations of biliary SN38, leading to gastrointestinal toxicity. The multi-organ perfusion model presented in this thesis holds potential to study these dynamic processes to understand the specific role of each organ contributing to the metabolism of the drug. To gain even a better understanding of organ specific drug metabolism during multi-organ perfusion, microdialysis emerges as a powerful tool as it allows for real-time monitoring and in-depth insights into the metabolic pathways. Microdialysis sampling is a technique often used in the field of neurosciences to study biochemical conversions in the extracellular fluid[52]. The techniques consists of a probe with a hollow fiber dialysis membrane which can easily be implanted in a (perfused) organ. This allows for real time monitoring of the extracellular fluid and thus real-time monitoring of PK processes like phase I and II metabolism[53], study drug unbound concentrations[54] or (blood flow dependent) tissue penetration. Until now, the use of microdialysis in organ perfusion has only be described in the field of *ex vivo* lung perfusion. Mazzeo et al.[55] described the use of microdialysis during *ex vivo* lung perfusion and reported that microdialysis was more effective and specific in studying lung metabolism compared to perfusate levels. Continuous sampling from the microdialysis flow in the intestine and liver would be beneficial and informative to study the distribution and

metabolism profile of drugs with complex ADME processes (e.g. phase I, phase II, EHC). Thereby in depth characterization of the metabolic pathway will enable better PBPK predictions.

Use of explanted human diseased organs for *ex vivo* perfusion research

The use of human tissues for pharmacological studies is superior over other species. In chapter 4, we showed the use of explanted human diseased livers for PK research. So far, the utilization of human diseased explanted livers is mentioned in a limited number of publications[56-58]. However, the applicability of human diseased livers for *ex vivo* perfusion research has major potential for instance to gain in depth information on disease-specific processes and the role in PK and even pharmacodynamic processes. For example, MAFLD is one of the most important causes of liver disease worldwide[59]. Non-alcoholic liver disease (NASH) is an advanced form of MAFLD and can potentially progress to cirrhosis and hepatocellular carcinoma. NASH is one of the most common indications for liver transplant, alongside alcoholic cirrhosis, hepatocellular carcinoma, hepatitis C related cirrhosis and cholestatic disease[59,60]. There are currently no therapies available for the treatment of MAFLD, NASH or ALD. Nevertheless, notable progress is being made in drug development regarding oligonucleotide-based treatments[61]. Oligonucleotide- based therapeutics are currently an emerging class of drugs which include short interfering RNA (siRNA) that degrade target mRNA[61]. So far, only a limited number of oligonucleotides have progressed to clinical stages[62]. The predominant challenge thus far has been securing the safe and effective intracellular delivery of these compounds in human tissues. A disadvantage of lipid nanoparticle delivery is for instance the high concentration needed and inducing a pro-inflammatory effect[63,64]. Given the abundance of disease targets in the liver which are susceptible to modulation, the liver is an interesting target for oligonucleotides therapies[61,65]. Therefore, *ex vivo* organ perfusion and especially *ex vivo* perfusion using diseased human livers would be a first step bridging the gap between preclinical *in vitro* and clinical *in vivo* studies. Utilizing explanted diseased human livers with NASH or ALD, uptake and gene modification can be assessed by leveraging the disease characteristics. Several oligonucleotides have been described which target NASH[63,66,67]. Linden et al.[67] for instance, demonstrated in a mice model the use of a conjugated antisense oligonucleotide which mediated silencing of the gene Pnpla3 and subsequently reduced liver steatosis score and fibrosis[67]. Exploring the application of these type of therapeutics in a liver perfusion model with explanted NASH or MAFLD

livers would provide a valuable opportunity to study tissue uptake, potential local toxicity effects or immune effects. First reports already describe the use of siRNA during *ex vivo* liver perfusion[68-70]. Bonaccorsi et al.[69] aimed to inhibit an apoptosis-associated gene using an siRNA approach in a rat transplant model to reduce ischemia reperfusion injury. The siRNA was administered during hypothermic machine perfusion (HMP) followed by liver transplantation. While the results on apoptosis inhibition by the siRNA remained inconclusive, the researchers were able to show hepatic uptake of the siRNA[71]. Recent studies have adapted machine perfusion to demonstrate the possibility to prolong organ perfusion duration[72-74], with perfusion of human and porcine livers for up to 7 days[75]. Prolonged perfusion would allow to study hepatic uptake of an oligonucleotide-based therapeutic and at the same time study changes in RNA and protein levels in time. Besides liver perfusion, first studies have also been reported with kidney perfusion. Thompson et al.[76] demonstrated the delivery of antisense oligonucleotide in a human kidney during perfusion and showed to block microRNAs function implicated in ischemia reperfusion injury.

Explantation of diseased organs followed by *ex vivo* organ perfusion for PK research is a concept which can be extrapolated to other research fields. The application of *ex vivo* organ perfusion may also find relevance in pediatrics as livers and kidneys are explanted due to conditions such as cancer[77-79]. In pediatric research, key research questions involve understanding the ontogeny of drugs transporters and drug metabolizing enzymes as well as studying age-related variations in the pharmacokinetics of specific drug classes in children[80,81]. *Ex vivo* organ perfusion complemented with PBPK modelling can subsequently contribute to the development of age-appropriate dosing guidelines. This concept can also be applied for other special population groups such as morbidly obese individuals for investigating specific pathophysiological changes related to obesity that impact drug metabolism[82,83]. An illustrative example is the study conducted by de Hoogd et al.[84] demonstrating reduced elimination of morphine glucuronide metabolites (morphine-3-glucuronide and morphine-6-glucuornide) in morbidly obese patients in comparison to healthy volunteers. Although the primary route of the glucuronide metabolites elimination is via renal excretion (80%), there was no difference in kidney function between the morbidly obese and healthy subject group. Therefore the researchers hypothesized, based on reports on Dubin-Johnson syndrome where dysfunctional mutations in the MRP2 gene caused impairment in biliary excretion of bilirubin glucuronides, that hepatic transporters in the biliary

elimination of morphine glucuronide metabolites plays a significant role in the morbidly obese subject group[85]. To test this hypothesis, *ex vivo* liver perfusion could be conducted if there are morbidly obese patients with an underlying liver disease awaiting transplantation[86]. With this approach, the metabolism and excretion as well as transporter abundance can be studied to investigate and characterize the underlying mechanism. Besides changes in CYP450 enzymes and uridine diphosphate glucuronosyltransferase (UGT) enzyme activity in morbidly obese patients affecting drug metabolism[82,87], hepatic blood flow can also be altered[87,88]. Hepatic clearance is a result of an interplay between CYP450 abundance and activity and hepatic flow. To understand the observed differences in midazolam clearance in morbidly obese adults or obese adolescents compared to healthy subjects[89,90], it would be of great value to study the impact of obesity on hepatic flow. *Ex vivo* perfusion using pressure driven perfusion machines is a solution to study the effect of obesity on hepatic flow as well as CYP3A4 activity.

How do *ex vivo* models translate to *in vivo* PK profiles?

Compared to traditional *in vitro* models, *ex vivo* (whole organ) models are a promising platform and thereby paving the way to apply PBPK modeling in a more reliable and accurate way. It is hypothesized that accurate predictions of PK profiles would result in better translation of preclinical data to *in vivo*, which is accompanied by a lower attrition rate[91-93]. In this thesis, multiple *ex vivo* liver perfusions were performed, generating concentration-time profiles of the disappearance of the drug from the perfusate and appearance of the drug into the bile. The concentration-time profiles give an estimate regarding the hepatic elimination rate and percentage biliary clearance. However, interpretation to clinical *in vivo* profiles lack as 'only' the hepatic extraction of a drug and the biliary clearance can be determined. This is also true for the previously published InTESTine system; a platform with *ex vivo* tissue explants to study (regional) intestinal absorption and permeability[94,95]. As mentioned in the introduction of this thesis, the intestines, liver and kidneys are key organs involved in ADME processes and together define the PK profile of a drug.

To study the potential of *ex vivo* platforms to predict the *in vivo* PK profile of a drug, we here combined preclinical *ex vivo* data from the InTESTine system, combined liver-kidney perfusion all integrated by PBPK modeling to predict *in vivo* PK profiles using the drug cocktail rosuvastatin, digoxin, metformin and furosemide. First, regional intestinal transport was assessed using the

InTESTine system. Figure 7.3 shows the regional transport P_{app} values derived from the InTESTine system with porcine intestinal tissue.
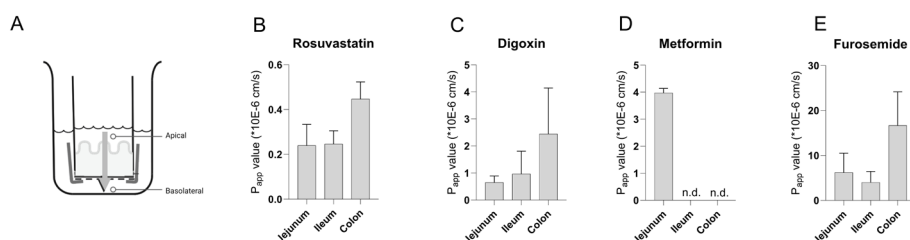
Figure 7.3 - Assessment of the regional intestinal transport of rosuvastatin, digoxin, metformin and furosemide using the InTESTine system with porcine intestinal tissue. (A) Schematic representation of the InTESTine system where porcine intestinal tissue is mounted in the system creating an apical (lumen) and basolateral (portal blood side) compartment. Determination of the regional permeability of (B) Rosuvastatin in jejunum (n=1), ileum (n=3), colon (n=2) tissue (C) Digoxin jejunum (n=6), ileum (n=3) and colon (n=4) tissue, (E) Metformin jejunum tissue (n=2) and (E) Furosemide jejunum (n=1), ileum (n=1) and colon (n=1) tissue.

The reported observed fraction absorbed of rosuvastatin, digoxin, metformin and furosemide *in vivo* is 0.50, 0.81, 0.55 and 0.53 respectively[95-98]. The reported range of the InTESTine system showed P_{app} values of 0 to ~18 (x10^{6}cm/s) translating to a F_a of 0 – 1[94]. Intestinal permeability of rosuvastatin was limited in the InTESTine system (mainly due to the fact that it is a strong BCRP substrate), with average P_{app} value of 0.21±0.09 for more proximal GI tract and 0.44±0.07 for distal GI tract, which does not correspond to the reported fraction absorbed of 0.50[98]. Comparable results were found for digoxin (average P_{app} 0.65±0.23, due to high affinity of digoxin for Pgp), and also showing higher P_{app} values in the distal parts of GI tract (P_{app}: 2.44±1.69) (Figure 7.3C). The absorption of metformin and furosemide across the intestinal wall showed to be faster with 3.98±0.16 for metformin jejunum and 8.74±6.01, 4.06±2.41 and 16.67±7.49 in jejunum, ileum and colon respectively for furosemide (Figure 7.3D-E).

To assess hepatic and renal clearance and subsequent biliary and renal excretion, the dual perfusion of liver+kidney was explored using the LiverAssist perfusion device (XVIVO, the Netherlands) (Figure 7.4). In this perfusion model the arterial blood supply is splitted to the 1) hepatic artery and 2) the renal artery. The liver receives also blood via the portal vein. The simultaneous perfusion of *ex vivo* kidney and liver is a novel and unique approach to determine the hepatic and renal clearance and excretion of drugs within one experiment[99]. The drug cocktail was dosed via the portal vein (1.4 mg

rosuvastatin, 0.056 mg digoxin, 74.2 mg metformin and 0.77 mg furosemide) and samples were taken from the perfusate, bile and urine.
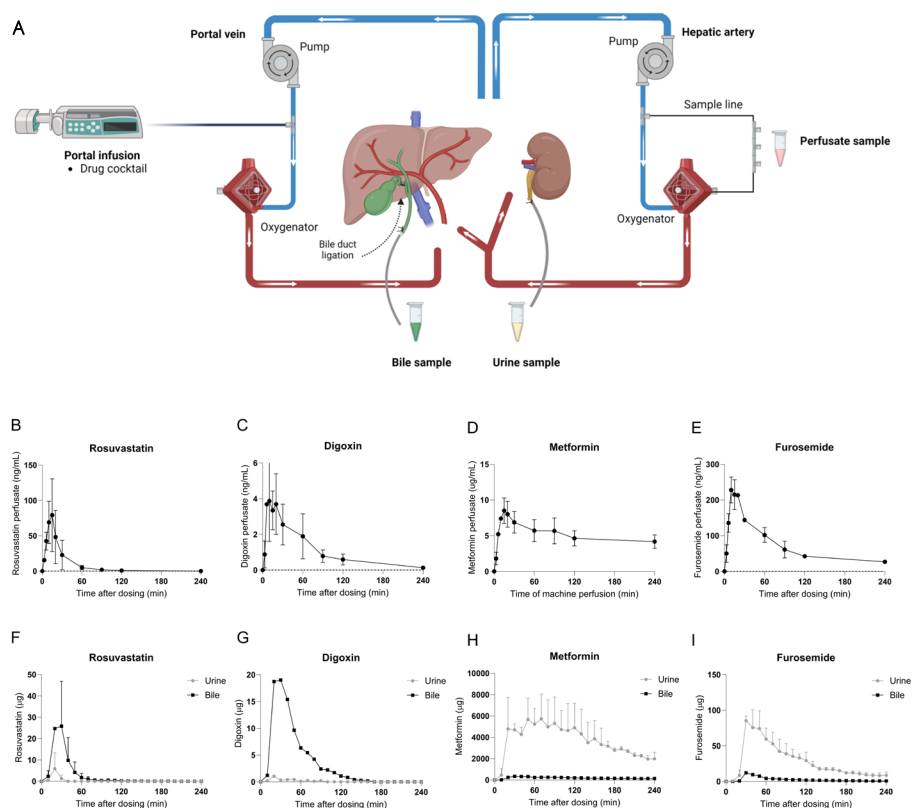

Figure 7.4 - Schematic representation of the perfused liver+kidney model using porcine organs and the perfusate and excretion profiles of rosuvastatin, digoxin, metformin and furosemide using the combined liver+kidney perfusion model. (A) The liver+kidney perfusion model: applied portal pressure of 8-11 mmHg and arterial pressure of 75-85 mmHg, with a total circulating volume of 2.5 L of perfusate. Drug cocktail was dosed to the portal vein of the liver mimicking oral dosing. Systemic perfusate profiles of (B) rosuvastatin dosed 1.4 mg, (C) Digoxin dosed 0.056 mg, (D) Metformin dosed 74.2 mg and (E) Furosemide dosed 0.77 mg. Urine and biliary elimination of (F) Rosuvastatin, (G) Digoxin, (H) Metformin (I) Furosemide. Data represents n=2 mean ± SD.

The combined liver+kidney perfusion model showed stable arterial and portal flow during 360 min of perfusion with constant bile and urine production (data not shown). Figure 7.4 shows the systemic profiles and excretion patterns after a single administration of the drug cocktail. Rosuvastatin was rapidly cleared from the circulation (Figure 7.4B) and was mainly eliminated via bile (20.2±5.8 %) and only a minor part was excreted into urine (2.1±1.5%). Digoxin was highly

biliary excreted (100%) and only a minor part was eliminated via urine (5.6%). Metformin clearance demonstrated slow uptake from the perfusate suggesting saturation of the OCT2 and MATE1/2 transporters, however was rapidly excreted into urine (120±29%) and to a minor extent via bile (6.5±0.3%). Furosemide was mainly excreted into urine (80.3±6.4%) and only a minor part in bile (7.7±1.8%). Data is in line with literature showing rosuvastatin and digoxin being mainly eliminated via bile and minorly into urine while metformin and furosemide are known to be mainly renally excreted[100-103]. To integrate *ex vivo* data into PBPK modeling, as a first step the concentration-time profiles of perfusate and cumulative amounts of bile and urine were fitted (Figure 7.5) to the developed liver+kidney PBPK model using R programming (R Studio, version 4.3.2). This liver+kidney PBPK model presented in Figure 7.6, generating the model-specific PK parameters CL_{bile}, CL_{urine}, K_{urine} and K_{bile} (Figure 7.6B).
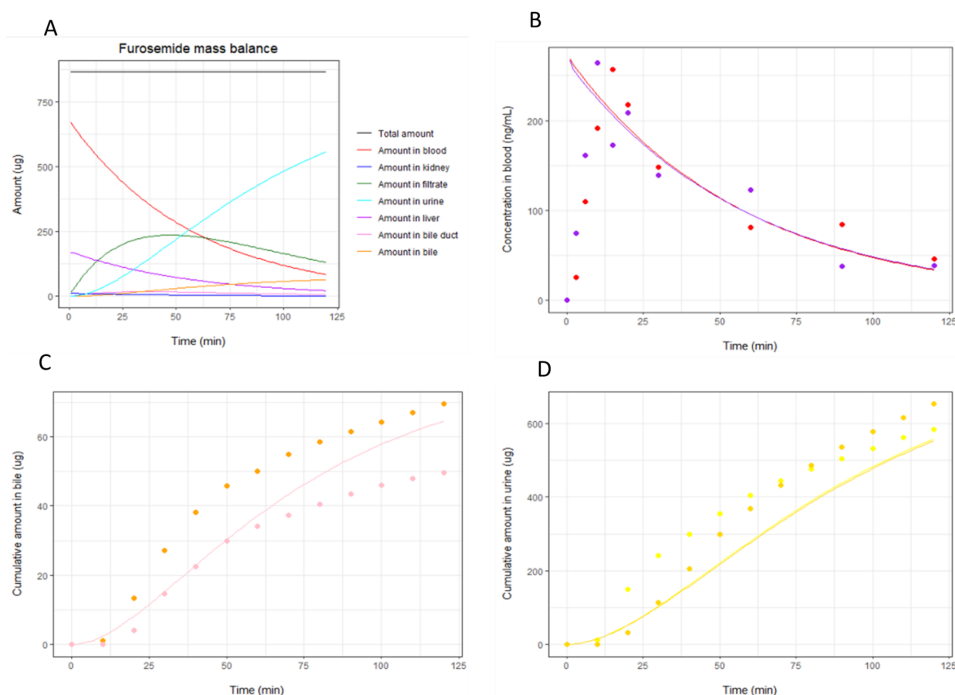

Figure 7.5 - Fitted concentration-time profiles of furosemide. (A) Furosemide mass balance per compartment (B) Concentration-time profile of furosemide perfusate perfusion experiment (C) cumulative amount of furosemide in bile and (D) Cumulative amount of furosemide in urine.
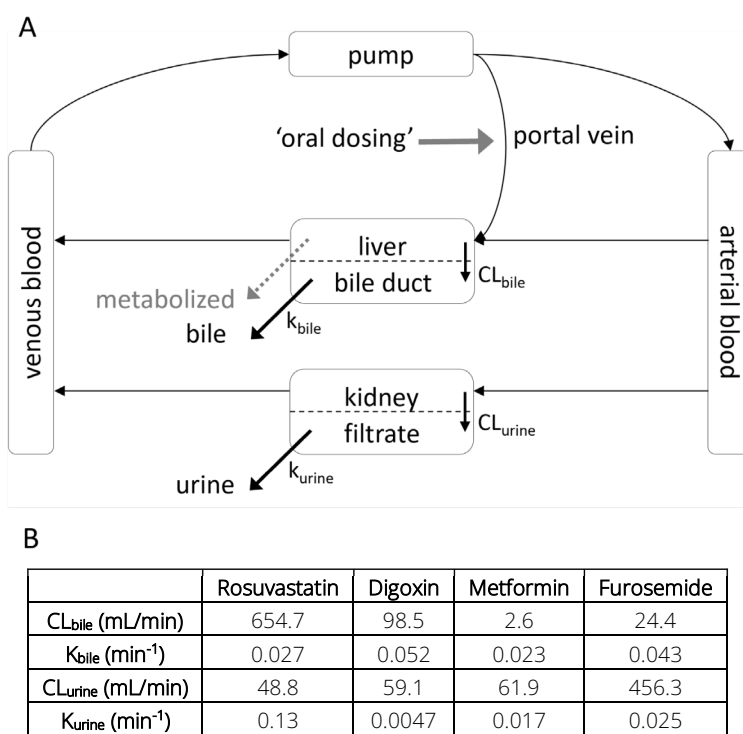
	Rosuvastatin	Digoxin	Metformin	Furosemide
CL_{bile} (mL/min)	654.7	98.5	2.6	24.4
K_{bile} (min^{-1})	0.027	0.052	0.023	0.043
CL_{urine} (mL/min)	48.8	59.1	61.9	456.3
K_{urine} (min^{-1})	0.13	0.0047	0.017	0.025

Figure 7.6 - Representation of the ex vivo liver+kidney PBPK model and simulated values derived from the sub PBPK model. (A) Schematic representation of the ex-vivo liver+kidney PBPK model and (B) Simulated pharmacokinetic parameters derived from the fitted ex vivo perfusion data of perfusate bile and urine determined in the generated ex vivo liver+kidney PBPK model.

Secondly, the PK parameters from the liver+kidney PBPK model (Figure 6A-B) together with the P_{app} data from the InTESTine system were integrated into a generic PBPK model using R programming. Figure 7.7 demonstrates the predicted concentration time profiles of the arterial blood following oral intake of the rosuvastatin, digoxin, metformin and furosemide. The predicted C_{max} and T_{max} of rosuvastatin showed to be within the range of the (lower) observed clinical values. Digoxin, displayed a systemic profile with a 7-fold lower C_{max} and a delay in T_{max} (T_{max} of 5 hours vs. 1.2 hours in vivo). Predictions for furosemide reached a maximum concentration at 0.105 mg/L which is nicely within the range of the clinically observed profiles. The T_{max} was predicted after 5 hours which was compared to clinical *in vivo* data showing a T_{max} of 1.2 hours, slightly delayed. In the case of metformin, our predictions showed a C_{max} level of 1.5 mg/L which is a 2-fold overestimation of the average C_{max} observed in clinical

profiles. Tmax was close to reported in vivo data (T_{max} of 4 hours vs 3.35 hours in vivo). Both furosemide and metformin showed an underestimation of the elimination of the drugs from the circulation.
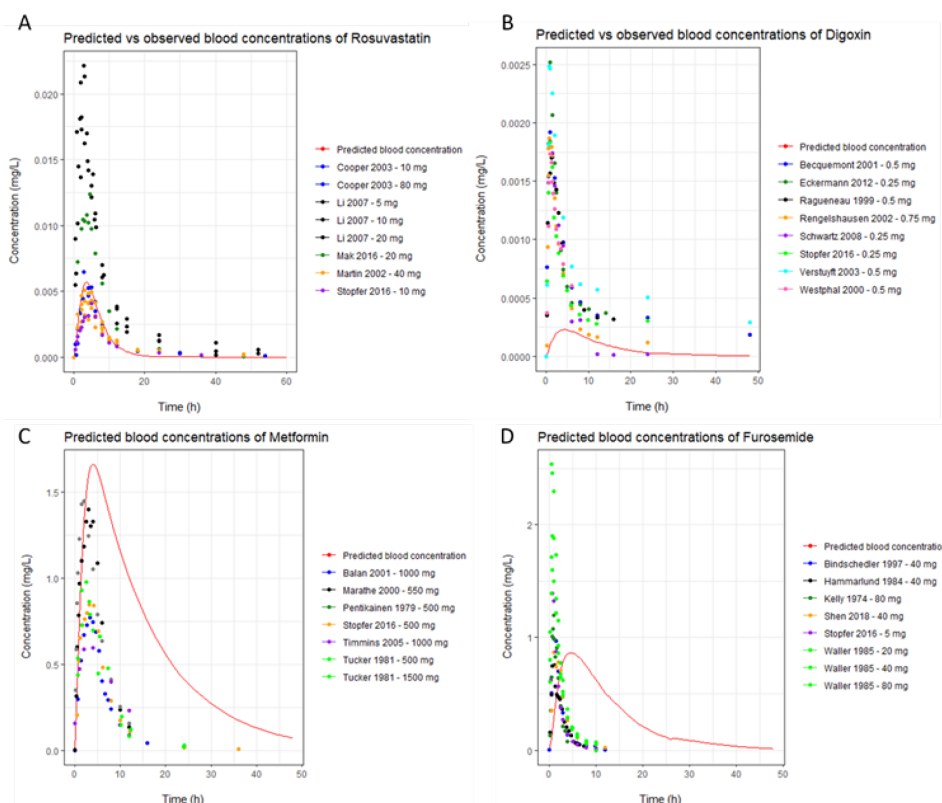

Figure 7.7 - Simulated blood concentration profiles after single oral dose of the drug cocktail. Simulation profiles of oral dosing of (A) 10 mg rosuvastatin, (B) 0.5 mg digoxin (C) 500 mg Metformin and (D) 40 mg furosemide. The simulation duration was 48 hours.

The prediction for C_{max} of rosuvastatin showed to be within the range of clinically observed data, but on the lower side. The intestinal transport of rosuvastatin showed to be relatively low when using porcine intestinal tissue. Rosuvastatin is a substrate for the BCRP efflux transporter, limiting the influx into while facilitating the efflux out of the cells[104]. Sjoberg et al.[105] reported a P_{app} value of 6.95±1.05 in human jejunum tissue while in porcine jejunum tissue a P_{app} value of 0.24 was measured. Vaessen et al.[44] demonstrated differences in abundance of BCRP expression between pig and human. A significant higher

expression of the protein was measured in jejunum tissue of pigs (0.75 pmol protein/g tissue) compared to human (0.45 pmol protein/g tissue), hypothesizing more efflux of rosuvastatin by BCRP in porcine intestinal tissue resulting in a lower permeability. Underestimation of the intestinal absorption resulted in a slightly lower C_{max} compared to clinical *in vivo* data[106-109]. However, important to note is the variation observed in clinical studies. Cooper et al.[106] demonstrated a C_{max} of 53.5 ng/mL after an oral dose of 80 mg rosuvastatin, while Li et al.[107] showed a C_{max} of 45 ng/mL after an oral dose of 40 mg rosuvastatin. These differences highlight the importance of considering and understanding the variability in drugs response among individuals. Similar as rosuvastatin, the same effect was observed for digoxin regarding intestinal transport and regional variability[110]. Although a fraction absorbed of 80% is observed in human, *ex vivo* tissue models and the Caco-2 model report rather low values of intestinal permeability which are not in line with a fraction absorbed of 80%[94,95,105]. Using the *ex vivo* data, the prediction of C_{max} showed to be 7 fold lower[111-116]. The protein expression of OATP2B1 (furosemide) and OCT1 (metformin) showed no major difference between intestinal regions[44,110] and the P_{app} values were in line with literature[95,105,117]. The predicted C_{max} levels showed to be close to *in vivo* observed data for metformin[118-122] as well as furosemide[103,120,123-126]. However, the predicted systemic profiles for metformin and furosemide showed delayed elimination compared to *in vivo* profiles with CL_{urine} as a factor contributing to the elimination. In a clinical study by Stopfer et al.[120] human subjects receiving the drug cocktail showed complete elimination of furosemide after 8 hours and metformin after 24 hours while in our model this process takes approximately 48 hours. This indicates an underestimated rate of renal elimination during *ex vivo* experiments compared to *in vivo* which could be the result of diminished *ex vivo* kidney function during normothermic perfusion. However, there are currently no established parameters for *ex vivo* kidney function. Parameters such as flow, urine output, creatine clearance and fractional sodium excretion are commonly investigated[127-130]. Multiple studies demonstrate the creatine clearance (GFR) during *ex vivo* kidney perfusion. In these studies, using slaughterhouse kidneys, GFR values around the 1.0 – 5.0 mL/min are measured[130-132]. In contrast, Lødrup et al.[133] measured the GFR from a single kidney *in vivo* and showed an average GFR of 33.9±8.9 mL/min thus indicating that *ex vivo*, kidney GFR is diminished compared to *in vivo*. Inulin is often used as a model compound to measure the GFR and Markgraf et al.[130] studied inulin clearance as function assessment test in perfused kidneys derived from laboratory pigs and slaughterhouse pigs with different time of

warm ischemia (WIT). The researchers demonstrated that none of the slaughterhouse derived kidneys were within the limits for consideration of 'functional kidneys' which was determined by the inulin uptake and excretion behavior independent of the WIT[130]. Together, the combination of *ex vivo* data with PBPK modeling provides a first 'real' insight into *ex vivo* kidney function by studying the clearance of transporter mediated drugs and subsequent translation to in vivo situation. This could aid in the generation of function assessment tests or parameters to study kidney function in an *ex vivo* environment which is needed in the field of transplantation.

The *ex vivo* models are complex models and may better represent physiological conditions than purely *in vitro* data and thereby enhancing the models' predictive capabilities. This is particularly relevant when studying transporter mediated processes as transporter mediated processes are typically more complicated than that of drug metabolizing enzymes. However, translation of the *ex vivo* data towards *in vivo* profiles with PBPK modeling has some challenges. First, we used a perfusate with at total concentration of 1% albumin which is lower compared to the physiological concentrations ranging between 3.5 - 5.0% albumin[134]. Many of our kidney perfusion experiments showed the inability to produce urine when using a perfusate consisting of red blood cells with plasma. Lowering the albumin concentration in the perfusate showed urine production by the *ex vivo* kidneys. Since urine production is essential to measure the renal elimination of a compound, we chose to use these sub-physiological concentrations. Many drugs are however highly bound to plasma proteins and changes into plasma protein concentration will therefore affect the elimination rate from the perfusate into the organ[135]. Although e*x vivo* to *in vivo* extrapolation was performed to adjust for the percentage of albumin in the system, it introduces additional uncertainties to the data. Moreover, to better fit the experimental data, tissue concentrations are needed which can easily be obtained from the *ex vivo* perfused organ.

Here we present for the first time the use of porcine *ex vivo* tissue models in combination with PBPK modeling, predicting PK profiles which are close to clinical observed human profiles. Currently, more abundant data is available regarding transporter abundance in intestine, liver and kidney between pig and humans[44,136,137] which can be used to refine profiles with greater accuracy. The use of human tissues in *ex vivo* models have been described before by our

group for intestine[94] and liver[138], showing the potential for even further enhancement of PK prediction in human.

Conclusion

In conclusion, in this thesis we aimed to study to pharmacokinetic application of pressure driven normothermic organ perfusion. Using a novel pressure driven perfusion machine, we endeavored to bridge the fields of transplantation and pharmacology. Our studies demonstrated the utilization of NMP to examine various drug PK processes such as the hepatic first pass effect, hepatic clearance, biliary excretion, transporter function and DDI using porcine and human explanted diseased livers. The use of porcine livers was an appropriate substitute for human livers to mechanistically study transporter contribution in drug uptake, drug excretion and to study DDI. These studies enabled the investigation of OATP1B1/1B3 mediated DDI, with results aligning closely with clinical data. Moreover, explanted diseased human livers showed to be suitable for perfusion research and can serve as a basis to explore the differences in hepatic handling of drugs for patients with different types of hepatic impairment. Hepatic clearance of rosuvastatin and digoxin showed to be the most affected by cirrhosis while no major differences were observed for the renally cleared drugs metformin and furosemide. The 3-fold lower portal flow in cirrhotic livers showed to diminish the hepatic extraction of rosuvastatin showing the importance of portal flow in a preclinical model to determine hepatic clearance. Furthermore, optimalisation of the liver perfusion model was studied by infusion of a (un)conjugated bile acid pool to replicate physiological conditions for a more accurate assessment of hepatic PK processes. This approach demonstrated that the infusion of (un)conjugated bile acids alleviated the burden of the *de novo* bile acid synthesis and enhanced liver function pointing towards potential advancements in liver preservation and transplantation techniques. The possibilities of the pressure driven perfusion system are numerous, as we demonstrated the development and application of multi-organ perfusion to understand the interplay between the intestine and liver by characterization of the first-pass effect and pre-systemic CYP3A4 metabolism. Use of perfusion showed to be an excellent tool to study drug concentrations in blood flows and tissues which are otherwise impossible to reach, thereby generating a novel and in depth insights into the ADME profile of drugs.

References

1. Benet LZ, Sodhi JK. Investigating the theoretical basis for in vitro–in vivo extrapolation (ivive) in predicting drug metabolic clearance and proposing future experimental pathways. The AAPS journal 2020;22:120.
2. Honek J. Preclinical research in drug development. Medical Writing 2017;26:5-8.
3. Mori D, Kashihara Y, Yoshikado T, Kimura M, Hirota T, Matsuki S, Maeda K, et al. Effect of OATP1B1 genotypes on plasma concentrations of endogenous OATP1B1 substrates and drugs, and their association in healthy volunteers. Drug metabolism and pharmacokinetics 2019;34:78-86.
4. Takehara I, Yoshikado T, Ishigame K, Mori D, Furihata K-i, Watanabe N, Ando O, et al. Comparative study of the dose-dependence of OATP1B inhibition by rifampicin using probe drugs and endogenous substrates in healthy volunteers. Pharmaceutical research 2018;35:1-13.
5. Nevzorova YA, Boyer-Diaz Z, Cubero FJ, Gracia-Sancho J. Animal models for liver disease–A practical approach for translational research. Journal of hepatology 2020;73:423-440.
6. Guillouzo A. Liver cell models in in vitro toxicology. Environmental health perspectives 1998;106:511-532.
7. Chiang JY. Bile acid regulation of gene expression: roles of nuclear hormone receptors. Endocrine reviews 2002;23:443-463.
8. Chiang JY. Bile acids: regulation of synthesis: thematic review series: bile acids. Journal of lipid research 2009;50:1955-1966.
9. Chiang JY. Bile acid metabolism and signaling. Comprehensive physiology 2013;3:1191.
10. De Fabiani E, Mitro N, Gilardi F, Caruso D, Galli G, Crestani M. Coordinated control of cholesterol catabolism to bile acids and of gluconeogenesis via a novel mechanism of transcription regulation linked to the fasted-to-fed cycle. Journal of Biological Chemistry 2003;278:39124-39132.
11. Halilbasic E, Claudel T, Trauner M. Bile acid transporters and regulatory nuclear receptors in the liver and beyond. Journal of hepatology 2013;58:155-168.
12. Alqahtani S, Mohamed LA, Kaddoumi A. Experimental models for predicting drug absorption and metabolism. Expert Opinion on Drug Metabolism & Toxicology 2013;9:1241-1254.
13. FDA U. In vitro drug interaction studies—cytochrome P450 enzyme-and transporter-mediated drug interactions guidance for industry. Food and Drug Administration (FDA), Center for Drug Evaluation and Research (CDER), Silver Spring, MD 2020.
14. Giacomini K, Huang SM. Transporters in drug development and clinical pharmacology. In: Wiley Online Library; 2013. p. 3-9.
15. Stevens LJ, Zhu AZ, Chothe PP, Chowdhury SK, Donkers JM, Vaes WH, Knibbe CA, et al. Evaluation of normothermic machine perfusion of porcine livers as a novel preclinical model to predict biliary clearance and transporter-mediated drug-drug interactions using statins. Drug Metabolism and Disposition 2021;49:780-789.
16. Lau YY, Okochi H, Huang Y, Benet LZ. Pharmacokinetics of atorvastatin and its hydroxy metabolites in rats and the effects of concomitant rifampicin single doses: relevance of first-pass effect from hepatic uptake transporters, and intestinal and hepatic metabolism. Drug metabolism and disposition 2006;34:1175-1181.
17. Luo Z, Liu Y, Zhao B, Tang M, Dong H, Zhang L, Lv B, et al. Ex vivo and in situ approaches used to study intestinal absorption. Journal of pharmacological and toxicological methods 2013;68:208-216.
18. Galetin A, Gertz M, Houston JB. Potential role of intestinal first-pass metabolism in the prediction of drug–drug interactions. Expert opinion on drug metabolism & toxicology 2008;4:909-922.

19. Kanebratt K, Diczfalusy U, Bäckström T, Sparve E, Bredberg E, Böttiger Y, Andersson T, et al. Cytochrome P450 induction by rifampicin in healthy subjects: determination using the Karolinska cocktail and the endogenous CYP3A4 marker 4β-hydroxycholesterol. Clinical Pharmacology & Therapeutics 2008;84:589-594.

20. Eshmuminov D, Becker D, Borrego LB, Hefti M, Schuler MJ, Hagedorn C, Muller X, et al. An integrated perfusion machine preserves injured human livers for 1 week. Nature biotechnology 2020;38:189-198.

21. Lau N-S, Ly M, Dennis C, Jacques A, Cabanes-Creus M, Toomath S, Huang J, et al. Long-term ex-vivo normothermic perfusion of human split livers: a unique model to study new therapeutics and increase the number of available organs. 2023.

22. Schuler MJ, Becker D, Mueller M, Bautista Borrego L, Mancina L, Huwyler F, Binz J, et al. Observations and findings during the development of a subnormothermic/normothermic long-term ex vivo liver perfusion machine. Artificial Organs 2023;47:317-329.

23. Attard JA, Osei-Bordom D-C, Boteon Y, Wallace L, Ronca V, Reynolds G, Perera M, et al. Ex situ normothermic split liver machine perfusion: protocol for robust comparative controls in liver function assessment suitable for evaluation of novel therapeutic interventions in the pre-clinical setting. Frontiers in surgery 2021;8:627332.

24. Huang V, Karimian N, Detelich D, Raigani S, Geerts S, Beijert I, Fontan FM, et al. Split-liver ex situ machine perfusion: a novel technique for studying organ preservation and therapeutic interventions. Journal of Clinical Medicine 2020;9:269.

25. Thorne AM, Lantinga V, Bodewes S, de Kleine RH, Nijkamp MW, Sprakel J, Hartog H, et al. Ex situ dual hypothermic oxygenated machine perfusion for human split liver transplantation. Transplantation direct 2021;7.

26. Derungs A, Donzelli M, Berger B, Noppen C, Krähenbühl S, Haschke M. Effects of cytochrome P450 inhibition and induction on the phenotyping metrics of the Basel cocktail: a randomized crossover study. Clinical Pharmacokinetics 2016;55:79-91.

27. Chen K-F, Jones HM, Gill KL. Physiologically based pharmacokinetic modeling to predict drug-biologic interactions with cytokine modulators: are these relevant and is interleukin-6 enough? Drug Metabolism and Disposition 2022;50:1322-1331.

28. Abdel-Razzak Z, Loyer P, Fautrel A, Gautier J-C, Corcos L, Turlin B, Beaune P, et al. Cytokines down-regulate expression of major cytochrome P-450 enzymes in adult human hepatocytes in primary culture. Molecular pharmacology 1993;44:707-715.

29. Dallas S, Sensenhauser C, Batheja A, Singer M, Markowska M, Zakszewski C, NVS Mamidi R, et al. De-risking bio-therapeutics for possible drug interactions using cryopreserved human hepatocytes. Current drug metabolism 2012;13:923-929.

30. Mimura H, Kobayashi K, Xu L, Hashimoto M, Ejiri Y, Hosoda M, Chiba K. Effects of cytokines on CYP3A4 expression and reversal of the effects by anti-cytokine agents in the three-dimensionally cultured human hepatoma cell line FLC-4. Drug metabolism and pharmacokinetics 2015;30:105-110.

31. Abdel-Razzak Z, Corcos L, Fautrel A, Campion J-P, Guillouzo A. Transforming growth factor-beta 1 down-regulates basal and polycyclic aromatic hydrocarbon-induced cytochromes P-450 1A1 and 1A2 in adult human hepatocytes in primary culture. Molecular Pharmacology 1994;46:1100-1110.

32. Aitken AE, Morgan ET. Gene-specific effects of inflammatory cytokines on cytochrome P450 2C, 2B6 and 3A4 mRNA levels in human hepatocytes. Drug Metabolism and Disposition 2007;35:1687-1693.

33. Guillén MI, Donato MT, Jover R, Castell J, Fabra R, Trullenque R, Gómez-Lechón MJ. Oncostatin M down-regulates basal and induced cytochromes P450 in human hepatocytes. Journal of Pharmacology and Experimental Therapeutics 1998;285:127-134.

34. de Jong LM, Jiskoot W, Swen JJ, Manson ML. Distinct effects of inflammation on cytochrome P450 regulation and drug metabolism: lessons from experimental models and a potential role for pharmacogenetics. Genes 2020;11:1509.

35. Klein M, Thomas M, Hofmann U, Seehofer D, Damm G, Zanger UM. A systematic comparison of the impact of inflammatory signaling on absorption, distribution, metabolism, and excretion gene expression and activity in primary human hepatocytes and HepaRG cells. Drug Metabolism and Disposition 2015;43:273-283.

36. Gravante G, Ong S, Metcalfe M, Sorge R, Sconocchia G, Orlando G, Lloyd D, et al. Cytokine response to ischemia/reperfusion injury in an ex vivo perfused porcine liver model. In: Transplantation proceedings; 2009: Elsevier; 2009. p. 1107-1112.

37. Chung WY, Gravante G, Al-Leswas D, Alzaraa A, Sorge R, Ong SL, Pollard C, et al. Addition of a kidney to the normothermic ex vivo perfused porcine liver model does not increase cytokine response. Journal of Artificial Organs 2012;15:290-294.

38. Weissenbacher A, Stone JP, Lo Faro ML, Hunter JP, Ploeg RJ, Coussios CC, Fildes JE, et al. Hemodynamics and metabolic parameters in normothermic kidney preservation are linked with donor factors, perfusate cells, and cytokines. Frontiers in medicine 2022;8:801098.

39. Hosgood SA, Moore T, Qurashi M, Adams T, Nicholson ML. Hydrogen gas does not ameliorate renal ischemia reperfusion injury in a preclinical model. Artificial Organs 2018;42:723-727.

40. De Beule J, Keppens D, Korf H, Jochmans I. Differential Cytokine Levels during Normothermic Kidney Perfusion with Whole Blood-or Red Blood Cell-Based Perfusates—Results of a Scoping Review and Experimental Study. Journal of Clinical Medicine 2022;11:6618.

41. Volpin G, Cohen M, Assaf M, Meir T, Katz R, Pollack S. Cytokine levels (IL-4, IL-6, IL-8 and TGFβ) as potential biomarkers of systemic inflammatory response in trauma patients. International orthopaedics 2014;38:1303-1309.

42. Damas P, Ledoux D, Nys M, Vrindts Y, De Groote D, Franchimont P, Lamy M. Cytokine serum level during severe sepsis in human IL-6 as a marker of severity. Annals of surgery 1992;215:356.

43. Hosgood SA, Moore T, Kleverlaan T, Adams T, Nicholson ML. Haemoadsorption reduces the inflammatory response and improves blood flow during ex vivo renal perfusion in an experimental model. Journal of Translational Medicine 2017;15:1-10.

44. Vaessen SF, van Lipzig MM, Pieters RH, Krul CA, Wortelboer HM, van de Steeg E. Regional expression levels of drug transporters and metabolizing enzymes along the pig and human intestinal tract and comparison with Caco-2 cells. Drug metabolism and disposition 2017;45:353-360.

45. Englund G, Rorsman F, Rönnblom A, Karlbom U, Lazorova L, Gråsjö J, Kindmark A, et al. Regional levels of drug transporters along the human intestinal tract: co-expression of ABC and SLC transporters and comparison with Caco-2 cells. European Journal of Pharmaceutical Sciences 2006;29:269-277.

46. Gertz M, Harrison A, Houston JB, Galetin A. Prediction of human intestinal first-pass metabolism of 25 CYP3A substrates from in vitro clearance and permeability data. Drug Metabolism and Disposition 2010;38:1147-1158.

47. Paine MF, Shen DD, Kunze KL, Perkins JD, Marsh CL, McVicar JP, Barr DM, et al. First-pass metabolism of midazolam by the human intestine. Clinical Pharmacology & Therapeutics 1996;60:14-24.

48. Paine MF, Khalighi M, Fisher JM, Shen DD, Kunze KL, Marsh CL, Perkins JD, et al. Characterization of interintestinal and intraintestinal variations in human CYP3A-dependent metabolism. Journal of Pharmacology and Experimental Therapeutics 1997;283:1552-1562.

49. Bachmann F, Duthaler U, Krähenbühl S. Effect of deglucuronidation on the results of the Basel phenotyping cocktail. British Journal of Clinical Pharmacology 2021;87:4608-4618.

50. van de Steeg E, Schuren FH, Obach RS, van Woudenbergh C, Walker GS, Heerikhuisen M, Nooijen IH, et al. An ex vivo fermentation screening platform to study drug metabolism by human gut microbiota. Drug Metabolism and Disposition 2018;46:1596-1607.

51. Gupta E, Lestingi TM, Mick R, Ramirez J, Vokes EE, Ratain MJ. Metabolic fate of irinotecan in humans: correlation of glucuronidation with diarrhea. Cancer research 1994;54:3723-3725.

52. Davies MI. A review of microdialysis sampling for pharmacokinetic applications. Analytica Chimica Acta 1999;379:227-249.

53. Gunaratna C, Kissinger PT. Application of microdialysis to study the in vitro metabolism of drugs in liver microsomes. Journal of pharmaceutical and biomedical analysis 1997;16:239-248.
54. Brill MJ, Houwink AP, Schmidt S, Van Dongen EP, Hazebroek EJ, van Ramshorst B, Deneer VH, et al. Reduced subcutaneous tissue distribution of cefazolin in morbidly obese versus non-obese patients determined using clinical microdialysis. Journal of Antimicrobial Chemotherapy 2014;69:715-723.
55. Mazzeo AT, Fanelli V, Boffini M, Medugno M, Filippini C, Simonato E, Costamagna A, et al. Feasibility of lung microdialysis to assess metabolism during clinical ex vivo lung perfusion. The Journal of Heart and Lung Transplantation 2019;38:267-276.
56. Schreiter T, Sowa J, Mathé Z, Treckmann J, Bröcker-Preuß M, Baba H, Gieseler R, et al. Long-term maintenance of human liver tissue by ex-vivo perfusion of liver sections. Zeitschrift für Gastroenterologie 2014;52:P_3_19.
57. Melgert BN, Olinga P, Weert B, Slooff MJ, Meijer DK, Poelstra K, Groothuis GM. Cellular distribution and handling of liver-targeting preparations in human livers studied by a liver lobe perfusion. Drug metabolism and disposition 2001;29:361-367.
58. Villeneuve J-P, Dagenais M, Huet P-M, Lapointe R, Roy A, Marleau D. Clearance by the liver in cirrhosis. III. Propranolol uptake by the isolated perfused human liver. Canadian journal of physiology and pharmacology 1996;74:1327-1332.
59. Younossi Z, Anstee QM, Marietti M, Hardy T, Henry L, Eslam M, George J, et al. Global burden of NAFLD and NASH: trends, predictions, risk factors and prevention. Nature reviews Gastroenterology & hepatology 2018;15:11-20.
60. Müller PC, Kabacam G, Vibert E, Germani G, Petrowsky H. Current status of liver transplantation in Europe. International Journal of Surgery 2020;82:22-29.
61. Sehgal A, Vaishnaw A, Fitzgerald K. Liver as a target for oligonucleotide therapeutics. Journal of hepatology 2013;59:1354-1359.
62. Roberts TC, Langer R, Wood MJ. Advances in oligonucleotide drug delivery. Nature Reviews Drug Discovery 2020;19:673-694.
63. An G. Pharmacokinetics and Pharmacodynamics of GalNAc‐Conjugated siRNAs. The Journal of Clinical Pharmacology 2023.
64. Andersson P, den Besten C: Preclinical and clinical drug-metabolism, pharmacokinetics and safety of therapeutic oligonucleotides. In: Advances in nucleic acid therapeutics, 2019; 474-531.
65. Griffett K, Burris TP. Development of LXR inverse agonists to treat MAFLD, NASH, and other metabolic diseases. Frontiers in medicine 2023;10:1102469.
66. Alkhouri N, Reddy GK, Lawitz E. Oligonucleotide‐Based Therapeutics: An Emerging Strategy for the Treatment of Chronic Liver Diseases. Hepatology 2021;73:1581-1593.
67. Lindén D, Ahnmark A, Pingitore P, Ciociola E, Ahlstedt I, Andréasson A-C, Sasidharan K, et al. Pnpla3 silencing with antisense oligonucleotides ameliorates nonalcoholic steatohepatitis and fibrosis in Pnpla3 I148M knock-in mice. Molecular metabolism 2019;22:49-61.
68. Bonaccorsi-Riani E, Gillooly A, Brüggenwirth IM, Martins PN. Delivery of genetic load during ex situ liver machine perfusion with potential for CRISPR-Cas9 gene editing: an innovative strategy for graft treatment. Hepatobiliary Pancreat Dis Int 2021;20:503-505.
69. Bonaccorsi-Riani E, Gillooly AR, Iesari S, Brüggenwirth IM, Ferguson CM, Komuta M, Xhema D, et al. Delivering siRNA compounds during HOPE to modulate organ function: a proof-of-concept study in a rat liver transplant model. Transplantation 2022;106:1565-1576.
70. Gillooly AR, Perry J, Martins PN. First report of siRNA uptake (for RNA interference) during ex vivo hypothermic and normothermic liver machine perfusion. In: LWW; 2019.
71. Thijssen MF, Brüggenwirth IM, Gillooly A, Khvorova A, Kowalik TF, Martins PN. Gene silencing with siRNA (RNA interference): a new therapeutic option during ex vivo machine liver perfusion preservation. Liver Transplantation 2019;25:140-151.
72. Butler AJ, Rees MA, Wight DG, Casey ND, Alexander G, White DJ, Friend PJ. Successful extracorporeal porcine liver perfusion for 72 hr1. Transplantation 2002;73:1212-1218.

73. Liu Q, Nassar A, Buccini L, Iuppa G, Soliman B, Pezzati D, Hassan A, et al. Lipid metabolism and functional assessment of discarded human livers with steatosis undergoing 24 hours of normothermic machine perfusion. Liver Transplantation 2018;24:233-245.

74. Vogel T, Brockmann JG, Pigott D, Neil DA, Muthusamy ASR, Coussios CC, Friend PJ. Successful transplantation of porcine liver grafts following 48-hour normothermic preservation. PLoS One 2017;12:e0188494.

75. Eshmuminov D, Becker D, Bautista Borrego L, Hefti M, Schuler MJ, Hagedorn C, Muller X, et al. An integrated perfusion machine preserves injured human livers for 1 week. Nature biotechnology 2020;38:189-198.

76. Thompson ER, Sewpaul A, Figuereido R, Bates L, Tingle SJ, Ferdinand JR, Situmorang GR, et al. MicroRNA antagonist therapy during normothermic machine perfusion of donor kidneys. American Journal of Transplantation 2022;22:1088-1100.

77. Finegold MJ, Egler RA, Goss JA, Guillerman PR, Karpen SJ, Krishnamurthy R, O'Mahony CA. Liver tumors: pediatric population. Liver Transplantation 2008;14:1545-1556.

78. Mangus RS, Tector AJ, Kubal CA, Fridell JA, Vianna RM. Multivisceral transplantation: expanding indications and improving outcomes. Journal of gastrointestinal surgery 2013;17:179-187.

79. Dhakal P, Giri S, Siwakoti K, Rayamajhi S, Bhatt VR. Renal cancer in recipients of kidney transplant. Rare tumors 2017;9:9-13.

80. HJ Krekels E, Danhof M, Tibboel D, AJ Knibbe C. Ontogeny of hepatic glucuronidation; methods and results. Current drug metabolism 2012;13:728-743.

81. Thakur A, Parvez MM, Leeder JS, Prasad B. Ontogeny of drug-metabolizing enzymes. Enzyme Kinetics in Drug Metabolism: Fundamentals and Applications 2021:551-593.

82. van Rongen A, Välitalo PA, Peeters MY, Boerma D, Huisman FW, van Ramshorst B, van Dongen EP, et al. Morbidly obese patients exhibit increased CYP2E1-mediated oxidation of acetaminophen. Clinical pharmacokinetics 2016;55:833-847.

83. Smit C, De Hoogd S, Brüggemann RJ, Knibbe CA. Obesity and drug pharmacology: a review of the influence of obesity on pharmacokinetic and pharmacodynamic parameters. Expert opinion on drug metabolism & toxicology 2018;14:275-285.

84. de Hoogd S, Välitalo PA, Dahan A, van Kralingen S, Coughtrie MM, van Dongen EP, van Ramshorst B, et al. Influence of morbid obesity on the pharmacokinetics of morphine, morphine-3-glucuronide, and morphine-6-glucuronide. Clinical pharmacokinetics 2017;56:1577-1587.

85. König J, Rost D, Cui Y, Keppler D. Characterization of the human multidrug resistance protein isoform MRP3 localized to the basolateral hepatocyte membrane. Hepatology 1999;29:1156-1163.

86. Delacôte C, Favre M, El Amrani M, Ningarhari M, Lemaitre E, Ntandja-Wandji LC, Bauvin P, et al. Morbid obesity increases death and dropout from the liver transplantation waiting list: A prospective cohort study. United European Gastroenterology Journal 2022;10:396-408.

87. Zhang T, Krekels EH, Smit C, Knibbe CA. Drug pharmacokinetics in the obese population: challenging common assumptions on predictors of obesity-related parameter changes. Expert Opinion on Drug Metabolism & Toxicology 2022;18:657-674.

88. Rolle A, Paredes S, Cortinez L, Anderson B, Quezada N, Solari S, Allende F, et al. Dexmedetomidine metabolic clearance is not affected by fat mass in obese patients. British Journal of Anaesthesia 2018;120:969-977.

89. Brill MJ, Välitalo PA, Darwich AS, van Ramshorst B, Van Dongen H, Rostami–Hodjegan A, Danhof M, et al. Semiphysiologically based pharmacokinetic model for midazolam and CYP3A mediated metabolite 1-OH-midazolam in morbidly obese and weight loss surgery patients. CPT: pharmacometrics & systems pharmacology 2016;5:20-30.

90. van Rongen A, Brill MJ, Vaughns JD, Välitalo PA, van Dongen EP, van Ramshorst B, Barrett JS, et al. Higher midazolam clearance in obese adolescents compared with morbidly obese adults. Clinical pharmacokinetics 2018;57:601-611.

91. DiMasi JA, Hansen RW, Grabowski HG. The price of innovation: new estimates of drug development costs. Journal of health economics 2003;22:151-185.

92. Zhang Y, Chan HF, Leong KW. Advanced materials and processing for drug delivery: the past and the future. Advanced drug delivery reviews 2013;65:104-120.

93. Waring MJ, Arrowsmith J, Leach AR, Leeson PD, Mandrell S, Owen RM, Pairaudeau G, et al. An analysis of the attrition of drug candidates from four major pharmaceutical companies. Nature reviews Drug discovery 2015;14:475-486.

94. Stevens LJ, van Lipzig MM, Erpelinck SL, Pronk A, van Gorp J, Wortelboer HM, van de Steeg E. A higher throughput and physiologically relevant two-compartmental human ex vivo intestinal tissue system for studying gastrointestinal processes. European Journal of Pharmaceutical Sciences 2019;137:104989.

95. Westerhout J, van de Steeg E, Grossouw D, Zeijdner EE, Krul CA, Verwei M, Wortelboer HM. A new approach to predict human intestinal absorption using porcine intestinal tissue and biorelevant matrices. European Journal of Pharmaceutical Sciences 2014;63:167-177.

96. Harrison LI, Gibaldi M. Physiologically based pharmacokinetic model for digoxin disposition in dogs and its preliminary application to humans. Journal of pharmaceutical sciences 1977;66:1679-1683.

97. Hu L-D, Liu Y, Tang X, Zhang Q. Preparation and in vitro/in vivo evaluation of sustained-release metformin hydrochloride pellets. European journal of pharmaceutics and biopharmaceutics 2006;64:185-192.

98. Jamei M, Bajot F, Neuhoff S, Barter Z, Yang J, Rostami-Hodjegan A, Rowland-Yeo K. A mechanistic framework for in vitro–in vivo extrapolation of liver membrane transporters: prediction of drug–drug interaction between rosuvastatin and cyclosporine. Clinical pharmacokinetics 2014;53:73-87.

99. Stevens LJ, Donkers JM, Dubbeld J, Vaes WH, Knibbe CA, Alwayn IP, van de Steeg E. Towards human ex vivo organ perfusion models to elucidate drug pharmacokinetics in health and disease. Drug metabolism reviews 2020;52:438-454.

100. Bergman E, Lundahl A, Fridblom P, Hedeland M, Bondesson U, Knutson L, Lennernäs H. Enterohepatic disposition of rosuvastatin in pigs and the impact of concomitant dosing with cyclosporine and gemfibrozil. Drug metabolism and disposition 2009;37:2349-2358.

101. Lau YY, Wu C-Y, Okochi H, Benet LZ. Ex situ inhibition of hepatic uptake and efflux significantly changes metabolism: hepatic enzyme-transporter interplay. Journal of Pharmacology and Experimental Therapeutics 2004;308:1040-1045.

102. Graham GG, Punt J, Arora M, Day RO, Doogue MP, Duong J, Furlong TJ, et al. Clinical pharmacokinetics of metformin. Clinical pharmacokinetics 2011;50:81-98.

103. Waller ES, Massarella JW, Tomkiw MS, Smith RV, Doluisio JT. Pharmacokinetics of furosemide after three different single oral doses. Biopharmaceutics & drug disposition 1985;6:109-117.

104. Takano M, Yumoto R, Murakami T. Expression and function of efflux drug transporters in the intestine. Pharmacology & therapeutics 2006;109:137-161.

105. Sjöberg Å, Lutz M, Tannergren C, Wingolf C, Borde A, Ungell A-L. Comprehensive study on regional human intestinal permeability and prediction of fraction absorbed of drugs using the Ussing chamber technique. European Journal of Pharmaceutical Sciences 2013;48:166-180.

106. Cooper KJ, Martin PD, Dane AL, Warwick MJ, Schneck DW, Cantarini MV. Effect of itraconazole on the pharmacokinetics of rosuvastatin. Clinical Pharmacology & Therapeutics 2003;73:322-329.

107. Li Y, Jiang X, Lan K, Zhang R, Li X, Jiang Q. Pharmacokinetic properties of rosuvastatin after single-dose, oral administration in Chinese volunteers: a randomized, open-label, three-way crossover study. Clinical therapeutics 2007;29:2194-2203.

108. Mak W, Tan S, Wong J, Chin S, Lim A. Pharmacokinetic Comparison and Bioequivalence Study of Two Rosuvastatin 20 mg Formulations in Healthy Volunteers. J Bioequiv Availab 2016;8:095-098.

109. Martin PD, Warwick MJ, Dane AL, Brindley C, Short T. Absolute oral bioavailability of rosuvastatin in healthy white adult male volunteers. Clinical therapeutics 2003;25:2553-2563.

110. Drozdzik M, Gröer C, Penski J, Lapczuk J, Ostrowski M, Lai Y, Prasad B, et al. Protein abundance of clinically relevant multidrug transporters along the entire length of the human intestine. Molecular pharmaceutics 2014;11:3547-3555.

111. Becquemont L, Verstuyft C, Kerb R, Brinkmann U, Lebot M, Jaillon P, Funck-Brentano C. Effect of grapefruit juice on digoxin pharmacokinetics in humans. Clinical Pharmacology & Therapeutics 2001;70:311-316.

112. Eckermann G, Lahu G, Nassr N, Bethke TD. Absence of pharmacokinetic interaction between roflumilast and digoxin in healthy adults. The Journal of Clinical Pharmacology 2012;52:251-257.

113. Ragueneau I, Poirier JM, Radembino N, Sao AB, Funck-Brentano C, Jaillon P. Pharmacokinetic and pharmacodynamic drug interactions between digoxin and macrogol 4000, a laxative polymer, in healthy volunteers. British journal of clinical pharmacology 1999;48:453-456.

114. Schwartz JI, Agrawal NG, Wehling M, Musser BJ, Gumbs CP, Michiels N, De Smet M, et al. Evaluation of the pharmacokinetics of digoxin in healthy subjects receiving etoricoxib. British journal of clinical pharmacology 2008;66:811-817.

115. Verstuyft C, Schwab M, Schaeffeler E, Kerb R, Brinkmann U, Jaillon P, Funck-Brentano C, et al. Digoxin pharmacokinetics and MDR1 genetic polymorphisms. European journal of clinical pharmacology 2003;58:809-812.

116. Westphal K, Weinbrenner A, Giessmann T, Stuhr M, Franke G, Zschiesche M, Oertel R, et al. Oral bioavailability of digoxin is enhanced by talinolol: evidence for involvement of intestinal P-glycoprotein. Clinical Pharmacology & Therapeutics 2000;68:6-12.

117. Rozehnal V, Nakai D, Hoepner U, Fischer T, Kamiyama E, Takahashi M, Yasuda S, et al. Human small intestinal and colonic tissue mounted in the Ussing chamber as a tool for characterizing the intestinal absorption of drugs. European Journal of Pharmaceutical Sciences 2012;46:367-373.

118. Marathe PH, Wen Y, Norton J, Greene DS, Barbhaiya RH, Wilding IR. Effect of altered gastric emptying and gastrointestinal motility on metformin absorption. British journal of clinical pharmacology 2000;50:325-332.

119. Pentikäinen P, Neuvonen P, Penttilä A. Pharmacokinetics of metformin after intravenous and oral administration to man. European journal of clinical pharmacology 1979;16:195-202.

120. Stopfer P, Giessmann T, Hohl K, Sharma A, Ishiguro N, Taub M, Zimdahl-Gelling H, et al. Pharmacokinetic evaluation of a drug transporter cocktail consisting of digoxin, furosemide, metformin, and rosuvastatin. Clinical Pharmacology & Therapeutics 2016;100:259-267.

121. Timmins P, Donahue S, Meeker J, Marathe P. Steady-state pharmacokinetics of a novel extended-release metformin formulation. Clinical pharmacokinetics 2005;44:721-729.

122. Tucker G, Casey C, Phillips P, Connor H, Ward J, Woods H. Metformin kinetics in healthy subjects and in patients with diabetes mellitus. British journal of clinical pharmacology 1981;12:235.

123. Hammarlund M, Paalzow L, Odlind B. Pharmacokinetics of furosemide in man after intravenous and oral administration. Application of moment analysis. European journal of clinical pharmacology 1984;26:197-207.

124. Shen H, Holenarsipur VK, Mariappan TT, Drexler DM, Cantone JL, Rajanna P, Gautam SS, et al. Evidence for the validity of pyridoxic acid (PDA) as a plasma-based endogenous probe for OAT1 and OAT3 function in healthy subjects. Journal of Pharmacology and Experimental Therapeutics 2019;368:136-145.

125. Bindschedler M, Degen P, Flesch G, De Gasparo M, Preiswerk G. Pharmacokinetic and pharmacodynamic interaction of single oral doses of valsartan and furosemide. European journal of clinical pharmacology 1997;52:371-378.

126. Michael RK, Ralph EC, Arden WF, Barbara MK. Pharmacokinetics of orally administered furosemide. Clinical Pharmacology & Therapeutics 1974;15:178-186.

127. Hosgood S, Barlow A, Hunter J, Nicholson M. Ex vivo normothermic perfusion for quality assessment of marginal donor kidney transplants. Journal of British Surgery 2015;102:1433-1440.

128. Pool MB, Hamelink TL, van Goor H, van den Heuvel MC, Leuvenink HG, Moers C. Prolonged ex-vivo normothermic kidney perfusion: The impact of perfusate composition. PLoS One 2021;16:e0251595.

129. Kaths JM, Hamar M, Echeverri J, Linares I, Urbanellis P, Cen JY, Ganesh S, et al. Normothermic ex vivo kidney perfusion for graft quality assessment prior to transplantation. American Journal of Transplantation 2018;18:580-589.

130. Markgraf W, Mühle R, Lilienthal J, Kromnik S, Thiele C, Malberg H, Janssen M, et al. Inulin clearance during ex vivo normothermic machine perfusion as a marker of renal function. ASAIO Journal 2022;68:1211-1218.

131. van Leeuwen LL, Ruigrok MJ, Kessler BM, Leuvenink HG, Olinga P. Targeted delivery of galunisertib using machine perfusion reduces fibrogenesis in an integrated ex vivo renal transplant and fibrogenesis model. British Journal of Pharmacology 2023.

132. Venema LH, Leuvenink HG. Development of a porcine slaughterhouse kidney perfusion model. Transplantology 2022;3:6-19.

133. Lødrup AB, Karstoft K, Dissing TH, Nyengaard JR, Pedersen M. The association between renal function and structural parameters: a pig study. BMC nephrology 2008;9:1-9.

134. Moman RN, Gupta N, Varacallo M. Physiology, albumin. 2017.

135. Gülden M, Seibert H. Influence of protein binding and lipophilicity on the distribution of chemical compounds in in vitro systems. Toxicology in vitro 1997;11:479-483.

136. Henze LJ, Koehl NJ, O'Shea JP, Kostewicz ES, Holm R, Griffin BT. The pig as a preclinical model for predicting oral bioavailability and in vivo performance of pharmaceutical oral dosage forms: a PEARRL review. Journal of pharmacy and pharmacology 2019;71:581-602.

137. Elmorsi Y, Al Feteisi H, Al-Majdoub ZM, Barber J, Rostami-Hodjegan A, Achour B. Proteomic characterisation of drug metabolising enzymes and drug transporters in pig liver. Xenobiotica 2020;50:1208-1219.

138. Stevens LJ, Dubbeld J, Doppenberg JB, van Hoek B, Menke AL, Donkers JM, Alsharaa A, et al. Novel explanted human liver model to assess hepatic extraction, biliary excretion and transporter function. Clinical Pharmacology & Therapeutics 2023.

ADDENDUM

Nederlandse samenvatting

De karakteriseren van het farmacokinetische profiel van een stof is een uitdagend en ingewikkeld proces met een lage slagingskans. Preklinische experimenten zijn een belangrijk onderdeel in het proces van medicijn ontwikkeling met als doel om informatie te voorzien over het veiligheidsprofiel en de werkzaamheid van het medicijn. Dit maakt dat het essentieel is dat alle aspecten van medicijn zoals de absorptie, distributie, metabolisme en excretie (ADME) gekarakteriseerd zijn. Om ADME processen te karakteriseren zijn preklinische ex vivo modellen zeer waardevol en kunnen ze worden beschouwd als de schakel tussen *in vitro* en *in vivo* modellen zoals besproken in deel I van deze dissertatie. In Hoofdstuk 2 wordt een overzicht gegeven van de huidige preklinische ex vivo modellen om medicijn absorptie, metabolisme en excretie te bestuderen. Daarnaast wordt de toepassing om drug-drug interacties (DDI) in gezondheid en de toepassing van ziekte (ex vivo) modellen bediscussieerd. Het gebruik van normotherme machine perfusie in het veld van transplantatie onderzoek heeft laten zien dat orgaan functie en dynamische processen op een representatieve manier kunnen worden bestudeerd. Toepassing voor het preklinische farmacologie veld zou een toepassing kunnen zijn; de intacte morfologische structuur van het orgaan, applicatie van fysiologische bloedstroom en de aanwezigheid van intacte galwegen en urine structuren zijn belangrijke karakteristieken nodig om bepaalde ADME processen in kaart te brengen. Deze hiervoor genoemde aspecten zijn vaak afwezig in preklinische simplistische *in vitro* modellen maar zijn van essentieel belang om inzichten te bieden in transporter affiniteit, DDI en eliminatie routes. Het doel van deze dissertatie was het exploreren van de toepasbaarheid van *ex vivo* orgaanperfusie om farmacologische processen in darm, lever en nier te karakteriseren. In de verschillende hoofdstukken hebben we het gebruik van o.a. leverperfusie en multi-orgaan perfusie laten zien dat farmacokinetische processen zoals DDI, endogene substraten processen, pre-systemische darm en lever metabolisme en excretieprofielen kunnen karakteriseren.

In deel II van deze dissertatie hebben we de toepasbaarheid van normotherme machine perfusie (NMP) van de lever bestudeerd om medicijn farmacokinetiek en het metabolisme van endogene substraten te karakteriseren. Als eerste stap hebben we in hoofdstuk 3 het perfusie model met varkenslevers opgezet en onderzocht of het model een geschikt platform is om klinische geobserveerde OATP-gemedieerde DDI na te bootsen. We hebben aangetoond dat NMP van

varkenslevers een nieuw en betrouwbaar model is om OATP-gemedieerde DDI te bestuderen. We hebben de DDI effecten op hepatische klaring, galexcretie en perfusate(metaboliet) profielen van verschillende statines bestudeerd. De rangorde in de mate van DDI die we in onze experimenten hebben gevonden kwamen goed overeen met klinisch gevonden mate van DDI waarbij de laagste DDI werd gevonden voor Pitavastatine en de hoogste interactie voor Atorvastatine. Dit wijst naar het potentiële toepassing van het nieuwe ex vivo model in de vroege fase van geneesmiddel ontwikkeling.

Het vertalen van preklinische bevindingen met behulp van dierlijke materiaal, zoals het varkenslever model, naar de klinische setting blijft uitdagend vanwege onder andere de verschillend in de eiwitexpressie van transporters en CYP-enzymen. Bovendien kan een leveraandoening en ziekte zoals cirrose leiden tot morfologische afwijkingen en verschillen de eiwit expressie van verschillende transporters en CYP-enzymen waardoor de farmacokinetische profielen van medicijnen worden beïnvloed. Met de huidig beschikbare preklinische modellen blijft het een uitdaging om effecten van deze pathologische veranderingen op het farmacokinetische profiel te bestuderen. In hoofdstuk 4 hebben we het gebruik van geëxplanteerde humane levers laten zien als toepassing voor machine perfusie. Met het model hebben we de invloed van cirrose op de hepatische extractie, galklaring en DDI van 4 geneesmiddelen voor verschillende transporter substraten onderzocht. We hebben succesvol 7 cirrotische levers en 4 niet-cirrotische levers voor 360 minuten geperfundeerd waarbij viabiliteit en functionaliteit behouden bleven. De hepatische klaring van rosuvastatine en digoxine bleken het meest te worden beïnvloed door cirrose, deze stoffen lieten een toename zien in Cmax van respectievelijk 11.5 en 2.89 keer vergelijke met niet-cirrotische levers. Er werden geen grote verschillen waargenomen voor metformin en furosemide. De interactie van rosuvastatine of digoxine met een interacterend geneesmiddel was duidelijker in niet-cirrotische levers vergeleken met cirrotische levers. Het bestuderen van de farmacokinetiek van geneesmiddelen met behulp van geëxplanteerde humane levers kan als basis dienen om verschillen in de hepatische klaring van geneesmiddelen voor patiënten met leverziekten te bestuderen.

Een voordeel van het perfusiemodel is het bepalen van specifieke functies van het hele orgaan zoals het karakteriseren van het hepatische first-pass effect en de biliaire excretie in een geïsoleerde omgeving zonder de aanwezigheid van andere systemische effecten. De lever is echter een centraal orgaan in het

menselijke lichaam en via is via de poortader in connectie met de darmen die voedingsstoffen, galzouten en hormonen transporteert richt de lever. Deze (endogene) stoffen remmen en/of stimuleren vaak bepaalde processen in de lever zoals lipide metabolisme, glucose huishouding en het galzoutmetabolisme. Galzouten regelen hun eigen homeostase door negatieve terugkoppeling op de biosynthese van galzouten. Galzouten remmen CYP27A2, CYP7A1 en CYP8B1 door FXR activatie. Na activatie zal het ook galzout import remmen en export stimuleren en daarbij voorkomen dat galzouten in de lever accumuleren wat toxisch kan zijn. Echter, de momenteel gebruikte NMP protocollen, die veel worden toegepast in zowel klinische als onderzoek setting, limiteren de nabootsing van de *in vivo* galzout fysiologie. Tijdens perfusies wordt namelijk alleen taurocholaat (TCA) gebruik als galzout infusie wat slechts een van de vele geconjugeerde circulerende galzouten is. Dit legt een aanzienlijke last op de lever tijdens NMP gezien de novo synthese van galzouten aanslaat maar er geen teruggave is van een gevarieerde galzout pool. In hoofdstuk 5 hebben we dit bestudeerd en geprobeerd de de novo synthese van galzouten te karakteriseren door het profileren van de galzout excretie in de gal, cholesterol homeostase te karakteriseren en hebben we de genexpressie van transporter eiwitten tijdens machine perfusie in kaart te brengen. We hebben aangetoond dat de galzout synthese (g/h) bovengemiddeld is tijdens machineperfusie wat resulteerde in een afname van perfusaat cholesterol levels in varkensperfusies. Bovendien was er een afname in de expressie van genen gerelateerd aan de galzout synthese en een toename van de genexpressie van genen gerelateerd aan cholesterol metabolisme en een afname van galzout afhankelijke opname en efflux transporter expressie. Het vervangen van TCA infusie door een representatievere galzout pool met (on)geconjugeerde galzouten heeft veelbelovende resultaten opgeleverd. De infusie van een fysiologische relevante geconjugeerde galzoutmix resulteerde in een verminderde levels van ALT en AST en behield stabiele perfusaat cholesterol waarden. Daarnaast konden we een link leggen tussen galzout klaring en leverfunctie.

In deel III hebben we farmacokinetische processen bestudeerde door middel van perfusie van abdominale organen. Real-time karakteriseren van het first-pass effect van oraal toegediende geneesmiddelen, bestaande uit darm absorptie en metabolisme, transport via de poortader en hepatobiliaire processen, blijft een uitdaging. In hoofdstuk 6 laten we de ontwikkeling en applicatie van een ex vivo varkens perfusie model zien met abdominale

organen wat het potentieel laat zien voor het bestuderen van ADME gerelateerde processen. Met behulp van dit model konden we pre-systemische extractie van midazolam karakteriseren voor zowel de darm als lever. Als gevolg daarvan kon de orale biobeschikbaarheid worden bepaald. De hepatische extractie (F_H) en darm extractie (F_G) en de berekende orale bio beschikbaarheid hieruit waren in overeenstemming met *in vivo* data van varkens. Door deze aanpak kunnen waardevolle inzichten worden verkregen in de absorptie en metabolisme van nieuwe geneesmiddelen waardoor de ontwikkeling en optimalisatie van geneesmiddelen in ontwikkeling voor humaan gebruik.

In conclusie, in deze dissertatie hebben we ons gericht op de farmacokinetische toepassing van NMP. Met behulp van deze techniek hebben we geprobeerd de vakgebieden van transplantatie en farmacologie samen te brengen. De verschillende studies hebben aangetoond dat NMP ingezet kan worden om verschillende farmacokinetische processen van geneesmiddelen in kaart te brengen zoals het hepatische first-pass effect, hepatische klaring, galkaring, transporterfunctie en DDI met behulp van geëxplanteerde zieke humane levers en uit het slachthuis verkregen varkenslevers. Het gebruik van varkenslevers bleek een geschikt alternatief voor menselijke levers om de mechanistische bijdrage van transporters in geneesmiddelopname, geneesmiddeluitscheiding en DDI te bestuderen. Deze studies maakten het mogelijk om DDI, gemedieerd door OATP1B1/1B3, te onderzoeken, met resultaten die goed in overeenstemming waren met klinische data. Bovendien bleken geëxplanteerde zieke humane levers geschikt te zijn voor perfusieonderzoek en kunnen ze dienen als basis om de verschillen in hepatische verwerking van geneesmiddelen bij patiënten met verschillende soorten leveraandoeningen beter te bestuderen. De hepatische klaring van rosuvastatine en digoxine bleek het meest beïnvloed door cirrose, terwijl er geen grote verschillen werden waargenomen voor de renaal geklaarde geneesmiddelen metformine en furosemide. De 3-voudig lagere portale flow in cirrotische levers verminderde de hepatische extractie van rosuvastatine, wat het belang van portale flow in een preklinisch model voor het bepalen van hepatische klaring aantoont. Verder werd de optimalisatie van het leverperfusiemodel bestudeerd door infusie van een (on)geconjugeerde galzuurpool om fysiologische omstandigheden na te bootsen voor een nauwkeurigere beoordeling van hepatische farmacokinetisce processen. Deze strategie toonde aan dat de infusie van (on)geconjugeerde galzuren de belasting van de de novo galzuursynthese verlichtte en de leverfunctie

verbeterde, wat wijst op potentiële vooruitgangen in leverpreservatie en transplantatietechnieken. De mogelijkheden van het perfusiesysteem bleken talrijk, zoals we aantoonden bij de ontwikkeling en toepassing van multi-orgaanperfusie om de interactie tussen de darm en lever te begrijpen door karakterisatie van het first-pass effect en pre-systemische CYP3A4 metabolisme. Het gebruik van perfusie bleek een uitstekend hulpmiddel te zijn om geneesmiddelconcentraties in bloedstromen en weefsels te bestuderen die anders onmogelijk te bereiken zijn, waardoor nieuwe en diepgaande inzichten kunnen worden verkregen in het ADME-profiel van geneesmiddelen.

Curriculum Vitae

Lianne Stevens was born on November 5th, 1992 in Twello, the Netherlands. After completing her secondary school at the Heemgaard in Apeldoorn in 2011, she started the bachelor Nutrition and Health at Wageningen University. While working on her bachelor thesis under supervision of Prof.dr. Witkamp, exploring the pharmacokinetic effects of omega-3 fatty acids on inflammation, she developed a growing interest in pharmacology. After successful completion in 2014, she continued with the master program Nutrition and Health with the specialization of Molecular Nutrition and Toxicology. During her master program she did her MSc thesis at the division of Toxicology at Wageningen. Thereafter, she performed her internship at TNO, where she worked on an organ on-a-chip project. After finalization of her internship and thereby her master program in December 2016, she worked for 2 years as scientist at TNO at the division of Human Cell Biology. In January 2019 she started her 5-year PhD project under the supervision of Prof.dr. Ian Alwayn, Prof.dr. Catherijne Knibbe and dr. Evita van de Steeg. In this role she worked for 4 days a week on the PhD project one day per week as a scientist on TNO projects. The results of this PhD project are described in this thesis, entitled: Pumping new life into preclinical pharmacokinetics; exploring the pharmacokinetics application of ex vivo organ perfusion. After completion of her PhD project, she started as a scientist preclinical development at ProQR Therapeutics in Leiden.

List of publications

This thesis

Stevens, L. J., Donkers, J. M., Dubbeld, J., Vaes, W. H., Knibbe, C. A., Alwayn, I. P., & van de Steeg, E. (2020). Towards human ex vivo organ perfusion models to elucidate drug pharmacokinetics in health and disease. Drug metabolism reviews, 52(3), 438-454.

Stevens, L. J., Zhu, A. Z., Chothe, P. P., Chowdhury, S. K., Donkers, J. M., Vaes, W. H., Knibbe, C.A.J., Alwayn I.P.J., & van de Steeg, E. (2021). Evaluation of normothermic machine perfusion of porcine livers as a novel preclinical model to predict biliary clearance and transporter-mediated drug-drug interactions using statins. Drug Metabolism and Disposition, 49(9), 780-789.

Stevens, L. J., Dubbeld, J., Doppenberg, J. B., van Hoek, B., Menke, A. L., Donkers, J. M., Alsharaa A., de Vries A., Vaes W.H.J., Knibbe C.A.J., van de Steeg E., & Alwayn, I. P. (2023). Novel explanted human liver model to assess hepatic extraction, biliary excretion and transporter function. Clinical Pharmacology & Therapeutics. 114(1), 137-147.

Stevens, L. J., Doppenberg, J. B., van de Steeg E., Alwayn, I. P., Knibbe C.A.J.& Dubbeld, J (2024) Ex vivo Gut-Hepatobiliary organ perfusion model to characterize oral absorption, first pass gut and liver metabolism biliary excretion: application to midazolam. European Journal of Pharmaceutical Sciences 2023, 196, 106760

Stevens, L. J., Donkers, J.M., Doppenberg, J.B., Caspers, M., Dubbeld, J., Heming B., Tramper, N., Kleinjan. L., de Waart, R., Oude Elferink, R., van de Steeg, E., & Alwayn, I.P.J Unraveling and enhancing the dynamics of hepatic bile acid and cholesterol metabolism during ex vivo normothermic machine perfusion; a path to improved liver function through conjugated bile acid infusion. Submitted

Other

Stevens, L. J., van Lipzig, M. M., Erpelinck, S. L., Pronk, A., van Gorp, J., Wortelboer, H. M., & van de Steeg, E. (2019). A higher throughput and physiologically relevant two-compartmental human ex vivo intestinal tissue system for studying gastrointestinal processes. European Journal of Pharmaceutical Sciences, 137, 104989.

Amirabadi, H. E., Donkers, J. M., Wierenga, E., Ingenhut, B., Pieters, L., Stevens, L.J., Donkers, T., Westerhout. J., Masereeus, R., Bobeldijk-Pastorova, I. & van de Steeg, E. (2022). Intestinal explant barrier chip: long-term intestinal absorption screening in a novel microphysiological system using tissue explants. Lab on a Chip, 22(2), 326-342.

Dankwoord

Bloed, zweet en tranen heeft het gekost om deze thesis tot stand te brengen. Het waren 5 leerzame en intensieve jaren en ik ben erg dankbaar voor alle ervaringen en inzichten die ik heb opgedaan. Ik heb het geluk gehad om vanuit verschillende disciplines begeleiding te ontvangen en wil graag een aantal mensen speciaal bedanken.

Allereerst Ian Alwayn, hartelijk dank voor je begeleiding en support tijdens het promotietraject. Daarnaast wil ik je bedanken voor de inkijk in de wondere wereld van orgaantransplantatie: ik vond het heel bijzonder om als iemand zonder medische achtergrond, orgaantransplantie van heel dichtbij mee te maken.

Catherijne Knibbe, ik keek altijd uit naar de afspraken op de vrijdagmiddag op het LACDR om nieuwe resultaten te bespreken. Je klinische perspectief was ontzettend waardevol in dit onderzoek en je enthousiasme inspireerde mij telkens weer, waarvoor dank!

Evita van de Steeg, dit onderzoek heb ik aan jou te danken! Ik heb de afgelopen jaren ontzettend veel van je creativiteit en oplossingsgerichtheid mogen leren. Daarnaast denk ik met veel plezier terug aan de congressen die we de afgelopen jaren samen hebben bezocht, dat was altijd erg gezellig!

Jeroen Dubbeld, je stond letterlijk dag en nacht klaar om mij te helpen met de humane lever- en multiorgaan perfusies. Dankzij jouw inzet hebben we kunnen laten zien dat deze nieuwe modellen ontzettend waardevol zijn voor o.a. farmacologisch onderzoek. Ik heb altijd met veel plezier met je samengewerkt!

Bijzonder veel dank wil ik uitspreken naar de patienten en donoren die hebben bijgedragen aan dit onderzoek. Onderzoek kunnen doen met humaan materiaal is een voorrecht en blijft ontzettend belangrijk voor transleerbare resultaten.

Slachterij & Vleesverwerking Visser B.V. uit Lunteren; oneindig veel dank dat we wekelijks langs mochten komen om bloed en organen op te halen voor onderzoek. Dank voor jullie behulpzaamheid en gastvrijheid.

TNO-collega's, hartelijk dank voor jullie support de afgelopen jaren! Met name Lisanne, Linda, Bo en Angelique; zonder jullie hulp in het slachthuis en op het lab had ik hier nu niet gestaan. Wat was het soms toch lachen in het slachthuis; de gesprekken met de slachters en varkens die soms rakelings langs je heen vlogen. Ik kijk er met een grote glimlach op terug. Irene, dankjewel voor de vele koffie momentjes. Joanne, dank voor (wetenschappelijke) discussies op ons kantoortje in Zeist, later in de kantoortuin in Leiden. Eva, Michelle, Maria and Marit; academic buddies within TNO. Thank you for your support, coffee breaks and scientific discussions!

Studenten; Babette, Emma, Naomi, Bo, Lisa en Sophie. Dank voor jullie bijdragen aan de verschillende onderzoeken van dit proefschrift! Ik vond het erg leuk om met jullie samen te werken en te begeleiden tijdens jullie (afstudeer)stages.

Mede promovendi en PI's en onderzoekers van de afdeling transplatatiechirurgie, dank! De kritische vragen tijdens de donderdagmiddag besprekingen brachten mij telkens een stapje verder. Daarnaast was het erg interssant om een inkijkje te krijgen in de klinische onderzoeken, hier heb ik veel van geleerd.

Hardloopgenootjes van Phoenix atletiek en Leiden atletiek, EJC Apollo 11, T.M.S.D.C.D.C Scotia en in het speciaal Clan Teachers, Benthe en Sharon. Dank allen voor jullie steun en de afleiding van het onderzoek die ik af en toe hard nodig had: jullie hebben mij soepeltjes door mijn PhD tijd heen gesleept.

Pap en mam, dankjewel voor jullie onvoorwaardelijke steun. Het doorzettingsvermogen wat ik van jullie heb meegekregen heeft mij tot hier gebracht, daar ben ik jullie ontzettend dankbaar voor. Lieve zus en broertje, dankjewel dat jullie er (extra) voor mij waren de afgelopen jaren. Schoonfamilie, dank voor jullie steun en medeleven tijdens mijn promotietraject.

Lieve Wijnand, bedank voor je oneindige support de afgelopen jaren. Je hebt mij er doorheen gesleept, zonder jou was het niet gelukt.